

# Scour holes

A data-driven risk-based analysis for  
scour holes in the Rhine-Meuse Delta

I.M. (Igor) Koevoets



Rijkswaterstaat  
Ministerie van Infrastructuur en Waterstaat

*(This page is intentionally left blank)*

# Scour holes

A data-driven risk-based analysis for scour holes in the Rhine-Meuse Delta

by

I.M. (Igor) Koevoets

to obtain the degree of

**Master of Science**

in Hydraulic Engineering

at the Delft University of Technology,

at the faculty of Civil Engineering and Geosciences,

to be defended publicly on Tuesday August 27, 2019 at 15:30.

|                   |  |
|-------------------|--|
| Student number:   | 4297121  |
| Project duration: | December, 2018 – August, 2019                      |
| Thesis committee: | Prof. dr. ir. M. Kok    TU Delft                   |
|                   | Dr. ir. S. van Vuren    TU Delft & Rijkswaterstaat |
|                   | Ir. J.C. Pol            TU Delft & HKV             |
|                   | Ir. J.G. Stenfert        HKV                       |
|                   | Ir. P. Neeffjes         Rijkswaterstaat            |

An electronic version of this thesis is available at <http://repository.tudelft.nl/>.

**Cover image:** River Spui, picture made by Igor Koevoets



Rijkswaterstaat  
Ministerie van Infrastructuur en Waterstaat

*(This page is intentionally left blank)*

# Preface

This thesis is the final product of my Master of Science in Hydraulic engineering at the Delft University of Technology. The research has been carried out in collaboration with HKV Consultants and Rijkswaterstaat WNZ. I would like to thank everyone at HKV and Rijkswaterstaat who helped me during my research.

I would like to thank my graduation committee for their help and feedback during the several committee meetings. First of all, I would like to thank Saskia van Vuren for proposing the research topic and putting me in touch with HKV and Rijkswaterstaat. Special gratitude to my daily supervisor Joost Stenfert for helping me with the entire research and giving me a lot of feedback. Next, I would like to thank Pim Neeffjes for the pleasant discussions and his advice. Furthermore, thanks to Joost Pol for his input and valuable comments. Finally, I would like to thank Matthijs Kok for being the chair of my graduation committee and for the guidance.

Since this thesis marks the end of my time as a student, I want to thank all my friends for an enjoyable time in Delft and during the many city trips. Special thanks go to Maarten Kroll for reading and giving feedback on my report.

Lastly, I would like to thank my family for their support during my entire study, thank you!

*Igor Koevoets  
Delft, August 2019*

*(This page is intentionally left blank)*

# Summary

## Introduction

There are over 100 scour holes located in the Rhine-Meuse Delta. Some of the scour holes are stable and some have a more dynamic behaviour. These scour holes are growing in surface area and in depth. The scour holes form a potential hazard for the stability of hydraulic structures, the erosion of the protected cover layers of cables, pipelines and tunnels and the stability of dikes near the scour holes. Despite, the locations in the river branches with scour holes are known, a quantified risk per location is lacking. A method for the quantification of the risk of scour holes is missing.

The scope of this research is limited by the hazard of dike instability and associated flood risk of scour holes. A data-driven method for the flood risk assessment of scour holes has been developed and applied, as an example, to one scour hole. Next to the risk assessment of this case scour hole, risk mitigation measures are analysed for this particular scour hole.

## Data-driven risk assessment method

The dynamic behaviour of a scour hole is coupled with the safety assessment of the flood defence next to the scour hole in the method for the risk assessment of scour holes. The scour hole development is predicted with a data-driven extrapolation tool. In the tool, the differences between historical measured bathymetry data are extrapolated in a probabilistic way to predict the future dimensions of a scour hole.

For the predicted future scour hole, the probability of occurrence of a flow slide is calculated with the methods given in the Wettelijk Beoordelingsinstrumentarium (WBI). This probability is calculated with 9 parameters representing the subsoil properties, the river cross-section and scaling conditions for the local circumstances. The river cross-section parameters can be determined from the predicted future scour hole together with land elevation data. The post flow slide profile is, together with the retrogression length of a flow slide, relevant for the determination whether a flow slide could affect the water-retaining function of a dike.

The probability of flooding is determined for the failure mechanism overtopping. Conditional scenarios for flow slide with different retrogression states and application of emergency repairs after a flow slide are used in the calculation of the probability of flooding.

In order to quantify the risk, the probability of flooding is multiplied with the consequences of a flood. Two types of consequences of flooding are used: 1) economic damage and 2) Loss of life. Both consequences have already been determined in the nationwide flood risk assessment 'Veiligheid Nederland in Kaart'.

## Case study

A quickscan is executed for the selection of a scour hole for the case study. In the quickscan, scour holes are identified with a high probability of occurrence of a flow slide and with affection of the water-retaining function of a dike. According to the quickscan, there are at least four locations in the connecting branches of the Rhine-Meuse Delta with a potential risk for flow slides with the affection of the flood defence next to the scour holes. These locations are:

1. In the Spui near rkm 1004.8
2. In the Spui near rkm 1007.5
3. In the Oude Maas near rkm 982.1
4. In the Noord near rkm 983.8

In this research, the scour hole in the Spui near rkm 1004.8 is used as a case study for which the flood risk is quantified. The historical growth of this scour hole resulted in an increase in the probability of occurrence of a flow slide in the period between 2014 and 2018. By extrapolation of the historical measured bathymetry data, the scour hole dimensions are predicted for 2023. Based on the predicted dimensions, the probability of occurrence of a flow slide will further increase.

In order to assess the probability of flooding, the probability of occurrence of a flow slide is combined with the probability of retrogression states, the probability of successful repair after a flow slide and the probability of exceedance of the critical overtopping discharge. The yearly probability of flooding next to these scour holes increases from 1/94,300 in 2018 to 1/58,000 for the expected mean scour hole in 2023. Multiplying these probabilities with the consequences of a flood gives an increase of the yearly risk from €54,955 in 2018 to €94.627 in 2023.

Two measures for the mitigation of the flood risk are analysed for the case scour hole: 1) placing of riprap on the entire underwater slope and 2) filling the entire scour hole with sand. With the implementation of the first measure, the probability of occurrence of a flow slide will be negligible, while the second measure only reduces this probability. The placement of riprap has larger investment costs than the filling of the scour hole (€944,384 versus €102.296). On the other hand, the lifespan is also larger, due to the erosion of the filling material, the second measure has a shorter lifespan. Both measures are economically feasible since the investment costs are smaller than the benefits (risk reduction). The benefit-cost ratio for placing riprap is 2.28 and for filling the scour hole with sand the benefit-cost ratio is 1.40.

### **Conclusions and recommendations**

This research shows that the flood risk near scour holes can be quantified with the usage of open data and that the implementation of risk mitigation measures can be economically beneficial. The economic feasibility depends on the original probability of flooding, the magnitude of the consequences, the effectiveness in risk reduction and the total investment costs.

A sensitivity study on the probability of flooding of the case scour hole is performed. This study shows the exact post flow slide profile as the most sensitive aspect of the probability of flooding, followed by the subsoil properties. Subordinate to these two aspects is the dynamic behaviour of the scour hole, which determines the exact scour hole dimensions and depth.

In the risk assessment method, overtopping is the only included direct failure mechanism. It is recommended to extend the risk assessment method with other direct failure mechanisms. Besides, the method can also be extended with other types of risk, like the stability of hydraulic structures and the erosion of the protected cover layers.

The quickscan is only applied for three connecting branches in this research. It is recommended to apply the quickscan also to the remaining river branches in the Rhine-Meuse Delta. The data-driven risk assessment method has been applied to one scour hole in this research. It is recommended to apply this method to all scour holes, which are identified as a potential threat in the quickscan.

# Contents

|   |           |
|---|-----------|
| List of Symbols   | ix        |
| Abbreviations   | xi        |
| List of Figures   | xiii      |
| List of Tables  | xvii      |
| <b>1 Introduction</b>   | <b>1</b>  |
| 1.1 Background information . . . . .  | 1         |
| 1.2 Problem statement . . . . .   | 2         |
| 1.3 Data-driven risk-based approach . . . . .                                   | 2         |
| 1.4 Objective . . . . .   | 4         |
| 1.5 Outline of the report . . . . .   | 5         |
| <b>2 Preparation for risk assessment</b>  | <b>7</b>  |
| 2.1 Rhine-Meuse Delta system . . . . .  | 7         |
| 2.2 Scour hole problems in the Rhine-Meuse Delta . . . . .                      | 11        |
| 2.3 Current management strategies . . . . .                                     | 13        |
| <b>3 Hazard identification: scour hole development</b>                          | <b>17</b> |
| 3.1 Scour hole development processes . . . . .                                  | 17        |
| 3.2 Tool for scour hole development prediction . . . . .                        | 19        |
| 3.3 Illustration of the probabilistic scour hole development approach . . . . . | 25        |
| 3.4 Discussion about scour hole development prediction . . . . .                | 27        |
| <b>4 Risk identification: flood safety</b>                                      | <b>29</b> |
| 4.1 Indirect failure mechanism: flow slide . . . . .                            | 29        |
| 4.2 Direct failure mechanisms . . . . .   | 35        |
| 4.3 Probability of flooding . . . . .   | 39        |
| 4.4 Consequences . . . . .  | 41        |
| 4.5 Risk quantification . . . . .   | 42        |
| <b>5 Risk assessment</b>  | <b>45</b> |
| 5.1 Locations with potential risk . . . . .                                     | 45        |
| 5.2 Method for risk assessment of individual scour holes . . . . .              | 46        |
| 5.3 Case Spui rkm 1004.8 . . . . .  | 47        |
| 5.4 Sensitivity analysis . . . . .  | 53        |
| <b>6 Risk management</b>  | <b>57</b> |
| 6.1 Risk tolerability . . . . .   | 57        |
| 6.2 Risk mitigation measures . . . . .  | 57        |
| 6.3 Risk management for case Spui rkm 1004.8 . . . . .                          | 59        |
| <b>7 Conclusions, discussions &amp; recommendations</b>                         | <b>65</b> |
| 7.1 Conclusions . . . . .   | 65        |
| 7.2 Discussion . . . . .  | 67        |
| 7.3 Recommendations . . . . .   | 68        |
| References  | 71        |
| Appendices  | 75        |
| <b>A Extra literature</b>   | <b>75</b> |

---

|          |  |            |
|----------|--|------------|
| <b>B</b> | <b>Scour hole prediction approach</b>                    | <b>89</b>  |
| <b>C</b> | <b>Flow slide quantification tool</b>                    | <b>101</b> |
| <b>D</b> | <b>Fictive scour hole development scenarios</b>          | <b>109</b> |
| <b>E</b> | <b>General method for risk assessment of scour holes</b> | <b>117</b> |
| <b>F</b> | <b>Quickscan for the connecting branches</b>             | <b>123</b> |
| <b>G</b> | <b>Risk assessment scour hole rkm 1004.8</b>             | <b>137</b> |

# List of Symbols

| Symbol                          | Description   | Units                 |
|---------------------------------|---|-----------------------|
| $E(D)$                          | Expected value of the risk  | [€/yr]                |
| $\Delta E(D)$                   | Present value of risk reduction   | [€]                   |
| $D$                             | Height of the steepest slope of the new profile                         | [m]                   |
| $D_{50.mean.kar}$               | Characteristic mean particle diameter                                   | [m]                   |
| $D_{pv}$                        | Present value of the potential damage                                   | [€]                   |
| $F_{cohesivelayers}$            | Factor for the presence of interference layers                          | [-]                   |
| $F_E$                           | Evacuation fraction   | [-]                   |
| $F_D$                           | Mortality fraction  | [-]                   |
| $F(FS)$                         | Frequency of occurrence of a flow slide:                                | [1/yr]                |
| $H$                             | Total height of the submerged slope                                     | [m]                   |
| $H_{channel}$                   | Channel depth   | [m]                   |
| $H_{m0}$                        | Significant wave height   | [m]                   |
| $H_r$                           | Fictive calculation height  | [m]                   |
| $I$                             | Total investment costs  | [€]                   |
| $L$                             | Retrogression length  | [m]                   |
| $L_{section}$                   | Length of the dike section  | [km]                  |
| $N_{loss}$                      | Loss of life estimation   | [-]                   |
| $N_{par}$                       | Number of people at risk  | [-]                   |
| $OLW$                           | Agreed low water level  | [m + NAP]             |
| $P_{f,0}$                       | Initial failure probability   |                       |
| $P_{f,new}$                     | Failure probability after risk reduction investment                     | [1/yr]                |
| $P(q_o > q_c)$                  | Probability of exceedance critical overtopping discharge                | [1/yr]                |
| $P(FS)$                         | Probability of occurrence of a flow slide:                              | [1/yr]                |
| $P(L > L_{max})$                | Probability of exceedance of the maximum allowable retrogression length | [-]                   |
| $P(Repair)$                     | Probability of a successful repair after a flow slide                   | [-]                   |
| $P(RS_i)$                       | Probability of occurrence of retrogression state i                      | [-]                   |
| $P(S_i)$                        | Probability of occurrence of subsoil scenario i                         | [-]                   |
| $RS_i$                          | Retrogression state i   |                       |
| $S$                             | Sediment transport per unit width                                       | [m <sup>3</sup> /s/m] |
| $S_i$                           | Subsoil scenario i  |                       |
| $T_{data}$                      | Period between the recording date of the two bathymetry datasets        | [yr]                  |
| $T_{prog}$                      | Prediction period   | [yr]                  |
| $T_{repair}$                    | Required time for emergency repair after a flow slide                   | [Days]                |
| $V_{local}$                     | Dynamic behaviour of the foreshore                                      | [m/yr]                |
| $V_{Zeeland}$                   | Characteristic value of dynamic behaviour of the foreshore in Zeeland   | [m/yr]                |
| $W_{max}$                       | Maximum scour hole width  | [m]                   |
| $Z$                             | Limit state function  |                       |
| $Z_n$                           | Position of the bed level   | [m]                   |
| $Z_{prog}(x + \Delta s_{prog})$ | Predicted bed level on location $(x + \Delta s_{prog})$                 | [m + NAP]             |
| $Z_{original}(x)$               | Original bed level in newest bathymetry data on location $(x)$          | [m + NAP]             |
| $\Delta Z$                      | Vertical difference between the two bathymetry datasets                 | [m]                   |

| Symbol            | Description   | Units     |
|-------------------|---|-----------|
| $\alpha_r$        | Calculation slope angle                                 | [°]       |
| $\beta$           | Slope angle of the steepest part of the new profile     | [°]       |
| $c$               | Ratio between surface area 1 and 2 of the profile       | [-]       |
| $d_i$             | Consequences of event i                                 | [€]       |
| $i$               | Local average slope                                     | [-]       |
| $p_i$             | Probability of event i                                  | [1/yr]    |
| $q_c$             | Critical overtopping discharge                          | [l/s/m]   |
| $q_o$             | Actual overtopping discharge                            | [l/s/m]   |
| $\Delta s_{prog}$ | Predicted horizontal displacement for period $T_{prog}$ | [m]       |
| $tp$              | Assessment water level                                  | [m + NAP] |
| $\gamma$          | Slope angle of the mildest part of the new profile      | [°]       |
| $\psi_{5m.kar}$   | State parameter   | [-]       |

# Abbreviations

|             |                                       |
|-------------|---------------------------------------|
| <b>AHN3</b> | Actueel Hoogtebestand Nederland       |
| <b>CPT</b>  | Cone Penetration test                 |
| <b>FORM</b> | First Order Reliability Method        |
| <b>HBN</b>  | Hydraulisch Belasting Niveau          |
| <b>LIR</b>  | Local individual risk                 |
| <b>NGD</b>  | Nautical Guaranteed Depth             |
| <b>rkm</b>  | River kilometer                       |
| <b>RMD</b>  | Rhine-Meuse Delta                     |
| <b>VNK2</b> | Veiligheid Nederland in Kaart         |
| <b>WBI</b>  | Wettelijk Beoordelingsinstrumentarium |

*(This page is intentionally left blank)*

# List of Figures

|      |   |    |
|------|---|----|
| 1.1  | Overview of the locations of the scour holes and the sedimentation/erosion rates in Rhine-Meuse Delta, including dredging activities. The scour holes are located in all branches. . . . .  | 1  |
| 1.2  | Source-Pathway-Receptor-Consequence model. . . . .  | 3  |
| 1.3  | Framework for research, based on the framework of Bowles et al. (2013). . . . .   | 5  |
| 2.1  | The Rhine-Meuse Delta with river names, Delta Works and bed level of the branches. . . . .  | 7  |
| 2.2  | Scour hole depth development in heterogeneous subsoil. . . . .  | 12 |
| 2.3  | Management area for Rijkswaterstaat(river manager) and waterboards (dike managers). . . . .   | 13 |
| 2.4  | Locations of the pilot study in the Oude Maas. . . . .  | 14 |
| 2.5  | Overview of the pilot nourishment plan and execution for the scour hole located at rkm 996 in the Oude Maas. . . . .  | 15 |
| 2.6  | Overview of the total costs of the six scenarios (in million euro), the initial costs are presented, with a distinction between ‘free’ and ‘partly bought’ sediment. For the maintenance costs over 20 and 50 years, it is assumed that all sediment is free. . . . . | 16 |
| 3.1  | Schematisation of purely horizontal extrapolation of a scour hole edge in Htrend. . . . .   | 20 |
| 3.2  | Schematisation of searching-lines for the horizontal extrapolation in Htrend. . . . .   | 20 |
| 3.3  | Schematisation of purely vertical extrapolation based on vertical erosion trends in Htrend. . . . .   | 21 |
| 3.4  | Schematisation extrapolation of combined horizontal and vertical trends in Htrend. . . . .  | 22 |
| 3.5  | Schematisation of the usage of bathymetry datasets for the calibration and verification of a particular scour hole Htrend. . . . .  | 23 |
| 3.6  | Steps for the scour hole development prediction in the probabilistic approach. . . . .  | 24 |
| 3.7  | Division of the scour hole in 8 areas, the bed level erosion rate relation is determined per area. . . . .  | 25 |
| 3.8  | Steps for the creation of the vertical erosion rate based on the relation between bed level and erosion rate. . . . .   | 26 |
| 3.9  | Accuracy of the 90th fractile values depending on the number of runs. . . . .   | 27 |
| 3.10 | Cross-section of the middle of the scour hole, with the historical bed level and the predicted future bed level. . . . .  | 27 |
| 3.11 | Prediction of the 2023-profile, with the original deterministic approach and the updated probabilistic approach. . . . .  | 28 |
| 4.1  | Pathway from flow slide to flooding. . . . .  | 29 |
| 4.2  | Overview of the indirect failure mechanism flow slide. . . . .  | 30 |
| 4.3  | Flow slide processes. . . . .   | 31 |
| 4.4  | Effect of a scour hole on the location of the characteristic river bottom point (effect 1). . . . .   | 33 |
| 4.5  | Effects of a scour hole on the post flow slide profile. . . . .   | 34 |
| 4.6  | Scenarios for scour hole development. . . . .   | 34 |
| 4.7  | Effect of flow slide on relevant direct failure mechanisms . . . . .  | 36 |
| 4.8  | Schematisation of overflow and wave overtopping . . . . .   | 37 |
| 4.9  | Events required for flooding for overflow and wave overtopping . . . . .  | 37 |
| 4.10 | Event tree for failure mechanism overtopping including conditional probability of flow slide . . . . .  | 40 |
| 4.11 | Schematisation of dike sections and ring segments in Veiligheid Nederland in Kaart (VNK2) . . . . .   | 42 |
| 5.1  | Overview of the scour hole locations in the Spui, Noord and eastern part of the Oude Maas. The scour holes with a potential danger for flow slide and scour holes with placed riprap are indicated. . . . .   | 45 |
| 5.2  | Overview of the relevant sections for the quickscan and the sections with a large probability of occurrence of a flow slide in the Spui, the Noord and eastern part of the Oude Maas. . . . .   | 46 |
| 5.3  | Overview of the data-driven method for risk assessment of scour holes. . . . .  | 47 |
| 5.4  | Bathymetry around the river bend in the Spui near rkm 1005 with indication of three scour holes. . . . .  | 48 |
| 5.5  | Historical locations of the scour hole edges. . . . .   | 48 |

|      |  |     |
|------|--|-----|
| 5.6  | Predicted locations of the scour edge in 2023 for three growth scenarios. . . . .  | 49  |
| 5.7  | Boundaries of the considered scour hole section. . . . .   | 49  |
| 5.8  | Dike geometry of the representative profiles for the retrogression states and the three used retrogression states for the case scour hole. . . . . | 50  |
| 5.9  | Representative profile for the sensitivity analysis. . . . .   | 54  |
| 5.10 | Parameter sensitivity on the return period range of $q_0 > q_c$ . . . . .  | 55  |
|      |  |     |
| 6.1  | Common method for placing riprap on a steep riverbank slope. . . . .   | 58  |
| 6.2  | Area for the placement of riprap and filling of the scour hole as risk mitigation measures. . . . .  | 60  |
|      |  |     |
| A.1  | Scour hole depth development in time for clear-water scour and live-bed scour. . . . .   | 76  |
| A.2  | Growth of a scour hole in the initial phase. . . . .   | 78  |
| A.3  | Growth of a scour hole in the development phase. . . . .   | 79  |
| A.4  | Growth of a scour hole in the stabilisation phase. . . . .   | 79  |
| A.5  | Two-dimensional flow regions in a scour hole . . . . .   | 79  |
| A.6  | Steps of the rule of thumb for flow slide in WBI. . . . .  | 82  |
| A.7  | Critical slope for breaching. . . . .  | 82  |
| A.8  | Determination of fictive calculation height and calculation slope angle based on most unfavourable total geometry . . . . .                        | 83  |
|      |  |     |
| B.1  | Schematisation of the steps for the scour hole prediction in the deterministic approach. . . . .   | 89  |
| B.2  | Location of the example cross-section for the analysis of the deterministic approach. . . . .  | 90  |
| B.3  | Vertical erosion rate input for Htrend. Blue indicates local erosion while red indicates sedimentation. . . . .                                    | 91  |
| B.4  | Example of scour hole development in a period of five years for two different erosion rate input files. . . . .                                    | 91  |
| B.5  | Effect of the usage of safety factor on the 5-year bathymetry extrapolation for two different erosion rate input files. . . . .                    | 92  |
| B.6  | Relation between historical data for the year on year erosion rate. . . . .  | 93  |
| B.7  | Relation between the yearly erosion rate and the bed level. For the years 2014-2018. . . . .   | 94  |
| B.8  | Relation between the yearly erosion rate and the bed level . . . . .   | 94  |
| B.9  | Schematisation of steps for the scour hole prediction in the probabilistic approach. . . . .   | 96  |
| B.10 | Steps for the creation of the vertical erosion rate based on the relation between bed level and erosion rate. . . . .                              | 97  |
| B.11 | Example of the vertical erosion rate data based on the historical relation between bed level and erosion rate. . . . .                             | 97  |
| B.12 | Example of 100 runs for the probabilistic approach, the bathymetry of 2016 and 2017 is used as input data for Htrend . . . . .                     | 99  |
| B.13 | Predicted 2023 profile, with three input bathymetry combinations: 2016-2017, 2017-2018 & 2016-2018. . . . .  | 99  |
|      |  |     |
| C.1  | Including rkms into the data for example case Oude Maas. . . . .   | 102 |
| C.2  | Extracting profiles from the datasets. . . . .   | 102 |
| C.3  | Example profile used for the tool description. . . . .   | 103 |
| C.4  | Profile split in lowest point of the example profile. . . . .  | 103 |
| C.5  | Determination of the dike top and dike toe for the right side of the example profile. . . . .  | 104 |
| C.6  | Determination of characteristic points of the example profile. . . . .   | 105 |
| C.7  | Determination of the slope angle, such that the ratio between the two area will be 1:1.4. . . . .  | 107 |
| C.8  | Determination of the slope angle, for each retrogression length a different slope angle can be found. . . . .                                      | 107 |
| C.9  | Determination of characteristic points of the example profile. . . . .   | 108 |
|      |  |     |
| D.1  | Scenarios for scour hole development. . . . .  | 109 |
| D.2  | Overview of the river branches taken into account for the creation of the reference situation. . . . .   | 110 |
| D.3  | Reference situation profiles. . . . .  | 111 |
| D.4  | Overview of probability for the wide profile including a scour hole of 26 m width, with an increasing depth. . . . .                               | 112 |

|      |   |     |
|------|---|-----|
| D.5  | Profile after a flow slide for the wide reference profile with and without a scour hole. . . . .  | 113 |
| D.6  | Overview of probabilities for the wide profile including a scour hole with increasing scour width located at the left riverside. . . . .                                  | 113 |
| D.7  | Overview of probabilities for the narrow side profile including scour holes with changing location of a scour edge with respect to the left riverside. . . . .            | 115 |
| E.1  | Overview of the data-driven method for risk assessment of scour holes. . . . .  | 118 |
| E.1  | Depth variation of the river Spui. . . . .  | 123 |
| E.2  | Relevant sections for flow slide on the river Spui. . . . .   | 124 |
| E.3  | $P(L > L_{max})_{section}$ for the right side of the river Spui. . . . .  | 125 |
| E.4  | $P(L > L_{max})_{section}$ for the left side of the river Spui. . . . .   | 125 |
| E.5  | Sections with with $P(L > L_{max})_{section} > 0.01$ on the river Spui. . . . .   | 126 |
| E.6  | Most interesting dike sections for flow slide on the river Spui. . . . .  | 132 |
| E.7  | Relevant sections for flow slide on the river Oude Maas. . . . .  | 132 |
| E.8  | $P(L > L_{max})_{section}$ for the right side of the river Oude Maas. . . . .   | 133 |
| E.9  | $P(L > L_{max})_{section}$ for the left side of the river Oude Maas. . . . .  | 134 |
| E.10 | Sections with with $P(L > L_{max})_{section} > 0.01$ on the river Oude Maas. . . . .  | 134 |
| E.11 | Most interesting dike section for flow slide on the river Oude Maas. . . . .  | 135 |
| E.12 | Relevant sections for flow slide on the river Noord. . . . .  | 135 |
| E.13 | Sections with with $P(L > L_{max})_{section} > 0.01$ on the river Noord. . . . .  | 136 |
| E.14 | Most interesting dike sections for flow slide on the river Noord. . . . .   | 136 |
| G.1  | Bathymetry around the river bend in the Spui near rkm 1005 with indication of three scour holes. . . . .  | 137 |
| G.2  | Historical locations of the scour hole edges. . . . .   | 138 |
| G.3  | Prediction of the location of the scour edge in 2023. . . . .   | 139 |
| G.4  | Riprap next to the scour hole. Based on riprap information from WSHD (WSHD, 2019). . . . .  | 139 |
| G.5  | Subsoil scenarios for dike-segment 20-01 from the SOS-database of the WBI. . . . .  | 140 |
| G.6  | Boundaries of the considered scour hole section. . . . .  | 141 |
| G.7  | Historical probability of occurrence of a flow slide for the individual river profiles of scour hole near rkm 1005 in the Spui. . . . .                                   | 142 |
| G.8  | Dike geometry of the section next to the scour hole. The river Spui is located on the left sides of the profiles. . . . .   | 143 |
| G.9  | Dike profiles after a flow slide for the three retrogression states. . . . .  | 143 |
| G.10 | Lithological cross-section at rkm 1004.6 of the river Spui. . . . .   | 146 |
| G.11 | Schematisation of usage of bathymetry datasets for the calibration and verification of the scour hole in Htrend. . . . .  | 148 |
| G.12 | Vertical erosion rate input data based on the historical average erosion in the period 2014-2018. Blue indicates local erosion while red indicates sedimentation. . . . . | 149 |
| G.13 | Overview of historical surfaces of the scour hole below a certain level. . . . .  | 149 |
| G.14 | Calibration results of surface area below a certain level. . . . .  | 150 |
| G.15 | Verification results of surface area below a certain level. . . . .   | 151 |

*(This page is intentionally left blank)*

# List of Tables

|      |   |     |
|------|---|-----|
| 2.1  | Overview of river branches with their length per subsystem together with the number and clusters of scour holes per branch. . . . .   | 11  |
| 3.1  | Spatial correlation for erosion rate and neighbours average erosion rate in 2017. . . . .   | 26  |
| 5.1  | Locations with potential risk and total number of scour holes in the connecting river branches.   | 46  |
| 5.2  | Overview of growth of the case scour hole . . . . .   | 48  |
| 5.3  | Overview of scour hole characteristic for the three growth scenarios. . . . .   | 49  |
| 5.4  | Historical probability of the occurrence of a flow slide for the dike section near the scour hole. .  | 50  |
| 5.5  | Probability of the occurrence of a flow slide in 2023 for different scour hole development scenarios. . . . .   | 50  |
| 5.6  | Conditional probability of occurrence of the retrogression states, for 2018 and the future scour hole scenarios. . . . .  | 51  |
| 5.7  | Conditional probability of exceedance critical overtopping discharge for the three retrogression states and original dike profile. . . . .                                    | 51  |
| 5.8  | Probability of exceedance and return period critical overtopping discharge( $q=5$ l/s/m) for the case with and without dike repair after a flow slide. . . . .                | 52  |
| 5.9  | Consequences of a flood with a breach near the scour hole for different water levels associated with their exceedance probability. . . . .                                    | 52  |
| 5.10 | Risk estimation for scour hole in 2018. . . . .   | 52  |
| 5.11 | Risk estimation for scour hole in 2023. . . . .   | 52  |
| 5.12 | Relevant probabilities for risk assessment of the scour hole and the representative profile for the sensitivity analysis. . . . .   | 53  |
| 5.13 | Parameters with their base values and variation ranges used in the sensitivity analysis. . . . .  | 54  |
| 6.1  | Calculated probabilities for the scour hole in 2018 and 2023 compared with the require probability with a contribution of 0.24 for the failure mechanism overtopping. . . . . | 59  |
| 6.2  | Relevant probabilities for the original scour hole and the scour hole filled with sand. . . . .   | 60  |
| 6.3  | Overview of investment items and unit prices for the implementation of measures. . . . .  | 61  |
| 6.4  | Overview of required material for the mitigation measures. . . . .  | 61  |
| 6.5  | Overview of investment costs for mitigation measures. . . . .   | 61  |
| 6.6  | Yearly risk reduction for the riprap measure. . . . .   | 62  |
| 6.7  | Yearly risk reduction for the filling measure. . . . .  | 62  |
| 6.8  | Net present values and benefit-cost ratios for the mitigation measures. . . . .   | 63  |
| 6.9  | Effect of sand price on feasibility mitigation measures. . . . .  | 63  |
| 6.10 | Effect of lifespan of the riprap measure on feasibility. . . . .  | 63  |
| 6.11 | Effect of lifespan of the filling measure on feasibility. . . . .   | 63  |
| 6.12 | Effect of the required time for emergency repairs on feasibility mitigation measure. . . . .  | 64  |
| A.1  | Subsoil parameter for the presence of interference layers. . . . .  | 85  |
| A.2  | Parameter distributions for the determination of the retrogression length with the volume balance. . . . .  | 86  |
| B.1  | Pearson's product moment correlation-coefficients for different erosion rates. . . . .  | 93  |
| B.2  | Pearson's product moment correlation-coefficients for the bed level and erosion rate relations. .   | 94  |
| B.3  | $\rho_{XY}$ for the bed level and erosion rate relations for the four areas of the scour hole. . . . .  | 95  |
| B.4  | Spatial correlation for erosion rate and neighbours average erosion rate in 2017. . . . .   | 95  |
| C.1  | Overview of the geometry parameters for the example profile. . . . .  | 105 |
| C.2  | Overview of the results for step 4. . . . .   | 106 |

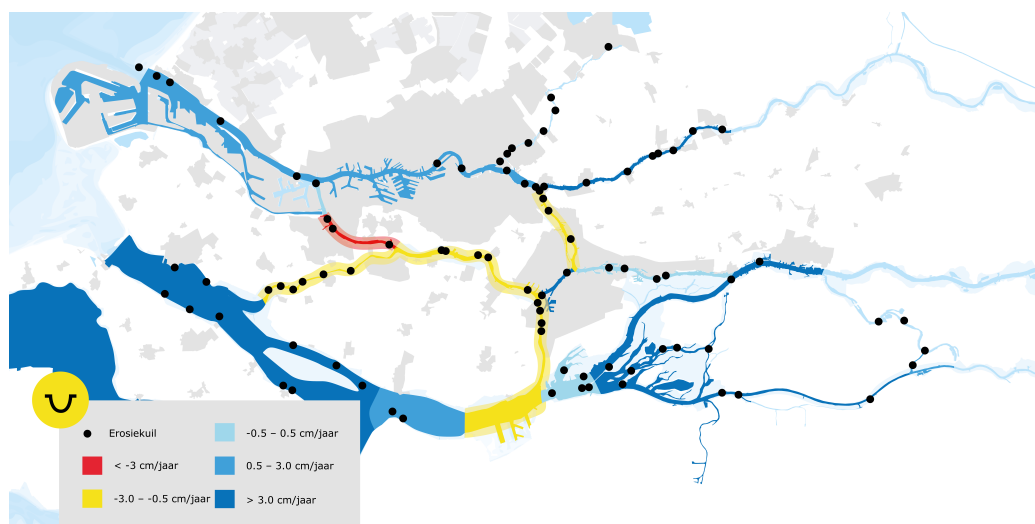
|      |   |     |
|------|---|-----|
| C.3  | Overview of the distributions of the variables of the post flow slide profile. . . . .  | 107 |
| C.4  | Determination of characteristic points of the example profile. . . . .  | 108 |
|      |   |     |
| D.1  | Overview of the river branches and subsoil scenario for the reference situation. . . . .  | 110 |
| D.2  | Probability of flow slide for median situation of the Spui and Oude Maas. . . . .   | 110 |
| D.3  | Characteristic points for the reference situation. . . . .  | 111 |
| D.4  | Probability flow slide for the wide profile, scenario 2: variation in width, scour depth=3.5m. . . . .  | 114 |
| D.5  | Probability flow slide for the narrow profile, scenario 3: variation in location for a scour hole with 25% of river width, depth=3.5m. . . . .                | 115 |
|      |   |     |
| E.1  | Relevant dike sections for the quickscan on the river Spui. . . . .   | 124 |
| E.2  | Sections on the right riverside with $P(L > L_{max})_{section} > 0.01$ . . . . .  | 125 |
| E.3  | Sections on the left riverside with $P(L > L_{max})_{section} > 0.01$ . . . . .   | 126 |
| E.4  | Check for riprap on right riverside of Spui. . . . .  | 127 |
| E.5  | Check for riprap on left riverside of Spui . . . . .  | 129 |
| E.6  | Time development $P(L > L_{max})_{section} > 0.01$ right side. . . . .  | 131 |
| E.7  | Time development $P(L > L_{max})_{section} > 0.01$ left side. . . . .   | 131 |
| E.8  | Relevant dike sections for the quickscan on the river Oude Maas, based on a smaller foreshore length than 300 m. . . . .                                      | 133 |
| E.9  | Sections on the Oude Maas right riverside with $P(L > L_{max})_{section} > 0.01$ . . . . .  | 133 |
| E.10 | Sections on the Oude Maas left riverside with $P(L > L_{max})_{section} > 0.01$ . . . . .   | 134 |
| E.11 | Relevant dike sections for the quickscan on the river Noord, based on a smaller foreshore length than 300 m. . . . .  | 135 |
| E.12 | Sections on the Noord right riverside with $P(L > L_{max})_{section} > 0.01$ . . . . .  | 136 |
|      |   |     |
| G.1  | Overview of development of the case scour hole. . . . .   | 138 |
| G.2  | Overview of growth of case scour hole. . . . .  | 138 |
| G.3  | Subsoil parameters for the subsoil scenarios for dike-segment 20-01. . . . .  | 140 |
| G.4  | Probability of the occurrence of a flow slide given the subsoil scenarios, for the dike near the scour hole. Unit = [1/yr] . . . . .                          | 142 |
| G.5  | Probability of the occurrence of a flow slide in 2023 for different scour hole development scenarios. Unit = [1/yr] . . . . .                                 | 142 |
| G.6  | Retgression lengths for the representative profiles. . . . .  | 143 |
| G.7  | Probability of the exceedance of the retrogression lengths for the 2018-geometry. Unit = [1/yr] . . . . .   | 144 |
| G.8  | Probability of occurrence of the retrogression states based on the 2018 profiles. Unit = [1/yr] . . . . .   | 144 |
| G.9  | Probability of occurrence of the retrogression states based on the lowest 5% scour hole prediction in 2023. Unit = [1/yr] . . . . .                           | 144 |
| G.10 | Probability of occurrence of the retrogression states based on the mean expected profile in 2023. Unit = [1/yr] . . . . .                                     | 144 |
| G.11 | Probability of occurrence of the retrogression states based on the largest 95% scour hole prediction in 2023. Unit = [1/yr] . . . . .                         | 144 |
| G.12 | Conditional probability of exceedance critical overtopping discharge. Unit = [1/yr] . . . . .   | 145 |
| G.13 | Probability of exceedance critical overtopping discharge( $q=5$ l/s/m). Unit = [1/yr] . . . . .   | 145 |
| G.14 | Probability of exceedance and return period critical overtopping discharge( $q=5$ l/s/m) for the case with and without dike repair after flow slide . . . . . | 146 |
| G.15 | Consequences of a flood with a breach near the scour hole for different water levels associated with their exceedance probability. . . . .                    | 147 |
| G.16 | Risk estimation for scour hole in 2018. . . . .   | 147 |
| G.17 | Risk estimation for scour hole in 2023. . . . .   | 147 |
| G.18 | Overview of historical surfaces of the scour hole below a certain level in [m <sup>2</sup> ]. . . . .   | 149 |
| G.19 | Overview of growth of Scour hole. . . . .   | 150 |
| G.20 | Calibration targets and tool result for surface area in [m <sup>2</sup> ]. . . . .  | 150 |
| G.21 | Calibration targets and tool result for deepest point and length. . . . .   | 151 |
| G.22 | Verification targets and tool result for surface area in [m <sup>2</sup> ]. . . . .   | 151 |
| G.23 | Verification targets and tool result for deepest point and length. . . . .  | 151 |

# Introduction

## 1.1. Background information

Over 100 scour holes are present in the Rhine-Meuse Delta, (hereafter referred to as RMD). The scour holes are located in the entire delta, as can be seen in figure 1.1. The presence of scour holes form a potential hazard for the stability of hydraulic structures, erosion of the protected cover layers of cables, pipelines and tunnels and the stability of dikes near the scour holes. (Platform Rivierkennis, 2018)

The RMD is a densely populated and intensively used area in the Netherlands. Therefore, the risk associated with the potential hazards and their direct consequences can be large. Many people will be affected by the consequences of potential hazards. Moreover, one of the world's largest ports is located in the delta. The Port of Rotterdam is an important factor for the Dutch economy. The potential hazards of scour holes can also lead to large indirect consequences for the Netherlands if the port activities are affected (Kuipers et al., 2018).



Source: Het verhaal van de Rijn-Maasmonding (Platform Rivierkennis, 2018)

Figure 1.1: Overview of the locations of the scour holes and the sedimentation/erosion rates in Rhine-Meuse Delta, including dredging activities. The scour holes are located in all branches.

The presence of scour holes in the RMD is known for years. The first scour holes were already identified in bed measurements data from 1967 (Koopmans, 2017). Other scour holes developed more recently. Some of the scour holes are stable and some have a more dynamic behaviour. These scour holes are growing in surface area and in depth. The largest scour holes are over 20,000 [m<sup>2</sup>] and have a bed level difference of over 7.0 [m] with the surrounding river bed. Besides, new scour holes can arise and grow in size rapidly.

A scour hole is a local deepening of the river bed. At locations with a lot of local erosion of the river bed, scour holes can develop. The heterogeneous subsoil together with the physical system behaviour of the RMD are the main reasons for the presence and dynamic behaviour of scour holes. During the formation of the delta, alternating layers of highly-erodible layers of sand and poorly-erodible layers of clay were deposited. The heterogeneity of the subsoil in combination with high flow velocity due to the tidal current leads to differences in local erosion and sedimentation rates along the river branches. If a poorly-erodible cover layer of a highly-erodible layer erodes entirely, the highly-erodible layer is exposed to the flow and erosion can occur. The high erodibility will lead to a rapid increase in depth and size, which results in a scour hole. However, the scour holes are present in both, branches with overall net erosion as well as branches with net sedimentation. (Huisman & Hoitink, 2017)

The presence of scour holes in the RMD is not a unique phenomenon. In more deltas over the world, the presence of scour holes with their potential hazards are known. Scour holes are for example identified in the Venice lagoon in Italy (Ferrarin et al., 2018), in the tidal creeks of South Carolina, USA (Kjerfve et al., 1979) and in the Bahia Blanca Estuary in Argentina (Ginsberg & Perillo, 1999). In these areas, the scour holes are mainly located at tidal channel junctions, while in the RMD the scour holes are also located in the middle of river branches, as can be seen in figure 1.1.

## 1.2. Problem statement

The locations of scour holes in the RMD are identified and the physical processes for the development are known. The presence and the dynamic behaviour of scour holes form a potential problem for the river management authority, Rijkswaterstaat. The scour holes may induce stability problems of hydraulic structures and flooding in the areas around scour holes. The growth in size and depth of scour holes is causing a further increase in the probability of hazards and the associated risk.

Measures like filling scour holes can be taken to slow down or stop the growth of the scour holes and reduce the risk. Rijkswaterstaat is currently executing a pilot study to get insight into the effectiveness of some measures (Sieben, 2018). But to assess the cost-efficiency and risk reduction associated with these measures, the most risk full locations must be identified. However, this insight in risk full scour holes is still lacking since a method for the quantification of the risk near scour holes is missing.

With a risk quantification method, the risk of scour holes can be quantified, which is preferred for four reasons. Firstly, it becomes clear what the expected damage due to the growth of scour holes is. Secondly, this value can be compared for different scour holes in order to prioritize the scour holes. Thirdly, an estimation can be given for the effectiveness and evaluation of a specific measure. Namely, the costs of implementing measures must be in proportion with the estimated reduction in expected damage. Finally, the cost-effectiveness of several measures can be compared if the risk is analysed in a quantitative way. In this way, the risk quantification can assist in the decision-making process by delivering information about the cost-effectiveness of measures.

## 1.3. Data-driven risk-based approach

In this research, the scour holes are analysed with a data-driven risk-based approach in order to assess and quantify the risk of scour holes in the RMD. The three main aspects of the risk assessment in this thesis are a quantification of the probability of occurrence of a hazard, the probability of scour hole growth and the consequences of a hazard. These aspects are determined with the usage of open data.

In general, a risk evaluation follows after a risk assessment, in order to determine the need for actions to deal, mitigate or compensate for risks.

### Risk assessment and risk management

Risk assessment is the structured process that identifies, quantifies and evaluates the risk for a system. In general, a risk assessment is performed for decision-makers or responsible parties to identify and evaluate the risk, such that they can decide on the acceptability of risk and the necessity of further treatment. The two basic elements of a risk assessment are the likelihood of a hazard and the consequences. (Bowles et al., 2013; Jonkman, 2007)

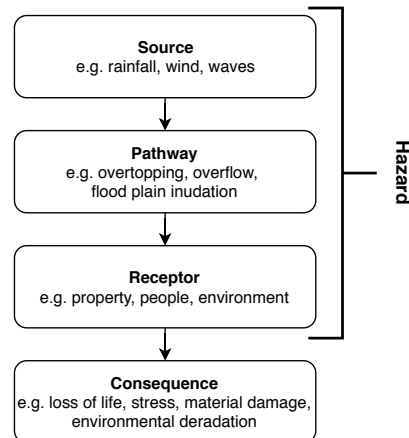
In the case, the risk exceeds an acceptable level, decision-makers or the responsible party can decide to undertake risk-reducing or mitigation measures. These measures are evaluated in the second part of the risk-based approach, the *'risk reduction and control'* part (Jonkman, 2007).

In this thesis, the quantification of risk is called risk assessment and the evaluation of risk-reducing or mitigation measures is called risk management.

### Hazards, consequences and risks

Key terms in a risk-based approach are hazards, consequences and risk. The term 'risk' is widely used in different disciplines, the meaning of risk is related to safety, economic, environmental and social issues. Since it is used in different disciplines, there can be a misunderstanding in the technical terminology associated with risk assessment. In some disciplines, the words 'hazard' and risk are treated as synonyms, while in the technical field there is a difference between these two terms (Gouldby et al., 2005).

The difference between 'hazards' and 'risk' can become clear from the Source-Pathway-Receptor-Consequence model. The model and examples of the different terms are given in figure 1.2 For a risk, there must be a hazard and consequences. A hazard consists of a source, pathway and receptor. A hazard will not lead to a harmful outcome if the consequences are small. A hazard is thus not necessarily a risk.



Source: Gouldby et al. (2005)

Figure 1.2: Source-Pathway-Receptor-Consequence model.

### Definition of hazard

In this research, the definition of hazard proposed by Gouldby et al. (2005) will be used:

*A physical event, phenomenon or human activity with the potential to result in harm. A hazard does not necessarily lead to harm.*

The occurrence of a hazard has a certain frequency or probability. The unit used for the frequency is the return period in years, while the unit for the probability of a hazard is occurrence per year [1/yr]. For large return periods (small frequencies), the probability of occurrence is approximately  $1/\text{return period}$  and the values are interchangeable (Jonkman, 2007).

### Definition of consequences

The following definition is used for consequences:

*An impact such as economic, social or environmental damage/improvement that may result from a flood. May be expressed quantitatively (e.g. monetary value), by category (e.g. High, Medium, Low) or descriptively (Gouldby et al., 2005).*

From this definition follows that the consequences of an event can be described quantitatively and qualitatively. This research focusses on risk quantification, therefore, the consequences are expressed quantitatively in monetary value. The unit used for consequences is Euro.

### Definition of risk

In the hydraulic engineering field, risk can be often related to flooding (Jonkman et al., 2018). The definition of flood risk adopted by the European Commission is:

*'Flood risk' means the combination of the probability of a flood event and of the potential adverse consequences for human health, the environment, cultural heritage and economic activity associated with a flood event.*

For flood risk management, the risk is often related to the expected value of the consequences. The following definition for risk is then used:

*Risk is the probability of a flood event multiplied by the consequences.*

This definition is derived from the general definition given by Kaplan & Garrick (1981)

*Risk is a set of scenarios ( $s_i$ ), each of which has a probability ( $p_i$ ) and a consequence ( $d_i$ ).*

There is no default unit for risk, the unit depends on the unit of the probability and the unit of the consequences. Often the consequences are expressed in monetary value and the unit for risk is then Euro per year. The expected value of the risk,  $E(D)$  can be expressed as Eq. 1.1 for a set of multiple discrete scenarios. The usage of the expected value of risk makes it possible to quantify and compare risk for different situations.

$$E(D) = \sum_{s_i=1}^n (p_i \times d_i) \quad (1.1)$$

### Probabilistic versus deterministic approach

A risk assessment is sometimes called the probabilistic approach (Jonkman, 2007). In the (civil) engineering field, two approaches are namely possible; the probabilistic (stochastic) approach and the deterministic approach. The deterministic approach is based on only one scenario for which all conditions are uniquely given. No uncertainties are taken into account in the deterministic approach. The probabilistic approach includes uncertainties and is based on the probability and consequences of all possible scenarios.

The chosen scenario in the deterministic approach is one of all possible scenarios, and thus also included in the probabilistic approach. The probabilistic approach provides a better basis for rational decision-making regarding risk since all scenarios and uncertainties are included as well in this approach.

### Scope of the research

This research focusses on a method for the risk quantification of scour holes in the RMD. However, the method may also be applied to scour holes that are located elsewhere. The method is elaborated for the risk associated with flooding in order to see which kind of steps are required for a risk assessment of scour holes. Other types of potential hazards are only shortly mentioned, but are not included in the risk assessment method in this thesis. However, the flood risk assessment method of scour holes can be used as an example for the risk quantification of other types of hazards near scour holes or along river branches in general.

## 1.4. Objective

This research has two objectives, both are related to the risk of scour holes. The first objective of the research is to obtain insight into the risk of scour holes in the RMD. The second objective is to evaluate measures for reducing the risk of the scour holes in the RMD.

These two objectives are covering an entire risk analysis, as described by Jonkman (2007) and Rosqvist & Tuominen (2004). The first objective is related to risk assessment of scour holes, while the second objective contains risk evaluation and the 'risk reduction and control' element, which is the risk management part.

The main research question for this thesis is:

*How to assess and reduce flood risk near scour holes in the Rhine-Meuse Delta?*

Based on the first objective the following sub-questions are formulated:

1. How can the development of scour holes be predicted and which processes and conditions play a role in the development of scour holes?
2. How to quantify the hazards and consequences of scour holes?
3. What is the impact of scour holes in the Rhine-Meuse Delta on flood risk and which scour holes form currently a threat?
4. What are the most sensitive aspects for the flood risk assessment near scour holes?

The following sub-question is related to the second objective:

5. What is the effect and economic feasibility of risk-reducing measures?

### 1.5. Outline of the report

This report follows the phases of the risk management framework proposed by Bowles et al. (2013) for the risk assessment of reservoirs in the UK. The risk management process in this research is applied to scour holes in the RMD. Small adaptations have been made to suit the framework for assessing risk of scour holes. The outline of the report and phases of the research, with associated steps, are indicated in figure 1.3.

The report consists of 7 chapters. Chapter 2, covers the *preparation phases* for the risk assessment. An introduction is given in the system of the RMD, the hazard related to scour holes and the policy of Rijkswaterstaat (the river management authority) with respect to the scour holes. The *identification phase* is presented in chapter 3 and chapter 4. In these chapters, the required methods for the risk assessment are given. In chapter 3 the method to predict the scour hole development and in chapter 4 the method to determine the flood risk. Both chapters are treated in a general way, such that the methods are applicable to individual scour holes. The methods are subsequently applied to one case scour hole in chapter 5. For the case scour hole, the risk is assessed in the *analysis phase*. Subsequently, the risk management elements are applied in the *evaluation phase* in chapter 6. For the case scour hole, risk mitigation measures are evaluated. Finally, the *conclusions, discussion and recommendations* are presented in chapter 7.

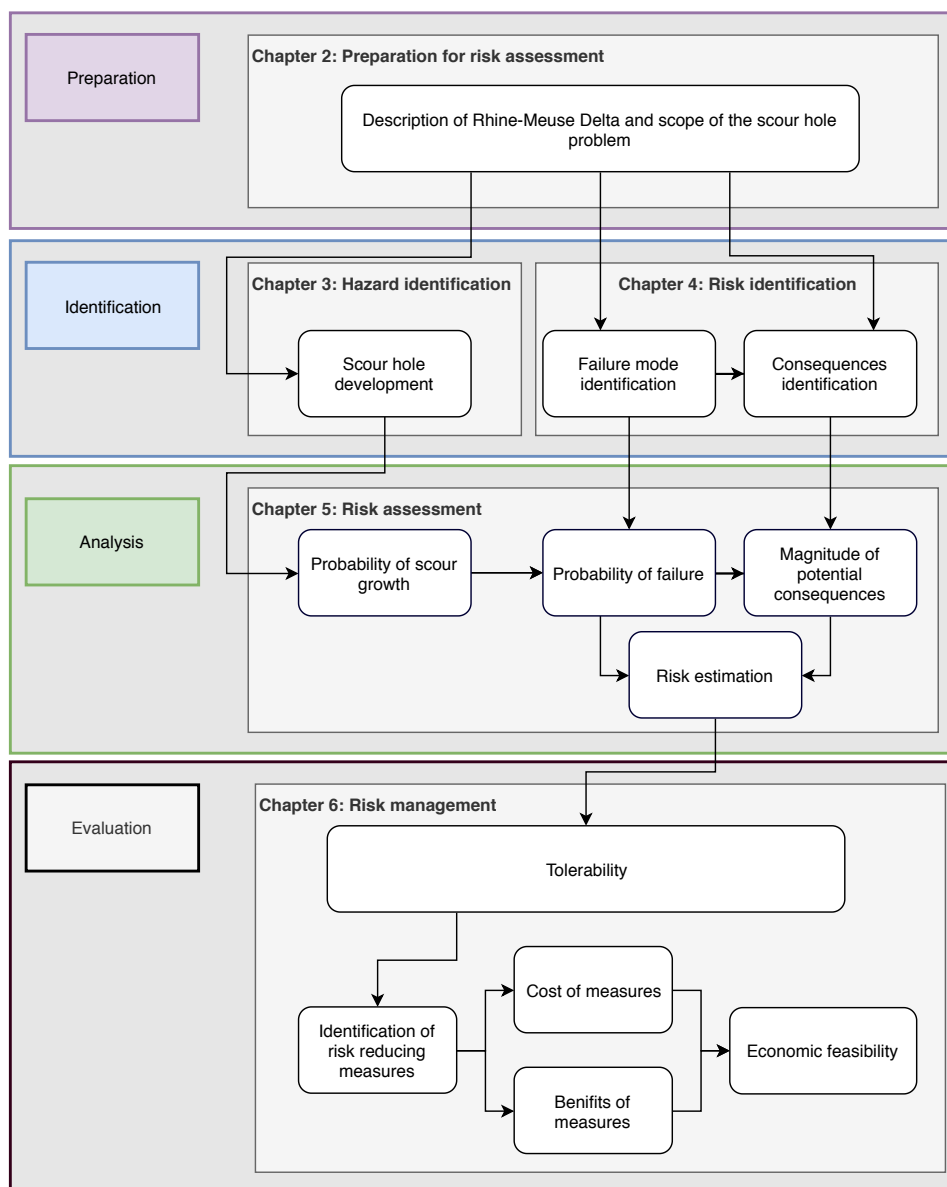


Figure 1.3: Framework for research, based on the framework of Bowles et al. (2013).

*(This page is intentionally left blank)*

## Preparation for risk assessment

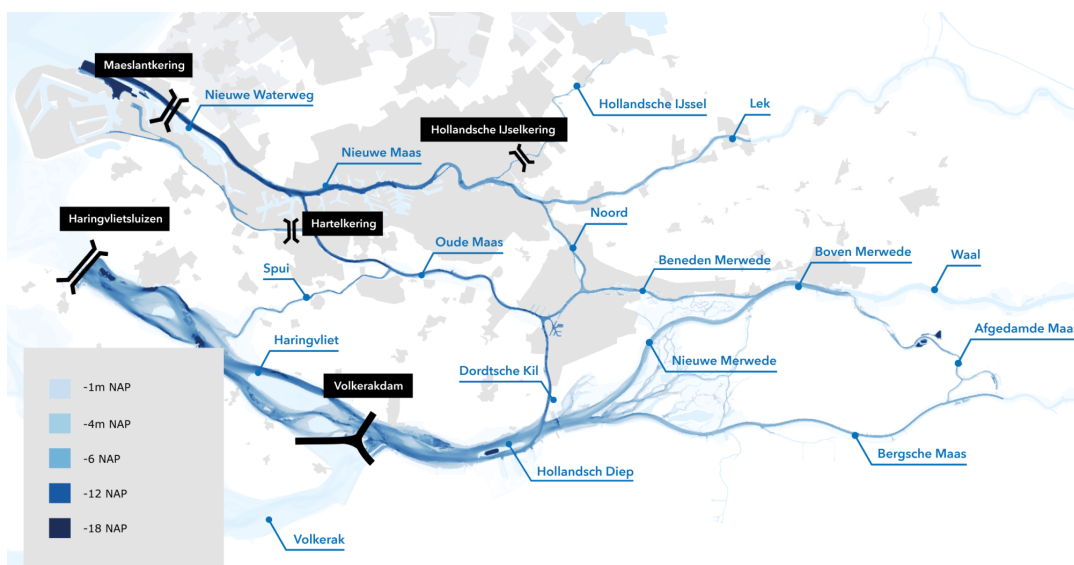
In order to do a risk assessment, the scope of the problem must be clear. Which is described in this chapter. First, an introduction is given about the RMD system, followed by a description of the scour hole problem in the delta. Finally, the current management strategies for the scour hole problem are explained.

### 2.1. Rhine-Meuse Delta system

The part of the Dutch river system with tidal influence is called the RMD. The Port of Rotterdam with the Nieuwe Waterweg, Europort and the Maasvlakte are located in the northern parts of the delta. The Haringvliet basin is the southern area boundary. The system area includes the part of Lek downstream of the weir of Hagestein and the part of the Meuse downstream of the weir of Lith (Platform Rivierkennis, 2018). An overview of all the river branches in the RMD is shown in figure 2.1.

The RMD can be separated into four subsystems (Huisman & Hoitink, 2017; Platform Rivierkennis, 2018):

1. The northern branches (Nieuwe Waterweg, Nieuwe Maas and Hollandsche IJssel).
2. The eastern branches (Lek, Boven Merwede, Beneden Merwede and Nieuwe Merwede).
3. The southern branches (Haringvliet and Hollandsch Diep).
4. The connecting branches (Spui, Oude Maas, Noord and Dordtsche Kil).



Source: Het verhaal van de Rijn-Maasmonding (Platform Rivierkennis, 2018)

Figure 2.1: The Rhine-Meuse Delta with river names, Delta Works and bed level of the branches.

The surrounding area of the RMD has the highest population density in the Netherlands and has an important contribution to the Dutch economy. Therefore, flood safety is an important issue in the delta. Flood levels in the delta occur during periods of high river discharge, extreme weather conditions and high tide.

### **2.1.1. Formation of the delta**

The formation of the RMD started at the end of the Pleistocene, the last glacial period about 11,000 years ago. First, a poorly-erodible clay layer was formed. This clay layer is called the layer of Wijchen and spreads out over a large part of the current delta (Koopmans, 2017). At the location of former channels, the layer of Wijchen could not be formed. At these locations, the layer is interrupted by the so-called channel belts, which are highly-erodible sand layers (Hijma, 2009).

Due to the sea level rise around 8,500 years ago, the delta became a sedimentation area and sediment settled down on top of the layer of Wijchen. Both, sediment from river and sea, settled down on top of the layer of Wijchen. Which resulted in the formation of alternating layers of sand, silt and clay. Moreover, under the influence of changing wave climate, tidal dynamics and decelerating sea level rise also peat layers started to form in the delta (Huisman & Hoitink, 2017).

The primarily formed layers are covered with a thick clay layer, which was formed about 2,500 years ago. The amount of clay and silt in the river Rhine and Meuse significantly increased due to human impacts, like deforestation for agriculture. Settling of this sediment during river floods formed this clay layer. River avulsion occurred more frequently and the Rhine mouth changed its course from Leiden to its current location. This resulted in a change of river discharges and sediment load. Consequently, the amount of settled sediment changed.

The river avulsion together with the changes in the settling of river and marine sediments resulted in a very heterogeneous lithology in the RMD. The several layers have a difference in thickness and erodibility. Besides, there is a strong local variation in the presence and thickness of layers in the subsoil. The heterogeneous subsoil has a large influence on river morphodynamics (Sloff et al., 2014).

### **2.1.2. Human interventions in the delta**

For decades, people have been trying to manage the river branches in the RMD with human interventions. The human influence on the delta started with the development of polders and dikes around 1,000 years ago. The first interventions were made to protect the land against flooding. In the last few hundred years, shipping became more important but at the same time, net sedimentation occurred in the rivers. Since 1850 the amount of measures to guarantee navigation depths has been increased rapidly (Vellinga et al., 2014). River training works were created to narrow and shorten the rivers. Moreover, human started to digging the Nieuwe Waterweg in 1872. The Nieuwe Waterweg improved the accessibility of the Port of Rotterdam for seagoing vessels.

After the flood in 1953, the Haringvliet barrier, the Volkerakdam and the Beerdam were constructed as a part of the Delta Works. The Haringvliet barrier created a blockage of the direct tidal influence in the Haringvliet and Hollandsch Diep, which transformed both into freshwater basins. The discharge and water levels in the several branches in the RMD changed after the closure of the Haringvliet. The tide can only enter and leave the delta through the Nieuwe Waterweg. This resulted in large flow velocities in the connecting branches between the Nieuwe Waterweg and the Haringvliet. The larger flow velocities resulted in structural erosion of the connecting branches up to a bed level degradation of 3.0 cm/year in the Oude Maas (Platform Rivierkennis, 2018).

### **2.1.3. Dynamics of the delta**

The combination of sea level, the tidal currents and river discharge results in characteristic dynamics in the delta. The hydraulic conditions (water levels, currents and flow velocities) affect the salt intrusions and the morphodynamics in the RMD.

#### **Hydraulics**

The tide influences the water levels in the entire RMD. However, the tidal ranges are varying over the delta. The largest mean tidal range of 1.75 [m] can be observed near Hoek van Holland. Along the Nieuwe Waterweg and the Nieuwe Maas, there is almost no reduction in the tidal range. Therefore, similar tidal ranges are

observed near Rotterdam. Due to the Haringvliet barrier, the tidal range in the Haringvliet has a maximum of only 0.5 [m]. In the connecting branches, the ranges are about 1.0 [m].

The river discharges enter the RMD through the Waal (70%), the Lek(18%) and the Meuse(12%). The water leaves the delta through the Nieuwe Waterweg and the Haringvlietsluices. Approximately 75% of the yearly river discharge flows through the Nieuwe Waterweg. (Platform Rivierkennis, 2018)

The combination of river discharge and tidal currents determines the flow velocities in the delta. Since the closure of the Haringvliet, two main flow direction can be distinguished in the connecting branches. In both direction the flow velocities are approximately equal. During mean river discharges conditions, the largest flow velocities are observed in the Nieuwe Waterweg (1.2-1.5 m/s) and the Oude Maas (1.0-1.2 m/s). (Platform Rivierkennis, 2018)

### Salt intrusion

The saltwater intrusion is a problem for mainly the northern river branches in the delta. A salt wedge travels back and forth with the tidal excursion in the Nieuwe Waterweg. The freshwater of the river discharge acts as a counter-pressure preventing the penetration of saltwater into the delta. During lower river discharge in the Nieuwe Waterweg the salt wedge travels further upstream and even up to the Lek and the Hollandsche IJssel, Spui and Lek.

### Morphodynamics

The distribution of the sedimentation within the delta is not equal (Huismans & Hoitink, 2017). By nature, the RMD is a sedimentation area. The tidal wave imports sediment from the North Sea and rivers Waal, Rhine and Lek import alluvial sediments. The erosion/sedimentation trends per river branch can be seen in figure 1.1 on page 1. The following trends can be observed:

- In the northern and eastern branches subsystem natural sedimentation occurs. However, in these branches the amount of dredging exceeds the accretion, which results in a bed degradation of 0.5 – 3.0 [cm/year].
- In the subsystem of the connecting branches erosion occurs. The erosion of the branches increased after the closure of the Haringvliet. The larger tidal wave in these branches generates high flow velocities which result in the erosion of the branches. The erosion rate is 0.5 – 3.0 [cm/year] for most of the connecting branches. In the western part of the Oude Maas, the erosion rate is even larger than 3.0 [cm/year].
- In the southern branches subsystem sedimentation occurs as well. The deposition is only partly compensated by dredging. This results in a net deposition of over 3.0 [cm/year] in the Haringvliet.

Over 100 scour holes are located in the RMD. The scour holes can be identified in all branches. The scour holes are not only located in the connecting eroding branches, but also in the branches with overall sedimentation. The scour holes in the connecting branches rapidly grew after the closure of the Haringvliet, due to the earlier mentioned increase of the flow velocities in these branches (Koopmans, 2017).

### 2.1.4. River functions affected by dynamics

The dynamics, mentioned in section 2.1.3, affect the following river functions in the RMD:

#### Navigation

In order to make inland navigation possible, the fairway of the river branches must be depth enough. During periods with low river discharge, there is a reduced water depth for navigation. The vessels must sail with a reduced depth and less cargo can be shipped.

For each river branch, a Nautical Guaranteed Depth (NGD) is defined based on water level statistics and the depth of inland vessels. If the bed level exceeds the NGD, dredging activities are required in order to keep the fairway depth enough. In the RMD, river branches with sedimentation are dredged in order to maintain the NGD. (Platform Rivierkennis, 2018)

### **Flood safety**

Flood safety, for which the safety requirements are strictly defined in the Dutch water Act, is an important issue in the RMD. The hydraulics and the morphodynamics influence the flood safety in the delta. The hydraulics determines the water levels, while the morphodynamics can affect the stability of the flood defences.

The flood defences must be stable and high enough to provide protection against flooding. Next to the regular flood defences (dikes, dunes and dams), there are also three storm surge barriers in the RMD: Maeslantkering, Hollandsche IJsselkering and the Hartelkering. These movable flood defences can be temporarily closed during high water levels (Platform Rivierkennis, 2018).

According to the Dutch Water Act, the safety of primary flood defences must be assessed every 12 years. The safety assessment is described in the Wettelijk Beoordelingsinstrumentarium (hereafter referred to as WBI). The primary flood defence must be checked on several aspects during the safety assessment (Rijkswaterstaat, 2017). Mitigation measures are required if a flood defence does not meet the safety requirements (Jonkman et al., 2018).

### **Drinking water**

A problem with drinking water can occur if there is saline water near the drinking water extraction points. The drinking water extraction points are located in the Spui, Lek and Hollandsche IJssel. In order to prevent the intrusion of saltwater to these points, the bed level gradually increases in the Nieuwe Waterweg (in Dutch known as 'Trapjeslijn'). However, during periods with low river discharge the saltwater wedge can travel up to these extraction locations and there are potential problems for freshwater supply in the RMD (Huismans & Hoitink, 2017).

### **2.1.5. Impact of climate change**

Long-term changes in river discharge, storm frequencies and sea level rise are the consequences of climate changes. This will also impact the morphology in the RMD (Huismans & Hoitink, 2017). Sea level rise will lead to higher mean water levels. Moreover, an increase of the tidal range with about 10 cm/century. The increase in tidal range will result in larger volumes of the incoming tide in the delta.

The following effects are the main direct effects of climate change and sea level rise for the morphology in the RMD:

- In theory, higher mean water levels will lead to lower flow velocities which result in sedimentation and an increase of bed levels. In the eastern branches of the RMD, it is expected that the rising bed level will lead to reduced water depth during periods with low river discharge.
- If the sedimentation of river branches cannot follow the sea level rise, a larger tidal inflow volume is expected. The larger tidal volume will increase the flow velocities in the connecting branches. Which will result in a more dynamic behaviour of the riverbed in the connecting branches (Haasnoot et al., 2018).
- The increased variability of precipitation will change the river discharges and will lead to a small increase in variability of the bed level in the Boven Merwede, Beneden Merwede and Nieuwe Merwede (Kind et al., 2019).

In order to prevent problems due to these direct effects, more river maintenance activities are necessary. With activities like continuously dredging in some river branches and dumping of sediment in other branches, the current situation can be retained (Kind et al., 2019).

Climate change will also have an impact on the river functions. A larger tidal volume will, for example, lead to more salt intrusion. The increased water levels will be an issue for flood safety. In the future, new human interventions are possibly required to deal with the effects of sea level rise and climate change. In the past, however, the effects of human interventions for flood safety have led to much larger morphological river changes than climate change effects. New human interventions like new sluices or closure works will change the system behaviour of the RMD completely. These effects are difficult to predict. But it can be assumed that it will have a much larger effect on the river morphology than the above-mentioned direct effects themselves (Kind et al., 2019).

## 2.2. Scour hole problems in the Rhine-Meuse Delta

### 2.2.1. Locations of scour holes

In the entire RMD scour holes are located and they can be found in all four subsystems of the delta. Deltares analysed the presence of the scour holes in the RMD, based on the bathymetry of 2014 (Huismans & van Duin, 2016). In figure 1.1 on page 1, the locations of the scour holes are indicated and in table 2.1, the number of scour holes per river branch for the four subsystems is shown. Some scour hole are located close to each other in so-called clusters. Due to these clusters, the number of locations of scour holes differs from the number of scour holes per river branch. As can be seen in table 2.1, the number of scour holes per subsystem is more or less equal (Huismans & van Duin, 2016).

| Northern branches         | Scour holes | Clusters | Southern branches      | Scour holes | Clusters |
|---------------------------|-------------|----------|------------------------|-------------|----------|
| Nieuwe Waterweg (20km)    | 12          | 5        | Haringvliet (28km)     | 10          | 10       |
| Nieuwe Maas (24km)        | 5           | 3        | Hollandsch Diep (20km) | 12          | 5        |
| Hollandsche IJssel (46km) | 10          | 8        | Biesbosch              | 5           | 5        |
|                           |             |          | Amer (12 km)           | 5           | 2        |
| Total                     | 27          | 16       | Total                  | 32          | 22       |

| Connecting branches | Scour holes | Clusters | Eastern branches       | Scour holes | Clusters |
|---------------------|-------------|----------|------------------------|-------------|----------|
| Spui (16km)         | 13          | 6        | Lek (62km)             | 12          | 8        |
| Oude Maas (30km)    | 15          | 9        | Boven Merwede (9km)    | 4           | 4        |
| Noord (9km)         | 6           | 4        | Beneden Merwede (15km) | 2           | 1        |
| Dordtsche Kil (9km) | 5           | 4        | Nieuwe Merwede (21km)  | 6           | 3        |
|                     |             |          | Bergsche Maas (25km)   | 3           | 3        |
|                     |             |          | Afgedamde Maas (17km)  | 4           | 4        |
| Total               | 39          | 23       | Total                  | 31          | 23       |

Source: Huismans & van Duin (2016)

Table 2.1: Overview of river branches with their length per subsystem together with the number and clusters of scour holes per branch.

There is a large variation in size and depth between the scour holes. For example, smaller scour holes have a surface area of 1,000 [m<sup>2</sup>] and a depth of 1.0 [m] with respect to the scour hole edge. The volume of smaller scour holes is around 500 [m<sup>3</sup>], while larger scour holes are over 20,000 [m<sup>3</sup>] and have a bed level difference of 7.0 [m] relative to the surrounding bed level. The larger scour holes are mainly located in the connecting branches. (Huismans & van Duin, 2016)

### 2.2.2. Types of scour holes in the Rhine-Meuse Delta

In the RMD, three different types of scour holes are presented. These types originate due to different hydrodynamic or geological conditions, like:

1. the presence of hydraulic structures or a local river geometry change;
2. an abrupt change in geological conditions;
3. the presence of old channel belts.

In general, scour holes are often located close to hydraulic structures or at locations where the geometry locally abruptly changes. The scour holes of this first type are formed due to the local change in hydrodynamic conditions. The shear force increases behind the structure due to an increase in turbulence and flow velocity. The increased shear force leads to larger erosion rates and finally to the formation of a scour hole (Hoffmans & Verheij, 1997).

The second type of scour hole originated due to an abrupt change in geological conditions instead of the change in hydrodynamic conditions. Due to the earlier mentioned river avulsion and changes in the settling of river and marine sediment, the subsoil of the RMD is very heterogeneous. The current riverbed is located close to the clay layer of Wijchen (Huismans & Hoitink, 2017). However, the heterogeneity of the subsoil is not constant over the delta. At some locations, the clay layer is thinner. Due to continuous erosion in the connecting river branches, the entire clay layer is eroded at some locations. At these locations, the bed level consists of high erodible sand. The critical flow velocity for this sediment is lower than in the surrounding

area, which results in strong local erosion. As indicated in figure 2.2 a scour hole can develop. Depending on the surrounding subsoil the hole can grow significantly in surface area and depth (Sloff et al., 2014).

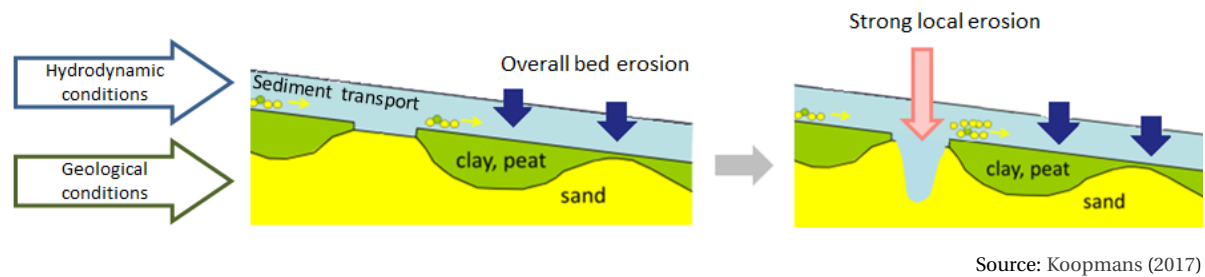


Figure 2.2: Scour hole depth development in heterogeneous subsoil.

The third type of scour hole developed at the location of old channel belts embedded in the subsoil. When the protecting layer above the old channel belt completely erodes, a scour hole can be formed in the old belt. The size of the scour hole is limited by the size of the old channel belt (Huisman & van Duin, 2016). This type of scour holes also originated due to local variation in the subsoil.

### 2.2.3. Influence of human interventions

In order to qualify the effect of the recent human interventions on the scour hole development, Koopmans (2017) and Huisman & van Duin (2016) made a reconstruction of scour hole development in time. They expected that the closure of the Haringvliet had led to the start of scour hole forming in the connecting branches. However, most of the scour holes in the Oude Maas are identifiable on bathymetry drawings from before the closure.

In the Dordtsche Kil, all scour holes developed in the period between 1970-1976. It is possible that the formation is caused by the closure of the Haringvliet. However, since no new scour holes developed in the Oude Maas after the closure, the development of scour holes in the Dordtsche Kil is probably more related to the deepening of the riverbed. During the dredging activities, the protected poorly-erodible layer could have been removed and the older channel belts could be exposed to the flow (Huisman & Hoitink, 2017).

Some scour holes show a strong development since the closure of the Haringvliet. Although the closure of the Haringvliet did not cause new scour holes, it potentially still enhanced the growth of the scour holes in the connecting branches (Huisman & Hoitink, 2017).

### 2.2.4. Potential hazards of scour holes

The presence of a scour hole in a river branch is not necessarily a problem. If a scour hole is located in the middle of a wide river far from any structure and from both riversides, there are no direct threats and such a scour hole is not a real problem. But if a scour hole is located near, or is growing towards a flood defence or any hydraulic structure (bridge, tunnel, cable & pipelines), there are potential hazards and the presence of a scour hole can lead to serious problems.

For Rijkswaterstaat, the river management authority of the RMD, three hazards due to scour holes are relevant. These hazards are 1) the stability of hydraulic structures; 2) the stability of flood defences and 3) the coverage of cables and pipelines. (Platform Rivierkennis, 2018)

The first potential hazard of scour holes is the stability of hydraulic structures. The presence of hydraulic structures, like bridge piers, groynes and tunnels can lead to the formation of a scour hole. The scour hole can subsequently be a hazard for the stability of the hydraulic structure itself.

The second potential hazard of scour holes is the stability of riverbanks and dikes. The presence of a scour hole increases the probability of occurrence of flow slides (in Dutch: zettingsvloeiingen or dijkvallen) due to the steep slopes and large depths (Sloff et al., 2014; Stouthamer & de Haas, 2011). During a flow slide, the foreshore turns into a sand-water mixture and slides (partly) away. The reduced foreshore length reduces the stability and reliability of dikes. In this way, scour holes influence flood risk if they are located close to riverbanks.

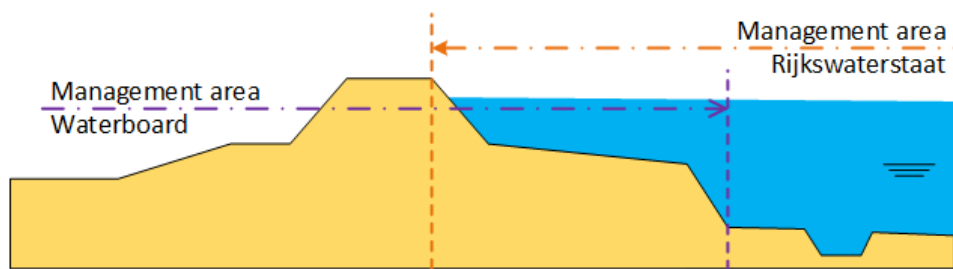


Figure 2.3: Management area for Rijkswaterstaat (river manager) and waterboards (dike managers).

The erosion of coverage of cables and pipelines is the third potential hazard. In the RMD, a lot of cables and pipelines are crossing the river branches. For example, liquids and gasses are transported through pipelines for the industrial activities in the port. The cables and pipelines are placed in the river bed and subsequently covered. Due to erosion or migration of scour holes, cables and pipelines can become unprotected. An unprotected cable or pipeline can easily be damaged by vessels. Therefore, the protection of unprotected cables and pipelines must be recovered or the cables and pipelines must be replaced. (Driessen et al., 2018).

### 2.2.5. Prioritization scour holes for flow slide

The hazard flow slide can have a large impact. A flow slide can result in a flood with associated damages and fatalities. Insight in the risk of flow slides is important for Rijkswaterstaat since a standardised risk assessment for this hazard can be applicable in large parts of the RMD.

The connecting branches subsystem has the largest probability of occurrence for flow slides, since in this subsystem the largest and deepest scour holes are located (Huisman & van Duin, 2016). In this subsystem, river branches erode, which can trigger the occurrence of flow slides, as will be explained in section 4.1. Moreover, due to the relatively small length of the foreshore in the connecting branches, there is a large probability that if a flow slide happens the flood defence will be affected.

Flood safety is a shared responsibility of Rijkswaterstaat and the waterboards, the dike managers. The waterboards are responsible for the maintenance and safety of dikes. While Rijkswaterstaat is responsible for a stable river bed, which is required for the safety of dikes. (Driessen et al., 2018)

For flow slide as a potential hazard of scour holes and in general for flood risk management, Rijkswaterstaat co-operates with the waterboards. There is a certain overlap in the management areas of the waterboards and Rijkswaterstaat. As indicated in figure 2.3, Rijkswaterstaat is responsible for the outer part of the dike up to the outer dike crest. While a waterboard is responsible for the area started from the dike toe.

## 2.3. Current management strategies

The core tasks for Rijkswaterstaat, as river management authority, are flood risk management, adequate water supplies, clean and healthy water, smooth and safe transport by water and a sustainable living environment (Rijkswaterstaat, 2015). The scour holes affect the flood risk management task.

The current policy with respect to scour holes is a calamity-driven management strategy. Therefore, there is only little attention to the presence of scour holes. Only if it has been detected that a situation is unsafe, some (emergency) measures are undertaken. In the past few years, the scour holes received more attention within the organization of Rijkswaterstaat because a couple of unsafe situations occurred nearby scour holes.

Rijkswaterstaat is analysing the effects of proactive management strategies, with continuous partly filling of scour holes. In order to increase the knowledge about filling aspects of scour holes, Rijkswaterstaat is executing a pilot study in the western part of the Oude Maas. In addition, Royal HaskoningDHV analysed different management strategies for the erosion and scour hole problems in the connecting branches, in order to analyse the costs of a proactive management strategy (Schuurman, 2018).

Both, the pilot study and the results of the management strategy analysis are shortly described in this section.

### 2.3.1. Pilot study

Rijkswaterstaat is currently executing a pilot study about nourishments in the Oude Maas. The sediment for the nourishment came available during the deepening of the Nieuwe Waterweg. Instead of selling the sediment or dumping it into the North Sea, Rijkswaterstaat used this 'free available' sediment for a pilot study about sediment nourishment in scour holes and eroding branches (Buschman et al., 2015). The nourishments for the pilot were executed at three locations in the Oude Maas in July 2018. The locations are indicated in figure 2.4.

The objectives of the pilot study are to learn in which way nourishments can contribute to 1) the stability of the bed level in eroding branches, and 2) the stability of the edges and/or bottom of scour holes. With the pilot study, Rijkswaterstaat will learn about the effective period and side effects of nourishments in eroding river branches.

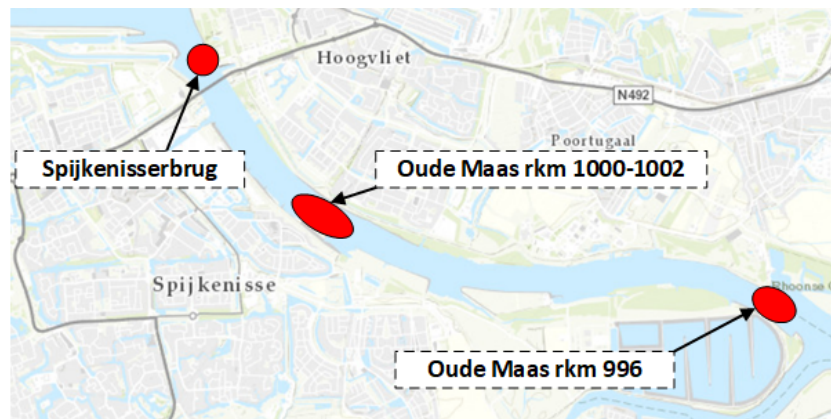


Figure 2.4: Locations of the pilot study in the Oude Maas.

#### Oude Maas 1000-1002

A layer of about 1.0 [m] is supplied on the relatively flat bottom between river km 1000-1002 in the Oude Maas. The average erosion rate for this river branch is 0.12 [m/year]. The nourishment restored the bed level to the level of about 8-10 years ago. Under the influence of the flow, the nourishment will be spread out over the river branch. Every month for the first two years after the nourishment, the bed level development will be measured, in order to monitor the spread out of the sediment (Sieben, 2018).

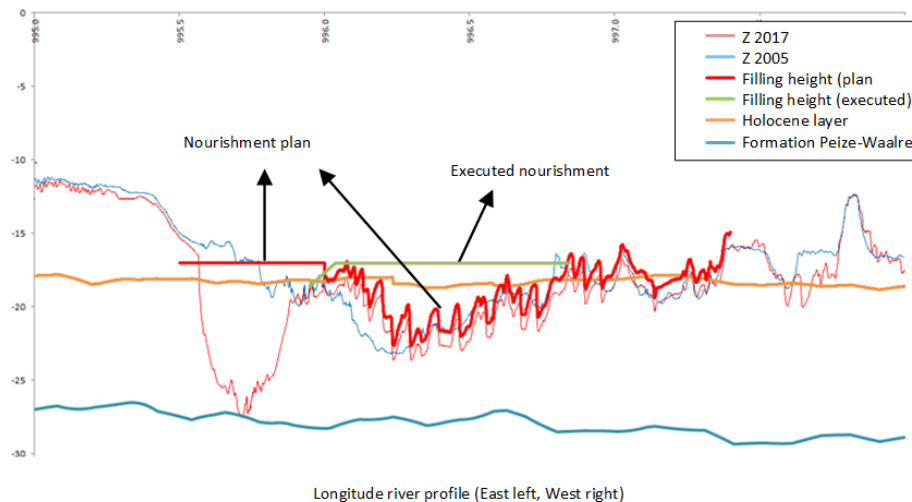
#### Oude Maas 996

For the second nourishment, sediment has been supplied in the scour hole located near river km 996, which is close to the river bifurcation with the river Spui. This scour hole is not stable. The scour hole has a growth rate of about 17 [m/year] in the upstream direction and 1.0 [m/year] towards the riversides. Before the nourishment, the east part of the scour hole was the deepest part of the scour hole, the bed level was lower than -25 [m + NAP]. The plan was to fill this deepest part up to -17 [m + NAP] and a layer of about 1.0 [m] in the remaining area of the scour hole. During the execution of the nourishments a mistake was made, the deepest part has not been filled. While, the remaining area has been filled up to -17 [m + NAP]. The nourishment plan and execution is schematically indicated in figure 2.5.

The bed level changes for this nourishment will also be monitored every two months in the first two years. Rijkswaterstaat will analyse the bed level changes in the scour hole and the effect of the nourishment on the stability of the scour hole edges and slopes. Possibly, the nourishment reduces the migration rate of the scour hole. (Sieben, 2018)

#### Spijkennisserbrug

The scour hole near the Spijkennisserbrug was a hazard for the stability of the Spijkennisserbrug and for the stability of the dike due to a large probability of occurrence of a flow slide. Rijkswaterstaat co-operates with the Waterboard Hollandse Delta, the dike manager, for the filling of this scour hole. First, the scour hole, with an initial bed level of -23 [m + NAP], has been filled up to -16 [m + NAP] and subsequently covered with 16 fascine mattresses with a geotextile (in Dutch: zinkstukken) with on top a layer of riprap (in Dutch: Stortsteen).



Source: Own creation based on Laurens Baars

Figure 2.5: Overview of the pilot nourishment plan and execution for the scour hole located at rkm 996 in the Oude Maas.

With this cover, the scour hole should be stable and the hazards for the stability of the Spijkenisserbrug and for the stability of the dike should be mitigated. The stability of the cover layer will be monitored during the regular yearly observations. (Ruckert & Sieben, 2019)

### 2.3.2. Scenario analysis

Several river management strategies to control the erosion trend and the scour holes problem are analysed in a scenario analysis performed by Schuurman (2018). Strategies for the long-term river management are compared with the current management strategy for the connecting river branches Oude Maas, Noord, Dordtsche Kil and Spui.

The base of the management scenarios is that sediment, which is dredged in the river branches with sedimentation, will be used as nourishments in the river branches with erosion.

The following scenarios are taken into account in the analysis.

- Scenario 0: Placing only bank protection where needed.
- Scenario A: Filling of scour holes once and subsequently placing riprap on top
- Scenario B: Yearly filling of scour holes.
- Scenario C: Placing of riprap over the entire river branches and filling of scour holes.
- Scenario D: Nourishments in eroding river branches, filling of scour holes once and placing riprap on top.
- Scenario E: Nourishments in eroding river branches and yearly filling of scour holes.

These scenarios are compared on costs and river functions. Per scenario, the total volumes of sediment and riprap is determined to maintain the river branches and mitigate the hazard of unstable riverbanks in the next 20 and 50 years. With unit prices, the total costs per scenario are determined for the period of 20 and 50 years.

In figure 2.6, the total costs are presented for the six scenarios. A distinction is made for the case that all sediment is free and the case that a part of the sediment must be bought. The volume of yearly dredged sediment is not enough to fill all scour holes at once in the first year. For the case with free sediment, both the sediment from the river branches and the extra required sediment are free. The initial costs and the total maintenance costs for a period of 20 and 50 years are shown in the figure. As can be seen, scenario C is by far the most expensive scenario. In this scenario, riprap is deposited in the entire river branches. This scenario is thus not realistic. Scenario 0, the current strategy, is not the cheapest management strategy for the maintenance of the connecting branches.

The conclusion of the analysis is that filling of scour holes is cheaper than the current strategy on the long-term. Due to scour hole growth and continuation of the erosion trend in the connecting river branches, more riverbank protection is needed in the future. In the end, the costs of this protection will be larger than the costs associated with (yearly) filling of scour holes.

|                                     | <b>0-scenario</b> | <b>Scenario A</b> | <b>Scenario B</b> | <b>Scenario C</b> | <b>Scenario D</b> | <b>Scenario E</b> |
|-------------------------------------|-------------------|-------------------|-------------------|-------------------|-------------------|-------------------|
| Once in year 0:                     | €112.2            | €80.8             | €46.4             | €1,082.0          | €85.3             | €50.9             |
| Once in year without sand purchase: | €112.2            | €77.6             | €36.3             | €1,076.6          | €79.2             | €37.8             |
| Yearly costs:                       | €0.0              | €0.0              | €1.1              | €0.0              | €0.7              | €1.4              |
| Total costs over next 20 years:     | €159.7            | €90.2             | €76.8             | €1,082.0          | €109.6            | €87.5             |
| Total costs over next 50 years:     | €299.2            | €199.2            | €217.4            | €1,082.0          | €136.2            | €132.6            |

Source: Scenario analysis (Schuurman, 2018)

Figure 2.6: Overview of the total costs of the six scenarios (in million euro), the initial costs are presented, with a distinction between 'free' and 'partly bought' sediment. For the maintenance costs over 20 and 50 years, it is assumed that all sediment is free.

# 3

## Hazard identification: scour hole development

Growth of a scour hole may lead to an increased probability of flooding and enlarged the risk in the near future. To assess the scour hole development, this chapter elaborates shortly on scour hole development processes. Subsequently, a data-driven method for the prediction of scour hole development based on purely historical bed level data is presented.

### 3.1. Scour hole development processes

Depending on the flow conditions around a scour hole and the interaction with sediment in the scour hole, the scour hole can grow in size or depth. The local hydrodynamic (flow velocities and turbulence) and geological conditions (composition of the subsoil) affect the scour hole development. The hydrodynamic conditions are the forcing conditions for erosion and the scour hole development, while the geological conditions determine the resistance against erosion.

The term scour is defined as local erosion, scour occurs when local transport capacity exceeds the supply from upstream (Schiereck & Verhagen, 2012). When the erosion leads to a local deepening which is significant with respect to the surrounding river bed, the local deepening is called a scour hole.

For each scour hole, the development varies strongly (Huismans & van Duin, 2016; Koopmans, 2017). Despite an equal discharge, there are not necessary similarities between the development of scour holes located in the same river branch. For example, in the Oude Maas, one scour hole (OMS-4a) grew 2.2 [m] in depth between 2009 and 2014, while another scour hole (OMS-3b) located 9 [km] downstream, became 0.4 [m] shallower in the same period (Huismans & van Duin, 2016). The differences between the development of scour holes occur due to a difference in interaction between hydrodynamic conditions and geological conditions.

The local hydrodynamic and geological conditions are varying over river branches in the RMD. The variation in hydrodynamic conditions is a result of changes in river geometry, presence of hydraulic structures or changes in the bed level. While the variation in geological conditions occurred during the formation of the delta. Differences in these conditions lead to the presence of a scour hole at one location and the absence of a scour hole at another location.

#### 3.1.1. Erosion processes

The flow velocities in combination with turbulence influence the transport capacity of sediment in a river. A spatial difference in flow velocity, turbulence or both leads to a spatial gradient of the transport capacity. A gradient leads to erosion or sedimentation. This follows from the conservation of mass. The general conservation of mass expression is given in Eq. 3.1. (Schiereck & Verhagen, 2012)

$$\frac{\partial z_b}{\partial t} + \frac{\partial S}{\partial x} = 0 \quad (3.1)$$

In which:

$$\begin{aligned} Z_b &= \text{Position of the bed level} && [\text{m}] \\ S &= \text{Sediment transport per unit width} && [\text{m}^3/\text{s}/\text{m}] \end{aligned}$$

From Eq. 3.1 follows that an increase in transport capacity leads to a reduction in bed level. A reduction in bed level is called erosion. On the other hand, a decrease in transport capacity leads to an increase in bed level, which is called sedimentation. (Schierreck & Verhagen, 2012)

In general, it can be said that non-cohesive sediment (e.g. sand) is easily erodible and cohesive sediment (e.g. clay and peat) is poorly erodible. The amount of transported sediment and the erodibility are determined by geological conditions. The transport of cohesive sediment differs from the transport of non-cohesive sediment.

The motion of non-cohesive sediment starts when the flow velocity is above a critical value. The motion can be described with Shields. According to Shields, the flow velocity in combination with turbulence leads to shear stress. If the shear stress is above the critical value the sediment starts to move. The only resistant force for non-cohesive material is the relative weight of a grain. (Schierreck & Verhagen, 2012)

The transport of cohesive sediment is more complex than the transport of non-cohesive sediment. Cohesive sediment must first break from the surrounding bed, which requires much larger forces. If a grain is loosened from the bed, a relatively small force is needed to transport the grain. (Hoffmans & Verheij, 1997). The transport of cohesive material can occur in two ways. The first is abrasive erosion, in which the grains are scrapped by the flow. This happens if the shear stress of the flow is above the critical shear stress of the grains. The critical shear stress depends on the cohesion of the sediment. The critical flow velocity can be determined from the critical shear stress. The second mode of transport is pulling-off entire sediment fragments. The critical shear stress for the pulling-off erosion depends on the undrained shear strength of the soil. (Sloff et al., 2014)

### 3.1.2. Development processes

Extensive international research has been performed on the development of scour holes located close to hydraulic structures. This type of scour hole is namely present worldwide. Less research is done for the development of scour holes due to changes in geological conditions. Bom (2017), Koopmans (2017), Stenfert (2017) and van Zuylen (2015) used the method for the prediction of scour holes behind a sill (Dutch: Drempe) with a non-erodible bed protection to predict the development of scour holes in heterogeneous subsoil. This method was used because of the similarities in two-dimensional flow pattern and slope steepness for a scour hole behind a sill and a scour hole in heterogeneous subsoil. The method is called Breusers theory. Stenfert (2017) analysed whether the method was applicable on a three-dimensional scour hole (variation in longitudinal, lateral and vertical direction).

Four stages can be distinguished in the development process from initial erosion till a stable scour hole, an initial phase, a development phase, a stabilisation phase and an equilibrium phase (Hoffmans & Verheij, 1997). These stages are described in Appendix A. The erosion processes and type of growth differs per stage. The last two stages are relevant for the scour holes currently present in the RMD.

For the development of scour holes, several processes are relevant. Some processes are relevant for two-dimensional situations (variation in longitudinal and vertical direction), while other processes are only relevant for three-dimensional situations. The following processes are relevant for a scour hole in a two-dimensional situation (Bom, 2017).

- The current development stage of the scour hole.
- Longitudinal recirculation.
- Mixing layer.

Next to the above-mentioned processes, the following additional processes are relevant for a three-dimensional situation:

- The curved recirculation zone.
- The horseshoe vortex.
- Flow contractions.

These processes influence the flow pattern inside a scour hole. In the case with uniform geological conditions and steady hydrodynamic conditions, the flow pattern can be used for a rough estimation of the scour hole development (Bom, 2017).

### 3.1.3. Tidal influence on scour hole development

The presence of tide in the RMD generates tidal currents and influence the hydrodynamic conditions in the delta. Especially in the connecting branches, large flow velocities can be observed. Tide generates currents with two main directions. Due to the constant reversing flow, there are no steady flow conditions around scour holes in the connecting branches.

The tide influences the scour hole development in two ways. Firstly, the high flow velocity results in the erosion of river branches and can initiate the development of a scour hole. Secondly, the constant reversing flow influences the shape and the maximum depth of the scour holes affected by the tidal current. According to the Breusers theory, scour holes have a steep upstream slope and a milder downstream slope (Hoffmans & Verheij, 1997). While there is only a small difference in the slopes of the scour holes in the connecting branches (Koopmans, 2017). The upstream slope is milder and the downstream slope steeper than expected. Moreover, the scour holes in the RMD are less deep than expected from the Breusers theory. Since the outflow of sediment is reduced by a steeper slope (van Zuylen, 2015).

## 3.2. Tool for scour hole development prediction

Although the influence of the basic processes on the hydrodynamic conditions in a scour hole are known, the application of it with numerical models is very complex. The flow pattern around scour holes is mainly three-dimensional. This means that the hydrostatic pressure distribution assumption, the basic assumption for most numerical models, is not valid for the flow around scour holes (Hoitink et al., 2017). Besides, the exact dynamic feedback between flow, sediment transport and morphology is hard to represent with numerical models.

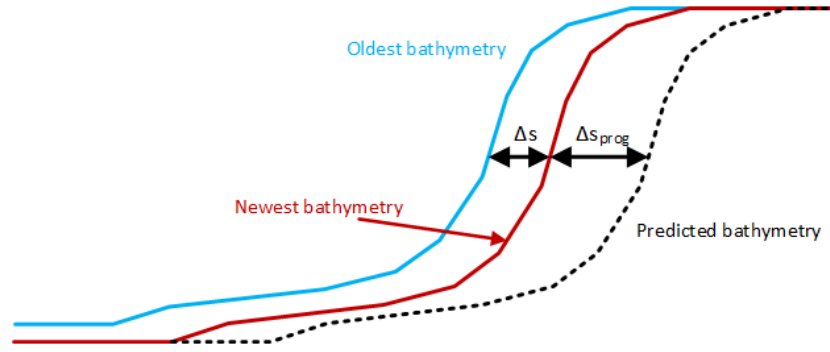
Modelling of the scour holes in the RMD is even harder due to the tidal influences. The reversing flow directions gives non-steady flow conditions around a scour hole. Even if a numerical model is able to reproduce the three-dimensional flow pattern in a scour hole, it will not represent the actual flow pattern. The usage of such models for the scour hole development gives an unreliable result (Hoitink et al., 2017). Besides, Breuser's scour hole development theory is not applicable for scour holes under tidal influence since applying the theory gives to large uncertainties (Koopmans, 2017).

Instead of predicting the scour hole development with a numerical model, the scour hole development can be predicted from historically measured bathymetry using extrapolation techniques. A tool called 'Htrend.exe' is available for this extrapolation (hereafter referred to as Htrend). The tool is developed by Rijkswaterstaat WVL and Rijkswaterstaat CIV and subsequently reviewed by Deltares in the KPP project river research ('Kenis Primaire Processen project rivierkundig onderzoek') in 2015 (de Ruiter et al., 2017). With the tool, the future bathymetry of an individual scour hole or a cluster of scour holes can be predicted.

In this thesis, the scour hole development will be predicted with Htrend. The usages of the tool has been updated, as will be explained later in section 3.2.4. The tool is purely data-driven and works on the principle of extrapolation of historical trends. Based on two historically measured bathymetry datasets, the tool gives a prediction of the bathymetry in the (near) future. The actual effect of the flow pattern in the scour on the scour hole development is represented in the measured bathymetry data. The effect of the local subsoil variance is represented as well. With the assumption that the effect in the past will continue in the future, the future bathymetry is predicted.

### 3.2.1. Description of data-driven extrapolation tool

The effect of the complex hydrodynamic condition and local geological conditions on the morphological development of a scour hole is simplified by considering only two processes in Htrend. The first process is a horizontal displacement of the scour hole edge. Followed by a vertical displacement of the scour hole bottom. The horizontal displacement results in a growth in surface, while the vertical displacement results in growth in depth.



Source: Own creation based on de Ruiter et al. (2017)

Figure 3.1: Schematisation of purely horizontal extrapolation of a scour hole edge in Htrend.

### Horizontal displacement

For the horizontal displacement, it is assumed that the historical displacement will continue in the future. The scour hole edge will shift in the horizontal direction with the same shape and magnitude as before (de Ruiter et al., 2017), see figure 3.1.

For each bathymetry point in the scour hole, searching-lines are created with intermediate steps in 360 degrees around each bathymetry point, as schematically indicated for two points in figure 3.2a. Along each line, a depth profile is created for the two bathymetry datasets. Subsequently, the vertical displacements between the two depth profiles ( $\Delta z$ ) and the average slopes ( $i$ ) are determined. The magnitude of the local horizontal displacement ( $\Delta s$ ) along the searching-line can then be determined from these values, as indicated in Eq. 3.2.

$$\Delta s_{prog} = \frac{\Delta Z}{i} \times \frac{T_{prog}}{T_{data}} \quad (3.2)$$

In which:

|                   |   |  |      |
|-------------------|---|--|------|
| $\Delta s_{prog}$ | = | Predicted horizontal displacement for period $T_{prog}$          | [m]  |
| $i$               | = | Local average slope  | [-]  |
| $\Delta Z$        | = | Vertical difference between the two bathymetry datasets          | [m]  |
| $T_{prog}$        | = | Prediction period  | [yr] |
| $T_{data}$        | = | Period between the recording date of the two bathymetry datasets | [yr] |

In order to cope small local changes, a minimum value is defined for the erosion rate, the erosion length (length of the searching-lines) and slope. Only if all minimum values are exceeded, the tool extrapolates the historical horizontal displacement. The tool calculated the new Z-value for each bathymetry point affected by a horizontal extrapolation along a searching-line as indicated in Eq. 3.3.

$$Z_{prog}(x + \Delta s_{prog}) = Z_{original}(x) \quad (3.3)$$

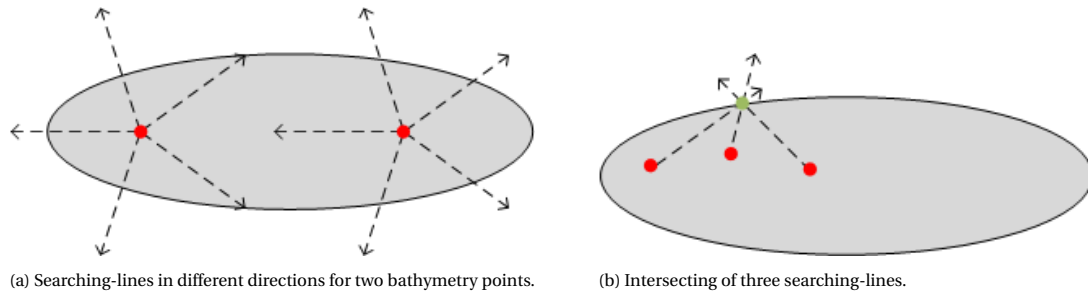


Figure 3.2: Schematisation of searching-lines for the horizontal extrapolation in Htrend.

In which:

$$\begin{aligned} Z_{prog}(x + \Delta s_{prog}) &= \text{Predicted bed level on location } (x + \Delta s_{prog}) && [\text{m} + \text{NAP}] \\ Z_{original}(x) &= \text{Original bed level in newest bathymetry data on location } (x) && [\text{m} + \text{NAP}] \end{aligned}$$

By creating searching-lines in all directions, potential horizontal displacements can be detected and subsequently extrapolated in all possible directions. In this way, the tool makes it possible to predict developments in different directions.

Due to the three-dimensional character of a scour hole and the intersection of searching-lines, a horizontal displacement for a specific bathymetry point can be detected on multiple searching-lines, as indicated for three searching-line in figure 3.2b. To deal with this, the minimum predicted Z-value (the lowest located value) of the intersecting searching-line will be used as final Z-value (de Ruiter et al., 2017). In this way, the covering horizontal trend will be represented in the predicted bathymetry.

### Vertical displacement

The prediction of the new bathymetry for the vertical extrapolation is based on the continuation of the historical erosion trend rate, as Eq. 3.4 shows.

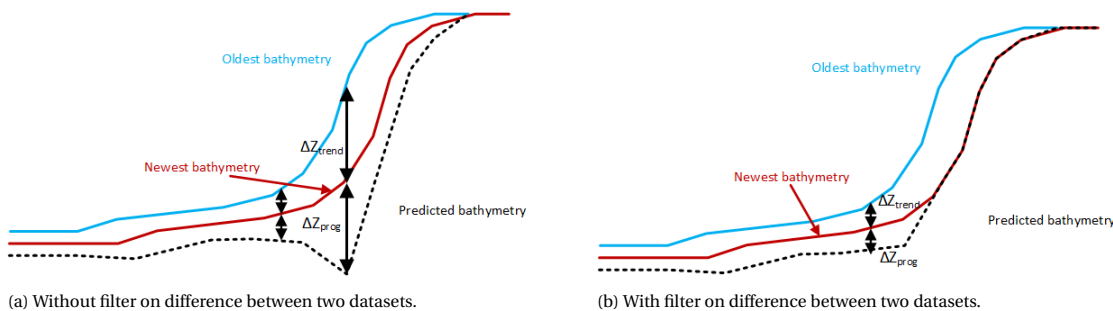
$$Z_{prog} = Z_{original} + \frac{\Delta Z}{\Delta t} \times T_{prog} \quad (3.4)$$

In which:

$$\begin{aligned} Z_{prog} &= \text{Predicted bed level} && [\text{m}] \\ Z_{original} &= \text{Original bed level in newest bathymetry data} && [\text{m}] \\ \frac{\Delta Z}{\Delta t} &= \text{Erosion trend rate} && [\text{m}/\text{yr}] \\ T_{prog} &= \text{Prediction period} && [\text{yr}] \end{aligned}$$

An additional dataset with vertical erosion rates is required for the vertical displacement. This dataset is not simply the difference between the two bathymetry datasets since extrapolating purely the vertical difference between two datasets will result in an extreme increase in depth near the edges, as shown in figure 3.3a.

For the generation of the vertical erosion rate file a correction is needed on the bed level differences of the two datasets. This can be for example a maximum allowable slope or another filter type. The effect of a filter on the slope is shown in figure 3.3b. For this example, only erosion rates on the milder slope parts are defined. For the steeper parts, the erosion rates are set to 0 [m/yr]. This results in only the extrapolation of vertical trends on mild slope parts.



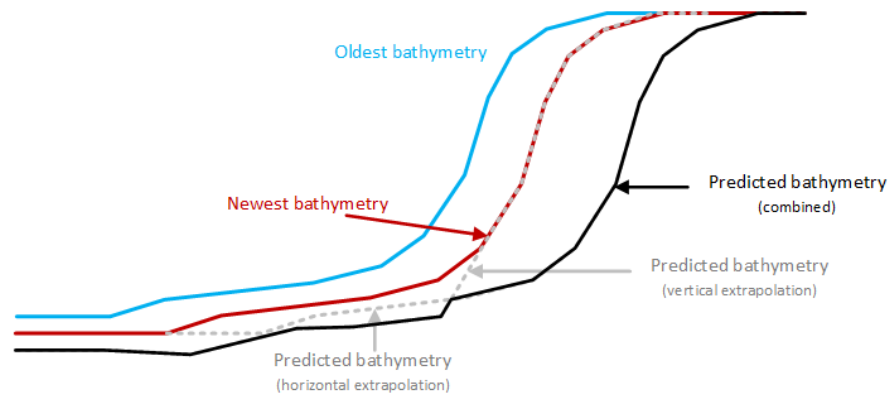
Source: Own creation based on de Ruiter et al. (2017)

Figure 3.3: Schematisation of purely vertical extrapolation based on vertical erosion trends in Htrend.

### Combined horizontal and vertical extrapolation

Both types of extrapolations are combined in Htrend. The two extrapolations will be executed separately and subsequently merged. For both extrapolations, an entire new bathymetry is determined. In the combined result, the lowest predicted Z-value of each bathymetry point is used. Such that the dominant process is represented in the new predicted bathymetry. The result of the combined extrapolation is schematically indicated in figure 3.4.

The two extrapolations are a complement to each other. In the purely horizontal extrapolation, only the steep slope parts are extrapolated and in the vertical extrapolation only the milder slope parts. If the extrapolations types are combined, all relevant parts of the scour hole will be extrapolated.



Source: Own creation based on de Ruiter et al. (2017)

Figure 3.4: Schematisation extrapolation of combined horizontal and vertical trends in Htrend.

### 3.2.2. Tool set-up

#### Input parameters

Three parameters must be defined for the detection of horizontal displacements in Htrend. These parameters are:

- Minimum erosion rate.
- Minimum length for erosion detection.
- Definition of a steep slope.

Next to these input parameters, a maximum slope as a filter for the vertical erosion rate must be defined.

#### Input data

Two historical bathymetry datasets and a vertical erosion rate dataset are required as input data for Htrend. The bathymetry is measured for all river branches in the RMD each year. The historically measured bathymetry is retrieved from Rijkswaterstaat CIV. The data is available per river branch, with a resolution of  $1 \times 1$  [m].

As input for Htrend, the bathymetry data around the scour hole of interest is selected from bathymetry datasets of entire river branches. The selected bathymetry can be directly used without adaptation as input.

The vertical erosion rate dataset has to be generated from the historical bathymetry datasets. For each point of interest around the scour hole, an erosion rate must be defined. Several methods are possible to generate this dataset, which will be explained later in section 3.3.2. After generating the vertical erosion rate dataset, the dataset must be filtered on the slope, in order to prevent extreme extrapolation on steep parts as indicated in figure 3.3.

#### Calibration and verification

Since the developments and dimensions of each particular scour hole are different, the input parameters must be calibrated per scour hole in order to represent the development of a particular scour hole. After the calibration of the input parameters, the scour hole development must be checked with a verification. If the input parameters are not defined well, a too large or too small scour hole development is given as tool result.

For the calibration and verification, the historical bathymetry of at least four different years are required. The usage of the datasets for the calibration and verification is schematically indicated in figure 3.5.

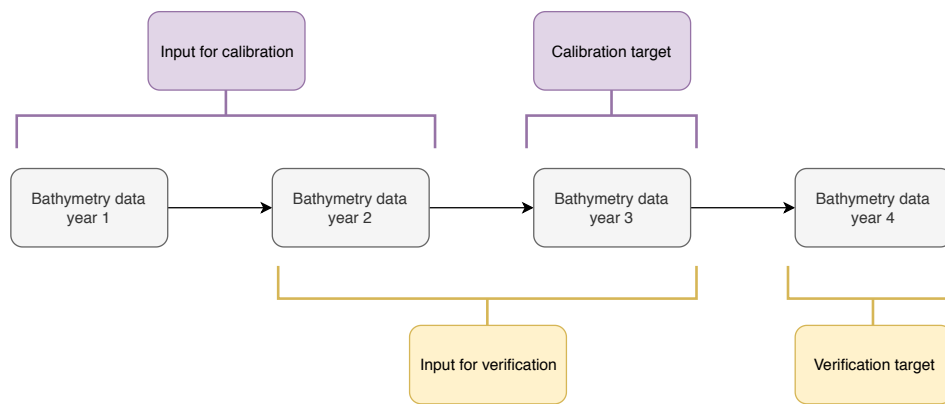


Figure 3.5: Schematisation of the usage of bathymetry datasets for the calibration and verification of a particular scour hole Htrend.

The first two datasets are used as input for Htrend for the calibration, such that the prediction of the scour hole bathymetry is close to the real bathymetry of the third dataset. Subsequently, the calibration must be verified, in order to see if the calibrated parameters also work on different datasets. For the verification, different input datasets are required. This can be, for example, the bathymetry of year 2 and 3. With these two datasets as input data, the bathymetry is predicted for year 4 and subsequently compared to real bathymetry of year 4.

The aim of the usage of the tool is to predict the development of the scour hole in the near future. The future size and depth of a scour hole are relevant for the risk analysis. In addition, the development of the lowest part of the scour hole is relevant, since this influences the average slope of the scour hole. Therefore, both representation of the scour hole dimensions and the lowest part are the targets of the calibration and verification.

### 3.2.3. Tool limitations

There are two limitations to the usage of Htrend. Firstly, the tool can only extrapolate erosion trends in horizontal and vertical directions. For both directions, local sedimentation trends can thus not be detected and extrapolated by the tool. At the locations with sedimentation, no extrapolation is done and the historical Z-value is given as future bed level. For each predicted future scour hole bathymetry, a growth in surface and depth is predicted due to this limitation.

Secondly, the tool is data-driven and not process-driven. Only the autonomous scour hole development can be predicted with the tool. The tool cannot be used to analyse the effects of future interventions in river branches on the scour hole development. A human intervention will lead to different local hydrodynamic conditions. These effects are not included in historical bathymetry data. Process-driven tools can predict new hydrodynamic conditions. However, with process-driven models the exact effect on the scour hole development is also difficult to predict.

### 3.2.4. Probabilistic use of Htrend

Htrend is developed as a deterministic tool for the extrapolation of scour hole development. The future bathymetry is predicted from a constant input dataset without taking uncertainties or variations into account. This means that the predicted bathymetry an indication is for the future scour hole bathymetry without uncertainties.

In this thesis, the tool is updated in order to predict the future scour hole bathymetry in a probabilistic way. This is achieved by making the input stochastic. The probabilistic approach gives a range of possible future scour hole shapes. This range gives, like the original deterministic approach, an indication for the future bathymetry. However, uncertainties in the prediction is included.

The original deterministic approach and the updated approach are described and analysed in Appendix B. In order to update the approach, a data-analysis is performed for the historical erosion trends, this analysis is also included in Appendix B.

### Stochastic input

In the probabilistic approach, the scour hole is predicted with a Monte Carlo simulation. Which means that a scour hole is predicted multiple times from randomly chosen input data. The scour hole development is predicted from input data files in Htrend. In the probabilistic approach, these input files are generated in a stochastic way. By choosing randomly data for the input files, a different result for each prediction is obtained and it is possible to define a range of the future bathymetry.

The horizontal and vertical extrapolation in Htrend are both made stochastic. Making the horizontal extrapolation stochastic is relatively simple. The horizontal extrapolation can be made stochastic by randomly choosing a combination of two historical bathymetry datasets as input files.

The vertical extrapolation is defined in a vertical erosion rate file. This file is made stochastic by generating the file randomly from the historical relation between the bed level and the erosion rate. Due to different geological conditions per scour hole and spatial variations within one scour hole this relation must be determined per particular scour hole. The determination of the relation and the generation of the vertical erosion rate file is illustrated in section 3.3.2.

### Approach description

The steps for the probabilistic approach for the prediction of the scour hole in three years are shown in figure 3.6. By repeating the last steps, the scour hole development can be predicted for a larger period.

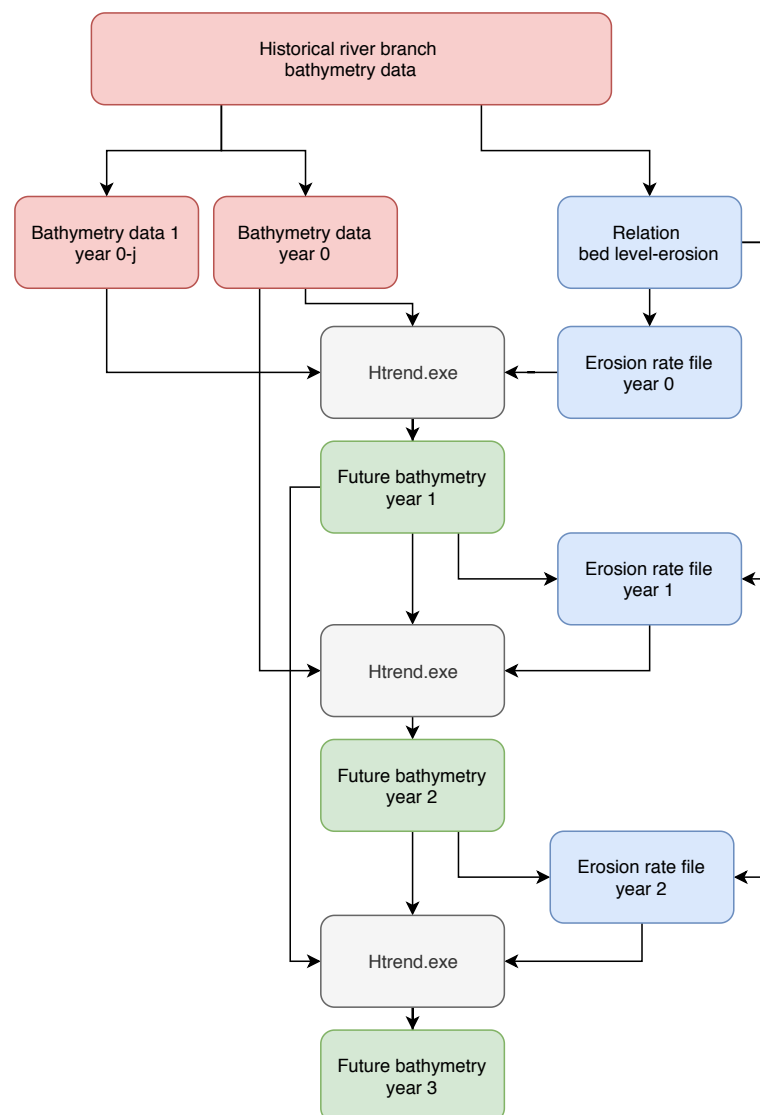


Figure 3.6: Steps for the scour hole development prediction in the probabilistic approach.

As can be seen, the future bathymetry of the year of interest is calculated with intermediate steps for each intermediate year. These steps are necessary in order to couple the local erosion rate of a specific year with the bathymetry of that year. Which results in yearly differences in local erosion rate.

### 3.3. Illustration of the probabilistic scour hole development approach

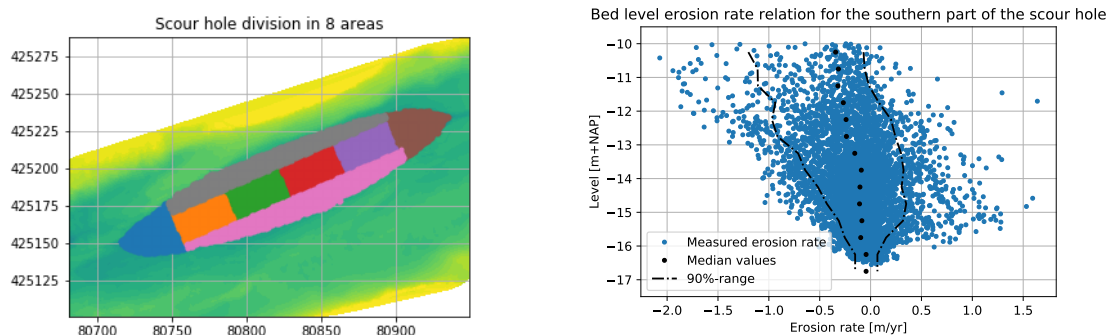
The steps of the probabilistic approach are illustrated for the scour hole near rkm 1005 in the river Spui. This scour hole will be used as a case study for the risk assessment in section 5.3. This scour hole had a length of 200 [m] and width of 47 [m] in 2018. In this example, the scour hole bathymetry is predicted for 2023.

For the prediction of the scour hole, five bathymetry datasets are used. These datasets are the bed level datasets of the entire river Spui measured in the period 2014-2018. The resolution of the bed level is 1x1 [m]. The bathymetry is yearly measured with a multibeam echo sounder by Rijkswaterstaat CIV.

#### 3.3.1. Determination of bed level erosion rate relation

The bed level erosion rate relation must be known for the generation of the vertical erosion rate file. The scour hole is divided into 8 areas, as indicated in figure 3.7a. The bed level erosion rate relation is determined for each area individually. These areas are chosen from the theoretical physical processes, such that the effect of the local different hydrodynamic conditions is represented in the bed level erosion rate relation.

Based on the bed level difference of two consecutive datasets, the erosion rate per bathymetry point (resolution 1x1 [m]) is determined per year in the period 2014-2018. All erosion rate values are stored per area together with their bed level values. In this way, the historical erosion rates are combined with the bed level. An example of the relation can be seen in figure 3.7b. In this figure, the historical erosion rate per bed level is shown together with the median and 90% confidence range for the southern area of the scour hole.



(a) Indication of the location of the 8 areas.

(b) Example of the bed level erosion rate relation for the southern (pink) area, including the median value and 90% confidence range.

Figure 3.7: Division of the scour hole in 8 areas, the bed level erosion rate relation is determined per area.

#### 3.3.2. Stochastic input

Htrend requires two bathymetry files and one vertical erosion rate file for the data-driven prediction of the future scour hole bathymetry. Both types of files are made stochastic in order to predict the scour hole in a probabilist way.

##### Bathymetry files

The historical bathymetry of 2016, 2017 and 2018 are used as input files for the prediction of the scour hole. With these datasets, three different input combinations are possible. These combinations are randomly used as input data for the scour hole development prediction.

##### Erosion rate file

The erosion rate file is generated from the initial bed level and the determined bed level erosion rate relations of the 8 areas. This generation is according to steps indicated in figure 3.8. First, the scour hole is divided into small areas of 6 × 6 [m]. Based on the mean bed level of the small area, an erosion rate for the whole area is randomly resampled from the historical bed level erosion rate relation. In order to keep spatial correlations,

for the entire small area, the same erosion rate is assessed. Finally, the erosion rate data is filtered for steep slopes to prevent extreme erosions at the scour hole edges.

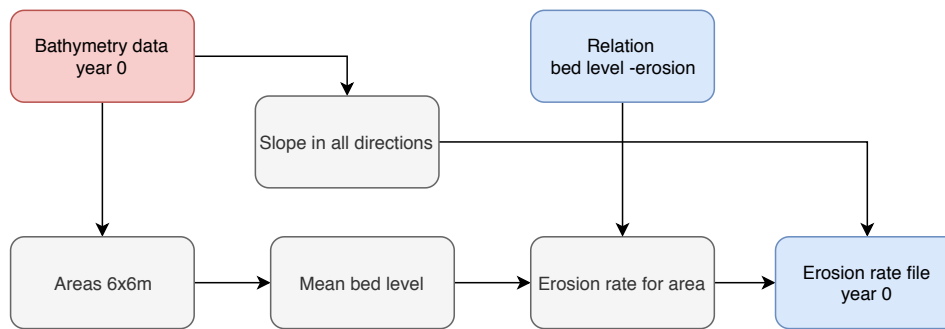


Figure 3.8: Steps for the creation of the vertical erosion rate based on the relation between bed level and erosion rate.

Since the erosion rate per area of  $6 \times 6$  [m] is randomly resampled, each time a different erosion rate for the same area is taken. The erosion rate file is thus each time different. For example, in the initial year 0, the mean bed level of a small area located in the southern part is  $-15.0$  [m + NAP] a random value of the historical observed erosion rates between  $-0.75$  and  $+1.50$  [m/yr] is selected. Say  $-0.5$  [m/yr], this value is assessed as erosion rate for the entire small area for the prediction of the scour in the first year. For the prediction of the scour hole in year 2, a new random value is chosen from the range of a bed level of  $-15.5$  [m + NAP]. For this bed level, the values for the erosion rate are between  $-0.50$  and  $+1.00$  [m/yr].

The size of the small areas is based on a spatial erosion rate variation analysis, in which the correlation-coefficient between the erosion rate and the neighbours' average erosion rate is analysed. For each point in the scour hole, the neighbours average erosion rate is calculated by taking several surrounding area sizes into account. By increasing the area the correlation between the erosion rate and the neighbours average rate decreases, as shown in table 3.1. In order to quantify the spatial dependency, the coefficient of determination is required. The coefficient of determination ( $\rho_{XY}^2$ ) gives the percentage of the variation in the values of X that can be explained or accounted for by variation of value Y (Taylor, 1990). For  $\rho_{XY} < 0.7$  the  $\rho_{XY}^2$  is below 0.5, which means that the erosion rate depends for less than 50% on the surrounding erosion rate. In general, the dependency for  $\rho_{XY}^2$ -values below 0.5 is considered as moderated or weak (Taylor, 1990). For the spatial erosion correlation, this holds for areas of  $6 \times 6$  [m].

| Area [m × m] | Spatial correlation |
|--------------|---------------------|
| 2x2          | 0.871               |
| 4x4          | 0.785               |
| 6x6          | 0.711               |
| 8x8          | 0.652               |
| 10x10        | 0.612               |
| 12x12        | 0.583               |
| 14x14        | 0.557               |
| 16x16        | 0.533               |

Table 3.1: Spatial correlation for erosion rate and neighbours average erosion rate in 2017.

### 3.3.3. Monte Carlo simulation

The bathymetry is predicted with 300 tool runs in a Monte Carlo simulation. This number is derived from the desired accuracy with the method proposed by van der Klis (2003). A desired accuracy of the lowest located point in the scour hole of plus or minus 5.0 [cm] of fractile  $p = 90$  is used for the determination of the number of runs.

In order to check these number of runs, the values corresponding to the 90<sup>th</sup>-fractile are plotted against the number of runs in figure 3.9. After approximately 250 runs, the bed level of the 90<sup>th</sup>-fractile remains constant. Running the tool 300 times is thus even more than enough to achieve the desired accuracy.

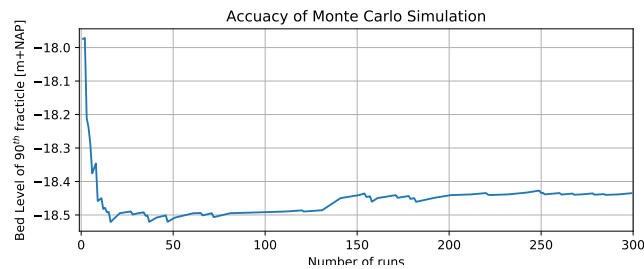


Figure 3.9: Accuracy of the 90th fractile values depending on the number of runs.

### 3.3.4. Output data

The tool runs 300 times, with a randomly chosen combination of bathymetry data and a unique generated erosion rate file for each year in each run. This gives for each bathymetry point in the scour hole 300 possible bed level values for 2023. Per bathymetry point, the expected value and 90% confidence interval can be determined. This is illustrated with an example in figure 3.10. In which the historical bed level and predicted bed level is shown for a cross-section of the middle of the scour hole.

Based on the 300 realisations for each bathymetry point, scenarios can be defined for the scour hole development. The mean scenario is retrieved by taking the mean value of the predicted range of each bathymetry point. The 5%-scenario and 95%-scenario are retrieved by taking the 5% or 95% value of each range. Scour hole characteristics, like scour hole width, length, surface area and maximum depth, can be determined for each defined scenario.

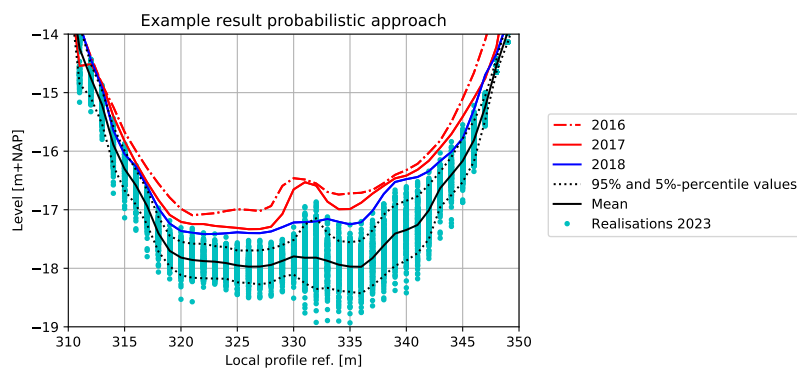


Figure 3.10: Cross-section of the middle of the scour hole, with the historical bed level and the predicted future bed level.

## 3.4. Discussion about scour hole development prediction

### Excluding of scour hole development processes

The future bathymetry is predicted with only the historical bathymetry data. This makes the method for the scour hole development a data-driven method. In the ideal case, the future bathymetry is predicted from a coupling between available data and physical processes. This coupling is difficult to make for the scour holes in the RMD since the actual physical processes are hard to determine due to the three-dimensional flow pattern in combination with the tidal influences. However, with only the measured bathymetry, it is already possible to predict the development of a scour hole.

The effect of the physical processes on the scour hole development is still incorporated in the bathymetry data. By dividing the scour hole into separate areas and subsequently determining the relation between the bed level and erosion rate per area, the effect of the physical process is included in the prediction of the future scour hole.

The result of the scour hole development prediction with the presented data-driven method is not necessarily less accurate than a prediction with numerical models. Namely, the current available numerical models with the scour hole development processes included, cannot give (yet) an accurate prediction of the scour hole development (Bom, 2017; Sloff et al., 2014).

### Approach comparison

The original method for the scour hole development prediction has been updated. In the original deterministic approach only one scenario run is done, this results in short computation time. On the other hand, no insight is obtained in the uncertainty of the realisation. The updated approach is more time consuming, but gives also insight in the uncertainty range.

In figure 3.11, the output results of the two approaches are shown, for a cross-section in the middle of the scour hole. As can be seen, the deterministic approach results in a larger yearly erosion rate and thus a lower located bed level than the average profile of the probabilistic approach. In the average profile of the probabilistic approach, there are less local variations in the bed level.

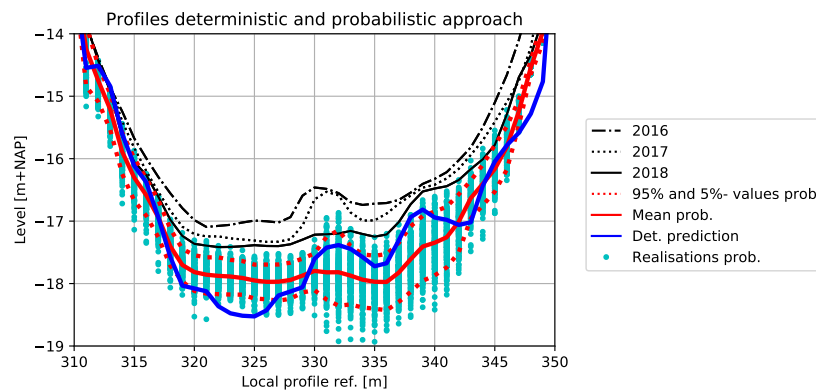


Figure 3.11: Prediction of the 2023-profile, with the original deterministic approach and the updated probabilistic approach.

### Bed level erosion rate relation

The variations in the realisations of the prediction of the future bathymetry are partly due to the sampling of the vertical erosion from the relation between the historical bed level and erosion rate. From the data analysis follows that the erosion rate reduces as the local bed level decreases. A possible explanation for this can be found in the geological conditions. The hydrodynamic conditions, like flow velocity and water levels, remained very likely the same in the observed period. Therefore, the smaller erosion rate could have been occurred due to the soil composition. The soil composition determines namely the critical condition for erosion. One type of soil layer can be less erodible compared to another soil layer, while the hydrodynamic forcing conditions are equal.

Since the bed level erosion rate relation is based on the historical data, this relation is only known up to a certain level. However, a scour hole is growing in depth, which means that the lowest part of a scour hole will be located at a level without any known information about this relation. In the current used method for the generation of the erosion rate file, it is now assumed that the relation for bed levels which were not present in the past, is the same as the relation in the lowest 0.5 [m] of the scour hole. This assumption can be invalid if the lower located soil composition is different. For example, if a highly-erodible layer is located close to the current bed level, a much high erosion rate can be expected for these bed levels.

# 4

## Risk identification: flood safety

Dike instability due to the occurrence of a flow slide has been identified as a large potential hazard of scour holes in the connecting branches in the RMD. The presence of scour holes induces larger probabilities for occurrence of flow slides. Flow slide is an indirect failure mechanism for dikes. The post flow slide profile (in Dutch: Restprofiel) increases the dike failure probability as a result of direct failure mechanisms. The occurrence of flow slides next to scour holes is, therefore, relevant for flood safety.

The probability of a flood and the consequences are the required aspects for the estimation of the risk of scour holes with respect to flood safety. In this chapter, the steps from flow slide to a flood are described, see figure 4.1. Next, the methods for the quantitation of the probability of occurrence of the different steps are given. In addition, the determination of the consequences of a flood is described in this chapter.

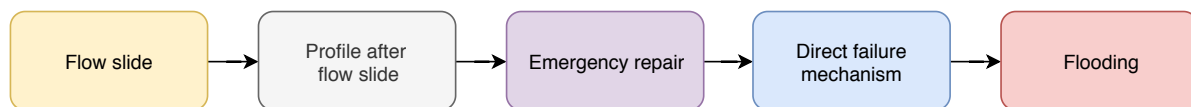


Figure 4.1: Pathway from flow slide to flooding.

### 4.1. Indirect failure mechanism: flow slide

#### 4.1.1. Flow slide processes

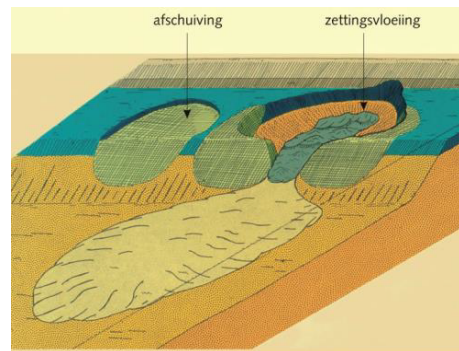
During a flow slide, the foreshore turns into a sand-water mixture and slides (partly) away. Two different processes can result in flow slides. These two processes are static liquefaction (in Dutch: verwekingsvloeiing) and breaching (in Dutch: bresvloeiing). For the occurrence of both processes, a trigger is required.

After a flow slide, the dike will have a new typical post flow slide profile, see figure 4.2. The post flow slide profile is equal for both processes.

#### Post flow slide profile

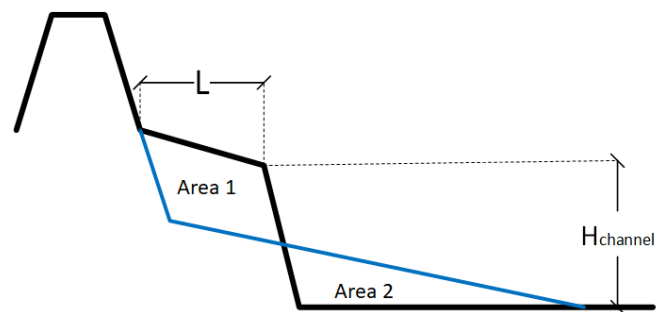
The post flow slide profile is a new stable profile, which is the result of a new equilibrium. As can be seen in figure 4.2, the characteristic post flow slide profile consists of two parts. The lower mild slope part and the upper steep slope. The transition between these two parts is often clearly visible in the profile. The transition point is approximately located on a height of 57% of the original channel height (Rijkswaterstaat, 2016b)

The retrogression length (in Dutch: inscharingslengte) is the horizontal distance of the affected foreshore by a flow slide. This is indicated with 'L' in figure 4.2. The retrogression length of a flow slide depends mainly on geometry properties of the original prior profile. Besides, the presence of riprap on the slope and the type of subsoil (Rijkswaterstaat, 2016b) influence the profile as well.



Source: Jonkman et al. (2018)

(a) Difference between flow slide (right) and sliding outer slope (left).



Source: Own creation, based on Rijkswaterstaat (2016b)

(b) Typical dike profile after the occurrence of a flow slide. A flow slide results in a milder slope.

Figure 4.2: Overview of the indirect failure mechanism flow slide.

If the retrogression length is larger than the acceptable retrogression length, a flow slide will affect the probability of occurrence of direct failure mechanism and so with this the safety level of a flood defence (Rijkswaterstaat, 2016b). The acceptable retrogression length depends on the actual length of the foreshore and is thus location specific. The length is often equal to the length of the foreshore and if necessary with a reduction for the influence zone of the flood defence. The length of the influence zone is determined by the direct failure mechanisms, like piping and macro instability of the outer slope.

### Static liquefaction

The first process which can lead to flow slides is static liquefaction. Static liquefaction can occur in loosely packed sand layers. A trigger, like a local vibration, can lead to the deformation of the grain skeleton. A vibration can occur due to a rapid fall or rise in water level, bed level erosion or an earthquake. The pore pressure increases and the effective stress reduces. The shear stress between particles decreases significantly due to the reduced effective stress. Depending on the location of the liquefaction area, particles slide directly down of the slope or a slip circle can occur, as indicated in figure 4.3a. (M. de Groot et al., 2007)

The process of flow slide due to liquefaction can be distinguished in different phases. The following four phases can be seen:

1. Gradual change of soil stresses due to erosion/sedimentation, such that the slope becomes metastable.
2. A trigger leads to a sudden increase in water pore pressure. Small shear deformations give a redistribution of effective stress and pore pressures.
3. Flow slide with a new redistribution of effective stress and pore pressures.
4. (Eventually): occurrence of new metastability of another part of the slope and a new flow slide.

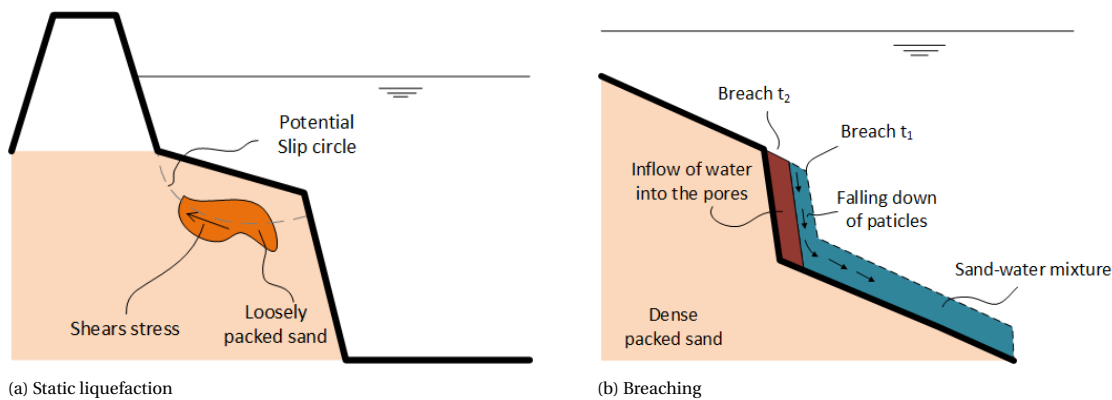
Flow slide can occur if a part of the slope is metastable. Metastability is a situation for which a small load or force can lead to liquefaction of a large part of the soil (Van den Berg, 2014). Metastability can occur if the following conditions hold for the soil:

1. Liquefaction favour conditions: the sand layer must have a sufficient thickness (at least 2-5 metres) and must be loosely packed
2. Steep slopes over a sufficient height difference.

These two conditions depend on each other; the critical slope for a denser packed sand layer is steeper.

### Breaching

Breaching is the process in which small layers of sand consecutively are falling down on a slope (M. de Groot et al., 2009). While liquefaction occurs for loosely packed sand, breaching occurs in densely packed sand layers. The process of breaching can take hours to days, where liquefaction can happen in just a few minutes. The densely packed sand layers make it possible to have relatively steep slopes. Due to erosion, a slope can become too steep and the slope becomes eventually unstable. The inflow of water into the pores leads to falling down of particles. The particles of the top layer together with the water leads to a sand-water mixture. The mixture is sliding down and can absorb extra particles from underlying layers while it slides down. The



Source: Own creation, based on Van den Berg (2014)

Figure 4.3: Flow slide processes.

following above-located layer can also slide down while it absorbed extra particles. This process continues until the whole slope is slid down. A schematic overview of breaching is shown in figure 4.3b.

The following conditions are necessary for the occurrence of breaching (Rijkswaterstaat, 2012):

1. The sediment of the submerged slope must consist of fine sand or silt particles.
2. A continuous slope without berms or protected areas on the slope.
3. The breaching material must be able to flow away.
4. The submerged slope must have a sufficient length and height.

For a flow slide due to breaching a trigger is also needed for initial breaching. This trigger can be one of the following physical processes:

- Local slip failure.
- Erosion of the slope.
- Liquefaction of loosely packed layer.
- Dumping or falling of sediment on the slope. The sediment can flow over the slope in a sand-water mixture.

#### 4.1.2. Quantification of probability of flow slides

In the Dutch safety assessment for flood defences, a method for the quantitation of the probability of flow slides is given. The method is described in detail in Appendix A.2. In Appendix C, the method is illustrated with an example calculation.

For the safety assessment regarding flow slide two aspects are relevant:

1. The probability of occurrence of a flow slide:  $P(FS)$ .
2. The retrogression length of the profile after a flow slide and the probability of exceedance of the maximum allowable retrogression length:  $P(L > L_{max}|FS)$ .

In many situations, there is no hazard for the occurrence of a flow slide. With a rule of thumb, it can be determined whether there is a potential hazard for flow slide on a specific location.

For locations with a potential hazard, an advanced method is described in the WBI, for the quantification of the probability of occurrence of a flow slide. The method is developed with the statistics of 145 out of 710 historical flow slides in the Dutch province of Zeeland (Rijkswaterstaat, 2012). Based on an estuary length of 190 [km], the frequency of flow slides is approximately 0.02 [1/km/yr]. The reference situation of the method is, therefore, the subsoil of Zeeland. With the introduction of scale parameters, the method is also applicable to river dikes (Arcadis, 2015).

The occurrence of a flow slide depends on the profile geometry and the subsoil. The profile geometry can often be determined from open data, like the AHN3. The subsoil properties are more difficult to determine, there is a large uncertainty due to the spatial variability of the subsoil. To deal with this uncertainty, subsoil

scenarios are introduced for the quantification of the probability of occurrence of a flow slide. For each dike-segment (part of a dike-trajectory) a certain amount number of subsoil scenarios are determined. These scenarios are stored as open-data in the WBI-software. (Rijkswaterstaat, 2016b)

#### Probability of occurrence of a flow slide

The probability of occurrence of a flow slide can be determined if the geometry and the subsoil scenarios are known. The probability must be determined per subsoil scenario and the total probability can be determined from the probability of occurrence of a specific subsoil scenario, as shown in Eq. 4.1.

$$P(FS) = \sum P(FS|S_i) \times P(S_i) \quad (4.1)$$

In which:

$$\begin{aligned} P(FS) &= \text{Total probability of flow slide} \\ P(S_i) &= \text{Probability of occurrence of subsoil scenario } i \end{aligned}$$

In the WBI, an equation is described for the frequency of occurrence of a flow slide given a specific subsoil scenario, see Eq. 4.2. Thereafter, the probability of occurrence can be calculated with Eq. 4.3.

$$F(FS|S_i) = \overbrace{\left( \frac{5}{\cot \alpha_r} \right)^5 \times L_{section} \times \frac{V_{local}}{V_{zeeland}} \times 0.025 \times}^{\text{Scaling}} \left[ \underbrace{0.5 \times \left( \frac{H_r}{24} \right)^{2.5} \times \left( \frac{1}{10} \right)^{-10(0.05 + \psi_{5m.kar})}}_{\text{Liquefaction}} + \underbrace{0.5 \times \left( \frac{H_{channel}}{24} \right)^5 \times \left( \frac{2 \times 10^{-4}}{d_{50.mean.kar}} \right)^5 \times F_{cohesivelayers}}_{\text{Breaching}} \right] \quad (4.2)$$

$$P(FS|S_i) = 1 - e^{-F(FS|S_i)} \quad (4.3)$$

This equation has been derived from the statistics of flow slides in Zeeland, by van den Ham et al. (2014) and subsequently updated for the WBI. The equation consists of three parts: a scaling part, static liquefaction part and breaching part. The several parameters of Eq. 4.2 can be divided into three groups: geometry parameters, subsoil parameters and scaling parameters.

The geometry parameters are representing the dike profile properties and can be determined from characteristic dike profile points. The following parameters are the geometry parameters in Eq. 4.2.

- Fictive calculation height  $H_r$
- Calculation slope angle  $\alpha_r$
- Channel depth  $H_{channel}$

The following parameters depend on the subsoil. These parameters must be determined for each subsoil scenario.

- Mean particle diameter  $D_{50.mean.kar}$
- State parameter  $\psi_{5m.kar}$
- Presence of interference layers  $F_{cohesivelayers}$

The scaling parameters are the following parameters:

- Dynamic behaviour of the foreshore  $V_{local}$
- Characteristic value of dynamic behaviour of the foreshore in Zeeland  $V_{zeeland}$
- Length of dike section  $L_{section}$

The explanations of these parameters, and the quantification methods are given in Appendix A.2.

### Exceedance of allowable retrogression length

There are two calculation methods available for the determination of  $P(L > L_{max}|FS)$ . For a flat foreshore, it can be determined with a First Order Reliability Method (FORM) calculation. For non-flat foreshores, which is in practice often the case, the  $P(L > L_{max}|FS)$  can be calculated by numerically solving of the volume balance between area 1 and 2 of the original and post flow slide profile, as indicated in 4.2. (Rijkswaterstaat, 2016b).

The volume balance must be solved with the distribution of the post flow slide profile parameters. The distribution of the parameters has been derived from the earlier-mentioned statistic of 145 historical flow slides in the Dutch province of Zeeland. By determining the post flow slide profile for the limit case  $L = L_{max}$  with the volume balance and subsequently comparing the determined slope of the milder profile part with the theoretical distribution of the milder slope part, the probability of exceedance of the limit case ( $P(L > L_{max}|FS)$ ) can be determined.

#### 4.1.3. Effect of the presence of scour hole on flow slide

The presence of scour holes in river branches increases the probability of flow slides. Both aspects of flow slide, the probability of occurrence of a flow slide and the probability of exceedance of the acceptable retrogression length can be affected by the presence of a scour hole.

##### Effect on probability of occurrence of flow slide

The relevant properties of a profile for flow slide are the geometry parameters ( $H_r$ ,  $\alpha_r$  and  $H_{channel}$ ). These parameters are determined from the characteristic profile points. The presence of a scour hole can lead to a lower located point representative for the river bottom, compared with a situation without a scour hole (hereafter referred to as effect 1). The lower located river bottom increases the value of  $H_{channel}$  and  $H_r$ , which is indicated in figure 4.4. According to Eq. 4.2 and 4.3, a larger  $H_{channel}$  and  $H_r$  results in a higher probability of occurrence of flow slide.

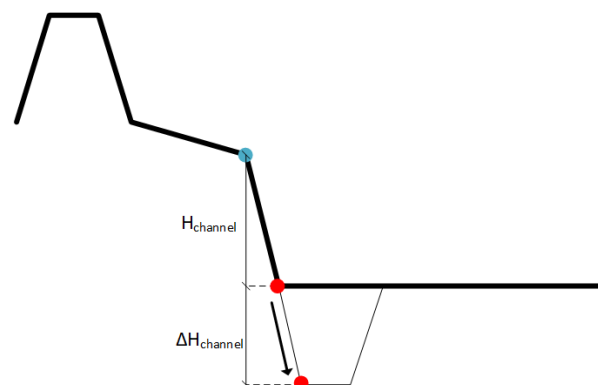


Figure 4.4: Effect of a scour hole on the location of the characteristic river bottom point (effect 1).

##### Effect on retrogression length

The presences of a scour hole may affect the post flow slide profile. The profile consists of two parts, a steep and a mild part. The transition point between the two parts depends on the total height of the profile (Rijkswaterstaat, 2016b). For the maximum allowable situation, the steep slope part starts directly at the dike toe. The slope angle of the mild slope part determines the probability of exceedance of the acceptable retrogression length, as explained in Appendix C. The presence of a scour hole can lead to a larger available surface area for soil material during a flow slide (the area below the new profile line). The larger available surface area results in a larger slope angle of the mild slope part, and thus in a larger probability of exceedance of the acceptable retrogression length (hereafter referred to as effect 2). This effect is schematically shown in figure 4.5a. As a third effect, a scour hole can result in an increase of the total height of the profile, as shown in figure 4.5b (hereafter referred to as effect 3). The location of the transition point is changed, which results in a larger surface area above the new profile line. The milder slope angle can change as a result. Depending on the size of the scour hole (effect 2), and the total increase in profile height (effect 3) the slope angle can be smaller or larger, resulting in a larger or a smaller probability of exceedance of the acceptable retrogression length.

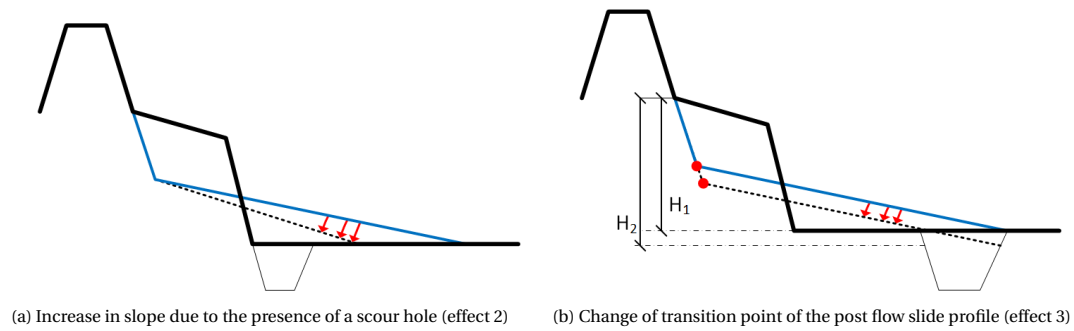


Figure 4.5: Effects of a scour hole on the post flow slide profile.

### Verification of the effects

The three effects are analysed and verified with fictive scour hole development scenarios in Appendix D. In these scenarios, a fictive scour hole is added to a reference profile, and one type of scour hole development is analysed per scenario. The developments are growth in depth (scenario 1), growth in scour hole width (scenario 2) and change of scour hole location with respect to the riverbanks (scenario 3), these scenarios are indicated in figure 4.6.

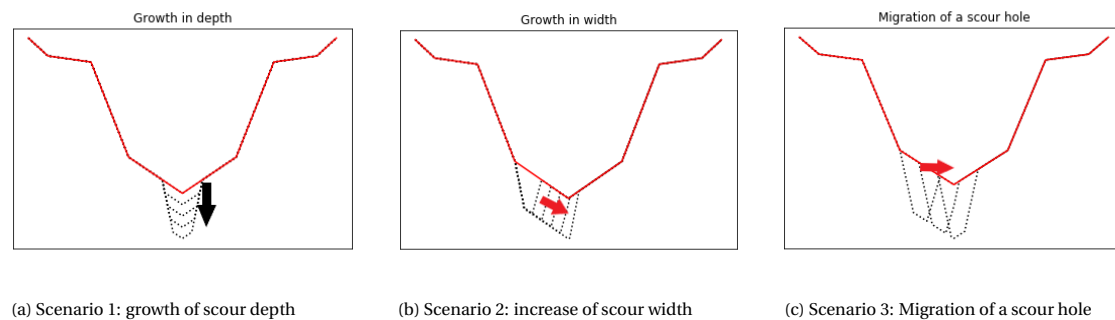


Figure 4.6: Scenarios for scour hole development.

The exact magnitude of the effect of scour hole development on  $P(FS)$  and  $P(L > l_{max}|FS)$  depends on the used reference profile, the dimension of the scour hole, location of the scour hole with respect to the riverside and the growth rate of the scour hole self. However, the following qualitative effects can be observed in the scour hole development analysis.

- If a scour hole increases only in depth, in the first instance only the  $P(L > l_{max}|FS)$  increases. For a certain depth, also the  $P(FS)$  increases.
- If a scour hole increases in width, the location of the characteristic point for the river bottom can be changed. Resulting in a larger  $P(FS)$  (effect 1). The increased scour width gives a larger area to fill. Therefore, the  $P(L > l_{max}|FS)$  increases due to effect 2.
- If a scour hole is migrating from one riverside to the other side. The  $P(FS)$  and  $P(L > l_{max}|FS)$  are affected for both riversides. These probabilities increase for the riverside in the direction of the migration, while both probabilities decrease for the other riverside.

#### 4.1.4. Relation of flow slide with water levels

In the context of flood safety, it is relevant to relate the occurrence of flow slides with the occurrence of certain water levels. Flooding can only happen during periods with high water levels. For both processes which can result in the occurrence of a flow slide, a trigger is required. The trigger cannot be determined from the profile after a flow slide. Many flow slides in the past have been, therefore, described as having occurred as a result of "spontaneous liquefaction", since no clear trigger have been observed (Kramer, 1988).

According to the article of Kramer (1988), in which the relation of 8 historical flow slides without a known trigger are compared with water levels, liquefaction flow slides can occur shortly after a rapid drawdown of the water level near the slopes. The drawdown does not necessarily have to be a large magnitude, small moderately rapid drawdown can already lead to a flow slide. Despite, the larger part of the analysed flow slides occurred during spring low water or periods of exceptionally low tide.

The trigger of breaching flow slide is often a small liquefaction flow slide, sliding or erosion of a part of the underwater slope. These triggers have a larger probability of occurrence during a large rapid drawdown of the water levels (Rijkswaterstaat, 2016b).

Both processes which can lead to flow slides are related to low water levels or drawdown of the water level. Flow slide will, therefore, not directly lead to flooding and failure of the flood defence due to resilient strength of the flood defence. For the safety assessment regarding flow slides, low water levels are considered instead of high water level. In the Dutch safety assessment, flow slide is considered as an indirect failure mechanism (Rijkswaterstaat, 2016b).

#### 4.1.5. Emergency repairs

After a flow slide, emergency or usual repairs can be made to restore the foreshore or the dike. Since the occurrence of flow slide is independent of the water level, there could be enough time for the repair without the occurrence of flooding. The required time and type of (emergency) repair depends on the retrogression length of a flow slide.

In order to restore the dike to the original geometry after a flow slide, a lot of soil must be moved. Therefore, it is often faster and cheaper to construct a new dike behind the affected area (in Dutch: *inlaagdijk*). However, this is only possible if there is enough space to construct a dike, otherwise the original dike must be restored.

The average required repair time for a successful repair is assumed to 60 days. This assumption is based on Van der Krogt (2015), in which is stated that probability of a successful repair within 14 days after the occurrence of a flow slide is 5% and a successful repair within 100 days has probability of 90%.

## 4.2. Direct failure mechanisms

A flow slide does not directly lead to flooding since it is an indirect failure mechanism, as discussed in section 4.1.4. After a flow slide, the flood defence can be (partly) damaged, but often the foreshore is only (partly) eroded. In both cases, the geometry of the dike profile is changed, resulting in reduced strength of the flood defence. This affects some direct failure mechanisms (van der Krogt et al., 2015).

In the context of this research, only the effect of flow slide on the direct failure mechanism overflow/overtopping is analysed in a quantitative way. The effects on other failure mechanisms are qualitatively described.

### 4.2.1. Flow slide and direct failure mechanisms

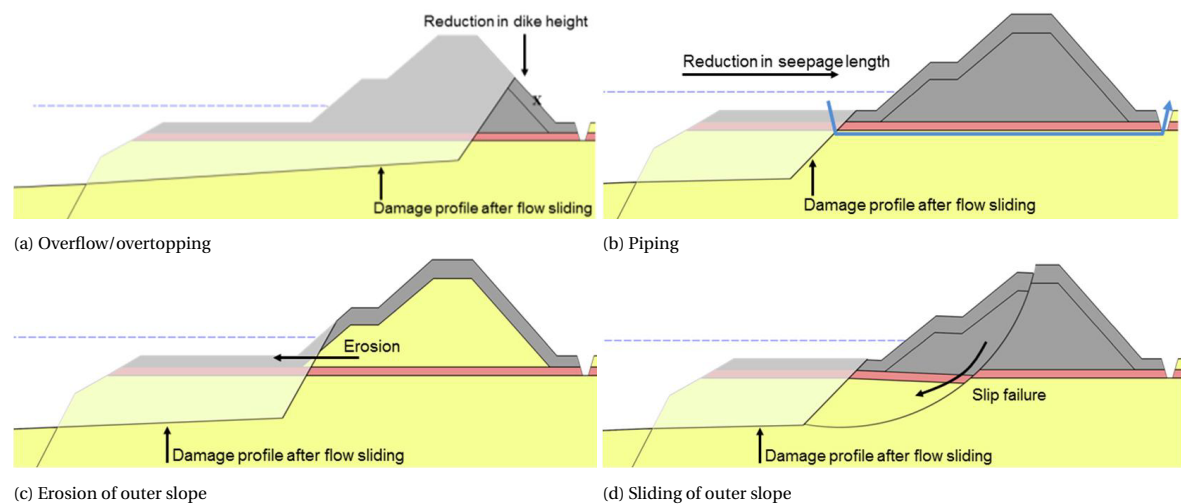
According to van der Krogt et al. (2015), a reduced foreshore length due to the occurrence of a flow slide affects the following four direct failure mechanisms:

- Overflow/overtopping
- Piping
- Erosion of the outer slope
- Macro-instability of the outer slope

The probabilities of occurrence of these mechanisms increase after a flow slide. The effects of flow slide on these mechanisms are schematically shown in figure 4.7. The effect of flow slide on other failure mechanisms, like, micro-instability and macro-instability of the inner slope can be neglected.

#### Overflow

Overflow occurs if the still water level is higher than the crest level of the flood defence. The water flows into the protected area behind the flood defence (Jonkman et al., 2018). If the retrogression length of a flow slide is larger than the foreshore length, a flow slide will damage the flood defence self and the crest height will be reduced. Resulting in an increase of the probability of overflow (van der Krogt et al., 2015). The reduced crest height due to a flow slide is shown in figure 4.7a.



Source: van den Ham (2015)

Figure 4.7: Effect of flow slide on relevant direct failure mechanisms

### Wave overtopping

During wave overtopping, the still water level remains below the crest level. The overtopping is a result of wave run up on the slope of the flood defence. Wave overtopping can damage the grass cover of the inner slope of the dike. This failure mechanism is typically relevant for sea dikes (Jonkman et al., 2018). However, ship induced waves are also present in river branches. A flow slide results in deepening of the foreshore and steepening of the dike slope. This results in less wave breaking on the foreshore and thus an increase in wave load and larger wave overtopping volumes. However, the resistance of the grass cover is usually large than the increased wave load. Therefore, the influence of flow slide on the failure mechanism wave overtopping can be neglected if only the foreshore is affected by a flow slide (Van der Krogt, 2015). If the crest height is reduced due to a flow slide, a higher overflow discharge can be expected and the effect of a flow slide can no longer be neglected.

### Piping

Pipes (cavities or channels) can form in the subsoil, if the hydraulic gradient towards the land-side is sufficiently high. The pipes can grow from the land-side towards the water-side and could undermine the dike. This can result in collapsing of the dike. The reduction of the foreshore due to a flow slide lead in a shortening of the seepage path and increases the probability of occurrence of the failure mechanism piping (Van der Krogt, 2015). Therefore, flow slide will influence the failure mechanism of piping, see figure 4.7b.

### Erosion outer slope

Erosion of the outer slope is also called revetment failure. Dikes are usually protected against erosion from waves and current with a revetment (cover layer). For river dikes, a grass layer on top of a clay layer is often sufficient as a cover layer against erosion. The main function of the cover layer is to prevent the soil body of a flood defence from direct contact with erosive forces (Jonkman et al., 2018). When the retrogression length of a flow slide is up to the cover layer, the cover layer can be damaged. The soil body is no longer protected against erosive forces and thus erosion can occur. Resulting in less soil mass and affection of the water retaining function of a dike. The interaction between flow slide and erosion of the outer slope cannot be neglected. The interaction is shown in figure 4.7c. (van der Krogt et al., 2015)

### Micro-instability

If the inner slope consists of permeable, granular material, grains of the inner slope can be pushed off the cover layer due to high pore pressure. This is called micro-instability and can result in internal erosion (Jonkman et al., 2018). Flow slides may influence the pore pressure distribution in the sand core of the dike. This can increase the probability of micro instability. However, this only happens if the impermeable cover of a sand dike is already damaged. Since this is part of the failure mechanism erosion outer slope. The interaction of flow slide and micro-instability can be ignored.

### Sliding inner slope

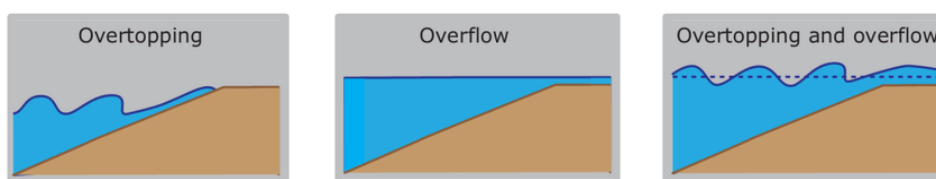
The inner slope can become unstable during rising water levels. Rising water gives higher pore pressures and lower effective stresses. This reduces the shear strength of the soil. For a stable slope, the resistance (shear strength and horizontal pressure of resisting volumes) is higher than the load (soil weight). A decrease in shear strength can lead to instability. A slide plane can develop (Jonkman et al., 2018). As described earlier, flow slide may influence the water pressure in the sand dike, which affects the shear strength. However, the interaction between inner slope stability and flow slide can be ignored for the same reasons as micro-instability.

### Sliding outer slope

Similar to the inner slope, the stability of the outer slope depends on the load (weight of the soil) and the resistance (shear stresses and resisting volumes of foreshore). Sliding of the outer slope can be initiated if the outside water level drops very quickly. The pore water inside the dike body cannot follow the water level. The load remains equal, while the resistance decreases due to lower horizontal pressure in the foreshore (Jonkman et al., 2018). A flow slide can also result in sliding of the outer slope. Since a flow slide reduces the soil volumes of the foreshore and thus decreases the resistance for sliding planes on the outer slope (van der Krogt et al., 2015). There is thus an interaction between flow slide and the stability of the outer slope. The effect is indicated in figure 4.7d.

### 4.2.2. Overtopping/overflow

The two failure mechanisms overflow and wave overtopping have similarities. In both, as schematically indicated in figure 4.8, water flows over the dike and inundation occurs. For overflow, the water level is higher than the crest level and there is a continuous flow of water over the dike. For wave overtopping the still water level is below the crest level and water flows only over the dike due to the run-up of waves. The discharge of water over the dike is significant lower for wave overtopping. Overtopping and overflow can occur at the same time, as indicated in figure 4.8(right). This happens if the still water level is above the crest level and at the same moment waves are present (Jonkman et al., 2018).



Source: S. den Hengst, 2012

Figure 4.8: Schematisation of overflow and wave overtopping

### Events for flooding

During overflow, there is a larger amount of water flowing over the dike. It can directly be stated that there is failure of the dike. This is not the case for wave overtopping, since the volume of water can be limited and no significant damages in the protected area occur. However, the overtopped water can damage the inner grass cover of the dike. Subsequently, erosion of the inner slope follows than, which results finally in a lower crest level and a continuous overflow. The events required for flooding for both mechanisms are shown in figure 4.9.

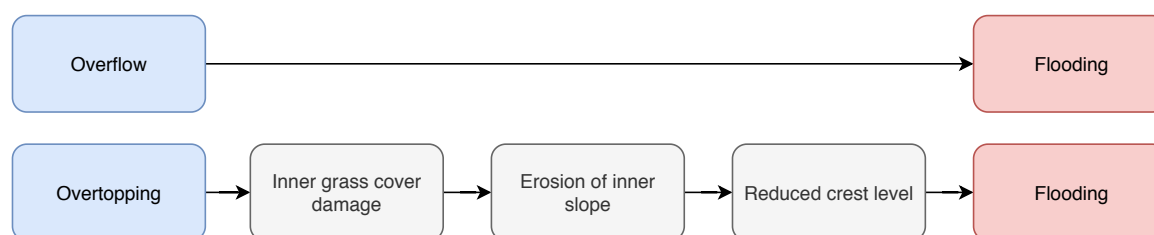


Figure 4.9: Events required for flooding for overflow and wave overtopping

### Limit state functions

The critical state of overflow is determined by the water level. If the water level is larger than the crest level overflow occurs, see Eq. 4.4. The limit state function for overflow, Eq. 4.5, follows from Eq. 4.4 :

$$h_w > h_c : failure \quad (4.4)$$

$$Z_{overflow} = h_c - h_w < 0 : failure \quad (4.5)$$

In which:

$$\begin{aligned} h_c &= \text{Dike crest height} & [\text{m} + \text{NAP}] \\ h_w &= \text{Still water level} & [\text{m} + \text{NAP}] \end{aligned}$$

The overtopped discharge determines the critical state for wave overtopping, as presented in Eq. 4.6. The critical discharge value depends on the grass cover resistant. If the overtopped discharge exceeds the critical value, a dike failure is considered. It is likely that only the grass cover is removed if the critical discharge is exceeded. The underlying soil may have some residual strength, which means that there is not directly flooding. However, this is not taken into account in the Dutch safety assessment (Jonkman et al., 2018).

$$q_o > q_c : failure \quad (4.6)$$

$$Z_{overtopping} = q_o - q_c < 0 : failure \quad (4.7)$$

In which:

$$\begin{aligned} q_c &= \text{Critical overtopping discharge} & [\text{l/s/m}] \\ q_o &= \text{Actual overtopping discharge} & [\text{l/s/m}] \end{aligned}$$

Usually, the probability of exceedance of the critical overtopping is larger than the probability of exceedance of the critical water level. The failure mechanism of overtopping is, therefore, more relevant than overflow.

### Overtopping discharge

The overtopping discharge depends on water levels, wave conditions, flood defence properties and energy dissipations in the foreshore and during the run-up. In the wave overtopping manual (EurOtop, 2018), the following expression is given for the calculation of the overtopping discharge for a design or assessment approach. This expression can be used if the wave conditions, water level and flood defence properties are known.

$$\frac{q}{\sqrt{g \times H_{m0}^3}} = \frac{0.026}{\sqrt{\tan \alpha}} \gamma_b \times \xi_{m-1,0} \times \exp \left[ - \left( 2.5 \frac{R_c}{\xi_{m-1,0} H_{m0} \gamma_b \gamma_f \gamma_\beta \gamma_v} \right)^{1.3} \right] \quad (4.8)$$

With a maximum of:

$$\frac{q}{\sqrt{g \times H_{m0}^3}} = 0.1035 \times \exp \left[ - \left( 1.35 \frac{R_c}{H_{m0} \gamma_f \gamma_\beta \gamma^*} \right)^{1.3} \right] \quad (4.9)$$

In which:

$$\begin{aligned} q &= \text{Overtopping discharge} & [\text{l/s/m}] \\ R_c &= \text{Freeboard} & [\text{m}] \\ g &= \text{gravitational constant} & [\text{m}^2/\text{s}] \\ H_{m0} &= \text{Significant wave height} & [\text{m}] \\ \xi_{m-1,0} &= \text{Iribarren number} & [-] \\ \tan \alpha &= \text{slope} & [-] \\ \gamma_b &= \text{Berm effect factor} & [-] \\ \gamma_{bf} &= \text{Roughness factor} & [-] \\ \gamma_\beta &= \text{Factor for oblique wave approach} & [-] \\ \gamma_v &= \text{Factor for vertical walls} & [-] \\ \gamma^* &= \text{Factor for non-breaking waves} & [-] \end{aligned}$$

### Critical overtopping discharge

The critical overtopping discharge depends on the erosion resistance of the inner slope. The quality of the grass in combination with the soil determine the erosion resistance. From tests follows that high-quality grass on a clay layer can resist an overtopping discharge of 30 [l/s/m] without failing. (Jonkman et al., 2018)

In the ‘Schematiseringshandleiding grasbekleding’ of the WBI (Rijkswaterstaat, 2018), distributions are given for the critical overtopping discharge for different wave height class and the quality of the grass layer. With these distributions, a detail safety assessment calculation can be done for the resistance of the grass cover in the WBI-software ‘Riskeer’.

In this research, a deterministic value of 5 [l/s/m] will be used for the critical overtopping discharge. This value is mentioned in simplified check in the WBI as the critical overtopping discharge for a closed grass cover on a clay layer of at least 0.4 [m] (Rijkswaterstaat, 2017). The effect of the usage of a deterministic value could be analysed in a sensitivity analysis.

### Hydra-NL

For the safety assessment regarding overtopping and overflow, the WBI-software Hydra-NL can be used. Hydra-NL is developed by HKV Lijn in Water and Rijkswaterstaat WVL (Duits, 2018). In Hydra-NL, for defined dike profiles the Hydraulisch Belasting Niveau (HBN) (in English: Hydraulic load level) for a specified overtopping discharge is determined. The HBN is determined from the combination of water levels, wave conditions and wave run-up. These local conditions on which the calculation of the HBN is based, are predefined in hydraulic boundary-condition databases and delivered together with the WBI-software. The minimum required crest level of a flood defence is equal to the HBN.

In Hydra-NL, the HBN is calculated together with the return period for exceeding the critical overtopping discharge. The calculation is done for all defined conditions of the hydraulic boundary-condition database. In addition, model uncertainties for water levels, wave heights and wave periods are taken into account. Moreover, for the water levels in the RMD, the failure probability of the storm surge barriers are included (Duits, 2018).

The calculation procedure in Hydra-NL is as follows:

1. Linking of dike trajectory locations to hydraulic location of the WBI-Database.
2. Assigning dike profiles to dike trajectory locations.
3. Calculation of HBN based on a specified critical overtopping discharge.

In the profile definition, a foreshore can be defined. When a foreshore is included in the profile, the hydraulic loading conditions are set to the beginning of the foreshore. With the foreshore-module of Hydra-NL, the wave energy dissipation on the foreshore is calculated and the new hydraulic conditions for the dike toe are determined. Based on these conditions the wave-overtopping is calculated.

The output of Hydra-NL is a frequency curve of the HBN. The return period of the HBN corresponding to the actual crest level (or any other level) can be determined from the frequency curve. For return periods larger than 1/100.000 year or smaller than 1/10 year, the return periods are obtained by extrapolation of the frequency curve (Duits, 2018).

## 4.3. Probability of flooding

With the assumption that exceedance of the critical overtopping discharge immediately lead to a flood, the probability of flooding due to overtopping is equal to the probability of exceedance of the critical overtopping discharge.

Scenarios are used for the calculation of the total probability of exceedance of the critical overtopping discharge. In this way, the probability of flow slide, successful emergency repairs and exceedance of the critical overtopping discharge are combined for the total probability calculation. The scenarios are presented in an event tree in figure 4.10. This event tree, represent the following equation for the probability calculation of exceedance of the critical overtopping discharge:

$$\begin{aligned}
 P(q_o > q_c) &= P(q_o > q_c | \text{No FS}) \times (1 - P(\text{FS})) \\
 &+ P(q_o > q_c | \text{FS} \& \text{Repair}) \times P(\text{FS}) \times P(\text{Repair}) \\
 &+ P(q_o > q_c | \text{FS} \& \text{No repair}) \times P(\text{FS}) \times (1 - P(\text{Repair}))
 \end{aligned}
 \tag{4.10}$$

In which:

|  |   |  |
|--|---|--|
| $P(q_o > q_c)$                                 | = | Total probability of exceedance critical overtopping discharge |
| $P(q_o > q_c   \text{No FS})$                  | = | $P(q_o > q_c)$ without flow slide                              |
| $P(q_o > q_c   \text{FS} \& \text{Repair})$    | = | $P(q_o > q_c)$ with flow slide and successful repair           |
| $P(q_o > q_c   \text{FS} \& \text{No Repair})$ | = | $P(q_o > q_c)$ with flow slide and without successful repair   |
| $P(\text{FS})$                                 | = | Probability of occurrence of a flow slide                      |
| $P(\text{Repair})$                             | = | Probability of a successful repair after a flow slide          |

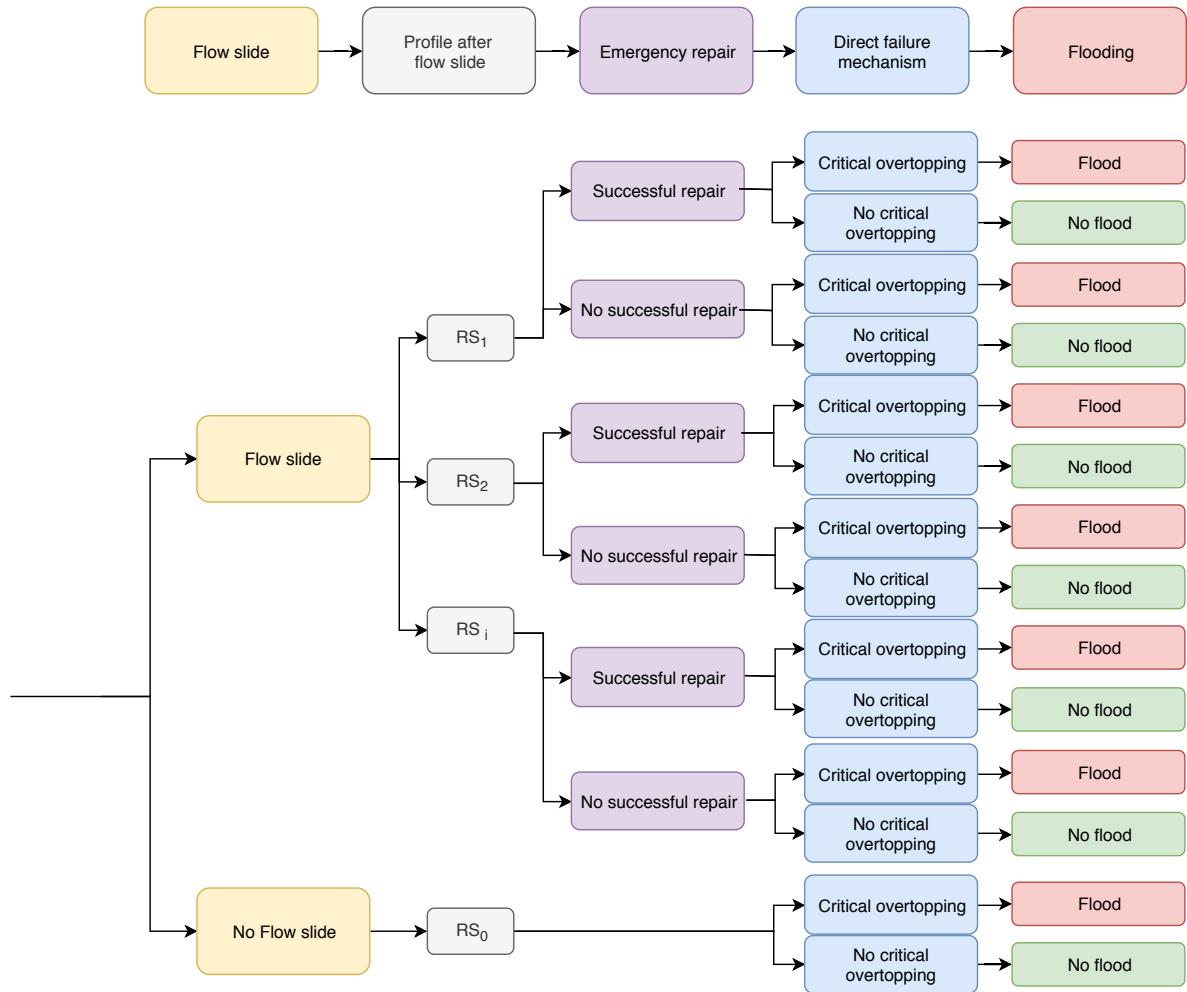


Figure 4.10: Event tree for failure mechanism overtopping including conditional probability of flow slide

The conditional probability of exceedance of the critical overtopping discharge depends on the retrogression length of the post flow slide profile. For example, the probability will be larger if there is a reduction of the crest height in the post flow slide profile compared with a situation in which only the foreshore is affected by a flow slide. Instead of using continuous foreshore lengths, some discrete retrogression states ( $RS_i$ ) are defined. The conditional probability  $P(q_o > q_c | \text{FS})$  can be determined from these retrogression states. These states can be, for example, a retrogression up to 50% of the foreshore, retrogression up to dike top or retrogression up to a dike height reduction of a few meters. The retrogression states self and the number of retrogression states must be based on the original dike profile and differs per location.

The conditional probability can subsequently be calculated with:

$$P(q_o > q_c | FS) = \sum_{i=1} P(q_o > q_c | RS_i \& FS) \times P(RS_i | FS) \quad (4.11)$$

In which:

$$\begin{aligned} PP(q_o > q_c | RS_i \& FS) &= \text{Probability of exceedance critical overtopping discharge given } RS_i \text{ and FS} \\ P(RS_i | FS) &= \text{Probability of occurrence of retrogression state } RS_i \text{ given flow slide} \end{aligned}$$

## 4.4. Consequences

It can be stated that a flood defence is failed, if there is an inflow of water into the area behind the flood defence. The water will damage objects and can cause fatalities in the affected area. The flood damage and fatalities are called hereafter consequences.

The magnitude of the consequences of a flood varies strongly per breach location. In densely populated areas, like large parts of the RMD, the consequences of a flood are much larger than in less populated rural areas. The exact damage depends on the land elevation of a dike ring, the land use functions and the location of a breach in the dike (Jonkman et al., 2018).

In the period between 2006 and 2014, a nationwide flood risk assessment study has been executed for the Netherlands, called Veiligheid Nederland in Kaart (VNK2) (Vergouwe et al., 2014). The consequences determined in VNK2 can be used for the risk assessment of scour holes in the RMD.

### 4.4.1. Type of consequences

In general, the consequences caused by a flood can be divided into tangible and intangible damages (Jonkman et al., 2018). The tangible damages can be expressed in monetary value and are, for example, damage of vehicles, buildings and infrastructure. While the intangible damages cannot be expressed in monetary value. Examples of intangible damages are fatalities and cultural, historical and environmental losses.

#### Economic damage

The economic damage is the sum of all tangible damages. To determine the total economic damages of a flood, insight is needed in flood characteristic, number and type of land use function affected by the flood, the value of objects in the affected area and the damage of land use functions given a certain level of flood (Jonkman et al., 2018).

#### Loss of life

A flood can result in fatalities. Not all people in the affected area will lose their life. A part of the people is able to leave the area before the flood (evacuation) and a part will survive. The potential loss of life depends on the flood characteristic and the number of people in the affected area. In addition, the possibilities to predict, warn and evacuate people determine the loss of life. The loss of life can be estimated according to Jonkman et al. (2018) as follows:

$$N_{loss} = F_D(1 - F_E) \times N_{par} \quad (4.12)$$

In which:

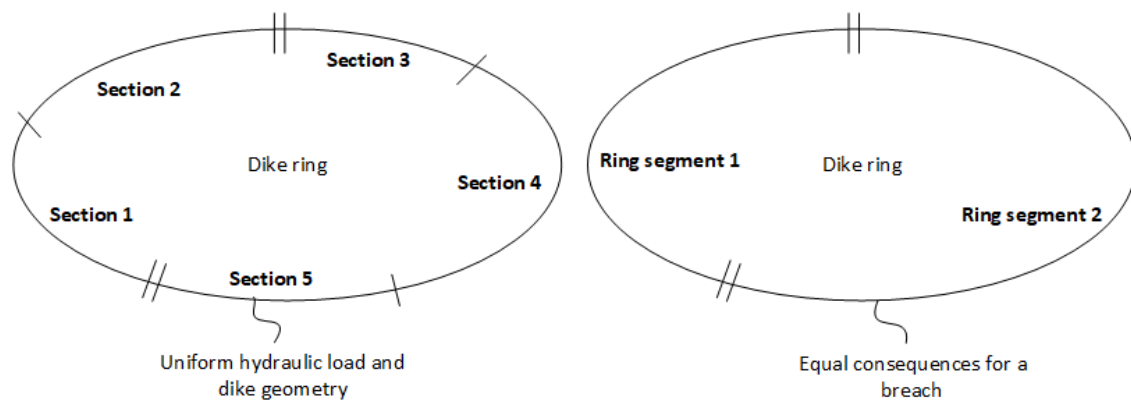
$$\begin{aligned} N_{loss} &= \text{Loss of life estimation} \\ N_{par} &= \text{Number of people at risk} \\ F_D &= \text{Mortality fraction} \\ F_E &= \text{Evacuation fraction} \end{aligned}$$

In order to compare and analyse the fatalities together with the economic damage in a cost-benefit analysis, the value of statistic life can be used. In the Netherlands, a value of €6.7 million per fatality is used for the analysis of flood defences. This value is obtained from surveys, which reveal how much people are willing to pay for safety measures. (Deltares, 2011; Jonkman et al., 2017)

#### 4.4.2. Risk assessment in the Netherlands

In VNK2, a risk assessment study is performed for 58 dike rings in the Netherlands. The actual probability of flooding and the consequences of flooding are determined, in order to analyse the flood risk in the Netherlands. The results of the study enable an evaluation of risk mitigation measures in order to protect the land in a cost-efficient way. The results are also used as input for the derivation of new flood safety standards. (Vergouwe et al., 2014)

In the study, a clear distinction is made for the probability of flooding and the consequences of flooding. For both, the dike ring is divided into several parts, as can be seen in figure 4.11. The probability of occurrence of several failure mechanisms is determined per dike section (in Dutch: dijkvak) and the consequences are determined as flood scenarios per ring segment (in Dutch: ringdeel). The hydraulic load and the dike geometry properties are uniform per dike section. For a ring segment holds that the total consequences of flood and the flooding pattern are equal regardless of the precise breach location within the segment. A ring segment can consist of multiple dike section. To get the probability of occurrence of a flood scenario, the different failure mechanisms of the multiple dike section are combined, including the dependencies between the failure mechanisms and the dike sections. (VNK2 Projectbureau, 2012)



Source: Own creation based on VNK2 Projectbureau (2012)

Figure 4.11: Schematisation of dike sections and ring segments in VNK2

Per dike ring, a certain amount of flood scenarios are determined. A flood scenario consists of failure of one or a combination of failing ring segments. The flood pattern, water depths, velocity and rise rate are determined for each flood scenario with flood propagation models. The flood pattern depends on the moment of the dike breach. There is more inflow of water if a dike fails during the highest outer water level than during lower water levels. In order to take this effect into account, the flood propagation models are run with different outer water levels.

Two types of damages are analysed for the flood scenarios. These are the expected economic damage (total tangible damages) and the expected fatalities. Other intangible damages are not taken into account in the analysis (B. R. de Groot, 2014). The expected economic damage is expressed in Euros per scenario and the expected fatalities in number per scenario. The consequences are determined in VNK2 with the consequence model HIS-SMM. Since each scenario has a different flood pattern, the consequences are also different for each scenario. (VNK2 Projectbureau, 2012)

#### 4.5. Risk quantification

According to the definition of risk given in Chapter 1, 'Risk is the probability of a flood event multiplied by the consequences, the probability of a flood and the consequences must be known for the risk quantification.

In general, the total flood probability is the sum of the probability of occurrence of different failure mechanisms, with their dependency and length effects taken into account. However, in this research, only the probability of flooding due to exceedance of the critical overtopping discharge next to a scour hole is analysed. The failure mechanism overtopping suits the best for the integration in a general approach for the risk

estimation of scour holes since the mechanism mainly depends on the dike geometry properties, which are relatively easy to determine without a large uncertainty. While other failure mechanisms also depend on subsoil properties, which are more difficult to determine, especially in the RMD because of the large variability in the subsoil.

The probability of a flood due to the presence of a scour hole can be determined with the event tree shown in figure 4.10. The consequences of a flood can be taken from the reports of VNK2.

The flood risk calculated with the probability of flooding due to overtopping is thus not equal to the total flood risk of a certain area. It is only the part of the total flood risk due to the presence of the scour hole for the failure mechanism overtopping.

*(This page is intentionally left blank)*

# 5

## Risk assessment

This chapter contains the risk assessment of scour holes. First, the locations with potential risk are identified for the connecting branches in the RMD. Subsequently, the method for the risk assessment of individual scour holes is given. This method is applied to one case study, a scour hole located in the Spui. Finally, a sensitivity analysis is executed in order to identify the important parameters in the risk assessment process.

### 5.1. Locations with potential risk

In Appendix F, a quickscan is applied for the identification of locations with potential risk is applied to three of the connecting river branches in the RMD. According to the quickscan, there are totally four locations in these branches with a potential risk for flow slide. These locations are shown in figure 5.1 and mentioned per river branch in table 5.1.

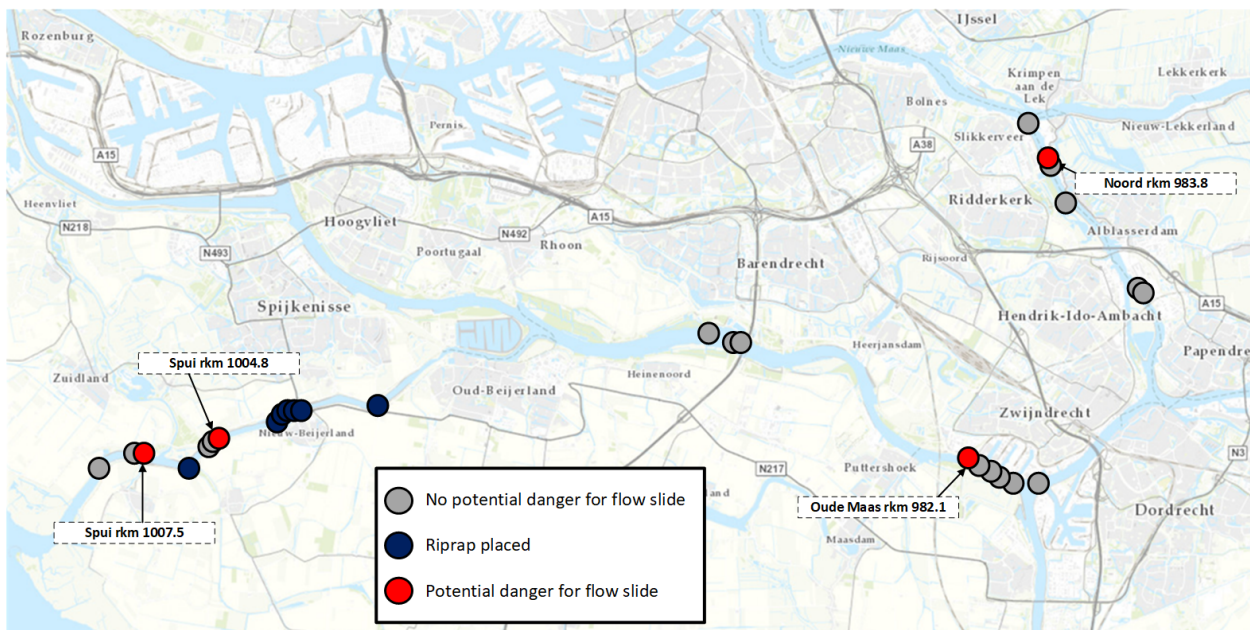


Figure 5.1: Overview of the scour hole locations in the Spui, Noord and eastern part of the Oude Maas. The scour holes with a potential danger for flow slide and scour holes with placed riprap are indicated.

For an entire river branch, the probability of occurrence of a flow slide ( $P(FS)$ ) and the probability of exceedance of the maximum allowable retrogression length are calculated. For these three river branches, river cross-section profiles are determined, each 10 [m] based on the Actueel Hoogtebestand Nederland (AHN3), baselinemodel (Helpdesk Water, 2015) and the most recent bathymetry data.

| River branch                   | Total scour holes | Locations with potential risk |
|--------------------------------|-------------------|-------------------------------|
| Spui (15km)                    | 13                | 2                             |
| Oude Maas (eastern part)(15km) | 10                | 1                             |
| Noord (9km)                    | 6                 | 1                             |
| Total                          | 29                | 4                             |

Table 5.1: Locations with potential risk and total number of scour holes in the connecting river branches.

For each river profile, the  $P(FS)$  is calculated with the method described in the WBI, as indicated in Eq. 4.2 and Eq. 4.3 (Rijkswaterstaat, 2016b). Subsequently, the  $P(L > L_{max}|FS)$  is determined with the volume balance applied to the post flow slide profile. For the calculation of  $P(FS)$  one subsoil scenario with conservative parameters is used in the quickscan. It is assumed that the maximum allowable retrogression length equals the actual local foreshore length.

The probabilities are only calculated for dike section with a foreshore length of less than 300 m. It is assumed that the probability of exceedance of the maximum allowable retrogression length is negligible for large foreshore lengths. The total probability is compared with the required probability of  $P_{required} = 0.01$  [1/yr/km] given in the WBI (Rijkswaterstaat, 2017).

The sections which are exceeding this value are indicated in figure 5.2. These sections are further analysed to determine the reason of the larger probability. The reason can be 1) the presence of a scour hole, 2) a steep slope or 3) an error in the determination. Finally, the presence of bank protection is checked for 1) and 2). The locations with a higher probability than 0.01 due to the presence of a scour hole without bank protections are identified as locations with potential risk for flow slide, see figure 5.1. The scour hole locations with placed riprap are also indicated in this figure.

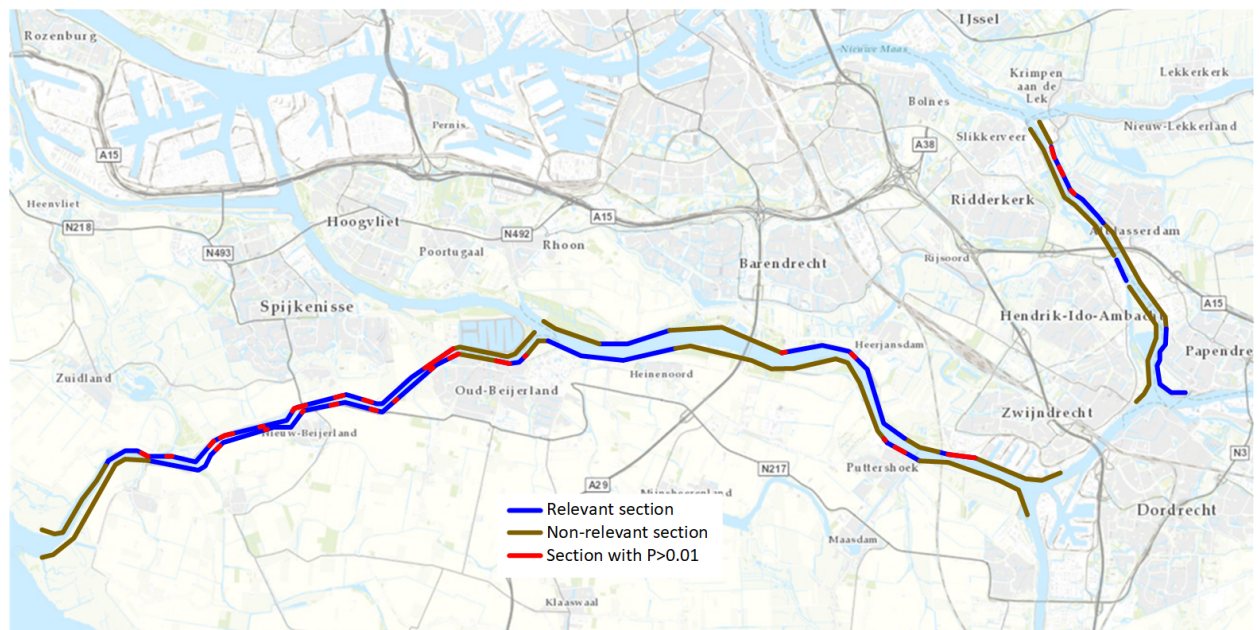


Figure 5.2: Overview of the relevant sections for the quickscan and the sections with a large probability of occurrence of a flow slide in the Spui, the Noord and eastern part of the Oude Maas.

## 5.2. Method for risk assessment of individual scour holes

For the scour holes identified as a potential risk for the occurrence of flow slide, the actual flood risk must be assessed. The scour hole development prediction, explained in chapter 3, is combined with the calculation methods for the probability calculation of flooding, mentioned in chapter 4, to a method for the risk assessment of scour holes. In Appendix E the method is explained. The method consists of 8 steps. In figure 5.3 an overview of the method is schematically indicated together with the relevant input and results per step.

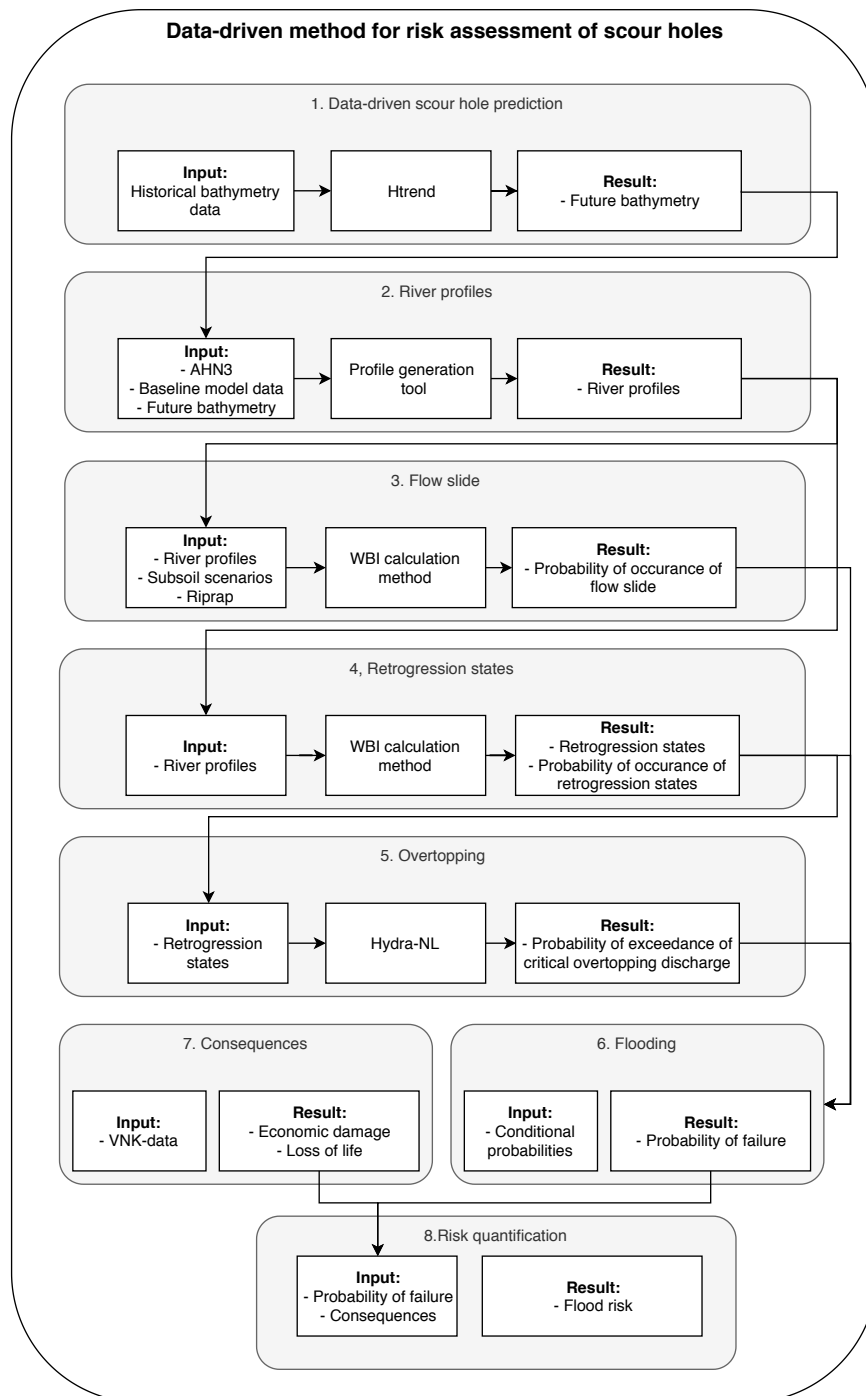


Figure 5.3: Overview of the data-driven method for risk assessment of scour holes.

### 5.3. Case Spui rkm 1004.8

At the Spui, around the river bend at rkm 1005, a cluster of three scour holes is located as shown in figure 5.4. The eastern scour hole of these three, is the most interesting scour hole in the context of this risk assessment since this scour hole is growing in depth and surface. Moreover, this scour hole is located close to the right riverbank and near the scour hole the foreshore length is relatively small.

The risk assessment for this scour hole is only performed for the right riverside. The dike on this riverside is part of dike-trajectory 20-3. The maximal acceptable flooding probabilities for this dike-trajectory is 1/10.000 [1/yr].

The edge level of this scour hole is located at  $-12.8$  [m + NAP]. All bed level points, which are lower located than this level are considered as part of the scour hole (Huismans & van Duin, 2016).

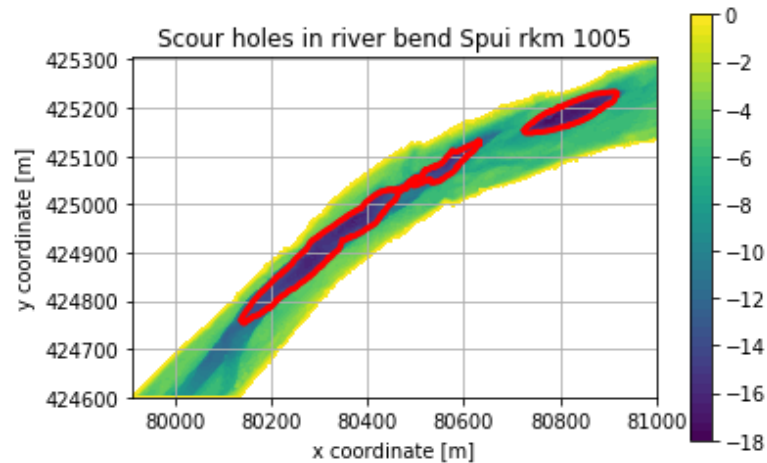


Figure 5.4: Bathymetry around the river bend in the Spui near rkm 1005 with indication of three scour holes.

This scour hole has currently a dynamic behaviour. The scour hole is growing in surface and in depth, as can be seen in table 5.2. The deepest point of the scour hole increases with about  $15 - 20$  [cm/year]. The scour hole is growing in length at both ends. This can be seen in figure 5.5. Besides, the scour hole is also growing in width. However, the growth in width is smaller than the growth in length. The scour hole is growing towards both riversides. The growth towards the left riverside (Northwest) is larger than towards the right riverside (Southeast).

| Year | Deepest point [m NAP] | Surface [m <sup>2</sup> ] | Length [m] | $W_{max}$ [m] |
|------|-----------------------|---------------------------|------------|---------------|
| 2014 | -16.98                | 6080                      | 182        | 44            |
| 2015 | -17.164               | 6281                      | 182        | 44            |
| 2016 | -17.379               | 6530                      | 190        | 46            |
| 2017 | -17.493               | 6725                      | 200        | 46            |
| 2018 | -17.705               | 6915                      | 200        | 47            |

Table 5.2: Overview of growth of the case scour hole

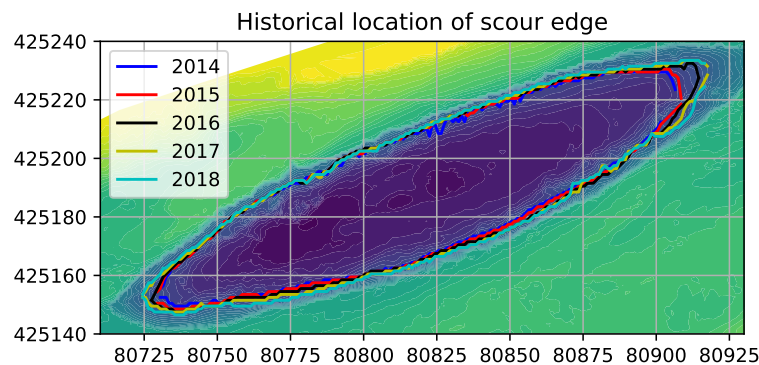


Figure 5.5: Historical locations of the scour hole edges.

The risk of this scour hole is assessed with the method shown in figure 5.3. The results per steps are briefly presented for the scour hole situation in 2018 and the predicted situation for 2023. The full calculations and step descriptions are given in Appendix G.

### 1. Data-driven scour hole prediction

With Htrend 300 runs are made for the prediction of the bathymetry in 2023. From these model results, a range of future scour hole bathymetry is determined. The bathymetry of 2016, 2017 and 2018 is used as input in Htrend for the horizontal extrapolation. The vertical erosion rate file, is in each run generated from the bed level erosion rate relation, based on the bathymetry in the period between 2014 and 2018.

The properties of the mean, 5% and 95% scour holes are presented in table 5.3. The predictions of the locations of the scour edges are indicated in figure 5.6.

| Scenario        | Deepest point [m NAP] | Surface [m <sup>2</sup> ] | Length [m] | $W_{max}$ [m] |
|-----------------|-----------------------|---------------------------|------------|---------------|
| 2018 scour hole | -17.705               | 6915                      | 200        | 47            |
| 5% percentile   | -17.895               | 6848                      | 206        | 46            |
| mean            | -18.252               | 7080                      | 210        | 48            |
| 95% percentile  | -18.672               | 7282                      | 212        | 49            |

Table 5.3: Overview of scour hole characteristic for the three growth scenarios.

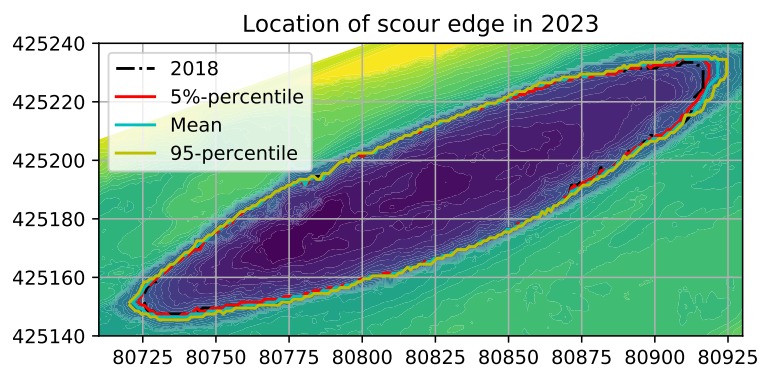


Figure 5.6: Predicted locations of the scour edge in 2023 for three growth scenarios.

### 2. River profiles

River cross-section profiles are generated from AHN3, baseline model data and bathymetry data. The predicted bathymetry for 2023 and the historically measured bathymetry in the period between 2014 and 2018 are used as bathymetry input. For each bathymetry dataset, 130 river profiles are generated, with an intermediate distance of 2.0 [m]. The scour hole had a length of 200 [m] in 2018. However, a larger section is considered in order to take future growth also into account. The considered section is shown in figure 5.7.

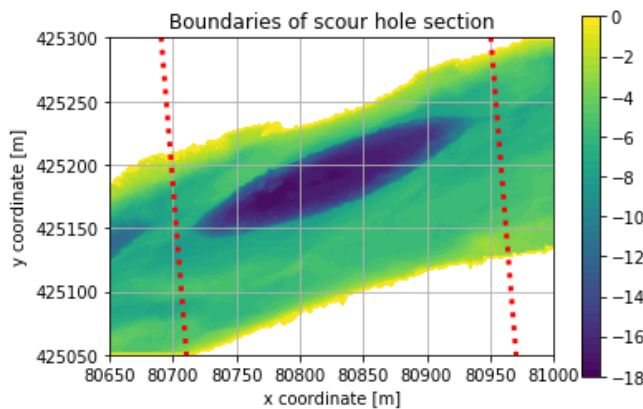


Figure 5.7: Boundaries of the considered scour hole section.

### 3. Flow slide

The probability of occurrence of a flow slide can be calculated from the river profiles geometries and subsoil parameters. The dike section next to the scour hole is located in dike-segment 20-01, for this dike-segment six subsoil scenarios are given in the WBI-Database (Helpdesk Water, 2017). For each scenario, the required subsoil parameters are estimated and the geometry parameters are determined for all generated river profiles for each year.

The values for the subsoil parameters differ from the values used in the quickscan. In the quickscan conservative parameters are used, while for the risk assessment of the scour hole more reliable values are used based on the subsoil scenarios of the WBI.

In table 5.4 the calculated probability of occurrence of a flow slide ( $P(FS)$ ) is shown together, based on the historically measured bathymetry. Subsequently, in table 5.5, the same is presented for the predicted bathymetry in 2023. As can be seen, the probability increased in the last couple of years. This will also continue in the near future according to all three scenarios.

| Year    | 2014   | 2015   | 2016   | 2017   | 2018   |
|---------|--------|--------|--------|--------|--------|
| $P(FS)$ | 0.0105 | 0.0104 | 0.0104 | 0.0107 | 0.0112 |

Table 5.4: Historical probability of the occurrence of a flow slide for the dike section near the scour hole.

| Scenario | 5% percentile | mean   | 95% percentile |
|----------|---------------|--------|----------------|
| $P(FS)$  | 0.0124        | 0.0152 | 0.0194         |

Table 5.5: Probability of the occurrence of a flow slide in 2023 for different scour hole development scenarios.

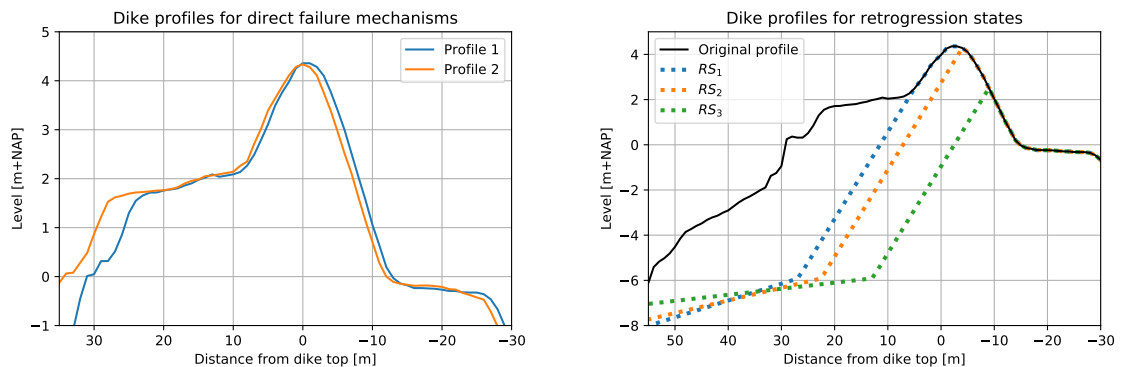
### 4. Retrogression states

The dike geometry over the considered section next to the scour hole is quite uniform. There is only a small deviation in the foreshore length. This length is between 17 and 21 [m]. Two of the 130 river profiles are used as representative profiles for the determination of the retrogression states and the probability of occurrence of these states.

The following retrogression states are used for the risk assessment:

1. Retrogression up to the dike toe ( $RS_1$ ).
2. Retrogression up to the dike top at landside ( $RS_2$ ).
3. Retrogression resulting of a dike height reduction of 2.0 m. ( $RS_3$ ).

The retrogression states and the two representative profiles are shown in figure 5.8. As can be seen in this figure, the profiles have different foreshore lengths.



(a) Representative dike profiles for determination of retrogression states. (b) Retrogression states.

Figure 5.8: Dike geometry of the representative profiles for the retrogression states and the three used retrogression states for the case scour hole.

The probability of occurrence of the retrogression states is determined with the volume balance between the original profile and the post flow slide profile. The probability depends on the scour hole dimensions and changes with the scour hole growth. In table 5.6, the probabilities are shown for 2018 and the three scenarios for the future scour hole. As can be seen in the table, the probability of occurrence of the first retrogression state decreases for the future scour hole scenarios, while the probability of the third retrogression state increases. A larger retrogression length after a flow slide can thus be expected due to the scour hole development.

|             | $P(RS_1 FS)$ | $P(RS_2 FS)$ | $P(RS_3 FS)$ |
|-------------|--------------|--------------|--------------|
| 2018        | 0.27         | 0.56         | 0.17         |
| 2023 (5%)   | 0.26         | 0.57         | 0.17         |
| 2023 (mean) | 0.23         | 0.57         | 0.20         |
| 2023 (95%)  | 0.19         | 0.57         | 0.24         |

Table 5.6: Conditional probability of occurrence of the retrogression states, for 2018 and the future scour hole scenarios.

## 5. Overtopping

The probability of exceedance of the critical overtopping discharge is calculated for the original dike profile and the three retrogression states in Hydra-NL. This is calculated for a critical overtopping discharge of 5.0 [l/s/m]. The probability of exceedance and the corresponding average return period to this probability are presented in table 5.7.

|                         | $q_c = 5.0$ [l/s/m]    |                    |
|-------------------------|------------------------|--------------------|
|                         |                        | Return period [yr] |
| $P(q_o > q_c RS_1\&FS)$ | $1.957 \times 10^{-8}$ | 51.100.000         |
| $P(q_o > q_c RS_2\&FS)$ | $1.570 \times 10^{-7}$ | 6.370.000          |
| $P(q_o > q_c RS_3\&FS)$ | $3.390 \times 10^{-2}$ | 29                 |
| $P(q_o > q_c No\ FS)$   | $4.739 \times 10^{-9}$ | 211.000.000        |

Table 5.7: Conditional probability of exceedance critical overtopping discharge for the three retrogression states and original dike profile.

The probability of exceedance of the critical overtopping discharge increases as the retrogression length becomes larger. The original probability is quite small due to the high crest level of the dike. Before the closure of the Haringvliet, the dikes next to the Spui were sea dikes and a larger crest height was required. The current dike has still this original height.

## 6. Flooding

The probability of flooding is assumed to be equal to the probability of exceedance of the critical overtopping discharge. With this assumption, the probability of flooding can be calculated with several earlier calculated conditional probabilities and the event tree shown in figure 4.10 (representation of Eq. 4.10).

The probability of flooding for the cases without emergency repairs and the cases with a successful application of emergency repairs are presented in table 5.8. The probability of successful application of emergency repairs is based on a required period of 60 days for the implementation of the repairs. The probability of successful repair can be calculated as follows:

$$P(\text{Repair}) = 1 - \frac{T_{\text{repair}}}{365} = 1 - \frac{60}{365} = 0.83 \quad (5.1)$$

|             | Repair time =60 days |                    | Without repairs      |                    |
|-------------|----------------------|--------------------|----------------------|--------------------|
|             | $P(q_o > q_c)$       | Return period [yr] | $P(q_o > q_c)$       | Return period [yr] |
| 2018        | $1.1 \times 10^{-5}$ | 94,300             | $6.5 \times 10^{-5}$ | 15,500             |
| 2023 (5%)   | $1.2 \times 10^{-5}$ | 80,800             | $7.5 \times 10^{-5}$ | 13,300             |
| 2023 (mean) | $1.7 \times 10^{-5}$ | 58,000             | $1.0 \times 10^{-4}$ | 9,500              |
| 2023 (95%)  | $2.6 \times 10^{-5}$ | 37,900             | $1.6 \times 10^{-4}$ | 6,200              |

Table 5.8: Probability of exceedance and return period critical overtopping discharge( $q=5l/s/m$ ) for the case with and without dike repair after a flow slide.

## 7. Consequences

In Veiligheid Nederland in Kaart (VНК2), the consequences of a flood with a breach location near the scour hole are determined. If there is a breach near the scour hole and a flood occurs, the entire urban area of Spijkenisse and the rural areas up to the Bernisse will be flooded. The total consequences depend on the outer water level at the moment of breaching, and are shown in table 5.9. (B. R. de Groot, 2014)

| Water level exceedance probability | Economic damage [M€] | Loss of life |
|------------------------------------|----------------------|--------------|
| 1/400 (tp-1d)                      | 2.495                | 80-330       |
| 1/4.000 (tp)                       | 2.910                | 100-415      |
| 1/40.000 (tp+1d)                   | 3.120                | 120-495      |

Source: B. R. de Groot (2014)

Table 5.9: Consequences of a flood with a breach near the scour hole for different water levels associated with their exceedance probability.

## 8. Risk quantification

Combining the probability of exceedance of the critical overtopping discharge with the consequences gives an estimation for the flood risk due to the presence of the scour hole for the failure mechanism overtopping. According to B. R. de Groot (2014), the consequences corresponding to the next, less favourable water level must be used for the risk estimation. For this scour hole, these are the consequences corresponding to an exceedance probability of 1/40.000 per year.

The risk estimation is given in table 5.10 for 2018 and in table 5.11 for 2023. This is performed for the case with repair measures after a flow slide. For 2023, the mean scenario with respect to the scour hole development is used. The two types of consequences are combined with the value of statistic life. The common used value of €6.7 million per fatality is used with the mean of the range of expected loss of life. An economic growth factor of 1.9% is used for the economical damage in 2023 (Deltares, 2011).

|                   | Probability            | × | Consequences             | Risk                        |
|-------------------|------------------------|---|--------------------------|-----------------------------|
| Economical damage | $1.061 \times 10^{-5}$ | × | 3,120,000,000            | = 33,099 [€/yr]             |
| Loss of life      | $1.061 \times 10^{-5}$ | × | (120 - 495)              | = 0.0013-0.0053 [People/yr] |
|                   | $1.061 \times 10^{-5}$ | × | $307.5 \times 6,700,000$ | = 21,1856 [€/yr]            |
| Total             |                        |   |                          | = 54,955[€/yr]              |

Table 5.10: Risk estimation for scour hole in 2018.

|                   | Probability            | × | Consequences             | Risk                        |
|-------------------|------------------------|---|--------------------------|-----------------------------|
| Economical damage | $1.724 \times 10^{-5}$ | × | 3,430,000,000            | = 59,104 [€/yr]             |
| Loss of life      | $1.724 \times 10^{-5}$ | × | (120 - 495)              | = 0.0021-0.0085 [People/yr] |
|                   | $1.724 \times 10^{-5}$ | × | $307.5 \times 6,700,000$ | = 35,523[€/yr]              |
| Total             |                        |   |                          | = 94.627[€/yr]              |

Table 5.11: Risk estimation for scour hole in 2023.

### Other direct failure mechanisms

The direct failure mechanism overtopping has only a relevant probability for the third retrogression state ( $RS_3$ ), for the other two retrogression states, the probability of exceedance of the critical overtopping discharge is significantly smaller. However, these two retrogression states can have an influence on other direct failure mechanisms.

For all retrogression states, the occurrence of piping can be neglected since there is a clay/peat layer with a thickness of at least 7.0 [m] present in the subsoil (MOS GRONDMECHANICA, 2019). No pipes can develop in cohesive layers with this thickness.

The effect on the erosion of the outer slope can be determined from the design conditions of the critical overtopping discharge. In  $RS_2$ , the grass cover of the dike is affected by flow slide. For this retrogression state, the design conditions corresponding to the critical overtopping discharge of  $q_c = 5.0$  [l/s/m] with the lowest wave height, are a water level of 3.10 [m + NAP] and  $H_{m0} = 1.06$  [m]. According to the 'Schematiseringshandleiding grasbekleding', the failure mechanism erosion of the outer slope cannot be neglected with these conditions Rijkswaterstaat (2018). Probability, the erosion of the outer dike is a more dominant direct failure mechanism for  $RS_2$ .

The retrogression states  $RS_1$  and  $RS_2$  can influence the stability of the outer slope. In both retrogression states, the foreshore is totally disappeared. Besides, in  $RS_2$  there is a different slope of the outer slope. The effect of the retrogression states on the macro-stability of the dike could be determined with numerical soil models. This has not been elaborated in the context of this research.

### Other hazards

For a broader view, it is relevant to indicate other potential hazards of this scour hole. The distance between the closest, near the scour hole located, groyne and the scour hole itself is over 200 [m]. No other hydraulic structures are nearby the scour hole. There are also no cables and pipelines near the scour hole. So, there is no potential hazard for the instability of some hydraulic structures or insufficient coverage of some cable, pipeline or tunnel.

## 5.4. Sensitivity analysis

To determine important and less important parameters in the risk assessment process for scour holes, a marginal sensitivity analysis is performed. In this analysis, the sensitivity of several parameters on the total probability of flooding (exceedance of the critical overtopping discharge) is determined. Insight into the sensitivity of this probability can be obtained by deterministic varying of the used parameters one by one and subsequently comparing the newly obtained probability with the probability of the base case.

### 5.4.1. Case for sensitivity analysis

The sensitivity analysis is applied on one river cross-section profile of the case scour hole, which is representing the entire scour hole. Applying the sensitivity analysis for the entire scour hole is namely difficult and requires a lot of calculations. The relative importance of the several parameters can also be determined from one representative river profile.

The representative river profile and its location are shown in figure 5.9. The location is on the west side of the scour hole, next to the lowest located point. The lowest point of the represented profile is located at -18.21 [m + NAP], the foreshore length is 17.2 [m].

The base values for the representative profile are given in table 5.13. Only one subsoil scenario is used in the sensitivity analysis. The base values are chosen such that the relevant probabilities, corresponding to the several steps of the risk assessment, are (almost) equal to the probability of the entire scour hole as predicted in the mean scenario for 2023. The probabilities corresponding to the several steps of the risk assessment are given in table 5.12 for the representative profile and the entire scour hole.

|              | $P(FS)$ | $P(RS_3 FS)$ | $P(NoRepair FS)$ | $P(q > q_{max} FS\&RS_3)$ | $P(q > q_{max})$      | Return period |
|--------------|---------|--------------|------------------|---------------------------|-----------------------|---------------|
| scour hole   | 0.0152  | 0.2035       | 0.1644           | 0.0339                    | $1.72 \times 10^{-5}$ | 58,000        |
| ref. profile | 0.0157  | 0.2093       | 0.1644           | 0.0339                    | $1.83 \times 10^{-5}$ | 54,500        |

Table 5.12: Relevant probabilities for risk assessment of the scour hole and the representative profile for the sensitivity analysis.

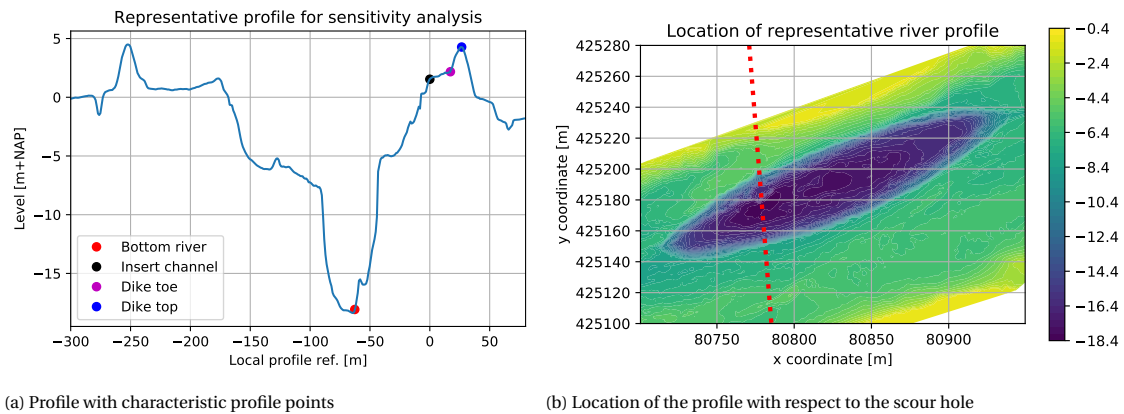


Figure 5.9: Representative profile for the sensitivity analysis.

### 5.4.2. Parameters

The sensitivities of 14 parameters are analysed in a marginal sensitivity analysis. These parameters are related to 1) the scour hole dimensions (river profile), 2) the calculation of the probability of occurrence of a flow slide, 3) the post flow slide profile and 4) remaining aspects. The parameters with their variation ranges are given in table 5.13. A new calculation is performed by replacing the minimum and maximum value of the range one by one for each parameter.

The ranges of the river profile parameters are based on the 5% and 95% predicted scour hole with the extrapolation tool. The ranges of the flow slide parameters are based on the minimum and maximum estimated values of the used subsoil scenarios as shown in Appendix G. In the WBI, distributions are given for the post flow slide profile parameters, the 5% and 95% characteristic values of the distributions are used as ranges for these parameters (Rijkswaterstaat, 2016b). The range for the critical overtopping discharge is based on values mentioned in Jonkman et al. (2018). The range of the required time till repair is chosen from the assumptions made in the report of Van der Krogt (2015).

| Type of data            | Parameter                       | Base value           | Range           | unit          |                   |
|-------------------------|---------------------------------|----------------------|-----------------|---------------|-------------------|
| River profile           | Location bottom river           | 62.7                 | 61.2 - 64.2     | [m]           |                   |
|                         | Level bottom river              | -18.07               | -17.86 - -18.60 | [m + NAP]     |                   |
|                         | Location Insert channel         | 0                    | -2.0 - 2.0      | [m]           |                   |
|                         | Level Insert channel            | 1.53                 | 1.00 - 2.00     | [m + NAP]     |                   |
| Flow slide parameters   | Mean particle diameter          | $D_{50,mean, kar}$   | 130             | 100-150       | [ $\mu\text{m}$ ] |
|                         | State parameter                 | $\psi_{5m, kar}$     | -0.10           | -0.15 - 0.05  | [-]               |
|                         | Presence of interference layers | $F_{cohesivelayers}$ | 2.0             | 1.0-3.0       | [-]               |
|                         | Dynamic behaviour foreshore     | $V_{local}$          | 0.1             | 0.01-0.30     | [m/yr]            |
|                         | Agreed low water level          | OLW                  | -0.30           | -0.60 - 0.00  | [m + NAP]         |
| Post flow slide profile | Slope steep part                | $\beta$              | 1:2.9           | 1:1.0 - 1:5.7 | [-]               |
|                         | Location of transition point    | $D/H$                | 0.43            | 0.331-0.528   | [-]               |
|                         | Ratio surface area 1 and 2      | $c$                  | 1.4             | 1.235-1.564   | [-]               |
| Remaining aspects       | Critical overtopping discharge  | $q_c$                | 5               | 1-10          | [l/s/m]           |
|                         | Time till repair                | $T_{repair}$         | 60              | 20-150        | [Days]            |

Table 5.13: Parameters with their base values and variation ranges used in the sensitivity analysis.

### 5.4.3. Results

The sensitivity of each parameter on the end result, the total probability of exceedance of the critical overtopping discharge is shown in figure 5.10. In this figure, the range of the return period of the exceedance of the critical overtopping discharge is shown. The ranges indicate the sensitivity of each parameter and the relative importance of the uncertainty of the parameters with respect to  $P(q_0 > q_c)$ .

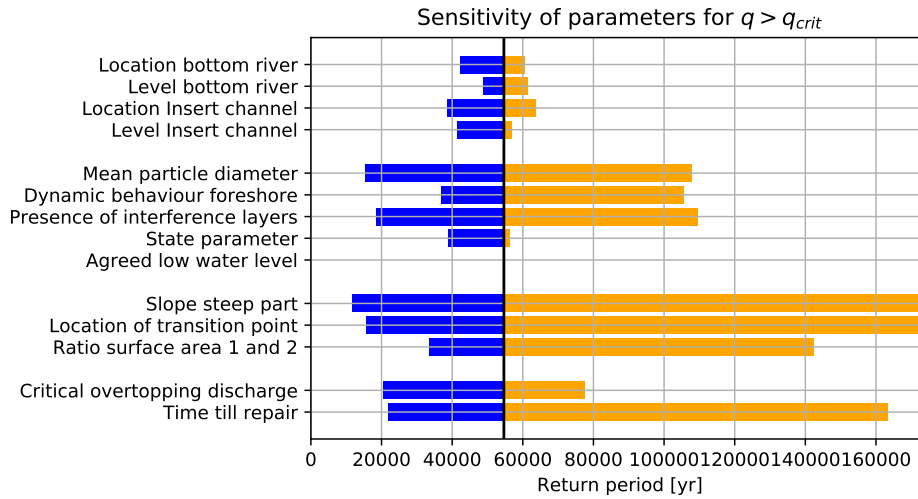


Figure 5.10: Parameter sensitivity on the return period range of  $q_0 > q_c$ .

As can be seen in figure 5.10, the parameters of the post flow slide profile are the most sensitive parameters for the result, followed by the flow slide parameters. This is not surprising since the variation range of these parameters is relatively larger than the variation range of the profile parameters.

In addition, the required time till repair of a dike after a flow slide, has a large sensitivity. If it is possible to implement emergency repairs faster, the  $P(q_0 > q_c)$  will be smaller and the associated risk as well.

*(This page is intentionally left blank)*

# 6

## Risk management

This chapter contains the evaluation phase of the risk-based approach for scour holes. First, the procedure for the evaluation of flood risk according to the Dutch safety standard is shortly explained. Subsequently, general risk-reducing measures for flow slide and scour hole growth are described. Finally, the assessed risk of the case scour hole is evaluated and the feasibility of risk mitigation measures is analysed.

### 6.1. Risk tolerability

In the Dutch Safety standard, the safety levels of the primary flood defences are clearly defined. In the Netherlands, the tolerability for flood risk is expressed as probability of flooding and not in terms of risk self. However, the safety levels are derived from the potential consequences of a flood. The standards are namely based on two principles (Kok et al., 2016):

1. Everyone has the same minimum level of protection, expressed as Local individual risk (LIR).
2. Based on societal risk and economic risk optimisation, a lower probability of flooding is appropriate for some dike-trajectories.

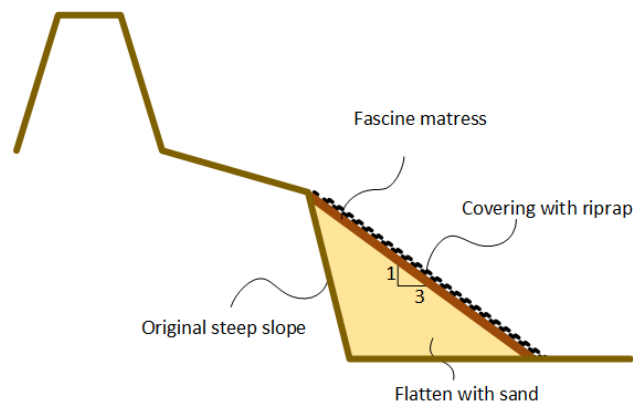
Based on these two principles, a safety level is determined in terms of probability of flooding per year per dike-trajectory. If a dike-trajectory does not satisfy to the safety level, mitigation measures are necessary in order to reduce the probability of flooding.

The safety standard holds for all failure mechanisms together for an entire dike-trajectory. The required failure probability for a specific failure mechanism at dike section level is determined by failure probability budgeting. The total probability is distributed over all mechanisms and dike sections. For each mechanism, a maximum contribution ( $w_{j,i}$ ) of the total allowable probability is specified. In the WBI, the default contribution for the failure mechanism overtopping is 24% for all dike sections together (Kok et al., 2016). However, during the safety assessment of a dike-trajectory it is allowed to deviate from the default values, as long as the total failure probability budget add up to the pre-described safety level. (Jonkman et al., 2018).

### 6.2. Risk mitigation measures

If a flood defence does not satisfy the required probability from the safety standards, mitigation measures are necessary. Default mitigation measures are often applied for direct failure mechanisms. For example, a typical mitigation measure for overtopping is a crest height increase. (Jonkman et al., 2018)

Increasing the crest height will not help to reduce the probability of exceedance of the critical overtopping discharge after a flow slide. In order to reduce this probability, measures can be applied to reduce the probability of occurrence of a flow slide. This can be achieved by making the underwater slope stable or reducing the height of the underwater slope. A slope height reduction can be established by filling a scour hole with sand and eventually covering the placed sand with a protection layer.



Source: Own creation based on Buschman et al. (2015)

Figure 6.1: Common method for placing riprap on a steep riverbank slope.

### 6.2.1. Stable underwater slope

According to the WBI, the probability of occurrence of a flow slide is reduced if riprap is placed on the lowest part of the slope up to the bottom level. If the riprap is present on the entire underwater slope, it can be assumed that the slope is stable and that the probability of occurrence of a flow slide is negligible. (Rijkswaterstaat, 2016b)

For Rijkswaterstaat and waterboards, the common method is to flatten the slope first with sand until a new slope of 1:3 is created. Subsequently, a cover layer of fascine mattress with on top riprap is placed on the placed sand to make the slope stable. This method is schematically shown in figure 6.1. This method has been applied by Rijkswaterstaat on the steep slope of the scour holes near Nieuw-Beijerland in 2017 and by the waterboard Hollandse Delta near the scour holes in the Dordtsche Kil in 2010 (Buschman et al., 2015). Moreover, this method is used in the scenario analysis for management strategies described in 2.3.2 (Schuurman, 2018).

### 6.2.2. Filling scour hole

A scour hole can be filled with sediment nourishments. However, if a scour hole is filled with sand, there is a large probability that the sand bed will erode again. Depending on the erosion rate, repeatedly nourishment have to be applied or after the filling, the scour hole must be covered with a protection layer. Examples of such protection layers are (Buschman et al., 2015):

- Gravel and stones
- Filter layers of riprap
- Fascine mattress with on top riprap
- Concrete block mats
- Phosphor and/or steel slacks
- Geotextile products like geotube, geocontainer and geobag
- Reinforced sediment
- Wood

Depending on the local conditions some solutions are less suitable or effective. For example, reinforced sediment has only been tested for locations with low flow velocities and not yet for high flow velocities. Geobags are, for example, more suitable for smaller scour holes. (Buschman et al., 2015)

The effectiveness of sand nourishment in scour holes is currently analysed within the pilot study described in section 2.3.1. At two locations, sand has been placed without a coverage layer. At the third location, the scour hole has been filled and subsequently covered with a fascine mattress with on top a layer of riprap. (Sieben, 2018).

In the scenario analysis for management strategies described in 2.3.2, scenarios are analysed in which scour holes are filling and coverage with riprap. These scenarios are compared with management scenarios in which only bank protection measures are implemented.

## 6.3. Risk management for case Spui rkm 1004.8

### 6.3.1. Risk tolerability

In section 5.3, the economic risk is assessed and the probability of exceedance of the critical overtopping is determined for the dike section next to the scour hole near rkm 1004.8. The calculated probability must be compared with the safety standard of dike-trajectory 20-3. The safety standard of the trajectory is  $P_{flooding} = 1/10.000$  [1/yr] (WSHD, 2017).

In table 6.1, the calculated failure probability of the years 2018 and 2023 are compared with the standard. For both years, the failure probability is below the required probability if the default contribution of 24% is used for overtopping. However, this does not directly mean that the dike-trajectory satisfies the safety standard. A large part of the total failure budget for the entire trajectory of 23 [km] is already required for only the failure mechanism of overtopping in the dike section of 260 [m] next to the scour hole.

|      | $P(q_0 > q_c)_{calculated}$ | $P(q_0 > q_c)_{required}$ | Allowable? | Percentage of total budget |
|------|-----------------------------|---------------------------|------------|----------------------------|
| 2018 | $1.1 \times 10^{-5}$        | $2.400 \times 10^{-5}$    | ✓          | 10.6%                      |
| 2023 | $1.7 \times 10^{-5}$        | $2.400 \times 10^{-5}$    | ✓          | 17.8%                      |

Table 6.1: Calculated probabilities for the scour hole in 2018 and 2023 compared with the require probability with a contribution of 0.24 for the failure mechanism overtopping.

Depending on the failure probability other failure mechanisms and the other dike section, the dike-trajectory would possibly not meet the safety standard.

### 6.3.2. Possible mitigation measures

Based on the calculated probability of exceedance of the critical overtopping discharge in 2023, risk mitigation measures are not directly necessary for the case scour hole according to the Dutch safety standards. Depending on the failure probability of other failure mechanisms and the other dike section, it can be necessary to take measures in order to let the entire dike section satisfy the safety standard. Risk mitigation measures for the dike-section next to the scour hole is, in that case, a good option since a large part of the total failure budget is required for this section.

Despite, measures are not directly necessary according to the WBI, measures can still be economical beneficial in the context of economic flood risk.

The effect of the following two mitigation measures on the probability of exceedance of the critical overtopping discharge is analysed.

1. Placing riprap on the entire slope
2. Filling entire scour hole up to -12.9 [m + NAP] without a coverage layer

The first measure is the common used measure to prevent flow slides. While the second measure is currently studied with the pilot study. During the execution of both mitigation measures, extra alertness is required for the occurrence of flow slides. Dumping of sediment and riprap can namely lead to local vibration in the soil. This can be an initiation trigger of the flow slide mechanism.

#### Placing riprap

Currently, upstream and downstream of the scour hole, there is riprap placed on the slope up to a level of -8 [m + NAP], but on the slope next to the scour hole there is no riprap placed. For this mitigation measure, riprap will be placed next to the scour until the bed level, as indicated in figure 6.2. The slope is first made less steep and subsequently covered with fascine mattresses with a layer of riprap.

As described in section 6.2.1, the probability of occurrence of a flow slide is negligible after placing the riprap on the entire slope (Rijkswaterstaat, 2016b). The total probability of exceedance of the critical overtopping discharge will be equal to  $P(q_0 > q_c | No FS)$ . It can be assumed that the riprap is stable and the new reduced probability holds for the entire lifespan of 50 years.

The measure of placing riprap on the slope changes the local river geometry, this can influence the local flow pattern and can initiate erosion next to the placed riprap or near the riverbank of the other riverside. After the execution of the measure, extra bathymetry surveys are required in order to detect possible erosion.

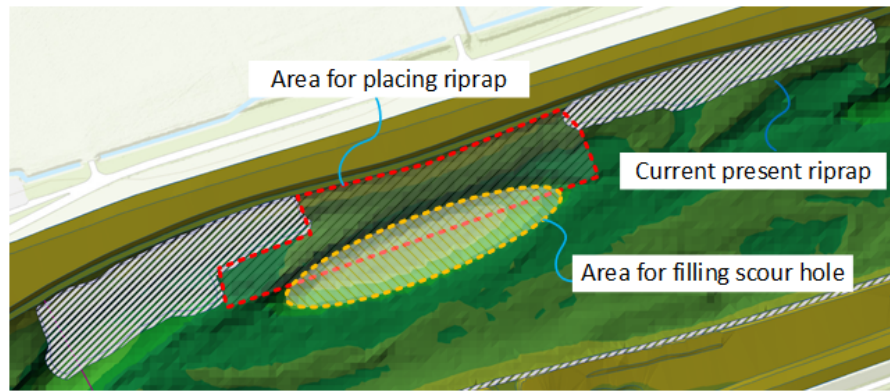


Figure 6.2: Area for the placement of riprap and filling of the scour hole as risk mitigation measures.

### Filling scour hole

In this measure, the entire scour hole is filled with sand to  $-12.9$  [m + NAP] without the placement of a cover layer.

A new calculation is executed for the total probability of exceedance of the critical overtopping discharge. The original and new calculated probabilities are shown in table 6.2. As can be seen, filling of the scour hole reduces the probability of occurrence of a flows slide. However, it can not be negligible. Besides, there is also an effect on the occurrence of the retrogression states.

|                            | $P(FS)$ | $P(S_1 FS)$ | $P(S_2 FS)$ | $P(S_3 FS)$ | $P(q > q_{max})$      | Return period |
|----------------------------|---------|-------------|-------------|-------------|-----------------------|---------------|
| Original scour hole (2018) | 0.0112  | 0.27        | 0.56        | 0.17        | $1.06 \times 10^{-5}$ | 94,300        |
| Placing riprap             | 0.0     | 0.27        | 0.56        | 0.17        | $4.74 \times 10^{-9}$ | 211,000,000   |
| Filled scour hole          | 0.0041  | 0.29        | 0.48        | 0.23        | $5.34 \times 10^{-6}$ | 187,100       |

Table 6.2: Relevant probabilities for the original scour hole and the scour hole filled with sand.

It is likely that the sand will erode in the years after the filling of the scour hole. The erosion rate of filling material is probably larger than the current observed erosion rates in the scour hole since the sediment has a different grain size, the placed sediment is looser packed and larger flow velocities are expected after the placement. (Schuurman, 2018). A conservative assumption is made with respect to the erosion, it is assumed that all placed sediment is eroded in five years and the scour hole will have the original geometry after five years. This assumption is based on the first results of the pilot study in the Oude Maas. After the first year approximately 20% of the placed sand has been eroded (Baars, 2019).

The erosion of the placed sediment needs to be monitored with bathymetry surveys. The total amount of required bathymetry surveys depends on the erosion development. It is assumed that yearly two extra surveys are required. The total amount of surveys will be thus 10 in 5 years.

### 6.3.3. Feasibility mitigation measures

The economic feasibility of the two mitigation measures is analysed. A measure is cost-effective if the investment costs are smaller than the present value of the risk reduction expressed in monetary terms, as indicated in Eq. 6.1 (Jonkman et al., 2017).

$$I < \Delta E(D) \quad (6.1)$$

In which:

$$\begin{aligned} I &= \text{Total investment costs} && [€] \\ \Delta E(D) &= \text{Present value of risk reduction} && [€] \end{aligned}$$

### Unit prices

The investment costs of the two measures are calculated with the unit prices presented in table 6.3. The same unit prices are used in the river management scenario analysis performed by Schuurman (2018). A unit

price of €0,0 is used as the direct material costs for sand. It can be assumed that transport costs are the only direct costs related to sand. The sand is available from the dredging activities in the Nieuwe Merwede, Boven Merwede and Beneden Merwede.

|              | Item                     | Unit                 | Unit price |   |
|--------------|--------------------------|----------------------|------------|---|
| Direct costs | Sand                     | €/m <sup>3</sup>     | 0          | 'Free' available, without transport costs |
|              | Riprap                   | €/m <sup>3</sup>     | 40         | Including transport and storage           |
|              | Fascine mattress         | €/m <sup>2</sup>     | 20         | Including transport and storage           |
|              | Bathymetry survey        | €/day                | 3,000      |   |
|              | Transport of sand        | €/m <sup>3</sup> /km | 0.048      |   |
| Other costs  | Mobilization             | €                    | 20,000     | Once                                      |
|              | Implementation costs     | %                    | 3.0        | % of direct costs                         |
|              | General costs            | %                    | 8.0        | % of direct costs                         |
|              | Profit                   | %                    | 2.5        | % of direct costs                         |
|              | Risk                     | %                    | 2.5        | % of direct costs                         |
| Extra        | Price fluctuation riprap | %                    | 10.0       | % of riprap costs                         |
|              | Engineering costs        | %                    | 2.0        | % of total costs                          |

Source: Based on Schuurman (2018)

Table 6.3: Overview of investment items and unit prices for the implementation of measures.

### Investment costs

For the investment costs calculation, the required amounts of material must be determined first. Based on the scour hole bathymetry of 2018, the amounts are calculated, see table 6.4.

| Material         | Unit           | Placing riprap | Filling scour hole |
|------------------|----------------|----------------|--------------------|
| Sand             | m <sup>3</sup> | 5,500          | 19,000             |
| Riprap           | m <sup>3</sup> | 12,000         | 0                  |
| Fascine mattress | m <sup>2</sup> | 12,000         | 0                  |

Table 6.4: Overview of required material for the mitigation measures.

The total costs are calculated with the unit prices of table 6.3 and the determined amount of material mentioned in table 6.4. The calculation is presented in table 6.5.

| Item                     | Placing riprap |   |       | € | Filling scour hole |         |        | €      |   |                |   |       |   |        |
|--------------------------|----------------|---|-------|---|--------------------|---------|--------|--------|---|----------------|---|-------|---|--------|
| Sand                     | 5,500          | × | 0     | = | 0                  | 19,000  | ×      | 0      | = | 0              |   |       |   |        |
| Riprap                   | 12,000         | × | 40    | = | 480,000            | 0       | ×      | 40     | = | 0              |   |       |   |        |
| Fascine mattress         | 12,000         | × | 20    | = | 240,000            | 0       | ×      | 20     | = | 0              |   |       |   |        |
| Bathymetry survey        | 3              | × | 3,000 | = | 9,000              | 10      | ×      | 3,000  | = | 30,000         |   |       |   |        |
| Transport of sand        | 5,500          | × | 43    | × | 0.048              | =       | 11,352 | 19,000 | × | 43             | × | 0.048 | = | 39,216 |
| <b>Total direct</b>      |                |   |       | = | <b>740,352</b>     |         |        |        | = | <b>69,216</b>  |   |       |   |        |
| Mobilization             | 20,000         | × | 1     | = | 20,000             | 20,000  | ×      | 1      | = | 20,000         |   |       |   |        |
| Implementation costs     | 740,352        | × | 0.03  | = | 22,211             | 69,216  | ×      | 0.03   | = | 2,076          |   |       |   |        |
| General costs            | 740,352        | × | 0.08  | = | 59,228             | 69,216  | ×      | 0.08   | = | 5,537          |   |       |   |        |
| Profit                   | 740,352        | × | 0.025 | = | 18,509             | 69,216  | ×      | 0.025  | = | 1,730          |   |       |   |        |
| Risk                     | 740,352        | × | 0.025 | = | 18,509             | 69,216  | ×      | 0.025  | = | 1,730          |   |       |   |        |
| <b>Total indirect</b>    |                |   |       | = | <b>138,456</b>     |         |        |        | = | <b>31,075</b>  |   |       |   |        |
| Price fluctuation riprap | 480,000        | × | 0.1   | = | 48,000             | 0       | ×      | 0.1    | = | 0              |   |       |   |        |
| Engineering costs        | 878,808        | × | 0.02  | = | 17,576             | 100,291 | ×      | 0.02   | = | 2,006          |   |       |   |        |
| <b>Total extra</b>       |                |   |       | = | <b>65,576</b>      |         |        |        | = | <b>2,006</b>   |   |       |   |        |
| <b>Total</b>             |                |   |       | = | <b>944,384</b>     |         |        |        | = | <b>102,296</b> |   |       |   |        |

Table 6.5: Overview of investment costs for mitigation measures.

### Risk reduction

The two measures reduce the economic risk of overtopping due to the presence of the scour hole. The risk reduction per year can be calculated with Eq. 6.2 (Jonkman et al., 2017).

$$\Delta E(D) = (P_{f,0} - P_{f,new}) \times D_{pv} \quad (6.2)$$

In which:

|             |   |   |        |
|-------------|---|---|--------|
| $D_{pv}$    | = | Present value of the potential damage               | [€]    |
| $P_{f,0}$   | = | Initial failure probability                         | [1/yr] |
| $P_{f,new}$ | = | Failure probability after risk reduction investment | [1/yr] |

The present value of the potential damage ( $D_{pv}$ ) can be calculated as follows:

$$D_{pv} = \frac{D_j}{(1+r)^t} \quad (6.3)$$

In which:

|       |   |                            |         |
|-------|---|----------------------------|---------|
| $D_j$ | = | Potential damage in year j | [€]     |
| $r$   | = | discount rate              | [%]     |
| $t$   | = | time reference             | [years] |

To calculate the total risk reduction for the entire lifespan of a measure, the risk reduction per year must be summed.

The risk reduction of the riprap measure is calculated with a constant initial failure probability over the entire lifespan of 50 years. The scour hole development is unclear for a period of 50 years. The probability for 2023 calculated in section 5.3 is used. The failure probability after the implementation of the mitigation measure remains also constant over the entire lifespan. Due to the usage of the present value, the yearly risk reduction reduces, as can be seen in table 6.6, in which the risk reduction is calculated for the riprap measure. The calculation is performed with an assumed discount rate of 5.5% and a yearly growth rate of 1.9% for the economical damage (Deltares, 2011).

|         | $P_{f,0}$              | $P_{f,new}$            | $D_{pv}$ [M€] | E(D) [€]  |
|---------|------------------------|------------------------|---------------|-----------|
| year 1  | $1.724 \times 10^{-5}$ | $4.739 \times 10^{-9}$ | 5,180         | 89,290    |
| year 2  | $1.724 \times 10^{-5}$ | $4.739 \times 10^{-9}$ | 5,003         | 86,243    |
| ⋮       | ⋮                      | ⋮                      | ⋮             | ⋮         |
| year 50 | $1.724 \times 10^{-5}$ | $4.739 \times 10^{-9}$ | 945           | 16,292    |
| Total   |                        |                        |               | 2,155,539 |

Table 6.6: Yearly risk reduction for the riprap measure.

For the risk reduction due to the filling of the scour hole, a variable  $P_{f,0}$  and  $P_{f,new}$  is used. It is assumed that both probabilities increase linearly in time. The  $P_{f,0}$  increases in a period of 5 years, from the initial probability in 2018 to the calculated probability for 2023. While the  $P_{f,new}$  increases in the same period from the new calculated probability to the initial probability of 2018. The risk reduction calculation for the 5-year lifespan of the filling of the scour hole is presented in table 6.7.

|        | $P_{f,0}$              | $P_{f,new}$            | $D_{pv}$ [M€] | E(D) [€] |
|--------|------------------------|------------------------|---------------|----------|
| year 1 | $1.061 \times 10^{-5}$ | $5.343 \times 10^{-6}$ | 5,180         | 27,275   |
| year 2 | $1.227 \times 10^{-5}$ | $6.660 \times 10^{-6}$ | 5,003         | 28,055   |
| year 3 | $1.393 \times 10^{-5}$ | $7.976 \times 10^{-6}$ | 4,833         | 28,750   |
| year 4 | $1.558 \times 10^{-5}$ | $9.292 \times 10^{-6}$ | 4,668         | 29,366   |
| year 5 | $1.724 \times 10^{-5}$ | $1.061 \times 10^{-5}$ | 4,508         | 29,906   |
| Total  |                        |                        |               | 143,351  |

Table 6.7: Yearly risk reduction for the filling measure.

### Results feasibility

The total investment costs are for both mitigation measures less than the risk reduction over the lifespan of the measures. Both measures are thus economical feasible since they are cost-effective. The net present values and the benefit-cost ratios for the two analysed mitigation measures are presented in table 6.8.

| Measure            | Risk reduction [€] | Investment costs [€] | NPV [€]   | Benefit-cost ratio |
|--------------------|--------------------|----------------------|-----------|--------------------|
| Placing riprap     | 2,155,539          | 944,384              | 1.211,155 | 2.28               |
| Filling scour hole | 143,351            | 102,296              | 41,055    | 1.40               |

Table 6.8: Net present values and benefit-cost ratios for the mitigation measures.

### 6.3.4. Reflection

Both measures are economically feasible, based on the made assumptions. The effects of three assumptions on the feasibility are analysed in this section.

#### Price of sand

It has been assumed that the sand required for filling of the scour hole and flatten of the slope is available for free, because of it can be dredged from the river branches with sedimentation. However, instead of reusing the sand, it can also be sold, therefore, sand is not really 'free'. The costs of both used mitigation measures are affected if this assumption is changed. In table 6.9, the effects on the investment costs and benefit-cost ratios are presented. As can be seen, the sand price influence the feasibility of the filling measure in a larger magnitude.

| Price sand [€/m <sup>3</sup> ] | Placing riprap       |                    | Filling scour hole   |                    |
|--------------------------------|----------------------|--------------------|----------------------|--------------------|
|                                | Investment costs [€] | Benefit-cost ratio | Investment costs [€] | Benefit-cost ratio |
| 0 (base)                       | 944,384              | 2.28               | 102,296              | 1.40               |
| 1                              | 950,892              | 2.27               | 124,777              | 1.15               |
| 2                              | 957,400              | 2.25               | 147,258              | 0.97               |
| 5                              | 976,922              | 2.21               | 214,700              | 0.67               |
| 10                             | 1,009,460            | 2.14               | 327,104              | 0.44               |

Table 6.9: Effect of sand price on feasibility mitigation measures.

#### Lifespan

The lifespan of the placing riprap measure is assumed to 50 years and the filling measure to 5 years. Changing these assumptions results in a difference in total risk reduction and benefit-cost ratio, as can be seen in table 6.10 and table 6.11. The assumption of free available sand is again used for the calculations. As can be seen, the riprap measure is still economically feasible if the lifetime reduces. While the filling measure is no longer feasible if the lifespan is less than 5 years.

| Lifespan [years] | Risk reduction [€] | Benefit-cost ratio |
|------------------|--------------------|--------------------|
| 20               | 1,309,955          | 1.39               |
| 40               | 1,964,125          | 2.08               |
| 50 (base)        | 2,155,540          | 2.28               |
| 60               | 2,290,807          | 2.43               |

Table 6.10: Effect of lifespan of the riprap measure on feasibility.

| Lifespan [years] | Risk reduction [€] | Benefit-cost ratio |
|------------------|--------------------|--------------------|
| 2                | 35,572             | 0.35               |
| 3                | 64,772             | 0.63               |
| 4                | 100,866            | 0.99               |
| 5 (base)         | 143,351            | 1.40               |

Table 6.11: Effect of lifespan of the filling measure on feasibility.

### Required time for emergency repairs

A required period of 60 days has been assumed for the implementation of emergency repairs after a flow slide. From the sensitivity analysis in section 5.4, follows that this period has a large sensitivity to the probability of flooding. The period required for the implementation of emergency repairs affects the risk reduction of both measures. This is shown in table 6.12.

| Time for emergency repairs | Placing riprap     |                    | Filling scour hole |                    |
|----------------------------|--------------------|--------------------|--------------------|--------------------|
|                            | Risk reduction [€] | Benefit-cost ratio | Risk reduction [€] | Benefit-cost ratio |
| 20 days                    | 718,513            | 0.76               | 47,786             | 0.47               |
| 40 days                    | 143,7026           | 1.52               | 95,571             | 0.93               |
| 60 days(base)              | 2,155,540          | 2.28               | 143,351            | 1.40               |
| 90 days                    | 3,233,310          | 3.42               | 215,035            | 2.10               |
| 120 days                   | 4,311,079          | 4.56               | 286,714            | 2.80               |
| 150 days                   | 5,388,849          | 5.71               | 358,392            | 3.50               |

Table 6.12: Effect of the required time for emergency repairs on feasibility mitigation measure.

### 6.3.5. Discussion

The implementation of risk reduction measures is not directly necessary according to the safety standards. However, both measures are economically beneficial and are effective in reducing the risk of flooding near the scour hole. The risk reduction and the benefit-cost ratio of placing riprap are larger than for the filling measure. The feasibilities of the measures depend on the made assumptions. If other values are assumed for the lifespan, sand price and time for implementation of emergency repairs, the filling measure is depending on the chosen values no longer economically beneficial. While the placement of riprap would possibly no longer be beneficial if other values are assumed for the lifespan and time for implementation of emergency repairs. Both types of measures can trigger new local erosion next to the scour hole. Depending on the occurrence of local erosion, addition measures could be required. This can affect the feasibilities of the measures.

The decision-makers, Rijkswaterstaat and the waterboard Hollandse Delta, must decide together if the implementation of a measure near the scour hole is desired and subsequently which measure have to be implemented. Placing riprap has larger investment costs, but results in a larger risk reduction and has a longer lifespan. Filling of the scour hole is relatively cheap, but the effectiveness and lifespan is currently not completely clear.

# 7

## Conclusions, discussions & recommendations

This chapter summarises the conclusions of the research. The conclusions are given per sub-question. Subsequently, recommendations are provided. The recommendations are subdivided into three groups; recommendations for further research, recommendations for the risk assessment method and recommendations for scour holes in the RMD and the case scour hole of this research.

### 7.1. Conclusions

The objectives of this research were to obtain insight into the risk of scour holes in the Rhine-Meuse delta and to evaluate possible measures for risk reduction. Based on these objectives, a main question with five sub-questions are mentioned in the introduction. The following conclusions can be made for the research questions.

#### 1. How can the development of scour holes be predicted and which processes and conditions play a role in the development of scour holes?

The hydrodynamic conditions (flow velocities and turbulence) inside a scour hole and the geological conditions (composition of the subsoil) around a scour hole determine the scour hole development. The hydrodynamic conditions are the forcing mechanism for scour hole growth, while the geological conditions are the resistant component. The tidal influence in the RMD results in complex continuously changing flow patterns inside a scour hole.

There is variability in local growth inside a particular scour hole due to local variation in the hydrodynamic and geological conditions. From the historical bathymetry data analysis follows that there is no yearly trend visible in the local scour hole development. This makes it, together with the continuously changing hydrodynamic conditions and the local variance of the geological conditions, very difficult to predict the scour hole development with numerical models.

The scour hole development can be predicted with a data-driven extrapolation tool. In this thesis, the currently available tool Htrend has been used as a basis for the scour hole development prediction. The tool is applied in an updated probabilistic way, such that uncertainties are considered. By extrapolation of differences between historically measured bathymetry data together with the historical relation between the measured local bed level and the measured erosion rate of that bed level, the future scour hole dimensions can be predicted from only measured bathymetry data.

#### 2. How to quantify the hazards and consequences of scour holes?

In this thesis, only the potential hazard of flooding due to the presence of scour holes is studied. However, similar steps can be applied for the quantification of other hazards like the stability of hydraulic structures, like bridges and groynes and the erosion of cover layers of cables, pipeline and tunnels.

In order to quantify any current or future hazard of a scour hole, the scour hole dimensions must be known. The probability of occurrence of any hazard can subsequently be determined based on the scour hole dimensions. The current scour hole dimensions can be determined from bathymetry surveys. The future scour hole dimensions can be predicted with the data-driven extrapolation tool.

The probability of flooding next to a scour hole can be increased due to the occurrence of a flow slide. In order to determine the probability of flooding, the occurrence of flow slides are used as conditional scenarios in the probability calculation of the direct failure mechanisms overtopping, piping and macro-stability of the inner slope. The probability of occurrence of a flow slide and the direct failure mechanisms can be quantified with the safety assessment method described in the WBI.

The consequences of a potential hazard depend on the type of hazard itself. For flooding, there are two types of consequences. After a flood, there are economic damages and loss of life. In order to express loss of life in monetary units, the value of statistic life can be used. For the other potential hazards of scour holes, these two types of consequences could also be used.

The magnitude of the consequences of a flood depends on the exact location of a dike breach. The two types of consequences of a flood are quantified in the Veiligheid Nederland in Kaart (VKNK2) analysis for many dike breach locations in the Netherlands. These values can be used for the risk assessment of scour holes.

### **3. What is the impact of scour holes in the Rhine-Meuse Delta on flood risk and which scour holes form currently a threat?**

There is a larger probability of occurrence of a flow slide of the foreshore next to a scour hole compared with a foreshore without a nearby located scour hole. The larger probability results in a larger probability of occurrence of a flood and therefore in a larger flood risk.

The dynamic behaviour of a scour hole affects the probability of occurrence of a flow slide in two ways. Firstly, the local river channel height increases due to a growth in depth resulting in a larger probability of occurrence. Subsequently, over a larger section length, there is an increased probability of occurrence, if a scour hole grows in size. Which results in a larger total probability of occurrence of a flow slide next to the scour hole.

The occurrence of a flow slide is independent of the water level and will often not directly lead to a flood. Therefore, flow slide is an indirect failure mechanism. After the occurrence of a flow slide, emergency repairs could be applied in order to reduce the probability of a flood. Without taking emergency repairs or in the period between the occurrence of a flow slide and the implementation of emergency repairs, there is an increased probability of flooding.

The RMD can be divided into four subsystems. In this thesis, the probability of occurrence of a flow slide is only checked in the subsystem of the connecting branches (Spui, Dordtsche Kil, Oude Maas and Noord). It has been assumed that the probability of occurrence of a flow slide is the largest in the connecting branches. Based on a quickscan for these branches, there are at least four scour holes with a larger probability for the occurrence of flow slide with affection of the flood defence next to the scour hole. Other scour holes in the connecting branches are stable, are not located nearby the riverbanks, have a larger foreshore between the river and the flood defence or the riverbanks have been stabilized with riprap.

The following scour holes are currently a threat:

1. In the Spui near rkm 1004.8
2. In the Spui near rkm 1007.5
3. In the Oude Maas near rkm 982.1
4. In the Noord near rkm 983.8

### **4. What are the most sensitive aspects for the flood risk assessment near scour holes?**

Different aspects with several associated parameters play a role in the assessment of the flood risk near scour holes. With a sensitivity analysis the importance of the parameters is determined. The most sensitive aspect is the post flow slide profile. Depending on the post flow slide profile, the whole dike or only the foreshore can be affected by a flow slide, which influences in the probability of flooding significantly. Followed by the subsoil properties, the subsoil properties are decisive for the probability of occurrence of a flow slide. Subordinate to these two aspects is the dynamic behaviour of the scour hole, which determines the exact scour hole dimensions and depth.

### 5. What is the effect and economic feasibility of risk-reducing measures?

Different types of risk mitigation measures can be implemented to reduce the flood risk near scour holes. Two types are analysed in this thesis. These types are 1) placing riprap on the entire underwater slope and 2) filling of the scour hole with sand. The sand can be dredged in other river branches in the RMD. After placing riprap on the entire underwater slope, the occurrence of flow slide can be neglected. However, direct failure mechanisms can still occur, therefore, the flood risk is not negligible. Filling of a scour hole with sand reduces the probability of occurrence of a flow slide and the flood risk. The occurrence of a flow slide cannot be neglected.

In this thesis, one scour hole in the Spui is analysed as case study. Based on a cost-benefit analysis for both measures, it becomes clear that the investment costs of placing riprap are much larger than filling of the scour hole with sand (€944,384 versus €102,296). The lifespan of the riprap measure is also expected to be larger. However, based on the assumption made for the investment costs, the lifespan of the measures and effectiveness in risk reduction, the implementations of both measures result in a positive net present value of the investment. The benefit-cost ratio for placing riprap is 2.28 and for filling the scour hole with sand the benefit-cost ratio is 1.40. Therefore, both measures are economically beneficial.

### Main question: How to assess and reduce flood risk near scour holes in the Rhine-Meuse Delta?

The first step of the method for the flood risk assessment near scour holes is to predict the future scour hole dimensions. With a data extrapolation tool, the scour hole development can be predicted and the future bed level bathymetry determined. Subsequently, the probability of occurrence of a flow slide and the corresponding post flow slide profile can be determined from a river cross-section profile, based on the predicted bathymetry and the land elevation height of the foreshore and dike. The probability of flooding can be subsequently determined from the probability of failure due to direct failure mechanisms based on the post flow slide profile. Finally, the flood risk can be assessed from the calculated probability of flooding multiplied with the consequences of a flood.

The flood risk can be reduced with risk mitigation measures, like placing riprap or filling the scour hole with sand. Both measures reduce the probability of occurrence of a flow slide and thus the probability of flooding. The implementation of risk mitigation measures can be economically beneficial, depending on the original probability of flooding, the magnitude of the consequences, the effectiveness in risk reduction and the total investment costs.

## 7.2. Discussion

In this thesis, a method has been developed for the risk assessment of scour holes in a quantitative way. A risk quantification method was missing but it was desired such that the risk of scour holes in the RMD could be assessed in a quantitative way. This discussion aims to evaluate the method itself and the results obtained with the usage of the method.

### Method for risk quantification

In the risk assessment method for scour holes, an earlier developed bathymetry data extrapolation tool (Htrend) has been used as a basis and applied in a probabilistic setting. Subsequently, the tool is used in combination with calculation methods from the WBI. Both aspects are discussed here.

The tool Htrend has been updated from a deterministic extrapolation tool to a probabilistic extrapolation tool to make it possible to predict the future scour hole bathymetry together with its uncertainty. The growth in depth of the scour hole is based on the historically measured relation between the erosion rate in the scour hole and the local bed level. This method has been chosen from a data-analysis of the case scour hole in the Spui. For the case scour hole, there was no historical trend in erosion visible in the bathymetry data. Therefore, the original deterministic approach was not suitable. As an alternative method the probabilistic approach is used. However, this method is chosen after an analysis of only one scour hole. As stated in this thesis, the dynamic behaviour of scour holes in the RMD are strongly varying, even if they are located close to each other, due to large variations in subsoil composition in the RMD. Therefore, the used method for the scour hole development prediction might be not direct suitable to other scour holes. First, the local dynamic behaviour in a particular scour holes with respect to the bed level need to be clear. When there is a trend recognizable in the historically measured bathymetry, the method is applicable to the scour hole.

Based on the predicted future bathymetry of a scour hole, the probability of occurrence of a flow slide can be determined with the method given in the WBI, as shown in Eq. 4.2. In order to calculate this probability, six parameters for subsoil and river cross-section profiles are required. There are currently no model uncertainties and uncertainties in the parameters taken into account. However, the sensitivity analysis shows that the result is especially sensitive to variations in these input parameters. Besides, the soil parameters are estimated from subsoil scenarios which hold for the entire dike-segment with a length of 8 [km], while mainly local subsoil properties are relevant for local occurrence of flow slides.

The scour hole growth in length and width is relevant for the probability of occurrence of a flow slide. The used case scour hole had a small historical growth in width. The predicted growth in width is also small, as a result of the extrapolation of the historical growth. However, the growth in width is relevant for the probability of occurrence of a flow slide, especially for a scour hole located close to the riverside. It is probably difficult to predict the exact growth in width for scour holes located close to riversides with the proposed probabilistic extrapolation method. This could result in an overestimation of the scour hole development of a scour hole which is growing towards a riverside. It is, therefore, important to monitor the scour hole development with bed measurements in order to check if the dynamic behaviour corresponds to the predicted development.

Moreover, usage of the method given in the WBI gives relatively large probabilities of occurrence of a flow slide. However, there are not many occurrences of flow slides known in the RMD. The mismatch between the probability and the actual number of observed flow slides in the RMD, can be due to 1) well implemented protection measures on riverbanks or 2) a not suitable calculation method for the probability of occurrence of a flow slide. On many locations in the connecting branches in the RMD, there is riprap present on the riverbanks, which could be an explanation for the difference. On the other hand, the used and only available calculation method is based on the historical occurrence of 710 flow slides along estuary banks in Zeeland. However, the riverbanks in the RMD are smaller and more diverse than in Zeeland. The difference is covered with scaling parameters in the calculation method. It is possible that the difference cannot fully be covered with these parameters. Next, the method is based on the assumption that only erosion of the foreshore can trigger a flow slide. However, there are more triggers possible, like rapid drawdown of the water level and dumping of sediments. The other triggers can have a larger probability of occurrence in Zeeland than in the RMD.

### **General flood risk near scour holes**

From the risk assessment of the case scour hole in the river Spui follows that there is an increased probability of flooding near the scour hole and this probability will increase in the near future. However, it cannot be stated that there is a large problem for the flood safety near this scour hole. Based on the quickscan executed in this thesis for the occurrences of flow slides in the connecting branches, there are only 4 of the 29 scour holes in the connecting branches RMD with a potential threat for flood risk. With the assumption that there is only a threat in the connecting branches for flow slide, it means that the magnitude of the total problem in the entire RMD is limited and probably manageable. This assumption has not been verified in this research. Besides, the actual flood risk is only assessed for one particular location. In addition, new scour holes can develop in the RMD and there could be more scour holes with a potential hazard for flow slide in the future.

The scour hole problem is manageable by regularly monitoring the exact scour hole development and stability of the foreshores next to the scour holes with a potential threat. The exact scour hole development will be clear and adequate measures can be implemented at the required moment. New scour holes can be detected by monitoring the entire river branches.

## **7.3. Recommendations**

### **7.3.1. Recommendations for further research**

For further research with respect to flood risk assessment near scour holes it is recommended to focus first on the method for quantification of the probability of occurrence of flow slide and the post flow slide profile. In a later stage, further research can be performed to the exact scour hole development.

### **Post flow slide profile**

The only currently available method for the determination of the post flow slide profile is based on a volume balance between the original profile and the post flow slide profile. This method is purely based on the river profile geometry and the distribution of the post flow slide profile properties, derived from historical flow slides in Zeeland. Aspects as soil properties, presence of riprap or vegetation are not taken into account. However, it can be assumed that these aspects have an influence on the post flow slide profile. A better method for the prediction of the post flow slide profile improves, in general, the reliability of the calculated probability of exceedance of a certain retrogression length. Besides, the known distributions for the post flow slide profile properties are based on the flow slides in estuary banks in Zeeland. It could be analysed if these same distributions hold for the post flow slide profile properties in riverbanks.

### **7.3.2. Recommendations for risk assessment method for scour holes**

#### **Other direct failure mechanisms**

In this research, only the effect of a flow slide on the direct failure mechanism overtopping is included in the risk assessment. However, a flow slide affects also other direct failure mechanisms. The effects on piping, macro-stability of the outer slope and erosion of the outer slope are not quantitatively analysed in this thesis. For a full risk assessment, it is recommended to also include these direct mechanisms.

#### **Other types of risk**

Next to flood risk, the presence of scour holes are a potential threat for the stability of hydraulic structures and the protecting coverage layers of cables, pipelines and tunnels. Despite, the consequences of these hazards are likely smaller than the consequences of a flood, the risk could still be assessed. For these two other types of risk, the scour hole development is also relevant and can be predicted with the same method as for flood risk.

#### **Application in river parts without scour holes**

For the quickscan, the several steps in order to calculate the probability of occurrence of flow slide have been scripted and coupled together in a tool. With the tool, it is possible to indicate directly all relevant locations for the failure mechanism flow slide of an entire river branch regardless of the presence of scour holes. The tool can also be used, in addition to the currently available software for the safety assessment for flood defences regarding flow slides.

### **7.3.3. Recommendations for scour holes in the RMD and the case scour hole**

#### **Application on other river branches and scour holes**

The potential threat of scour holes in three river branches in the RMD has been analysed with a quickscan. The quickscan is only executed for the connecting river branches, based on the assumption that the scour holes in the connecting river branches have, in general, the largest probability of occurrence of flow slide. By applying a quickscan for the remaining other river branches in the RMD, this assumption can be relatively simply be verified.

If it turns out that there are multiple scour holes affecting the probability of flooding for a same dike-trajectory. The total probability of flooding due to scour holes cannot be calculated by summing the individual probabilities. The dependencies of the occurrence of flow slides and the occurrence of flooding must be taken into account.

One of the four identified scour holes with a potential threat, is used as a case scour hole in this research. It is recommended to apply the same steps as applied for this scour hole on the three other scour holes. Then, the flood risk of these three other scour holes become also clear.

#### **Soil properties investigation**

The composition of the subsoil determines the scour hole development and the probability of flow slides. The soil properties of and local thickness of soil layers under the scour hole are currently unknown. With insight in these properties and the local variability in soil composition, the local scour hole development can be more precisely predicted.

Moreover, insight into the exact soil composition of the foreshore of the riverbank next to scour hole can result in a better estimation of the soil parameters required for the calculation of the probability of occurrence of a

flow slide. Better insight into the relevant soil properties can be obtained with Cone Penetration tests (CPTs) in the foreshore and especially close to the riverbank. Next to CPTs, it is advisable to analyse the particle sizes from soil samples retrieved from boreholes, in order to determine the local mean particle diameter.

#### **Implementation of risk mitigation measures**

The implementation of risk mitigation measures in the case scour hole is not directly required to meet the safety standard. However, filling the scour hole with sand or placing riprap on the underwater slope reduces the flood risk. Based on the assumptions made with respect to the effectiveness of the implementation and the investment costs, both measures are economically beneficial. It can thus be considered to fill the scour hole with sand dredged from the river branches in the RMD with sedimentation or placing riprap on the entire underwater slope.

The measure to fill the scour hole with sand can be reconsidered if the results from the pilot study to nourishments in scour holes in the Oude Maas are clear. The lifespan of the nourishment influence the feasibility of the measure. If it turns out that the filling material erodes rapid, the filling measure is less effective and probably no longer economically beneficial.

#### **Monitoring plan**

Results from the quickscan in the connecting river branches can be used by the Waterboard Hollandse Delta in order to improve their monitoring plan regarding bed level changes. The waterboard now monitors entire river branches in order to detect bed level changes which can initiate flow slides. In the results of the quickscan, the relevant locations with a large probability of occurrence are indicated, regardless of the presence of a scour hole and the placement of riprap. Monitoring is also relevant on locations with riprap in order to monitor the stability of the placed riprap. The monitoring plan of the waterboard can be adapted to more inspections on the locations with a large probability of occurrence of a flow slide (as indicated in the results of the quickscan and figure 5.2) and less frequently on the remaining river parts.

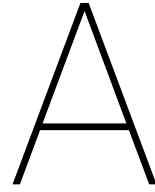
# References

- Arcadis. (2015). *Landelijke verkenning zettingsvloeiing* (Tech. Rep.). Rotterdam: Arcadis Nederland BV.
- Baars, L. (2019). *Suppletie Oude Maas: monitoring & analyse morfologie*.
- Bom, S. (2017). *Scour holes in heterogeneous subsoil; A numerical study on hydrodynamic processes in the development of the scour holes* (Master Thesis). TU Delft.
- Bowles, D., Brown, A., Hughes, A., Morris, M., Sayers, P., Topple, A., ... Gardiner, K. (2013). *Guide to risk assessment for reservoir safety management* (Vol. 2). Bristol: Environment Agency.
- Breusers, H. N. C. (1965). *Conformity and time scale in two-dimensional local scour*. Delft: Hydraulics Laboratory Delft, the Netherlands.
- Buschman, F., Forzoni, A., van den Ham, G. & Hijma, M. (2015). *Opvullen en afdekken ontgrondingskuilen in de Oude Maas* (Tech. Rep.). Delft: Deltares.
- de Groot, B. R. (2014). *Veiligheid Nederland in Kaart 2 Overstromingsrisico dijkringgebied 20, Voorne-Putten* (Tech. Rep.). Rijkswaterstaat WVL.
- de Groot, M., Stoutjesdijk, T. P., Meijers, P. & Schweckendiek, T. (2007). Verwekingsvloeiing in zand. *Geotechniek*(Oktober2007), 54–59.
- de Groot, M., van der Ruyt, M., Mastbergen, D. R. & van den Ham, G. (2009). Bresvloeiing in zand. *Geotechniek*(Juli 2009), 34–39.
- Deltares. (2011). *Maatschappelijke kosten-batenanalyse Waterveiligheid 21* (Tech. Rep.). Delft: Author.
- de Ruiter, T., Fioule, A. & Sieben, A. (2017). *Prognose bodemveranderingen met heterogene bodemdynamiek*.
- Driessen, T., Jong, W. D., Moll, R., Kruijff, A. D., Schropp, M., Treurniet, M., ... Sieben, A. (2018). *Impact van Basis Rivierbodempligging op beleid en beheer* (Tech. Rep.). Nijmegen: HASKONINGDHV NEDERLAND B.V.
- Duits, M. (2018). *Hydra-NL: Gebruikershandleiding* (Tech. Rep.). Lelystad: HKV lijn in water.
- EurOtop. (2018). *Manual on wave overtopping of sea defences and related structures*.
- Ferrarin, C., Madricardo, F., Rizzetto, E., Kiver, W. M., Bellafiore, D., Umgiesser, G., ... Trincardi, F. (2018). Journal of Geophysical Research : Earth Surface Geomorphology of Scour Holes at Tidal Channel Confluences. *Journal of Geophysical Research: Earth Surface*, 123, 1386–1406.
- Ginsberg, S. S. & Perillo, G. M. E. (1999). Deep-scour holes at tidal channel junctions , Bahia Blanca. *Marine Geology*, 160(1-2), 171–182.
- Gouldby, B., Samuels, P., Klijn, F., Messner, F., Os, A. V. & Sayers, P. (2005). *Language of Risk: Project definitions* (Tech. Rep. No. March). HR Wallingford UK.
- Haasnoot, M., Bouwer, L., Diermanse, F., Kwadijk, J., van der Spek, A., Essink, G., ... Mosselman, E. (2018). *Mogelijke gevolgen van versnelde zeespiegelstijging voor het Deltaprogramma* (Tech. Rep.). Delft: Delaters.
- Helpdesk Water. (2015). *Baselinemodel RijnMaaasMonding: Baseline-RMM-beno15.5-v2*.
- Helpdesk Water. (2017). *D-Soil Model 17.2*.
- Hijma, M. (2009). *From river valley to estuary: The early-mid Holocene transgression of the Rhine-Meuse valley, The Netherlands* (Phd Thesis). Utrecht University.

- Hoffmans, G. & Pilarczyk, K. (1995). Local scour downstream of hydraulic structures. *Journal of Hydraulic Engineering*, 121(4), 326–340.
- Hoffmans, G. & Verheij, H. J. (1997). *Scour manual*. Rotterdam: A.A. Balkema.
- Hoitink, A. J. F., Wang, Z. B., Vermeulen, B., Huismans, Y. & Kästner, K. (2017). Tidal controls on river delta morphology. *NATURE GEOSCIENCE*, 10(September), 637–645.
- Huismans, Y. & Hoitink, A. J. F. (2017). Towards control over Rhine-Meuse Delta channel network: a historical overview and contemporary research needs. *Advances in Water Resources (submitted)*.
- Huismans, Y. & van Duin, O. (2016). *Advies beheer rivierbodem van de Rijn-Maasmonding* (Tech. Rep.). Delft: Deltares.
- Jonkman, S. N. (2007). *Loss of life estimation in flood risk assessment* (Phd Thesis). TU Delft.
- Jonkman, S. N., Jorissen, R. E., Schweckendiek, T. & van den Bos, J. P. (2018). *Flood Defences: lecture notes CIE315* (3rd Edition ed.). TU Delft.
- Jonkman, S. N., Steenbergen, R., Morales-Napoles, O., Vrouwenvelder, A. & Vrijling, J. (2017). *PROBABILISTIC DESIGN: RISK AND RELIABILITY ANALYSIS IN CIVIL ENGINEERING. Lecture notes CIE4130* (Nov 2017 ed.). Delft: TU Delft.
- Kaplan, S. & Garrick, B. J. (1981). On The Quantitative Definition of Risk. *Risk Analysis Coastal engineering*, 1(1), 11–27.
- Kind, J., de Bruijn, K., Diermanse, F., Wojciechowska, K., Klijn, F., van der Meij, R., . . . Sloff, C. J. (2019). *Invloed Hoge Scenario 's voor Zeespiegelstijging voor Rijn- Maas Delta* (Tech. Rep.). Delft: Deltares.
- Kjerfve, B., Shao, C.-C. & Stapor jr, F. W. (1979). Formation of deep scour holes at the junction of tidal creeks: an hypothesis. *Marine Geology*, 33, M9—M14.
- Kok, M., Jongejan, R., Nieuwjaar, M. & Tanczos, I. (2016). *Fundamentals of Flood Protection*. Breda: Ministry of Infrastructure and the Environment and Expertise Network for Flood Protection (ENW).
- Koopmans, H. (2017). *Scour holes in tidal rivers with heterogeneous subsoil under anthropogenic influence* (Master Thesis). TU Delft.
- Kramer, S. L. (1988). Triggering of liquefaction flow slides in coastal soil deposits. *Engineering Geology*, 26, 17–31.
- Kuipers, B., van der Lugt, L., Jacobs, W., Streng, M., Jansen, M. & van Haaren, J. (2018). *Rotterdam effect* (Tech. Rep.). Rotterdam: Erasmus University.
- MOS GRONDMECHANICA. (2019). *Geotechnisch lengteprofiel: Traject 20-3 Voorne Putten (Opdr. 1801726)*. Rhooon: Retrieved from WSHD.
- Platform Rivierkennis. (2018). *Het verhaal van de Rijn-Maasmonding* (Tech. Rep.). RWS.
- Rijkswaterstaat. (2012). *Handreiking Toetsen Voorland Zettingsvloeiing t.b.v. het opstellen van het beheerder-soordeel (BO) in de verlengde derde toetsronde* (Tech. Rep.). Author.
- Rijkswaterstaat. (2015). *Beheer- en ontwikkelplan voor de rijkswateren 2016 - 2021* (Tech. Rep.).
- Rijkswaterstaat. (2016a). *Schematiseringshandleiding macrostabiliteit* (No. december 2016). Ministerie van Infrastructuur en Milieu.
- Rijkswaterstaat. (2016b). *Schematiseringshandleiding zettingsvloeiing* (No. december 2016). Ministerie van Infrastructuur en Milieu.
- Rijkswaterstaat. (2017). *Regeling veiligheid primaire waterkeringen 2017: Bijlage III Sterkte en veiligheid* (No. april 2016). Ministerie van Infrastructuur en Milieu.

- Rijkswaterstaat. (2018). *Schematiseringshandleiding grasbekleding* (No. april 2018). Ministerie van Infrastructuur en Milieu.
- Rosqvist, T. & Tuominen, R. (2004). Qualification of Formal Safety Assessment : an exploratory study. *Safety Science*(42), 99–120.
- Ruckert, C. & Sieben, A. (2019). Rijkswaterstaat vult erosiekuilen Oude Maas. *Land+Water: vakblad voor civiel- en milieutechniek*(3), 30–31.
- Schiereck, G. J. & Verhagen, H. J. (2012). *Introduction to Bed, bank an shore protection* (2nd ed.). Delft: VSSD.
- Schuurman, F. (2018). *Scenariostudie t.b.v. besluit sedimentbeheerplan RMM*. Amersfoort.
- Sieben, A. (2018). *Monitoringsbehoefte pilot Oude Maas*.
- Sloff, C. J., Van Spijk, A., Stouthamer, E. & Sieben, A. (2014). Understanding and managing the morphology of branches incising into sand-clay deposits in the Dutch Rhine Delta. *International Journal of Sediment Research*, 28(2), 127–138.
- Stenfert, J. (2017). *Scour holes in heterogeneous subsoil; An experimental study to improve knowledge of the development of scour holes in heterogeneous subsoil* (Master Thesis). TU Delft.
- Stouthamer, E. & de Haas, T. (2011). *Erodibiliteit en risico op zettingsvloeiing als maat voor stabiliteit van oevers, onderwatertaluds en rivierbodems van de Noord, de Oude Maas en het Spui* (Tech. Rep.). Utrecht: Geografie, Departement Fysische Geowetenschappen, Faculteit Utrecht, Universiteit.
- Taylor, R. (1990). Interpretation of the Correlation Coefficient A Basic Review. *Journal of Diagnostic Medical Sonography*, 6(1), 35–39.
- Van den Berg, F. (2014). *Innovaties HWBP Probleemveld Zettingsvloeiing*. Delft: Deltares.
- Van der Krogt, M. (2015). *Safety Assessment Method for Indirect Failure Mode Flow Sliding* (mastersthesis). TU Delft.
- van den Ham, G. (2015). *Faalmechanismebeschrijving zettingsvloeiing* (Tech. Rep.). Delft: Deltares.
- van den Ham, G., de Groot, M. B. & Mastbergen, D. R. (2014). A Semi-empirical Method to Assess Flow-Slide Probability. *Submarine Mass Movements and Their Consequences 6th International Symposium*, 37, 213–223.
- van der Klis, H. (2003). *Uncertainty Analysis applied to Numerical Models of River Bed Morphology* (Phd Thesis). TU Delft.
- van der Krogt, M., van den Ham, G. & Kok, M. (2015). Safety Assessment Method of Flood Defences for Flow Sliding..
- van Vuren, B. G. (2005). *Stochastic modelling of river morphodynamics Stochastisch modelleren van rivier-morfodynamica* (PhD Thesis). TU Delft.
- van Zuylen, J. (2015). *Development of scour in non-cohesive sediment under a poorly erodible top layer* (Master Thesis). TU Delft.
- Vellinga, N. E., Hoitink, A. J. E., van der Vegt, M., Zhang, W. & Hoekstra, P. (2014). Human impacts on tides overwhelm the effect of sea level rise on extreme water levels in the Rhine–Meuse delta. *Elsevier Coastal engineering*, 90, 40–50.
- Vergouwe, R., Sarink, H., Roode, N., Kooij, A. & Verheijen, J. (2014). *De veiligheid van Nederland in kaart: eindrapportage* (Tech. Rep.). Rijkswaterstaat Projectbureau VNK.
- VNK2 Projectbureau. (2012). *Flood risk in the Netherlands VNK2: The method in brief* (Tech. Rep.). Rijkswaterstaat WVl.
- WSHD. (2017). *Beoordeling veiligheid primaire waterkeringen 2017-2023: Normtraject 20-3 – Geervliet-Hekelingen*. Ridderkerk.
- WSHD. (2019). *Steen besorting*. Ridderkerk.

*(This page is intentionally left blank)*



## Extra literature

In this Appendix extra relevant literature is presented. First the scour hole development process are clarified. Followed by the safety assessment method regarding flow slide given in the Wettelijk Beoordelingsinstrumentarium (WBI).

### **A.1. Scour hole development**

Scour is defined as local erosion. It occurs if the local transport capacity exceeds the supply from upstream (Schierck & Verhagen, 2012). If the erosion leads to a local deepening which is significant with respect to the surrounding river bed, the local deepening is called a scour hole.

Koopmans (2017) and Huismans & van Duin (2016) showed with a data analysis that the scour hole development strongly varies per scour hole. Despite similar hydrodynamic conditions, there are not necessary similarities between scour holes located in the same branches. From the data analysis follow different trends, some scour holes are stable, while others are eroding or even sedimentating. For example, in the Oude Maas, one scour hole (OMS-4a) grew 2.2 [m] in depth between 2009 and 2014, while another scour hole (OMS-3b) located 9 [km] downstream, became 0.4 [m] shallower (Huismans & van Duin, 2016). An explanation for the strong variance in scour hole development is the presence of structures close to the scour hole, changes in river geometry and the varying composition of the subsoil.

#### **A.1.1. Conditions for erosion**

The differences between the development of scour holes occur due to a difference in hydrodynamic conditions and geological conditions. The hydrodynamic conditions are the forcing condition for erosion and the scour hole development, while the geological conditions determine the resistant against erosion.

The local hydrodynamic and geological conditions are varying over river branches in the RMD. The variation in hydrodynamic conditions are due to changes in river geometry, presence of hydraulic structures or changes in bottom level. While the variation in geological conditions is originated during the formation of delta. Differences in these conditions lead to the presence of a scour hole at one location and the absence of a scour hole at another location.

#### **Hydrodynamic conditions**

The velocities and forces in the river current are called the hydrodynamic conditions. For the scour process the near-bed flow velocity is relevant. In general, the flow velocity is determined by the river discharge. In some branches of the RMD, the flow velocity is dominated by the tidal current instead of the river discharge. The local flow velocity depends on the local water depth and river width. At the locations of structures, like bridge piers or groynes, the river, is narrowed resulting in higher flow velocity. On the other hand, a scour hole is a local deepening of the river bed. This local deepening leads to a local reduce in flow velocity at the locations of a scour hole.

The flow velocities in combination with turbulence influence the transport capacity of a river. A spatial difference in either velocity or turbulence or both, leads to a spatial gradient of the transport capacity. The gradient leads to erosion or sedimentation. This follows from the conservation of mass. The general conservation of mass expression is (Schierreck & Verhagen, 2012):

$$\frac{\partial z_b}{\partial t} + \frac{\partial S}{\partial x} = 0 \quad (\text{A.1})$$

In which:

$$\begin{aligned} Z_b &= \text{Position of the bed level} && [\text{m}] \\ S &= \text{Sediment transport per unit width} && [\text{m}^3/\text{s}/\text{m}] \end{aligned}$$

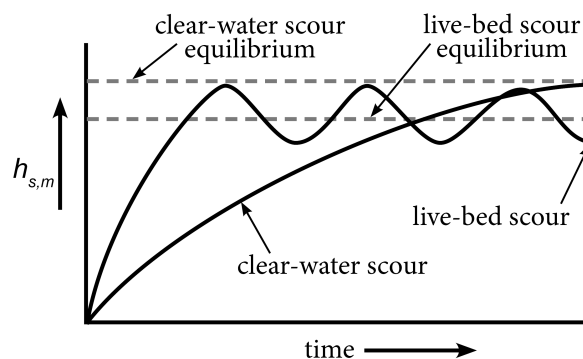
From Eq. A.1 follows that an increase in transport capacity lead to a reduction in bed level. A reduction in bed level is called erosion. On the other hand a decrease in transport capacity leads to an increase in bed level, which is called sedimentation (Schierreck & Verhagen, 2012).

Two types of scour are described by Schierreck & Verhagen (2012), the type depends on the upstream sediment transport.

- ( $S_2 > S_1 = 0$ ). When the upstream sediment supply is zero while there is downstream sediment transport the scour is called **clear-water scour**. The upstream supply can be zero if there is a lack of capacity due to a below critical flow velocity or because of a lack of erodible material.
- ( $S_2 > S_1 > 0$ ). The second type is known as **live-bed scour**. This is the scour when there is a sediment supply from upstream, but the downstream transport is larger. The downstream capacity can be larger due to an increase in flow velocity or due a difference in soil composition.

The scour process and the equilibrium depth depends on the type of scour. For clear-water scour the scour process reach its equilibrium at the moment when the flow velocity is reduced below the critical value. For the live-bed scour erosion within a scour hole also stops when the flow velocity is below the critical value. But due to the upstream sediment supply, sedimentation occurs. Resulting in bed level increase in the scour hole with corresponding increasing flow velocity. If the flow velocity increases above the critical value, erosion occur again. So, there is no real equilibrium for live-bed scour, but there is a dynamic equilibrium (Schierreck & Verhagen, 2012).

In figure A.1, the scour hole depth developments in time are shown for both types of scour holes. In this figure can be seen that the dynamic equilibrium depth for live-bed scour is smaller than the depth for clear-scour. The equilibrium for live-bed scour is sooner reached in time.



Source: Bom (2017) based on Hoffmans & Verheij (1997)

Figure A.1: Scour hole depth development in time for clear-water scour and live-bed scour.

### Geological conditions

The geological conditions, the conditions of the subsoil, determine the sediment transport. The transport of cohesive sediment (e.g. clay and peat) differs from the transport of non-cohesive sediment (e.g. sand).

#### *Non-cohesive sediment*

The motion of non-cohesive starts when the flow velocity is above a critical value. The motion can be described with Shields. According to Shields, the flow velocity in combination with turbulence leads to a shear stress. If the shear stress is above the critical value the sediment starts to move. The critical value depends on the relative weight of the sediment. Shields defined 7 stages of movement. In the first stage, there is only occasional movement at some location. While in the seventh stage there is general transport of all grains (Schierreck & Verhagen, 2012). The stage of transport depends on the ratio between the hydraulic load and strength of the sediment. This ratio is called the Shield-number, this is expressed in Eq. A.2.

$$\Psi_c = \frac{Load}{Strength} = \frac{\tau_c}{(\rho_s - \rho_w)gd} = \frac{u_{*,c}^2}{\Delta gd} \quad (A.2)$$

In which:

|           |   |   |                      |
|-----------|---|---|----------------------|
| $\Psi_c$  | = | Shield number   | [-]                  |
| $\tau_c$  | = | Critical shear stress                                 | [N/m <sup>2</sup> ]  |
| $\rho_s$  | = | Density of sediment                                   | [kg/m <sup>3</sup> ] |
| $\rho_w$  | = | Density of water                                      | [kg/m <sup>3</sup> ] |
| $g$       | = | Acceleration of gravity                               | [m/s <sup>2</sup> ]  |
| $d$       | = | Grain size  | [m]                  |
| $u_{*,c}$ | = | Critical bed shear stress                             | [m/s]                |
| $\Delta$  | = | Relative density ( $\frac{\rho_s - \rho_w}{\rho_s}$ ) | [-]                  |

For practical use the critical shear velocity  $u_{*,c}$  can be replaced by the Chezy coefficient. The Chezy coefficient is a roughness indicator based on bed-level properties and water depth.

$$u_{*,c}^2 = \frac{g}{C} \bar{u}_c^2 \quad (A.3)$$

In which:

|             |   |  |                       |
|-------------|---|--|-----------------------|
| $C$         | = | Chezy coefficient                                | [m <sup>1/2</sup> /s] |
| $\bar{u}_c$ | = | Depth average critical flow velocity coefficient | [m/s]                 |

Combining Eq. A.2 and A.3 gives:

$$\bar{u}_c = C \sqrt{\Psi_c \Delta d} \quad (A.4)$$

From this equation, it is clear that the critical velocity for movement of non-cohesive sediment depends on the stage of movement, the sediment properties and water depth.

#### *Cohesive sediment*

For non-cohesive material, the only resistant force is the relative weight of a grain. For cohesive sediment much large forces are needed to break the aggregates from the surrounding bed. If a grain is loosened from the bed, a relatively small force is needed to transport the grain. The transport of cohesive sediment is more complex than the non-cohesive sediment (Hoffmans & Verheij, 1997).

The transport of cohesive material can occur in two ways (Sloff et al., 2014). The first is abrasive erosion, in which the grains are scrapped by the flow. This happens if the shear stress of the flow is above the critical shear stress of the grains. The critical shear stress depends on the cohesion of the sediment. The critical flow velocity can be determined from the critical shear stress. The second mode of transport is pulling off entire sediment fragments. The critical shear stress for the pulling-off erosion depends on the undrained shear strength of the soil.

According to Hoffmans & Verheij (1997) no general design equations for the depth of scour holes are available. Because the most equations are related to a specific kind of sediment. The equations often include a parameter for cohesion. Hoffmans & Verheij (1997) suggest for a first estimation the following critical flow velocities:

- Fairly compacted clay: 0.5 [m/s]
- Stiff clay: 1.5 [m/s]

The classification of clay is based on the void ratio. Which is the ratio between volume of the voids to the volume of the solids of the sediment (Schierneck & Verhagen, 2012).

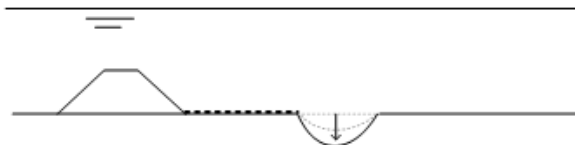
### A.1.2. Scour hole development stages

Since worldwide most scour holes are located close to hydraulic structures and could result in instability of structures, extensive international research has been done on this type of scour hole developments. Methods are developed to predict the equilibrium depth of this type of scour holes. For the prediction of the type of scour holes due to geological changes, less research is done. Bom (2017), Koopmans (2017), Stenfert (2017) and van Zuylen (2015) used the method for the prediction of scour holes behind a sill (Dutch: Drempel) with a non-erodible bed protection to predict the development of scour holes in heterogeneous subsoil. This method was used because of the similarities in two-dimensional flow pattern and slope steepness for a scour hole behind a sill and a scour hole in heterogeneous subsoil.

The method to predict the development of a scour hole behind a sill is called Breusers theory, which described the evolution of a two-dimensional scour hole based on clear-water scour. The development of a scour hole consists of four phases: an initial phase, a development phase, a stabilisation phase and an equilibrium phase (Hoffmans & Verheij, 1997).

#### Initial phase

In the initial phase, the flow is uniform and the bed is more or less flat. Bed material gets into suspension downstream of the non-erodible protection bed if the flow velocity is larger than the critical velocity. The suspended material will remain in suspension and flow away, which results in a small hole. The upstream slope will slightly increase. The growth in this phase is schematically presented in figure A.2. This phase ends if the uniform flow will be detached. The flow can then no longer follow the river geometry, resulting in a mixing layer with high turbulence intensities (Schierneck & Verhagen, 2012).

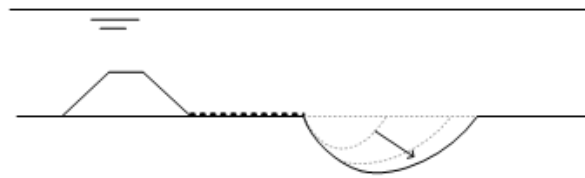


Source: Own creation, based on Hoffmans & Verheij (1997)

Figure A.2: Growth of a scour hole in the initial phase.

#### Development stage

In the development phase, several flow regions can be distinguished in the scour hole, as presented in figure A.5. The scour hole depth increase significantly. However, the ratio between the depth and the distance between the deepest point and the end of the bed protection remains constant. The upstream slope will remain constant as well, in this phase, see figure A.3

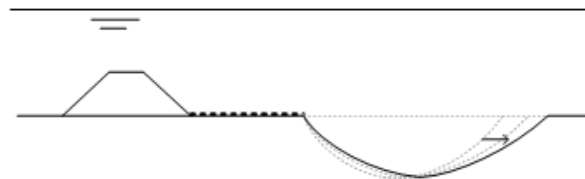


Source: Own creation, based on Hoffmans & Verheij (1997)

Figure A.3: Growth of a scour hole in the development phase.

**Stabilisation phase**

In the third phase, the stabilisation phase, the scour hole will only growth in length and no longer in depth. The erosion rate in the deepest point of the scour hole is low. The upstream slope of the scour hole becomes less steep, as indicated in figure A.4.



Source: Own creation, based on Hoffmans & Verheij (1997)

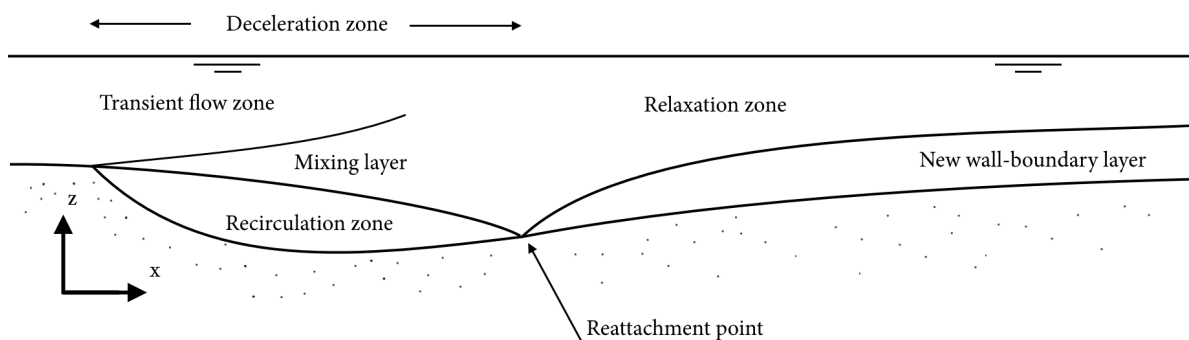
Figure A.4: Growth of a scour hole in the stabilisation phase.

**Equilibrium phase**

In the last phase, the scour hole will no have significant changes in depth or length. The scour hole is in equilibrium and therefore this phase is called the equilibrium phase.

**Flow regions**

The different flow regions are schematised in figure A.5. At the location of the scour edge, the flow will be detached due to the abrupt change in geometry. This results in a recirculation zone and a mixing layer downstream. In the recirculation zone, a return current is presented. This current has a lower flow velocity but more turbulence intensity compared to the initial situation. The mixing layer decelerates the main flow by approximately 30 % (Schierck & Verhagen, 2012). The declaration occurs due to the transport of mass and momentum. Within the mixing layer the high shear stresses give high turbulence intensities.



Source: Bom (2017) based on Hoffmans & Verheij (1997)

Figure A.5: Two-dimensional flow regions in a scour hole

### A.1.3. Development formulas

#### Depth development

The most important parameters of a scour hole are the scour hole depth and the timescale for the scour growth (Breusers, 1965). The depth determines in combination with the slopes, the size of a scour hole. According to Breusers (1965), the following relation can be found for the scour hole depth in the initial phase.

$$\frac{y_m}{h_0} = \left( \frac{t}{t_1} \right)^\gamma \quad (\text{A.5})$$

In which:

|          |   |                           |     |
|----------|---|---------------------------|-----|
| $y_m$    | = | Maximum scour hole depth  | [m] |
| $h_0$    | = | Local initial water depth | [m] |
| $t_1$    | = | Characteristic timescale  | [s] |
| $\gamma$ | = | Exponent                  | [-] |

The value for the exponent  $\gamma$  is determined by tests. A value between 0.34 and 0.38 can be used for two-dimensional scour holes (Hoffmans & Verheij, 1997). van Zuylen (2015) found during his experiments with a two-dimensional scour hole values of  $\gamma = 0.36 - 0.37$  for the initial stage of scour holes and higher values  $\gamma = 0.43$  for later stages. Stenfert (2017) could not fit the experimental results of a three-dimensional scour hole to a general  $\gamma$  value. Probably because of the fact that equilibrium scour hole depth during the experiments was smaller than the water depth. Which is one condition for Eq. A.5.

The characteristic timescale ( $t_1$ ), is the time which is needed for the development of a scour hole depth equal to the water depth ( $y_m = h_0$ ) (Hoffmans & Verheij, 1997). This timescale can be calculated with:

$$t_1 = \frac{K h_0^2 \Delta^{1.7}}{(\alpha \bar{u} - \bar{u}_c)^{4.3}} \quad (\text{A.6})$$

In which:

|           |   |  |                                   |
|-----------|---|--|-----------------------------------|
| $K$       | = | Calibration coefficient                | $[\text{m}^{2.3}/\text{s}^{3.3}]$ |
| $\alpha$  | = | Amplification factor for flow velocity | [-]                               |
| $\bar{u}$ | = | Local depth average flow velocity      | [m/s]                             |

The calibration coefficient  $K$  is dependent of the type of bed protection, for a hydraulic rough bed protection a value of 330  $[\text{m}^{2.3}/\text{s}^{3.3}]$  can be used. The amplification factor  $\alpha$  is used to assess the difference between the depth average flow velocity and the maximum flow velocity. According to Schiereck & Verhagen (2012), an amplification of  $\alpha = 5$  can be used to be on the safe side. However, the amplification factor can also be calculated with the relative turbulence intensity.

#### Equilibrium depth

Often the equilibrium depth is more important than the depth during the development process. According to Hoffmans & Verheij (1997), an estimation of the theoretical equilibrium depth can be obtained with Eq. A.7. However, a real equilibrium depth will never be reached for scour holes in the RMD since the water level is varying due to the tidal influence.

$$\frac{y_{max,e}}{h_0} = \frac{\alpha \bar{u}_c - \bar{u}}{\bar{u}_c} \quad (\text{A.7})$$

In which:

|             |   |                                      |     |
|-------------|---|--------------------------------------|-----|
| $y_{max,e}$ | = | Maximum equilibrium scour hole depth | [m] |
|-------------|---|--------------------------------------|-----|

#### Slope of the scour hole

The size of a scour hole depends on the depth and the steepness of the slope. According to Hoffmans & Pilarczyk (1995), the slope steepness of non-cohesive material, like sand, depends on the local velocity and the grain size diameter. The turbulence intensity, with a correction for bed roughness, affects the slope as well. With the following expression, the upstream slope of a scour hole in equilibrium can be estimated.

$$\beta = \arcsin \left( 2.9 \times 10^{-4} \frac{u_0^2}{\delta g d_{50}} + (0.11 + 0.75r_0) f_c \right) \quad (\text{A.8})$$

In which:

|          |   |  |       |
|----------|---|--|-------|
| $\beta$  | = | Angle of upstream slope                  | [°]   |
| $u_0$    | = | Local flow velocity                      | [m/s] |
| $d_{50}$ | = | Mean particle diameter                   | [m]   |
| $r_0$    | = | Relative turbulence intensity            | [-]   |
| $f_c$    | = | Roughness correction factor $F_c = C/40$ | [-]   |

In the case that the slope angle is larger than the internal friction angle, the slope cannot withstand the gravity forces. Shear stress due to the flow results in an unstable slope and the motion of particles. Depending of the initial packing of sediment, two mechanisms can occur. For loose packed material, liquefaction can occur, while for dense packed sediments breaching can occur. Both mechanisms result in a flow slide.

## A.2. Wbi method for safety assessment regarding flow slide

According to the Dutch Water Act, the safety of primary flood defence must be assessed every 12 years. The safety assessment is described in the safety standards. The primary flood defence must be checked on several aspects during the safety assessment (Rijkswaterstaat, 2017). Flow slide is taken into account for the safety assessment of the stability of the foreshore. The check of the stability of the foreshore is firstly based on a rule of thumb and the slope angle of the foreshore. In addition, a geotechnical check can be done. These checks give an indication for the possibility of occurrence of flow slides.

Until the introduction of the new WBI in 2017, these checks were sufficient (Rijkswaterstaat, 2012). A more advanced method to quantify the probability of occurrence has been developed during the 'Wettelijk Toets Instrumentarium' program. Based on expert judgement, statistics and knowledge about liquefaction and breaching, the probability of failure of a flood defence due to flow slide can be quantified. The calculation method of the probability of occurrence of flow slides is described for the first time in 'Handreiking zettingsvloeiing' from Rijkswaterstaat (2012). Firstly, the method was used as a second opinion for dike trajectories which were labelled as 'no judgement' according to the first checks, during the third assessment round (Arcadis, 2015). In the WBI, the method is updated and included in the obligatory safety assessment. The description is given in a separate document: 'Schematiseringshandleiding zettingsvloeiing' (Rijkswaterstaat, 2016b). In the rule of thumb, a clear distinction is made between flow slide due to static liquefaction and flow slide due to breaching. Each process has their own rule of thumb. While in the advanced method, no clear distinction is made for the two mechanisms. However, both processes are included in the advanced method.

For the safety assessment regarding flow slide two aspects are relevant:

1. The probability of occurrence of a flow slide.
2. The retrogression length of the profile after a flow slide.

### A.2.1. Rule of thumb

According to the WBI, the safety for flow slide can be assessed with the method presented in figure A.6a. The assessment consists of three steps (Rijkswaterstaat, 2017); 1) Would flow slide lead to damage of the flood defence? 2) Is flow slide possible based on the steepest slope? and 3) Is flow slide possible based on the total geometry?

In the first step (E.1), the possible consequence of a flow slide is analysed. If a flow slide occurs will it affect the water retaining function of a flood defence. In order to determine this, the actual profile must be compared with the assessment profile. The assessment profile for a foreshore without bed protection consists of two parts, a horizontal part and a sloping part. The horizontal part has a length of  $M = 2 \times H_{channel}$ . The slope part has a steepness of 1 : 15 for  $H_{channel} < 40m$  and 1 : 20 for  $H_{channel} > 40m$ . At the level of  $1/3 \times H_{channel}$ , the actual profile must be compared with the assessment profile. If the actual profile is within the assessment profile, flow slide can affect the water retaining function of the flood defence. The assessment profile for the affection of the water retaining function is shown in figure A.6b. In the situation shown in the figure, the actual

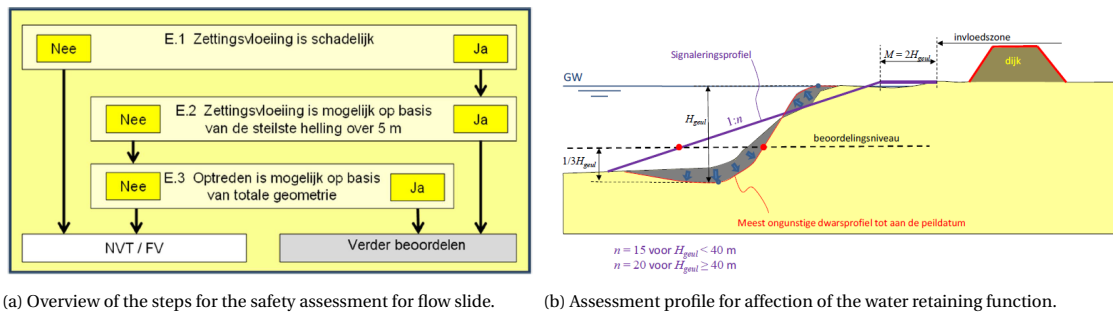


Figure A.6: Steps of the rule of thumb for flow slide in WBI.

Source: Rijkswaterstaat (2017)

profile is within the assessment profile, the occurrence of a flow slide will affect the water retaining function of the flood defence. The assessment profile shown in figure A.6b, holds only for unprotected slopes of the foreshore. For (partly) protected slopes with riprap, the assessment profile differs from this profile.

The second step (E.2) is the application of another simple rule of thumb. If the steepest slope of the submerged part, steeper is than 1:4 over at least 5.0 [m], it is assumed that flow slide can occur. If the steepest slope is milder than 1:4 flow slide can still occur based on the total geometry of the profile. Therefore, the total profile must be checked in the third step. The total profile must be checked for liquefaction and breaching (E.3).

Breaching can occur if a part of the slope of the dike profile in one of the sand or silt layers is too steep. The critical steepness depends on the vertical depth location. In figure A.7 the critical slopes are presented per depth interval. For depths larger than 40 [m], no critical slope is defined. According to Rijkswaterstaat (2017) no judgement can be made for the possibility of flow slide based on the total geometry for depths larger than 40 [m]. However, there are no depths larger than 40 [m] in the RMD. The critical slopes holds only for  $d_{50,mean} > 0.2$  [mm] and  $d_{15,mean} > 0.1$  [mm]. For smaller  $d_{50,mean}$  and  $d_{15,mean}$  also no judgement can be made. If the slope is milder than the critical slope, the probability of failure due to breaching flow sliding is negligible and no further calculation is required.

| Diepte-interval van onbestort deel van het onderwatertalud [m] | Maximale helling |
|--|------------------|
| 0 - 5  | 1:2              |
| 5 - 10   | 1:2.5            |
| 10 - 15  | 1:3              |
| 15 - 20  | 1:3.5            |
| 20 - 25  | 1:4              |
| 25 - 30  | 1:4.7            |
| 30 - 35  | 1:5.4            |
| 35 - 40  | 1:6              |

Source: Rijkswaterstaat (2017)

Figure A.7: Critical slope for breaching.

Next to breaching, also a rule of thumb for liquefaction must be checked. The rule of thumb for liquefaction is:

$$\cot(\alpha_r) \leq 7 \cdot \left( \frac{H_r}{24} \right)^{1/3} \quad (\text{A.9})$$

In which:

$$H_r = \text{Fictive calculation height} \quad [\text{m}]$$

$$\alpha_r = \text{Calculation slope angle} \quad [^\circ]$$

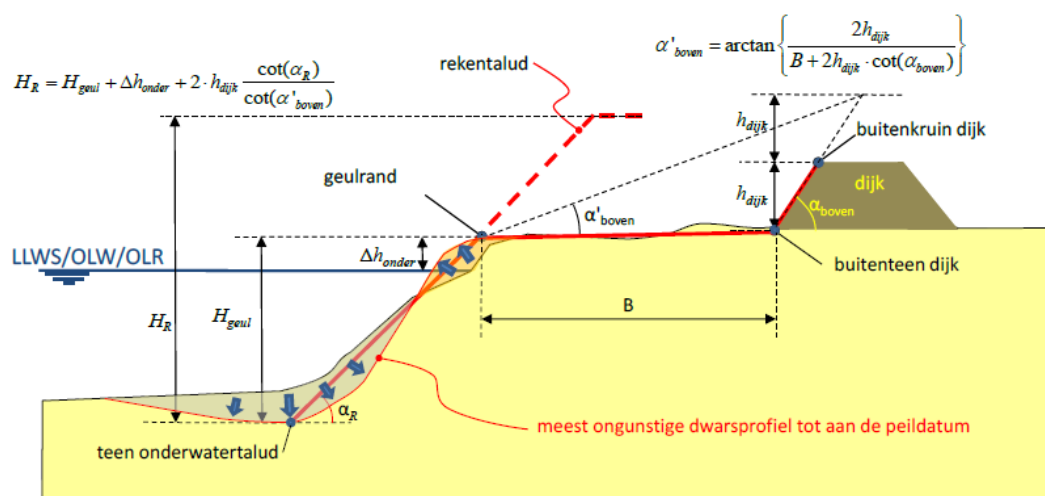
For liquefaction, a fictive calculation height must be used instead of the 'real' height. The fictive calculation height includes a correction for the height due to difference in submerged and emerged weight of sand

particles. The calculation slope angle is equal to the 'real' slope angle (Rijkswaterstaat, 2016b).

In figure A.8 is shown how  $\alpha_r$  and  $H_r$  can be determined. In order to determine  $\alpha_r$  and  $H_r$ , the following characteristic points of a dike profile are required:

- Bottom river channel
- Insert river channel
- Dike toe at riverside
- Dike top at riverside

The dike toe and dike top can often easily be determined from the dike profile. The determination of the bottom and insert of the river channel is more difficult since it is often not intermediately clear from a dike profile where these points are exactly located. These two points must, therefore, be determined in an iterative process. The points corresponding with the largest probability of occurrence of a flow slide, must be defined as bottom river channel and insert river channel (Rijkswaterstaat, 2016b). This can be done with Eq. A.10 of the advanced method. For the rule of thumb, these two points can be roughly estimated from a dike profile.



Source: Rijkswaterstaat (2017)

Figure A.8: Determination of fictive calculation height and calculation slope angle based on most unfavourable total geometry

### A.2.2. Quantification of probability of occurrence of flow slide

For the profiles that do not meet the criteria of the rule of thumbs, the advanced method of the WBI must be applied in order to determine the probability of occurrence of a flow slide. The method is developed with the statistics of 145 historical flow slides in the Dutch province of Zeeland (Rijkswaterstaat, 2012). The reference situation of the method is therefore the subsoil of Zeeland. With the introduction of scale parameters, the method is also applicable on river dikes (Arcadis, 2015).

The occurrence of a flow slide depends on the profile geometry and the subsoil. The subsoil properties can be determined with Cone Penetration tests (CPTs). However, there is a large uncertainty in the results from these tests. (The uncertainty is the consequences of spatial variability of the subsoil and uncertainty in the transformation of the results of the CPT to usable soil parameters (Rijkswaterstaat, 2017).) To deal with this uncertainty, subsoil scenarios are introduced for the quantification of the probability of occurrence of a flow slide. For each dike-trajectory a certain amount number of subsoil scenarios are determined. These scenarios are open and included in WBI-software.

The probability of occurrence of a flow slide must be determined per section (in Dutch: kans per Vak). A section is defined in the WBI as part of a flood defence with uniform properties and loads (Rijkswaterstaat, 2017).

In order to determine the probability per section, one representative profile for the entire section must be

determined. The following steps need to be applied on this representative profile to assess the safety per dike section regarding the indirect failure mechanism flow slide:

1. Determination of probability of occurrence of a flow slide per subsoil scenario:  $P(FS|S_i)$
2. Determination of probability of occurrence of a flow slide for all scenario:  $P(FS) = \sum P(FS|S_i)P(S_i)$
3. Determination of probability of exceedance of the acceptable retrogression length given a flow slide:  $P(L > L_{max}|FS)$
4. Determination of probability of exceedance of the acceptable retrogression length for a dike section:  $P(L > L_{max})_{section}$
5. Check if  $P(L > L_{max})_{section} < P_{required.section}$

### 1. Probability of occurrence of a flow slide per scenario

The first step in order to determine the probability of occurrence of a flow slide per subsoil scenario is to calculate the frequency of a flow slide. This can be calculated as follows:

$$F(FS|S_i) = \overbrace{\left( \frac{5}{\cot \alpha_r} \right)^5 \times L_{section} \times \frac{V_{local}}{V_{zeeland}} \times 0.025 \times}^{\text{Scaling}} \left[ \underbrace{0.5 \times \left( \frac{H_r}{24} \right)^{2.5} \times \left( \frac{1}{10} \right)^{-10(0.05 + \psi_{5m.kar})}}_{\text{Liquefaction}} + \underbrace{0.5 \times \left( \frac{H_{channel}}{24} \right)^5 \times \left( \frac{2 \times 10^{-4}}{d_{50.mean.kar}} \right)^5 \times F_{cohesivelayers}}_{\text{Breaching}} \right] \quad (\text{A.10})$$

From the frequency determined with Eq. A.10, the probability of occurrence can be calculated:

$$P(FS|S_i) = 1 - e^{-F(FS|S_i)} \quad (\text{A.11})$$

These equations are derived from the statistics of flow slides in Zeeland, by van den Ham et al. (2014) and subsequently updated for the WBI. Eq. A.10 consists of three parts: a scaling part, static liquefaction part and breaching part. The several parameters of Eq. A.10 can be divided into three groups: geometry parameters, subsoil parameters and scaling parameters.

The following parameters are geometry parameters. These parameters depend on the profile geometry, as described in the explanation of the rule of thumb.

- Fictive calculation height  $H_r$
- Calculation slope angle  $\alpha_r$
- Channel depth  $H_{channel}$

The following parameters depend on the subsoil. These parameters need to be determined per subsoil scenario.

- Mean particle diameter  $D_{50.mean.kar}$
- State parameter  $\psi_{5m.kar}$
- Presence of interference layers  $F_{cohesivelayers}$

The scaling parameters are the following parameters:

- Dynamic behaviour of the foreshore  $V_{local}$
- Characteristic value of dynamic behaviour of the foreshore in Zeeland  $V_{zeeland}$
- Length of dike section  $L_{section}$

The occurrence of static liquefaction depends on the total height including the flood defence self and the soil state (Rijkswaterstaat, 2017). For the total height the fictive calculation height ( $H_r$ ) must be used. For the soil state, the state parameter is used. The state parameter  $\psi_{5m.kar}$  indicates the sensitivity of sand for liquefaction. It is the difference between the actual void ratio and the void ratio in critical state with the

same effective stress. The state parameter can be determined from a cone penetration test (Rijkswaterstaat, 2016b).

The relevant height for breaching is the height of the channel ( $H_{channel}$ ). Instead of the soil state which is relevant for liquefaction, the grain size and the presence of interference layers is more relevant for breaching.

Interference layers in the subsoil, like clay or peat layers, are cohesive layers. If these layers are undermined due to erosion or by an up slope moving breach, the cohesive layers can sudden breakdown. This can be a trigger for a breach flow or a vertical increase of an already existent up slope moving breach. Due to this sudden height increase of the existent breach, the sand discharge of the breach flow and the erosion volume increase as well (van den Ham et al., 2014). The presence of interference layers increases the probability of occurrence of breaching.

A qualitative scaling parameter  $F_{cohesivelayers}$  is introduced for the presence of cohesive layers by van den Ham et al. (2014). The reference situation for this scaling parameter is the mean subsoil of the province of Zeeland. The values for the scaling parameter are presented in table A.1.

| Amount of cohesive layers                | $F_{cohesivelayers}$ |
|--|----------------------|
| Almost none peat or clay layers          | 1/3                  |
| Restricted amount of peat or clay layers | 1                    |
| Many peat or clay layers                 | 3                    |

Table A.1: Subsoil parameter for the presence of interference layers.

The dynamic behaviour of the foreshore is the migration velocity of the foreshore edge. Due to erosion or sedimentation, the location of the foreshore edge can migrate. The yearly-average change of the position of the foreshore is the  $V_{local}$ -parameter. For the reference situation of Zeeland, the yearly change is 1.0 [m]. This is also the value of the parameter  $V_{Zeeland}$ . The local yearly change can be determined from consecutively bathymetry surveys of the foreshore. If these are not available, the parameter can be determined from bottom bathymetry surveys.  $V_{local}$  can then calculated as follows:

$$V_{local} = \frac{dZ}{dt} \times \cot \alpha_r \quad (\text{A.12})$$

## 2. Probability of occurrence of a flow slide for all scenario

After determining the probability of occurrence per subsoil scenario the total probability of occurrence of flow slide for all scenarios can be determined. The total probability can be calculated with:

$$P(FS) = \sum P(FS|S_i) \times P(S_i) \quad (\text{A.13})$$

In which:

$$\begin{aligned} P(FS) &= \text{Total probability of flow slide} \\ P(S_i) &= \text{Probability of occurrence of subsoil scenario } i \end{aligned}$$

## 3. Determination of probability of exceedance of the acceptable retrogression length given a flow slide

After the determination of the total probability of occurrence of flow slide. The probability of exceedance of the acceptable retrogression length has to be determined.

In order to determine the retrogression length of a flow slide, the profile after a flow slide must be determined. A schematic overview of the new profile is shown in figure 4.2. During a flow slide, the sediment flows away from the foreshore and spread out. Due to the flow in two directions and the fact that the new profile consists of two different parts, the surfaces of the two indicated areas are not equal. The ratio between area 1 and 2 is approximately 1.4 : 1. However, the three-dimensional volumes are equal due to the spread out of a flow slide. The retrogression length can be calculated from geometric properties of the profile and the ration between the two areas. For a flat foreshore, this can be done as follows:

$$L = a \times x - D \times b \quad (A.14)$$

$$x = \frac{-cH + \sqrt{(cH)^2 + (1-c)\left(\frac{D^2b}{a} + H^2c\right)}}{(1-c)}$$

$$a = \cot \gamma - \cot \alpha$$

$$b = \cot \gamma - \cot \beta$$

In which:

|          |   |   |     |
|----------|---|---|-----|
| $L$      | = | Retgression length                                  | [m] |
| $H$      | = | Total height of the submerged slope                 | [m] |
| $D$      | = | Height of the steepest slope of the new profile     | [m] |
| $c$      | = | Ratio between surface area 1 and 2 of the profile   | [-] |
| $\gamma$ | = | Slope angle of the mildest part of the new profile  | [°] |
| $\beta$  | = | Slope angle of the steepest part of the new profile | [°] |

As an alternative for non-flat foreshores, which is in practice often the case, the retrogression length can be calculated by numerically solving of the volume balance between area 1 and 2 (Rijkswaterstaat, 2016b). The variables of Eq. A.14 have uncertainties. Based on the statistics of over 145 flow slides in the province of Zeeland, the expected value, deviation and type of distribution for the different variables are determined. These values and type of distribution are presented in table A.2.

| $X$            | $\mu(X)$ | $\sigma(X)$        | Distribution |
|----------------|----------|--------------------|--------------|
| $\cot(\gamma)$ | 16.8     | 7.1                | Lognormal    |
| $\cot(\beta)$  | 2.9      | 1.7                | Lognormal    |
| $D/H$          | 0.43     | 0.06               | Normal       |
| $c$            | 1.4      | 0.1                | Normal       |
| $\cot(\alpha)$ |          | $0.05 \times E(X)$ | Normal       |

Source: Rijkswaterstaat (2016b)

Table A.2: Parameter distributions for the determination of the retrogression length with the volume balance.

In order to determine whether the retrogression length is acceptable, the following limit state function is given in the WBI:

$$Z = L_{max} - L \quad (A.15)$$

The retrogression length is not acceptable when this limit state function has a negative value ( $Z < 0$ ). The probability of exceedance of the acceptable retrogression is equal to the probability of negative values in the limit state function, as given in Eq. A.16. The limit state function, Eq. A.15, can be solved with a fully-probabilistic method (Level III), like a Monte Carlo simulation, or an approximation method (Level II), like a First Order Reliability Method (FORM) calculation.

$$P(L > L_{max} | FS)_{section} = P(Z < 0) \quad (A.16)$$

#### 4. Determination of probability of exceedance of the acceptable retrogression length for a dike section

In order to determine the probability of exceedance of the acceptable retrogression length for a dike section, the conditional probability of exceedance need to be multiplied with the probability of occurrence of flow slide, as is shown in Eq. A.17.

$$P(L > L_{max})_{section} = P(L > L_{max} | FS) \times P(FS) \quad (A.17)$$

In which:

$$P(L > L_{max})_{section} = \text{Total probability of exceedance of acceptable retrogression length for a dike section}$$

### 5. Check if probability is not above the safety standard

The last step of the safety assessment regarding flow slide is to check if the calculated probability of exceedance of the acceptable retrogression in step 4 does not exceed the maximum allowable probability. The maximum allowable failure probability is defined as follows:

$$P_{required.section} = 0.01 \times L_{section} \quad (A.18)$$

As can be seen, the allowable probability is in proportion with the section length. Larger sections have also larger allowable probability. However, the allowable probability per kilometre is the same.

#### Application on scour holes

The above-described safety assessment method is developed for regular dike profiles. However, in the WBI it is mentioned that for non-flat beds, which is the case for the presence of scour holes, the same method can be applied. Profiles with scour holes must be checked in the first step of the rule of thumb. The actual profile including the scour hole have to be compared with the assessment profile. If according to this first step, the scour hole profile is within the assessment profile, the scour hole must be taken into account during the determination of the calculation slope angle and the fictive calculation height. Otherwise, the presence of the scour hole can be ignored in the safety assessment regarding flow slide (Rijkswaterstaat, 2016b).

*(This page is intentionally left blank)*

# B

## Scour hole prediction approach

In this Appendix, the original deterministic approach of the tool Htrend.exe is described. Subsequently, the local erosion rates inside the scour hole near rkm 1004.8 is analysed in a data analysis. Based on the results of the data analysis, the deterministic approach is updated to a probabilistic approach.

### B.1. Original deterministic approach

In the deterministic approach, only one input set is used. The set contains two historical bathymetry files and one file with erosion rate data. In this approach, the data is directly extrapolated over the interested period without taking uncertainties and distributions into account for the input data of Htrend. Moreover, no variations during the extrapolation period are taken into in the deterministic approach.

#### B.1.1. Approach description

The calculation steps in the deterministic approach are relatively simple. Since this approach can be used to predict the future bathymetry in the year of interest directly. No intermediate extrapolation steps are required for the prediction of the future bathymetry, the horizontal displacement trend is directly extrapolated for the future horizontal displacement. The steps of the deterministic approach are indicated in figure B.1.

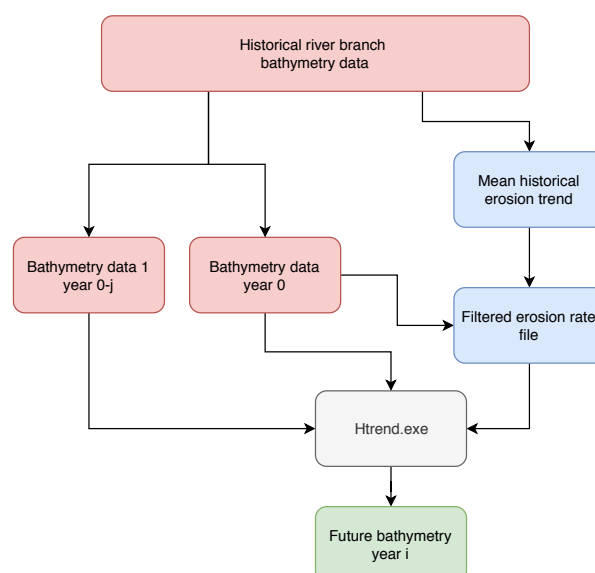


Figure B.1: Schematisation of the steps for the scour hole prediction in the deterministic approach.

### Bathymetry data

Two historical bathymetry datasets from different years are required as input for the calculation in Htrend. No modification are needed on the historical bathymetry data.

### Vertical erosion rate dataset

Htrend uses the vertical erosion rate dataset in addition to the horizontal extrapolation for the milder parts of the scour hole in order to predict the scour growth in depth. The local historical erosion rates for non-steep slopes are used as erosion rate-values in the deterministic approach. This can be the erosion rate of one specific year or the historical mean erosion rate for a couple of years. Historical bathymetry datasets are used for the determination of the historical vertical erosion rate dataset. The erosion rate data is subsequently filtered on bed slope, such that only non-steep parts will be extrapolated in the vertical.

### Safety factor

In order to deviate from historical trends, a safety factor can be introduced. By introducing the safety factor, several scenarios can be calculated in the deterministic approach. The safety factor can be used as an amplification factor or reduction factor on the historical trend. A different safety factor can be applied on the horizontal extrapolation and on the vertical extrapolation.

With the introduction of safety factors, Eq. 3.3 and Eq. 3.4 are updated to:

$$Z_{prog,h}(x + \Delta s_{prog} \times \gamma_h) = Z_{original}(x) \quad (B.1)$$

$$Z_{prog,v} = Z_{original} + \frac{\Delta Z}{\Delta t} \times T_{prog} \times \gamma_v \quad (B.2)$$

### B.1.2. Approach analysis

A cross-section of the scour hole near rkm 1004.8 in the river Spui is used as an example for the approach analysis. The cross-section is indicated in figure B.2.

The following two aspects of the deterministic approach are analysed:

1. Effect of the erosion trend file.
2. Effect of the safety factors.

In order to analyse these aspects, two different vertical erosion files and 5 safety factors are used as input data.

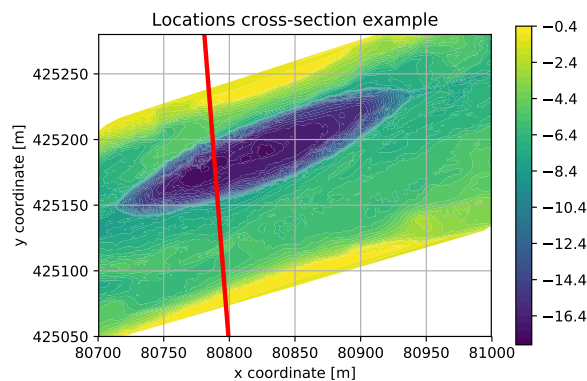
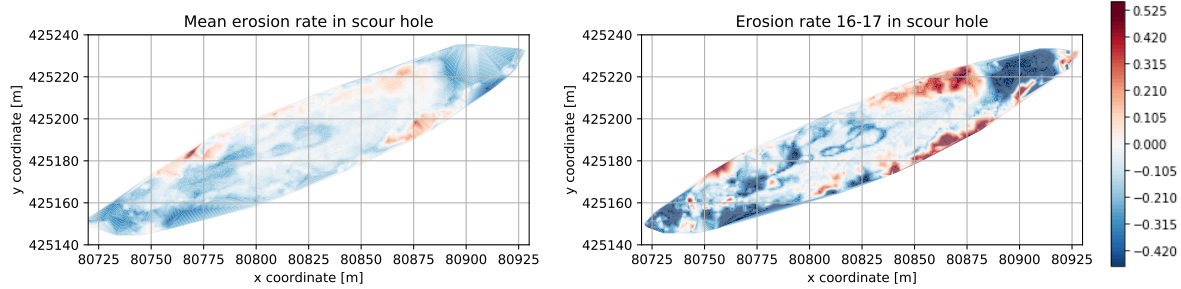


Figure B.2: Location of the example cross-section for the analysis of the deterministic approach.

### Input data

The historical bathymetry data of 2016 and 2017 are used as input data for Htrend. Two cases are compared for the vertical erosion. In the first case, the vertical erosion file is generated from the actual vertical erosion between 2016 and 2017, while in the second case the historical mean local erosion rate based on bathymetry datasets from 2014 till 2018 is used. The two erosion rate data can be seen in figure B.3. More and larger

spatial variation can be seen in the erosion rate data based on the actual erosion between 2016-2017 than in the mean erosion rate data.



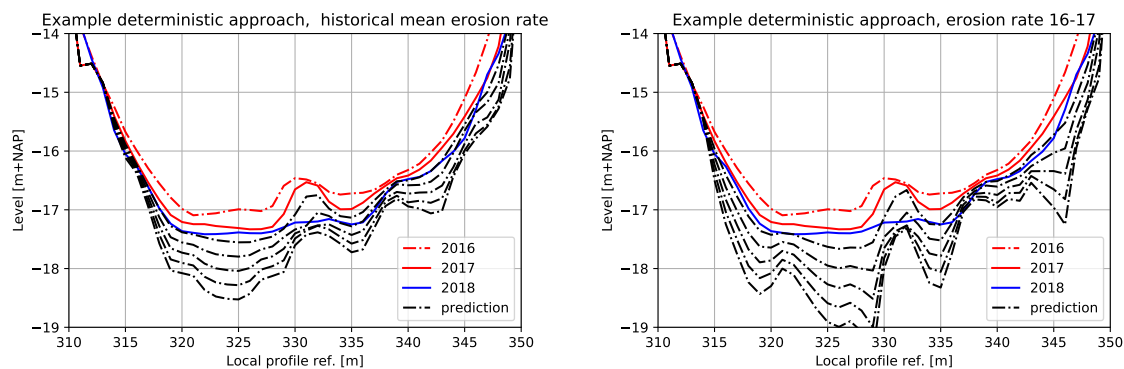
(a) Vertical erosion rate data based on the historical average erosion in the period 2014-2018.

(b) Vertical erosion rate data based on the erosion rate between 2016-2017.

Figure B.3: Vertical erosion rate input for Htrend. Blue indicates local erosion while red indicates sedimentation.

### Output profile

With Htrend the bathymetry is extrapolated for a period of 5 year. The scour hole development with the use of the two vertical erosion files the can be seen in figure B.4 for this period. The historical measured bathymetry of 2016, 2017 and 2018 are also presented in this figure.



(a) Vertical erosion rate based on the historical average erosion in the period 2014-2018.

(b) Vertical erosion rate based on the erosion rate between 2016-2017.

Figure B.4: Example of scour hole development in a period of five years for two different erosion rate input files.

### Vertical erosion trend effect

As can be seen, the scour hole is growing in depth and for the lowest part also in width for both cases. Due to the direct extrapolation of the historical vertical trend, there is a small depth increase at the location with a historical small erosion rate and a larger depth increase at the location with a historical larger erosion rate. This results in a spatial difference in the depth development of the scour hole.

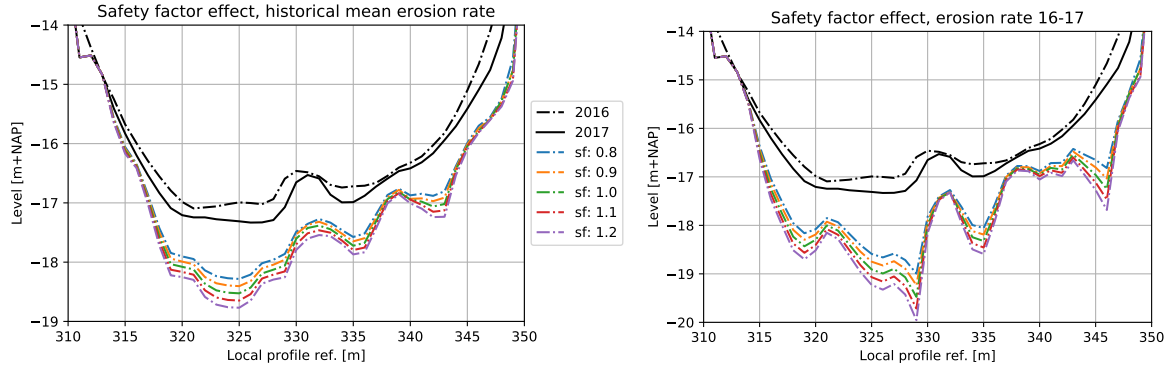
The development in the second case (erosion rate 2016-2017) is more extreme than in the first case (historical mean). The growth in depth and the spatial difference are larger. The growth in depth is larger due to the fact that the local erosion rate in a year can be larger than the historical mean erosion rate. Extrapolating this larger value results in a larger depth. The opposite holds for a local small erosion rate which result in a small or even no increase in depth. Due to this larger spatial difference are observed for the second case compared with the first case.

### Safety factor effect

In order to analyse the effect of safety factors, the bathymetry is extrapolated for 5 years. Safety factors in the range of 0.8-1.2 are used. The effect on the two cases is presented in figure B.5.

As can be seen in figure B.5, the shape of the extrapolated cross-section remains about the same if different safety factors are used, while the bed level differs. For safety factors smaller than 1.0 the erosion trend is

reduced, while for safety factor larger than 1.0 the erosion trend is increased as expected. The absolute effect of safety factor is larger on the vertical erosion displacements than on the horizontal displacements since the absolute values of the vertical displacements are larger.



(a) Safety factor effect with as vertical erosion trend input the historical mean erosion rate between 2016-2017.

(b) Safety factor effect with as vertical erosion trend input the erosion rate between 2016-2017.

Figure B.5: Effect of the usage of safety factor on the 5-year bathymetry extrapolation for two different erosion rate input files.

### Conclusions deterministic approach

The following conclusions can be made for the deterministic approach:

- Extrapolating vertical trends results at some location to a larger depth increase while at some other location there is almost no depth increase.
- Using the historical mean average vertical erosion rate for the vertical extrapolation results in less spatial depth variation and is better than the usage of the erosion rate of one specific year.
- Safety factors have larger effects on the vertical extrapolation than on the horizontal extrapolation.
- Safety factor can be used to reduce or increase erosion trends.

## B.2. Updated probabilistic approach

In contrast to the deterministic approach, uncertainties, yearly variations and distributions of parameters are taken into account in the probabilistic approach. The historical variations and distributions are identified in the historical data analysis and subsequently incorporated into the input files and parameters of Htrend. This results in a method to analyse scour hole development in a probabilistic way.

### B.2.1. Historical data analysis

The historical bathymetry (2014-2018) of the scour hole near rkm 1005 in the river Spui is used for the historical data analysis. With the bathymetry data, several analyses are done.

For the analyses the yearly and historical average erosion rate are required. These erosion rates can be calculated in the following ways:

$$\Delta Z_{m,n-mean} = \frac{Z_{m,n-latest} - Z_{m,n-oldest}}{T_{data}} \quad (B.3)$$

In which:

|                       |   |  |           |
|-----------------------|---|--|-----------|
| $\Delta Z_{m,n-mean}$ | = | Local historical mean erosion rate                               | [m/yr]    |
| $Z_{m,n-latest}$      | = | Local bed level in latest bathymetry data                        | [m + NAP] |
| $Z_{m,n-oldest}$      | = | Local bed level in oldest bathymetry data                        | [m + NAP] |
| $T_{data}$            | = | Period between the recording date of the two bathymetry datasets | [yr]      |

$$\Delta Z_{m,n-year i} = Z_{m,n-year i+1} - Z_{m,n-year i} \quad (B.4)$$

In which:

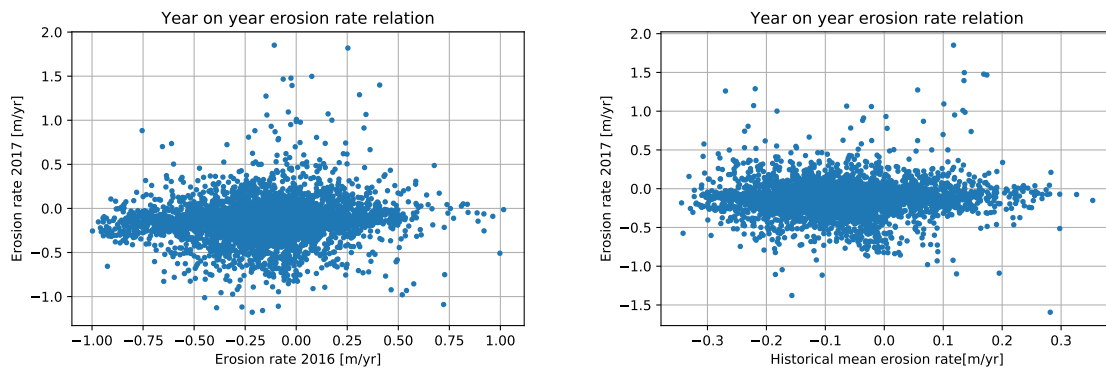
|                         |   |                               |           |
|-------------------------|---|-------------------------------|-----------|
| $\Delta Z_{m,n-year i}$ | = | Local erosion rate for year i | [m/yr]    |
| $Z_{m,n-year i+1}$      | = | Local bed level in year i+1   | [m + NAP] |
| $Z_{m,n-year i}$        | = | Local bed level in year i     | [m + NAP] |

**Year on year erosion rate**

In the deterministic approach, it is assumed that the historical erosion rate will continue in the near future. This assumption is valid if yearly erosion rate is linear dependent on the erosion rate in the previous year. The Pearson’s product moment correlation-coefficient ( $\rho_{XY}$ ) between the erosion rate of *year*  $i$  and *year*  $(i - 1)$  is then (close to) 1.0 (Jonkman et al., 2017).

In figure B.6, the erosion rate of 2017 is plotted against the erosion rate of 2016 and the average erosion in the period 2014-2016 for each relevant bathymetry point. A negative value means local erosion, while a positive value means local sedimentation. There is no direct relation visible between the erosion rate in 2017 and the historical erosion rate in the figure.

In table B.1, the correlation-coefficients of the presented data are presented. In this table the correlation-coefficients between other historical erosion rate are presented as well.



(a) Scatterplot erosion rate 2016 and 2017.

(b) Scatterplot historical mean erosion rate for and erosion rate 2017.

Figure B.6: Relation between historical data for the year on year erosion rate.

| Var X             | Var Y                       | $\rho_{XY}$ |
|-------------------|-----------------------------|-------------|
| Erosion rate 2017 | Erosion rate 2016           | 0.12        |
| Erosion rate 2017 | Mean erosion rate 2014-2016 | 0.05        |
| Erosion rate 2017 | Erosion rate 2015           | -0.03       |
| Erosion rate 2017 | Erosion rate 2014           | -0.05       |
| Erosion rate 2016 | Erosion rate 2015           | -0.08       |
| Erosion rate 2016 | Erosion rate 2014           | -0.16       |
| Erosion rate 2015 | Erosion rate 2014           | 0.01        |

Table B.1: Pearson’s product moment correlation-coefficients for different erosion rates.

As can be seen the correlation-coefficients are between -0.16 and +0.12. Which means that the yearly erosion rate is close to 0.0 and thus almost independent of the erosion rate in the previous year. The assumption in the deterministic approach that the future erosion rate will be equal to the historical erosion rate is therefore not valid.

**Bed level-erosion rate relation**

Since the year on year erosion rate is almost independent, another relation is required for the extrapolation of historical data to the future bathymetry. Due to erosion and sedimentation, the local bed level is changing each year. The relation between the local bed level and the local erosion rate is analysed for the period 2014-2018.

The yearly local erosion rate is determined for each year in the indicated period. The erosion data is subsequently filtered on the bed slope, in order to filter out the local erosion due to horizontal displacements of the scour hole edges. In figure B.7, the yearly local erosion rates are plotted against the local bed level of the same year for each bathymetry point in the scour hole.

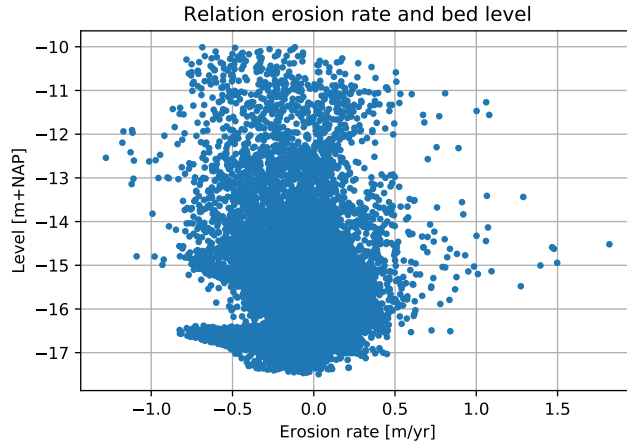


Figure B.7: Relation between the yearly erosion rate and the bed level. For the years 2014-2018.

Although, there is a lot of variation in the erosion rate for a specific bed level, a kind of relation can be seen in the figure. This follows also from the correlation-coefficient between the erosion rate of a specific year and the bed level in the same year, see table B.2.

| Var X                  | Var Y               | $\rho_{XY}$ |
|------------------------|---------------------|-------------|
| Erosion rate 2014      | Bed level 2014      | -0.149      |
| Erosion rate 2015      | Bed level 2015      | -0.300      |
| Erosion rate 2016      | Bed level 2016      | -0.176      |
| Erosion rate 2017      | Bed level 2017      | -0.114      |
| Erosion rate all years | Bed level all years | -0.184      |

Table B.2: Pearson's product moment correlation-coefficients for the bed level and erosion rate relations.

To check if the bed level erosion rate relation is equal for the entire scour hole. The scour hole is subdivided into four areas, as indicated in figure B.8. In table B.3 the correlation coefficient is calculated for each area the period. The bed level erosion rate relation differs per year and per area.

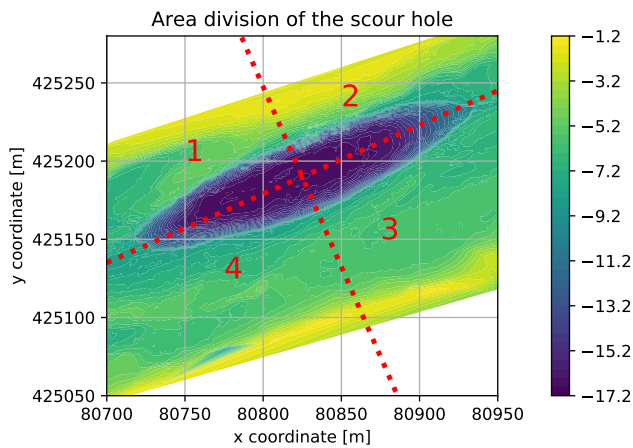


Figure B.8: Relation between the yearly erosion rate and the bed level

|           | Area 1 | Area 2 | Area 3 | Area 4 | Entire scour hole |
|-----------|--------|--------|--------|--------|-------------------|
| 2014      | -0.091 | -0.181 | -0.266 | -0.406 | -0.149            |
| 2015      | -0.022 | -0.356 | -0.255 | -0.460 | -0.300            |
| 2016      | -0.212 | -0.386 | -0.289 | -0.043 | -0.176            |
| 2017      | 0.020  | -0.138 | -0.429 | -0.003 | -0.114            |
| All years | -0.077 | -0.182 | -0.239 | -0.203 | -0.184            |

Table B.3:  $\rho_{XY}$  for the bed level and erosion rate relations for the four areas of the scour hole.

The following can be concluded from the correlation-coefficients in table B.3:

- The erosion rate has some negative dependence on the bed level.
- The bed level erosion rate relation is not uniform in the scour hole.
- The correlation between erosion rate and bed level is significantly higher than the correlation between the year on year erosion rates.

### Spatial erosion relation

The bed level erosion rate relation it follows that the relation is varying over the scour hole. In general, it is interesting to see how the erosion of a specific point relates to the erosion of the adjacent points. This is called the spatial erosion rate relation. The correlation-coefficient between the erosion rate and the neighbours' average erosion rate is used as indication for the spatial erosion relation. The erosion rate data of 2017 is used for the spatial erosion relation.

For each point in the scour hole, the neighbours average erosion rate is calculated. This is done by taking several surrounding area sizes into account. By increasing the area the correlation between the erosion rate and the neighbours average rate decreases, as shown in table B.4.

In order to say something about spatial dependency, the coefficient of determination is required. The coefficient of determination ( $\rho_{XY}^2$ ) gives the percentage of the variation in the values of X that can be explained or accounted for by variation of value Y (Taylor, 1990). For  $\rho_{XY} < 0.7$  the  $\rho_{XY}^2$  is below 0.5, which means that the erosion rate depends for less than 50% on the surrounding erosion rate. In general, the dependency for  $\rho_{XY}^2$ -values below 0.5 is considered as moderated or weak (Taylor, 1990). For the spatial erosion correlation, this holds thus for areas of 6x6m.

| Area [m × m] | Spatial correlation |
|--------------|---------------------|
| 2x2          | 0.871               |
| 4x4          | 0.785               |
| 6x6          | 0.711               |
| 8x8          | 0.652               |
| 10x10        | 0.612               |
| 12x12        | 0.583               |
| 14x14        | 0.557               |
| 16x16        | 0.533               |

Table B.4: Spatial correlation for erosion rate and neighbours average erosion rate in 2017.

### B.2.2. Approach description

The steps for the probabilistic approach are shown in figure B.9. As can be seen, the future bathymetry of the year of interest is calculated with intermediate steps for each intermediate year. These steps are necessary in order to get yearly differences in the development of the scour hole.

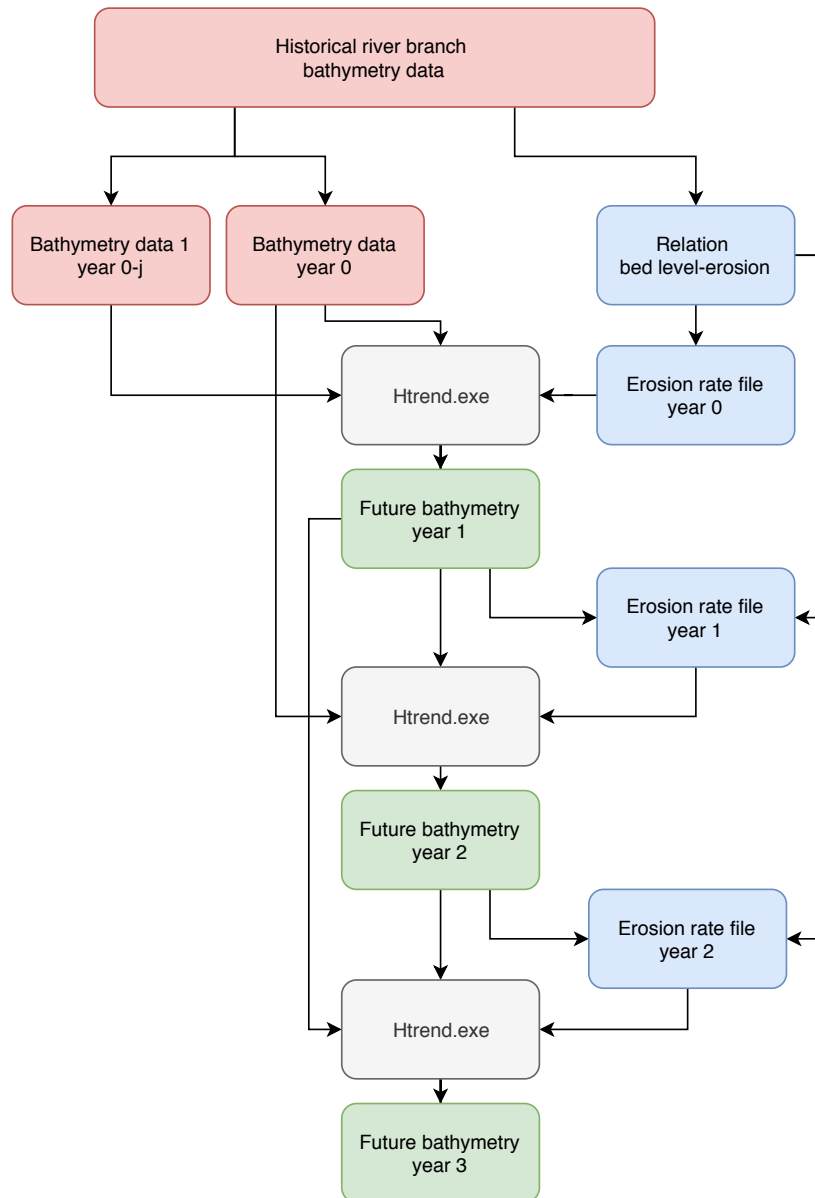


Figure B.9: Schematisation of steps for the scour hole prediction in the probabilistic approach.

### Bathymetry data

Again two historical bathymetry datasets are required as input. By using different combinations of historical bathymetry datasets, the variability in horizontal displacements can be determined. In this way, different historical horizontal displacements are used for the prediction of the future bathymetry. Each combination will give a (slightly) different prediction and thus the variability of the future bathymetry can become clear.

### Vertical erosion rate dataset

For the vertical erosion rate, no longer the historical mean erosion rate is used. Since this results in local too large differences. Moreover, analysing historical data gives almost no correlation between erosion rates of different years for the same location. While using mean-values, it is assumed that for each point the yearly erosion rate remains equal. Therefore, the historical relation between local bed level and erosion rate is used to generate an erosion rate data set. Analysing the historical data gives namely a correlation between the local bed level and the local erosion rate. Using the relation instead of mean-values gives for each year different erosion rates for the same location.

The steps for the creation of the vertical erosion rate are shown in figure B.10. First, the scour hole is divided

into small areas of  $6 \times 6$  [m]. Based on the mean bed level in the area, the erosion rate for the whole area is sampled from the bed level erosion rate relation. In order to keep the spatial correlation, for the entire area the same erosion rate is assessed. Finally, the erosion rate data is filtered for steep slopes. In order to prevent extreme erosions at the scour hole edges. An example of the vertical erosion data can be seen in figure B.11.

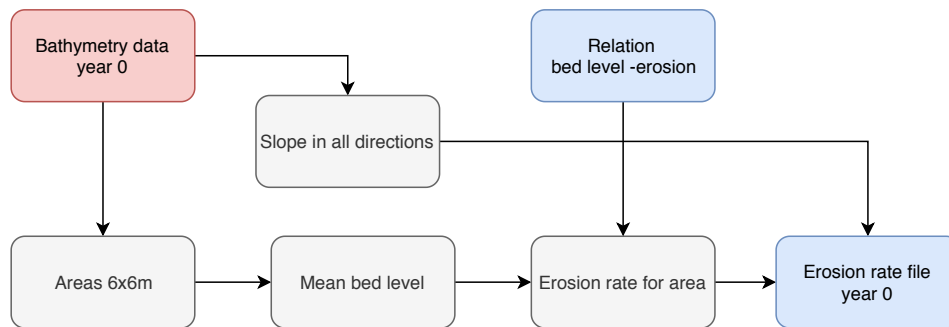


Figure B.10: Steps for the creation of the vertical erosion rate based on the relation between bed level and erosion rate.

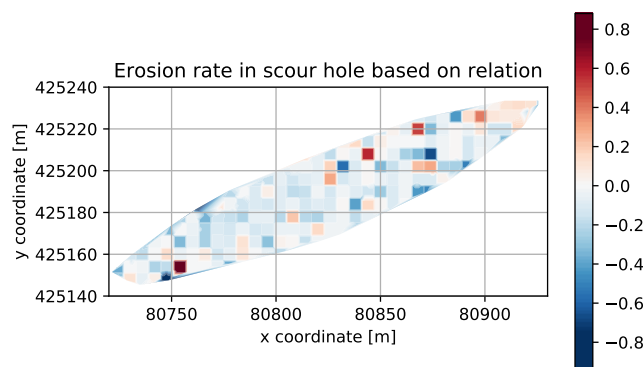


Figure B.11: Example of the vertical erosion rate data based on the historical relation between bed level and erosion rate.

### Approach steps

The following steps are done in the probabilistic approach in order to predict the future bathymetry of a scour hole:

1. Two datasets are selected from the historical available datasets.
2. The non-steep parts of the most recent input bathymetry dataset are selected from that bathymetry dataset.
3. For the non-steep parts the local erosion rate is sampled from the historical relation between bed level and erosion rate.
4. The sampled erosion rates are combined into an erosion rate dataset.
5. Htrend is used for the prediction of the bathymetry in the next year. The two bathymetry datasets and the erosion rate dataset are used as input for the extrapolation,
6. The above-mentioned steps are repeated while using the predicted bathymetry as most recent bathymetry and the previous most recent bathymetry as second input bathymetry.

These steps can be repeated several times in order to predict the bathymetry in a couple of years.

### Monte Carlo simulation

In order to get insight into the uncertainties and variability of the scour hole development, the above-described steps are done multiple times in a Monte Carlo simulation. The principle of a Monte Carlo simulation is to run a deterministic process several times with each time a different input. The input of each run are generated randomly from known input statistics and the correlation between the different inputs.

Since the tool input differs each run, the tool output will also be different for each simulation. By taking all the output from different simulations together, the results can be analysed in order to determine the expected value together with the uncertainty. Moreover, the confidence intervals can be determined from the results.

The amount of runs is an important factor of a Monte Carlo simulation. Since this amount determines the accuracy of the simulation and on the same time the required computation time. By increasing the number of simulation, the result will be more accurate, while the computation time increases. The number of simulation must be determined beforehand, in order to avoid either pointless computational time or an unacceptable reduction of the sample size (van Vuren, 2005).

According to van der Klis (2003) the required amount of runs can be estimated beforehand based on a small sample output of circa 20-30 runs. The amount of total required runs can then be estimated with Eq. B.5, in which  $N$  is the required sample size in order that the actual  $p^{th}$  fraction is within the estimates of the  $p - \Delta p^{th}$  and  $p + \Delta p^{th}$  fractiles.  $c_\alpha$  is the interval of the standard normal distribution that reflects the desired confidence interval, such that  $(P(-c_\alpha < \Phi < c_\alpha) = \alpha)$ .

$$N = p(1 - p) \left( \frac{c_\alpha}{\Delta p} \right)^2 \quad (\text{B.5})$$

The  $p^{th}$ -fraction and the  $c_\alpha$ -value are free choice, while  $\Delta p$  can be determined from the desired accuracy of fractile  $p$  and the small sample output.

### B.2.3. Approach analysis

The same cross-section as used in the deterministic approach analysis is used for the probabilistic approach analysis.

#### Input data

The historical bathymetry of 2016, 2017 and 2018 are used in the probabilistic approach. With this bathymetry data, three different combinations of input data are made and subsequently randomly used as input for Htrend.

The vertical erosion is generated from the historical bed level erosion rate relation. This relation is based on the scour hole development in the period 2014-2018, determined from the bathymetry data of the same period.

The bathymetry of the scour hole is predicted for 2023. Which means that the simulation period for the 2016-2017 combination is set to six years. The simulation period for the other two combinations is five years.

#### Number of runs

The number of required runs are determined with a small sample simulation. The bathymetry of 2017 and 2018 are used as input data for a simulation with 25 runs, in order to determine the total required number of runs with Eq. B.5. The desired accuracy of the lowest point of the example cross-section is used for the determination of the total required runs. The desired accuracy of the bed level of fractile  $p = 0.90$  is plus or minus 5.0 [cm] for a simulation of 6 years.

The sample simulation results in an average bed level of the lowest point of  $-18.15$  [m + NAP] and a standard deviation of  $0.1609$  [m]. According to the Gaussian distribution, the bed level for the  $90^{th}$  fractile is  $-18.36$  [m + NAP] The allowable confidence interval for the bed level is thus  $[-18.31; -18.41]$ . The corresponding fractiles for this interval are the  $83^{th}$  and  $94^{th}$  fractile. Resulting in  $\Delta P = 0.0551$ . Filling in Eq. B.5 results in:

$$N = 0.9(1 - 0.9) \left( \frac{1.96}{0.0551} \right)^2 = 115 \quad (\text{B.6})$$

According to the method proposed by van der Klis (2003), the required runs for one combination of bathymetry input is estimated to 115. This value is rounded to 100 runs for each combination of bathymetry input. This is allowed since the outcome of the method gives the order of magnitude of the number of runs and not an exact amount.

**Output profile**

In figure B.12, the outcome of 100 simulations with the probabilistic approach is shown for the bathymetry prediction for 2023. As can be seen the relations for each run slightly differs. The mean outcome and the 90% confidence interval can be determined for the realisations.

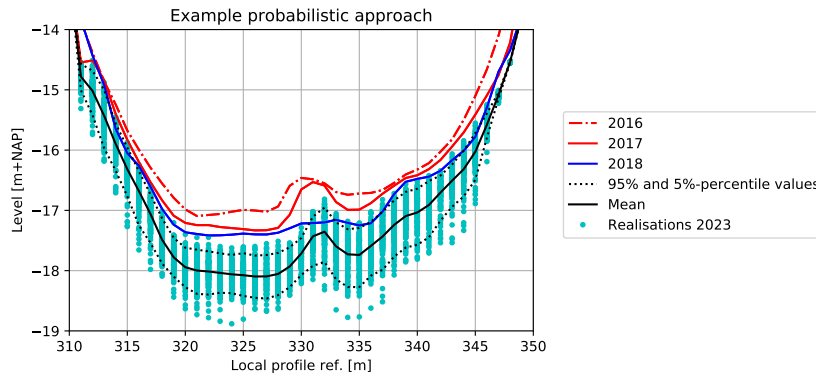


Figure B.12: Example of 100 runs for the probabilistic approach, the bathymetry of 2016 and 2017 is used as input data for Htrend

The accuracy of the output profiles must be checked, in order to verify that the correct amount of runs has been chosen. For a Monte Carlo simulation with 100 runs,  $\Delta P = 0.0588$  in order to have a 95% confident of the 90<sup>th</sup> fractile. From the output data follows that an accuracy of 5.0 [cm] corresponds to  $\Delta P = 0.0497$ . The desired accuracy of 5.0 [cm] is thus not met with 100 simulations. The actual accuracy of the 90<sup>th</sup> fractile with 95% confident is 6.0 [cm]

**Effect of different bathymetry input combinations**

As described, three different combinations of input bathymetry are simulated in the probabilistic approach. By simulating these combinations, three different ranges and mean output profiles are determined. The mean profiles of the three combinations are shown in figure B.13. As can be seen the profiles, slightly differs from each other, especially at the location of the hump in 2017. This hump is still visible in the predicted bathymetry for the combination with the bathymetry of 2016 and 2017.

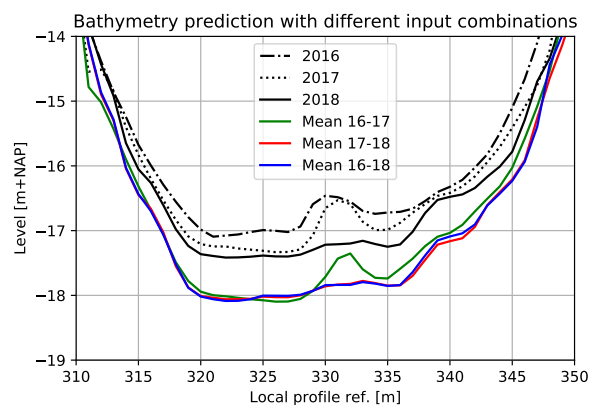
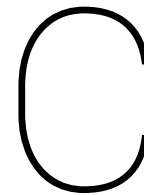


Figure B.13: Predicted 2023 profile, with three input bathymetry combinations: 2016-2017, 2017-2018 & 2016-2018.

The tool outputs of the three combinations can be combined in order to get rid of the effect of a local variation in one of the input bathymetry data. Moreover, by combining the outputs, a range can be created for the horizontal displacements of the scour hole edges.

*(This page is intentionally left blank)*



# Flow slide quantification tool

For the quantification of the probability of flow slide the stand-alone software D-Flowslide is available. The usage of this software is pre-described in the WBI (Rijkswaterstaat, 2017). However, D-Flowslide has some input and output limitations, therefore an own created tool is used for the calculation of the probability of flow slide. In this Appendix, the steps which are done in the tool are described.

## C.1. Part I: River profile generation

In the first part of the tool, river profiles are generated from three datasets. The river profile is a river cross-section perpendicular to the river-axis and contains the flood defences on both riversides and everything in between them, like foreshores, scour holes, local humps and of course the river channel self. The used datasets for the generation of the river profiles are data from the Actueel Hoogtebestand Nederland (AHN3), Baseline model of the Rhine-Meuse Delta from Helpdesk Water (2015) and bathymetry data of the fairway retrieved from Rijkswaterstaat CIV (Centrale informatievoorziening). The datasets have the same data format, therefore merging of the datasets is relatively easy.

The AHN3 contains the land elevation of the areas without water. The bathymetry datasets contains the measured bathymetry data of the fairway. Merging of only these two datasets will not give a complete river profile, since parts of the foreshore are missing. However, these parts are presented in the baseline model, and therefore this third dataset will also be used for the generation of the river profiles.

The baseline model contains also bathymetry data, however there are some differences between the data of bathymetry datasets and the baseline model. The bathymetry data contains the recently (in the past few year, different per river branch) measured bathymetry data for the fairway only. This data is up to +/- a depth of 3.0 [m], and does not contain the foreshores and dikes. The baseline model data is generated from a couple of datasets, like land height, foreshore surveys and bathymetry data. The baseline model contains different datasets like, the foreshores. This model has all the required data to generate a river profile from dike toe till dike toe. However, the baseline model data is generated in 2015 and the bathymetry data can be outdated.

In the first part of the tool, the three datasets are merged in order to get an entire reliable river profile. The AHN3 data is added to data of the baseline model to include the entire flood defence. The bathymetry data of the baseline model is replaced by the more recent bathymetry data from the CIV. In this way, entire river profiles can also be updated by adding only an updated version of the bathymetry data. It is also possible to get an approximation of historical river profiles, by replacing the bathymetry in the baseline with historical bathymetry data.

From the merged datasets, river profiles can be generated. The steps for this generation will be illustrated with an example. The example is for the Oude Maas between the bifurcation with the Spui and the Spijkenserbbrug.

## 1. Selecting relevant data

Firstly, the relevant data from the datasets must be selected. The bathymetry data consists already of separate files per river branch, while the baseline data is one large dataset for the entire Rhine-Meuse Delta and the AHN3 data is subdivided in separated files, containing the data of an area of  $6.25 \times 5.00$  [km]. The relevant data is selected by defining the coordinates of the required area.

## 2. Selecting lines for river profiles

Next to the river elevation data, more datasets are including in the baseline model. For the line selection, the 'rivierlijnen' dataset is used. This dataset contains the location of all defined River kilometers (rkms) in the Rhine-Meuse Delta. By selecting the rkms, the geometry of the river can be defined and coupled with the bathymetry data.

This is done for the example river branch, as can be seen in figure C.1a. Two rkms are added to the bathymetry. Since the starting points of the line are located at the foreshore of the river. The locations of the points need to be adjusted, in order to include the flood defence into the profile. In figure C.1b, this is done for the example river branch. The starting points and endpoints of the lines are now located outside the data domain.

The distance between two rkm lines is 1.0 [km]. In order to get river profiles with smaller intermediate distances, the points between two rkms are interpolated, see figure C.1c

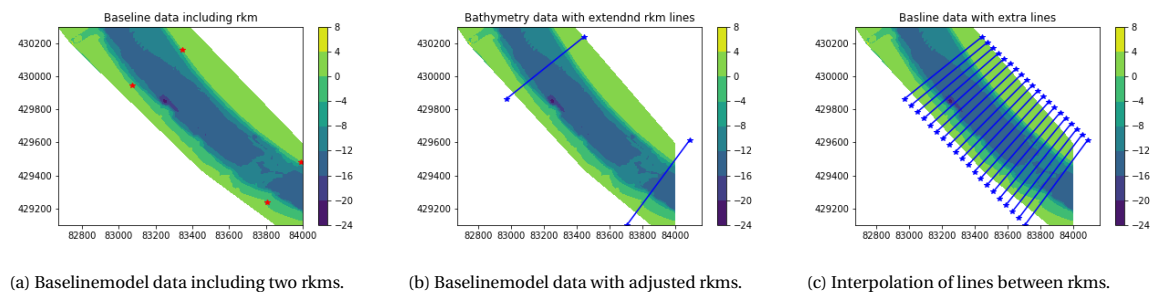


Figure C.1: Including rkms into the data for example case Oude Maas.

## 3. Extracting data along lines

Along the lines determined in step 2, the data is extracted from the three datasets. The accuracy is set to 1.0 [m], such that every meter on the line a profile data point is extracted. First, the data is extracted from the bathymetry dataset, see figure C.2a. For the points on the line without a data-value from the bathymetry dataset, the data is extracted from the AHN3, see figure C.2b. After extracting the data from the baseline model, there are still some points on the line without a data-value. These points are located outside the domain of the bathymetry data and the AHN3, the data for these point are extracted from the baseline model. In the last step, the profile is moved horizontally, such that the lowest located point is located at  $x=0.0$ . In this way, an entire reliable river profile is generated.

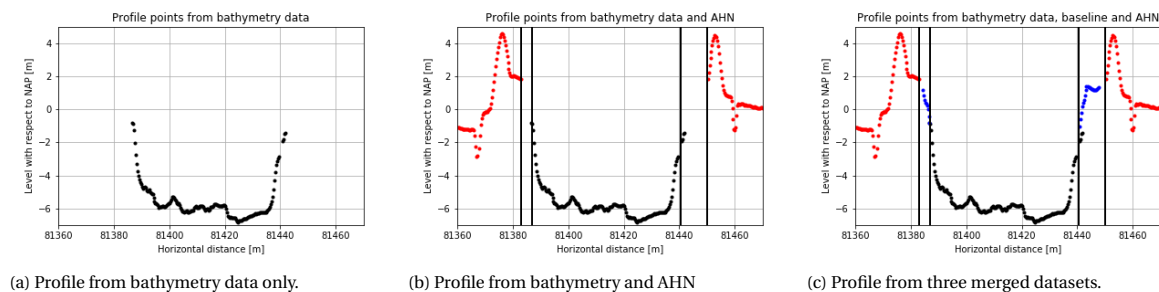


Figure C.2: Extracting profiles from the datasets.

## C.2. Part II: probability calculation

In the second part of the tool, the probability of occurrence of flow slide and the probability of exceedance of the acceptable retrogression length are calculated. The probabilities are calculated for an input river profile generated with the first part of the tool. The calculation is done for both riversides at the same time. In this description, an example profile is used in order to explain the different steps. The profile is shown in figure C.3, as can be seen in the figure, the river profile contains both riversides.

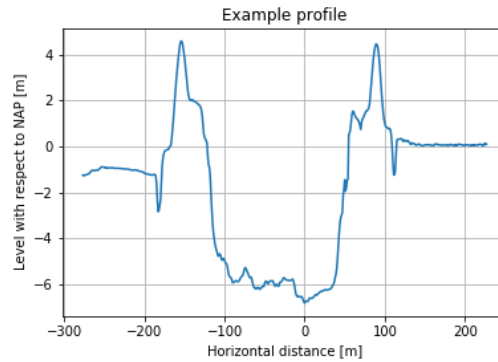


Figure C.3: Example profile used for the tool description.

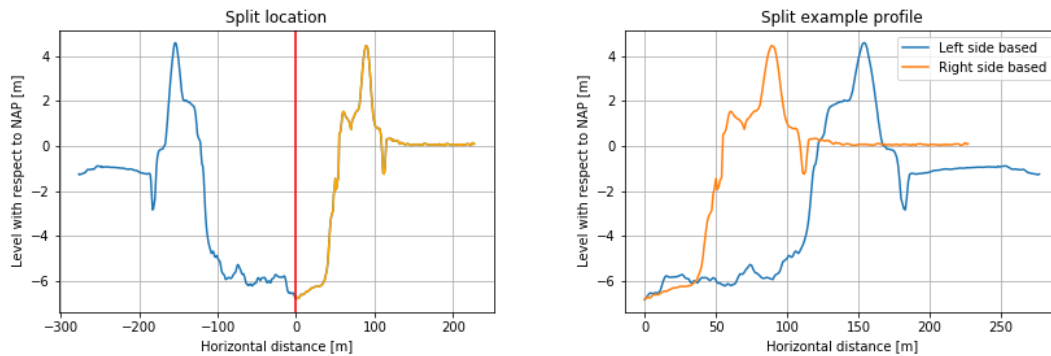
Part II contains several steps in order to calculate the probabilities of flow slide. The following steps are done in part II:

1. Profile split in lowest point.
2. Determination of characteristic profile points.
3. Calculation of geometry parameters ( $H_r$ ,  $\cot \alpha_r$ ,  $H_{channel}$ ).
4. Calculation of probability of occurrence of a flow slide.
5. Calculation of the probability of exceedance of the acceptable retrogression length.
6. Calculation of total probability.

Each step will be described below.

### 1. Profile split in lowest point

Firstly, the river profile is split into two parts. Such that a distinction between the two riversides is possible. The river profile is split in the lowest located point of the river profile and not in the river-axis. The lowest point is chosen because otherwise the effect of a possible located scour hole is not always included in both riverside if the profile is split in the river-axis. But, if the river profile is split in the lowest point, it is included. The two split profiles of the example profile are shown in figure C.4, the location of the split is also indicated in this figure.



(a) Split location

(b) Split profiles of the example profile

Figure C.4: Profile split in lowest point of the example profile.

## 2. Determination of characteristic profile points

In the second step, the characteristic profile points are determined. The required characteristic profile points in order to quantify the probability of flow slide are; 1) Bottom river channel, 2) Insert river channel, 3) Dike toe at riverside and 4) Dike top at riverside. These points are determined per riverside, thus for both split profiles separately.

### Dike top

The dike top at the riverside is determined first. The starting point for the determination is the highest located profile point. Most likely this point is located on the dike crest, but this is not necessarily directly the dike top at the riverside. A close-by (lower) located point could also be the dike top at river side, therefore this must be checked. From the highest located point, it is checked if any other profile point is located within a slope of 1:50. If this is the case, the closest point with a less mild slope than 1:50 will be the new starting point, and the same check is done for this point. This procedure is being done until no other point is located within a slope of 1:50. The slope value of 1:50 is an assumption based on trial and error on generated river profiles from the Spui and Oude Maas.

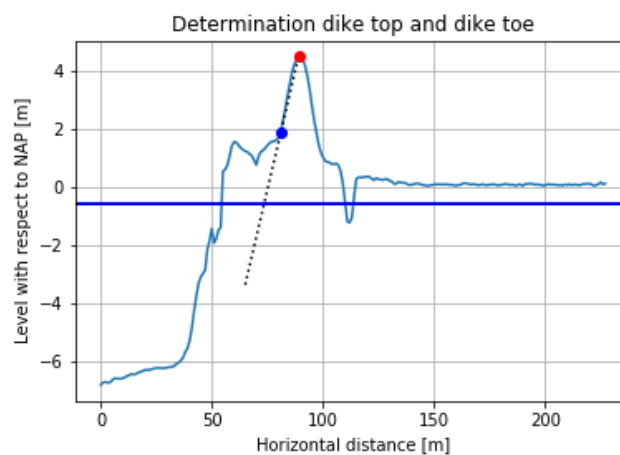


Figure C.5: Determination of the dike top and dike toe for the right side of the example profile.

### Dike toe

Next, the dike toe at riverside is determined. The starting point for this determination is the dike top. The slope between all profile points which are located above the defined water level (OLW) and the dike top is calculated. The profile point with the steepest slope up to the dike top is defined as dike toe.

This determination is shown in figure C.5, in which the split profile of the right riverside is shown. The water level (OLW), is indicated in the figure. For each point above the water level, the slope to the dike top (indicated with a red dot) is calculated. It turns out, the point located at  $x=81$  has the steepest slope to the dike top. This slope is indicated with the dashed line.

### Insert river channel and bottom river channel

The last two characteristic points are determined at the same moment in an iterative way. The starting points for the determination are the earlier defined dike top and dike toe. Each profile point below the dike toe could possibly be one of the two remaining characteristic points. There is only one limitation: the characteristic point of the river insert is always located above the characteristic point of the river bottom. As stated in Rijkswaterstaat (2016b), the probability of occurrence of a flow slide for all possible combination of the last two characteristic points have to be calculated. The method to calculate this probability of occurrence is explained in step 4. The two points corresponding to the highest probability are subsequently used as insert river channel and bottom river channel.

Please note, the insert of the river channel can be the same point as the dike toe. If this is the case, the dike profile is called in Dutch a *schaardijk*. A *schaardijk* does not have a foreshore and the dike is directly located on the river channel.

### Overview characteristic points

An overview of the characteristic points determined with the above-described method for the example profile is shown in figure C.6

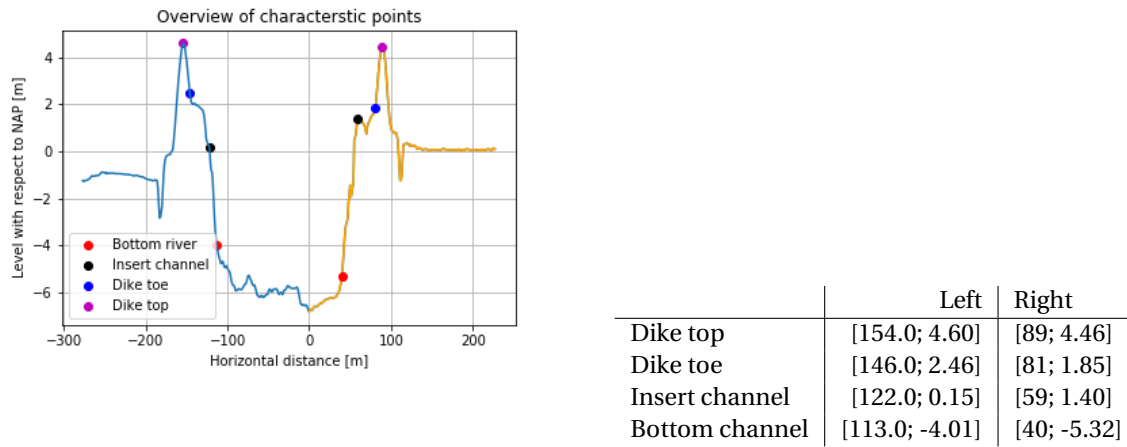


Figure C.6: Determination of characteristic points of the example profile.

### 3. Calculation of geometry parameters

With the characteristic profile points, determined in step 2, the geometry parameters ( $H_r$ ,  $\cot \alpha_r$ ,  $H_{channel}$ ) can be calculated. These parameters are calculated with the following equation:

$$H_r = H_{channel} + \Delta h_{below} + 2 \times h_{dike} \times \frac{\cot(\alpha_r)}{\cot(\alpha_{upper})}$$

$$\cot \alpha_r = \frac{Z_{insertchannel} - Z_{bottomriver}}{X_{insertchannel} - X_{bottomriver}} \quad (C.1)$$

$$H_{channel} = Z_{insertchannel} - Z_{bottomriver}$$

In which:

$$h_{below} = Z_{dike toe} - OLW$$

$$h_{dike} = Z_{dike top} - Z_{dike toe}$$

$$\alpha_{upper} = \arctan \frac{2 \times h_{dijk}}{B + 2 \times h_{dijk} + \cot \alpha_r} \quad (C.2)$$

For the example profile, the geometry parameters are presented in table C.1.

|                   | Left | Right |
|-------------------|------|-------|
| $H_r$ [m]         | 5.60 | 10.45 |
| $H_{channel}$ [m] | 4.17 | 6.71  |
| $\alpha_r$        | 2.16 | 2.83  |

Table C.1: Overview of the geometry parameters for the example profile.

#### 4. Calculation of probability of occurrence of a flow slide

From the geometry parameters, subsoil parameters and the scaling parameters, the probability of occurrence of a flow slide can be calculated by filling in Eq. C.3 and Eq. C.4. First, the frequency of occurrence of a flow slide is calculated, followed by the probability.

$$F(FS|S_i) = \left( \frac{5}{\cot \alpha_r} \right)^5 \times L_{section} \times \frac{V_{local}}{V_{zeeland}} \times 0.025 \times \left[ 0.5 \times \left( \frac{H_r}{24} \right)^{2.5} \times \left( \frac{1}{10} \right)^{-10(0.05 + \psi_{5m.kar})} + 0.5 \times \left( \frac{H_{channel}}{24} \right)^5 \times \left( \frac{2 \times 10^{-4}}{d_{50.mean.kar}} \right)^5 \times F_{cohesivelayers} \right] \quad (C.3)$$

$$P(FS|S_i) = 1 - e^{-F(FS|S_i)} \quad (C.4)$$

For the example profile, the subsoil parameters and scaling parameters are presented in table C.2a. With these parameters and the geometry parameters shown in table C.1, the frequency and probability of occurrence are calculated. These are presented in table C.2b.

| Parameter:           | Value:               |
|----------------------|----------------------|
| $D_{50.mean.kar}$    | $150 \times 10^{-6}$ |
| $\psi_{5m.kar}$      | 0.026                |
| $F_{cohesivelayers}$ | 0.33                 |
| $V_{local}$          | 0.87 [m/yr]          |
| $L_{section}$        | 1.0 [km]             |
| Agreed low water     | -0.30 [m + NAP]      |

(a) Subsoil scenario parameters and scaling parameter

|                    | Left  | Right |
|--------------------|-------|-------|
| $F(FS S_i)$ [1/yr] | 0.111 | 0.135 |
| $P(FS S_i)$ [1/yr] | 0.104 | 0.126 |

(b) Frequency and probability of occurrence of a flow slide for the example profile

Table C.2: Overview of the results for step 4.

#### 5. Calculation of the probability of exceedance of the acceptable retrogression length

For this step, the entire river profile is needed instead of the split profiles. The steps described below are applied on both riversides.

##### Determination of slope angle

It has been assumed that the maximum allowable retrogression length is up to the dike toe. This assumption is based on the fact that if the retrogression length is beyond the dike toe, the dike self will be affected. Therefore, the maximum allowable situation and the starting point for the calculation of probability of exceedance of the acceptable retrogression length, is the determined dike toe in step 3. For this point, the dike profile after a flow slide is determined based on the variables given in Rijkswaterstaat (2016b). The distributions of these variables are presented in table C.3. The new profile consists of two parts, a steep and a mild part. The transition between the two slopes (D/H-value) is approximately on 43% of the total profile height. (Rijkswaterstaat, 2016b). The slope angle of the mild part is the most relevant variable for the determination of the new profile. According to Rijkswaterstaat (2016b), as a simplification, only  $\cot(\gamma)$  can be considered as stochastic variable and the expected value remaining variables should be taken. The value of the slope angle of the mild profile part is determined in an iterative way. Until, the ratio between the two areas, the area above and the area below the new profile, 1:1.4 is. This ratio is due to the three-dimensional flow of soil during a flow slide. The iterative process is schematically indicated in figure C.7.

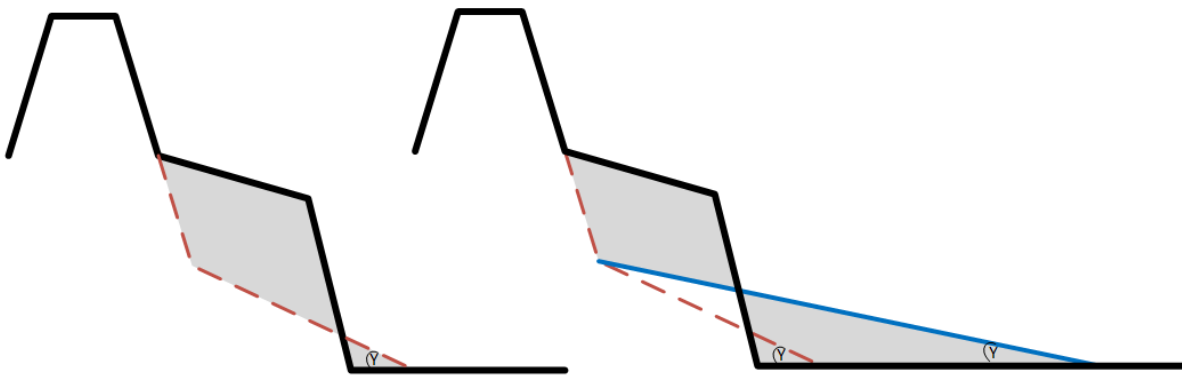


Figure C.7: Determination of the slope angle, such that the ratio between the two area will be 1:1.4.

|                | $\mu(x)$ | $\sigma(x)$ | Distribution type | underlying normal distribution<br>$\mu(y)$ | $\sigma(y)$ |
|----------------|----------|-------------|-------------------|--|-------------|
| $\cot(\gamma)$ | 16.8     | 7.1         | Lognormal         | 2.82                                       | 0.38        |
| $\cot(\beta)$  | 2.9      | 1.71        | Lognormal         | 2.05                                       | 0.47        |
| $D/H$          | 0.43     | 0.06        | Normal            |  |             |
| $ratio$        | 1.4      | 0.1         | Normal            |  |             |

Source: Rijkswaterstaat (2016b)

Table C.3: Overview of the distributions of the variables of the post flow slide profile.

### Determination probability of exceedance

For the, in an iterative way, determined slope angle, the corresponding probability of exceedance of that slope angle can be determined with the known distribution of the mild slope angle, presented in table C.3. Smaller slope angles have a larger probability of exceedance of the slope angle. The probability of exceedance of the slope angle for the maximum allowable situation is equal to the probability of exceedance of the acceptable retrogression length. Because for each profile point of the foreshore a unique new profile after a flow slide can be determined. Each new profile has a slope angle with a corresponding probability of occurrence. How larger the retrogression length, how milder the slope angle and how less likely it occurrence is. This is indicated in figure C.8. Thus concluding, how milder the slope of the new profile for the maximum allowable situation, the smaller the probability of exceedance of the acceptable retrogression length.

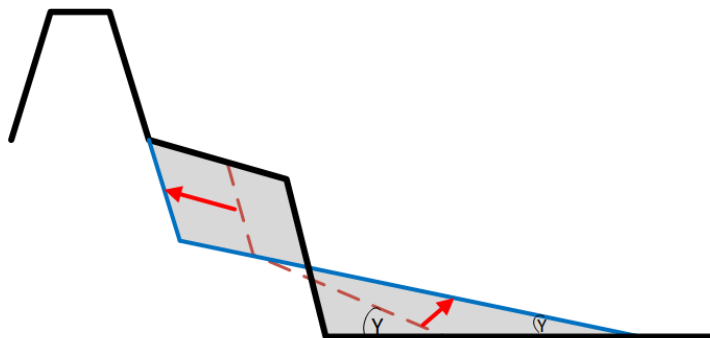
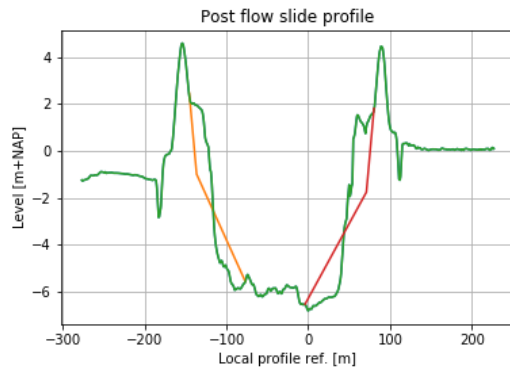


Figure C.8: Determination of the slope angle, for each retrogression length a different slope angle can be found.

### Probability for the example profile

For the two riversides of the example profile, the new profile after flow slides on both riversides is determined. The new profiles are shown in figure C.9. For the right riverside, the profile is quite similar to the original profile, Due to the fact that the dike toe is located close to the river channel. The relevance of the entire river profile can be seen for the left riverside. The new profile is beyond the lowest located profile point. The entire scour hole will be filled for a flow slide. If only the split profile was used, a wrong area was taken into account

for the determination of the slope angle. Which would have resulted to a wrong slope angle. In the table of figure C.9, the slope  $\cot(\alpha_r)$  of the two new profiles are shown together with the corresponding probability of exceedance of that slope. The probability of exceedance of the slope is thus equal to the probability of exceedance of the acceptable retrogression length.



|   | Left  | Right |
|---|-------|-------|
| $\cot \alpha_r$                         | 13.01 | 15.68 |
| $P(\cot \alpha > \cot \alpha_r)$ [1/yr] | 0.748 | 0.570 |
| $P(L > L_{max} FS)$ [1/yr]              | 0.748 | 0.570 |

Figure C.9: Determination of characteristic points of the example profile.

## 6. Calculation of total probability.

In the last step, the two calculated probabilities are multiplied, as shown in Eq. C.5. For the example profile, this is done in table C.4.

$$P(L > L_{max})_{section} = P(L > L_{max}|FS) \times P(FS) \quad (C.5)$$

|                            | Left  | Right |
|----------------------------|-------|-------|
| $P(FS S_i)$ [1/yr]         | 0.104 | 0.126 |
| $P(L > L_{max} FS)$ [1/yr] | 0.748 | 0.570 |
| $P(L > L_{max})_{section}$ | 0.078 | 0.072 |

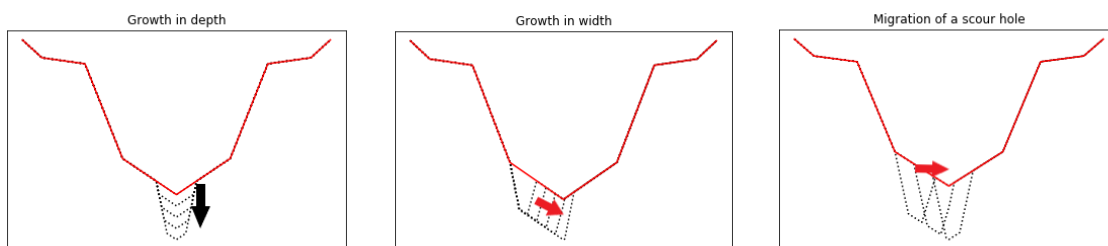
Table C.4: Determination of characteristic points of the example profile.

# D

## Fictive scour hole development scenarios

In this Appendix, the effect of the presence of scour holes on the indirect failure mechanism flow slide is analysed with the usage of fictive scour hole development scenarios. In these scenarios, a fictive scour hole is added to a reference profile, and one type of scour hole development is analysed. The developments are growth in depth (scenario 1), growth in scour hole width (scenario 2) and change of scour hole location with respect to the riverbanks (scenario 3), these scenarios are indicated in figure D.1.

In order to apply the scenario, first, a reference situation is created, based on the actual situation in the Rhine-Meuse Delta. Followed by the analysis of the effect of scour holes in different scenarios.



(a) Scenario 1: growth of scour depth

(b) Scenario 2: increase of scour width

(c) Scenario 3: Migration of a scour hole

Figure D.1: Scenarios for scour hole development.

### D.1. Creation of reference situation

From the baseline model and bathymetry data, river profiles are generated every 10.0 [m] over the river branches of the Spui and the Oude Maas. These river branches are indicated in figure D.2a, the properties of these river branches are shown in table D.1a.

For the reference situation, only one subsoil scenario is used for simplicity reasons. The parameters of this subsoil scenario are shown together with the location-specific scaling parameters in table D.1b. The scaling parameters and subsoil parameters are retrieved from the example given in Rijkswaterstaat (2016b). A section length of 1.0 [km] has been chosen in order to get as a final unit, probability per km per year. The agreed low water level value corresponds to the value of the OLW-Value of the Oude Maas near Goidschalxoord is used. This location is near the bifurcation of the Oude Maas and the Spui.

For each generated river profile of the Spui and the Oude Maas, the four relevant characteristic profile points; dike top, (dike toe, insert river channel and insert river bottom) are determined for both riversides. The median characteristic points are selected and the points are merged to a median river profile. The median river profiles for the Spui and Oude Maas are shown in figure D.2b.

|                 | Spui    | Oude Maas |
|-----------------|---------|-----------|
| River km up.    | SP 996  | OM 980    |
| River km down.  | SP 1010 | OM 994    |
| Total length    | 14 [km] | 14 [km]   |
| Profile density | 10 [m]  | 10 [m]    |
| Scour holes     | 13      | 10        |

(a) Properties of river branches for reference situation.

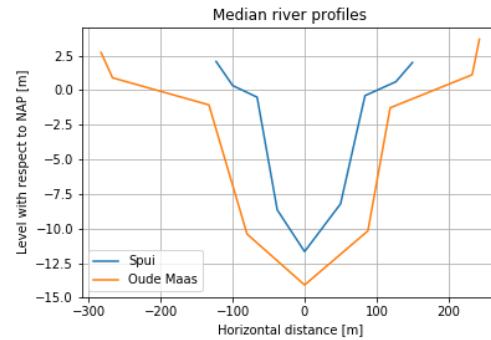
| Parameter:           | Value:               |
|----------------------|----------------------|
| $D_{50.mean.kar}$    | $150 \times 10^{-6}$ |
| $\psi_{5m.kar}$      | 0.026                |
| $F_{cohesivelayers}$ | 0.33                 |
| $V_{local}$          | 0.87 [m/yr]          |
| $L_{section}$        | 1.0 [km]             |
| OLW                  | -0.30 [m + NAP]      |

(b) Subsoil scenario parameters and scaling parameter.

Table D.1: Overview of the river branches and subsoil scenario for the reference situation.



(a) River branches taken into account for the reference situation.



(b) Median river profile for Spui and Oude Maas.

Figure D.2: Overview of the river branches taken into account for the creation of the reference situation.

As can be seen in figure D.2b, there are differences between the two median river profiles. The river Spui is, for example, narrower and shallower than the Oude Maas. The river Oude Maas has a wider foreshore than the Spui. For both branches, there can be a small difference observed between the two riversides. The two median profiles are thus not symmetrical.

|                            | Spui   |        | Oude Maas |           |
|----------------------------|--------|--------|-----------|-----------|
|                            | Left   | Right  | Left      | Right     |
| $P(FS)$                    | 0.0421 | 0.0087 | 0.0029    | 0.0292    |
| $P(L > L_{max} FS)$        | 0.4319 | 0.1632 | 0.0019    | 0.0128    |
| $P(L > L_{max})_{section}$ | 0.0182 | 0.0014 | 5.850e-06 | 3.744e-04 |
| $P_{required}$             | 0.01   | 0.01   | 0.01      | 0.01      |
| Acceptable?                | No     | Yes    | Yes       | Yes       |

Table D.2: Probability of flow slide for median situation of the Spui and Oude Maas.

For the median profiles, the probability of occurrence of a flow slide  $P(FS)$  and probability of exceedance of the acceptable retrogression length  $P(L > L_{max}|FS)$  for both riversides are calculated in table D.2. As can be seen, the left riverside of the median profile of the river Spui does not satisfy the required probability of exceedance of the acceptable retrogression length given in the WBI. The right riverside of the Spui and both riversides of the Oude Maas do satisfy the required probability. For the median profile of the Oude Maas, the probability of exceedance of the acceptable retrogression length is even very small, this is the effect of the relative wide foreshore in this river branch. The median situation for the Spui suits better to analyse the effect of the presence of scour holes in the river profile since the probability of exceedance are in the same order of magnitude as the required probability in the WBI.

For the reference situation, the median profile of the river Spui will be slightly modified. Two symmetric profiles are made from the median profile, for each riverside one profile. The two profiles are called; 1) 'Narrow profile' and 2) 'Wide profile'. The narrow profile is based on the characteristic points of the median profile of the left riverside, while the wide profile is based on the median profile of the right riverside.

The two profiles are shown in figure D.3, the characteristic points are presented in table D.3. Based on

the characteristic points the relevant profile parameters  $H_r$ ,  $\cot \alpha_r$  and  $H_{channel}$ , are determined, these are shown in the table as well.

For the two reference profiles, the probability of occurrence of flow slide and the probability of exceedance the acceptable retrogression length are given in table D.3. Since the two reference profiles are symmetrical, these two probabilities are equal for both riversides of each profile. The probabilities of exceedance of the maximum allowable retrogression deviate slightly from the median profiles presented in table D.2, due to the small profile adaptation in order to make the profiles symmetrical.

|                              | Narrow profile | Wide profile   |
|------------------------------|----------------|----------------|
| Dike top                     | [118.0; 2.035] | [145.0; 2.000] |
| Dike toe                     | [100.0; 0.451] | [130.0; 0.733] |
| Insert river channel         | [68.0; -0.086] | [89.0; 0.130]  |
| Bottom river channel         | [40.0; -8.503] | [53.0; -7.858] |
| Base point                   | [0.0; -11.706] | [0.0; -11.706] |
| River width bottom level [m] | 80             | 106            |
| $H_r$ [m]                    | 9.122          | 8.828          |
| $\cot \alpha_r$              | 3.327          | 4.507          |
| $H_{channel}$ [m]            | 8.417          | 7.988          |
| $P(FS)$                      | 0.0424         | 0.0087         |
| $P(L > L_{max} FS)$          | 0.4342         | 0.1614         |
| $P(L > L_{max})_{section}$   | 0.0184         | 0.0014         |

Table D.3: Characteristic points for the reference situation.

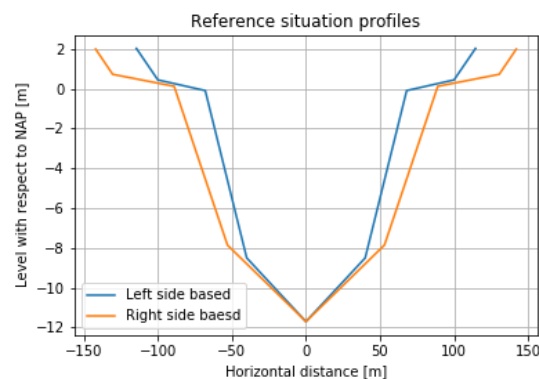


Figure D.3: Reference situation profiles.

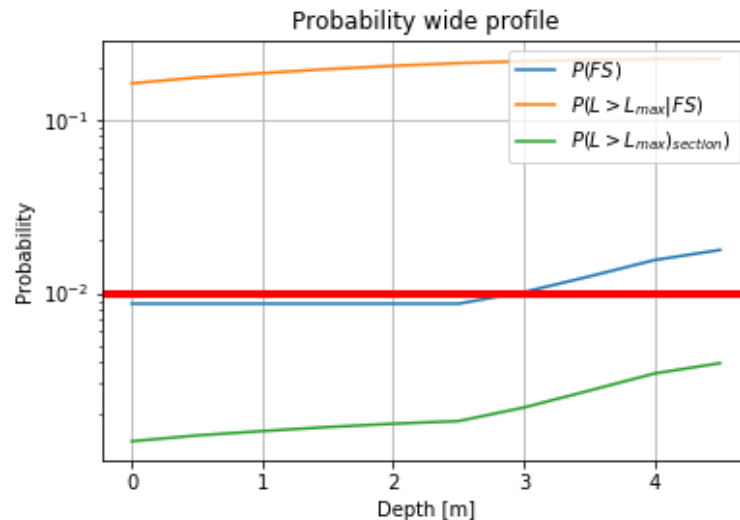
### Scenario 1: Growth in depth

In the first scour hole scenario, a scour hole is located right in the middle of the river branch, such that a symmetrical situation is created and the effect of the scour hole is equal on both riversides. The scour hole is only growing vertically in depth, the scour edges remain on the same place. This scenario is applied for scour holes with a width of 25%, 50%, 75% and 100% of the river branch. The scenario has been added to both references profiles. For the wider profile, the results of a scour hole with of 25% of the river are presented in figure D.4. The other results were similar, for all four scour hole widths in both reference situations, the following results are observed.

- The total probabilities of a flow slide which will result in a larger than acceptable retrogression length, increase if the scour holes become deeper.
- For a certain depth, eventually all scour hole situation do not longer satisfy to the required safety standard given in the WBI.
- In the first instance, only the  $P(L > L_{max}|FS)$  increases, after a certain depth also the  $P(FS)$  increases.

The total probability of a flow slide which will result in a larger than acceptable retrogression length, increase if the scour holes become deeper.

The effect on  $P(FS)$  can be clearly seen in figure D.4. In the first instance, the  $P(FS)$  is not affected, but for a certain depth, this probability increases. For the example shown in figure D.4, this is a depth of 3.0 [m]. The  $P(FS)$  increases because the geometry parameters  $H_{channel}$  and  $H_r$  has been increased due to a change of the characteristic point for the river channel bottom. The  $P(L > L_{max}|FS)$  increases slightly due to the larger available filling area for soil during a flow slide..



(a) Scour width: 26 m (25% river width)

| Depth [m]  | $P(FS)$ | $P(L > L_{max} FS)$ | $P(L > L_{max})_{section}$ |
|------------|---------|---------------------|----------------------------|
| ref. (0.0) | 0.0087  | 0.161               | 0.0014                     |
| 0.5        | 0.0087  | 0.174               | 0.0015                     |
| 1.0        | 0.0087  | 0.185               | 0.0016                     |
| 1.5        | 0.0087  | 0.195               | 0.0017                     |
| 2.0        | 0.0087  | 0.204               | 0.0018                     |
| 2.5        | 0.0087  | 0.211               | 0.0018                     |
| 3.0        | 0.0101  | 0.217               | 0.0022                     |
| 3.5        | 0.0125  | 0.220               | 0.0027                     |
| 4.0        | 0.0155  | 0.222               | 0.0035                     |
| 4.5        | 0.0177  | 0.223               | 0.0040                     |

(b) Probability scour width in the wide profile: 25% of river width

Figure D.4: Overview of probability for the wide profile including a scour hole of 26 m width, with an increasing depth.

### Scenario 2: Increase in scour width

A scour hole is placed at the left side of the profile, in the second scenario. The width of the scour hole is increasing. The results for the wide profile are shown in figure D.6 as an example. The numerical values are given in table D.4 The initial scour hole has a width of 25 [m] and a depth of 3.5 [m]. Compared with the reference situation without a scour hole, the total probability,  $P(L > L_{max})_{section}$ , on left riversides increases if a scour hole is added to the reference profile at the left riverside. This is due to the following effects:

1. The change of the characteristic bottom profile point.
2. The larger available filling area for soil during a flow slide.

For the right riverside, the  $P(L > L_{max})_{section}$  decreases. This is remarkable since the available filling area for soil increases, and thus a larger probability is expected. However, taken into account the change in the transition location of the two slope parts of the new profile, a larger amount of lower situated soil is flowing away during a flow slide. This larger soil amount results in a milder slope and thus a smaller  $P(L > L_{max}|FS)$ .

Both aspects, a change in transition location and the milder slope, can be seen in figure D.5, in which the profiles after a flow slide are shown for the reference case with and without the scour hole.

Looking to the probabilities for wider scour holes on the left riverside, it can be seen that the  $P(FS)$  will not change. The  $P(L > L_{max}|FS)$  is increasing in the first instance and will decrease slightly for wide scour holes. The increase is due to effect 2, wider scour holes have a larger area to fill and results in a steeper slope and thus a larger  $P(L > L_{max}|FS)$ . The later decrease of  $P(L > L_{max}|FS)$  is due to effect 3, the endpoint of the new profile is than located in the scour hole. Resulting in a lower located end point and thus a lower located transition location between the two profile points. This gives a larger amount of lower situated soil which flow away during a flow slide and thus a milder slope in the new profile.

On the right riverside, the  $P(L > L_{max}|FS)$  decreases with respect to the reference situation without a scour hole due to effect 3. When the scour hole grows in width, the  $P(L > L_{max}|FS)$  increases again due to effect 2. First, the  $P(FS)$  remains equal, but for a scour hole width larger than 60 [m] the  $P(FS)$  increases due to effect 1.

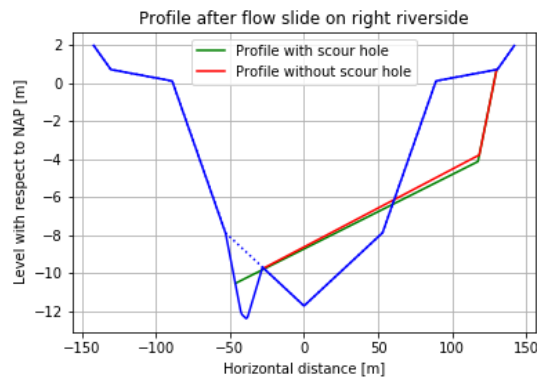
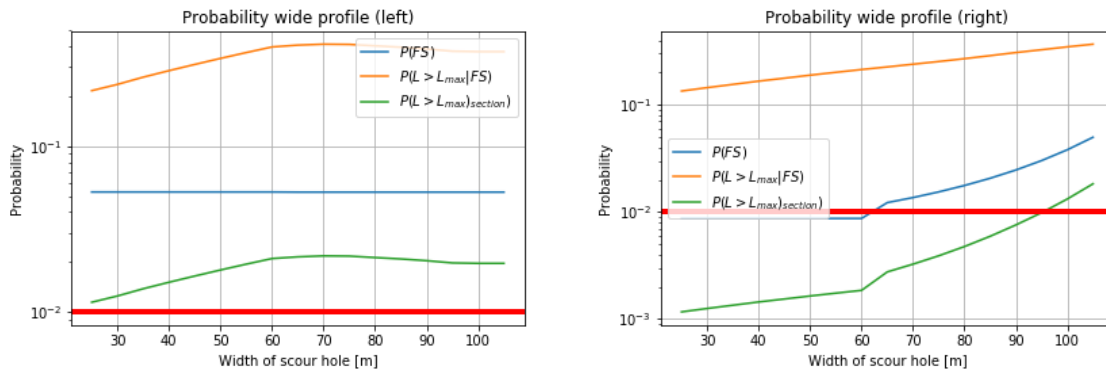


Figure D.5: Profile after a flow slide for the wide reference profile with and without a scour hole.



(a) Probability for left riverside.

(b) Probability for right riverside.

Figure D.6: Overview of probabilities for the wide profile including a scour hole with increasing scour width located at the left riverside.

| Width [m]  | Left side |                     |                            | Right side |                     |                            |
|------------|-----------|---------------------|----------------------------|------------|---------------------|----------------------------|
|            | $P(FS)$   | $P(L > L_{max} FS)$ | $P(L > L_{max})_{section}$ | $P(FS)$    | $P(L > L_{max} FS)$ | $P(L > L_{max})_{section}$ |
| ref. (0.0) | 0.0087    | 0.161               | 0.0014                     | 0.0087     | 0.161               | 0.0014                     |
| 25.0       | 0.0529    | 0.216               | 0.0114                     | 0.0087     | 0.134               | 0.0012                     |
| 30.0       | 0.0529    | 0.236               | 0.0125                     | 0.0087     | 0.145               | 0.0013                     |
| 35.0       | 0.0529    | 0.261               | 0.0138                     | 0.0087     | 0.155               | 0.0013                     |
| 40.0       | 0.0529    | 0.285               | 0.0151                     | 0.0087     | 0.166               | 0.0014                     |
| 45.0       | 0.0529    | 0.311               | 0.0164                     | 0.0087     | 0.177               | 0.0015                     |
| 50.0       | 0.0529    | 0.338               | 0.0179                     | 0.0087     | 0.189               | 0.0016                     |
| 55.0       | 0.0529    | 0.367               | 0.0194                     | 0.0087     | 0.201               | 0.0017                     |
| 60.0       | 0.0529    | 0.397               | 0.021                      | 0.0087     | 0.213               | 0.0019                     |
| 65.0       | 0.0528    | 0.407               | 0.0215                     | 0.0122     | 0.226               | 0.0028                     |
| 70.0       | 0.0528    | 0.412               | 0.0218                     | 0.0136     | 0.239               | 0.0033                     |
| 75.0       | 0.0528    | 0.411               | 0.0217                     | 0.0154     | 0.253               | 0.0039                     |
| 80.0       | 0.0528    | 0.403               | 0.0213                     | 0.0177     | 0.269               | 0.0048                     |
| 85.0       | 0.0528    | 0.395               | 0.0209                     | 0.0206     | 0.287               | 0.0059                     |
| 90.0       | 0.0528    | 0.386               | 0.0204                     | 0.0246     | 0.307               | 0.0076                     |
| 95.0       | 0.0528    | 0.374               | 0.0197                     | 0.0301     | 0.326               | 0.0098                     |
| 100.0      | 0.0528    | 0.372               | 0.0196                     | 0.038      | 0.347               | 0.0132                     |
| 105.0      | 0.0528    | 0.372               | 0.0196                     | 0.0498     | 0.368               | 0.0183                     |

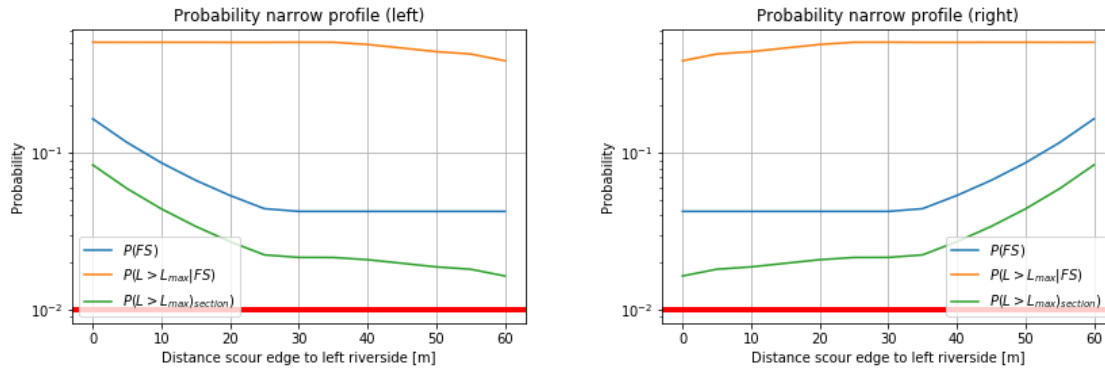
Table D.4: Probability flow slide for the wide profile, scenario 2: variation in width, scour depth=3.5m.

### Scenario 3: Migration of the scour hole

In the third situation, a scour hole is again placed at the left riverside. The location with respect to the riverbank is now varying while the scour width remains the same, see right figure of figure D.1. The scour hole migrates in this scenario from the left riverside towards the right riverside. For this scenario, two cases are applied on both reference profiles: a scour hole width of 25% and 50% of the river width.

As example, the results of a scour hole width of 25% of the river width are presented in figure D.7. The scour hole has a width of 20 [m] and a depth of 3.5 [m]. Since the profile with a scour hole is not symmetric, the probabilities on both riversides are not equal. Compared with the reference situation without a scour hole, the total probability on left riversides increases and decreases on the right riverside if the scour hole is located at the left riverside. This was also observed for scenario 2, in the wide reference profile.

Both probabilities,  $P(FS)$  and  $P(L > L_{max}|FS)$ , are thus larger on the left riverside than on the right riverside. If the scour hole migrates from the riverbank towards the other, the  $P(FS)$  for the left riverside decreases, while  $P(L > L_{max}|FS)$  is not changed. For the right riverside, the opposite is observed, the  $P(FS)$  remains equal, while  $P(L > L_{max}|FS)$  increases. The  $P(FS)$  for the left riverside changes again due to the change of characteristic channel bottom point. When the scour hole is located over 25 [m] from the riverside, the scour hole does no longer affect the  $P(FS)$ , this hold for both riversides. The  $P(L > L_{max}|FS)$  for the left riverside is not changing in the first phase, when the location of the scour hole varies, since the available surface area for the soil material remains equal. When the scour hole is located far from the riverside (over 40 [m]), the  $P(L > L_{max}|FS)$  decreases. The scour hole is no longer filled entirely after a flow slide and the effect of the presence of a scour hole on the  $P(L > L_{max}|FS)$  is reduced.



(a) Probability for left riverside, scour width 20 m

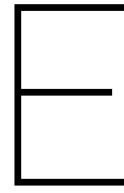
(b) Probability for right riverside, scour width 20 m

Figure D.7: Overview of probabilities for the narrow side profile including scour holes with changing location of a scour edge with respect to the left riverside.

| Edge dist. [m] |      |       | Left side |                     |                            | Right side |                     |                            |
|----------------|------|-------|-----------|---------------------|----------------------------|------------|---------------------|----------------------------|
|                | left | right | $P(FS)$   | $P(L > L_{max} FS)$ | $P(L > L_{max})_{section}$ | $P(FS)$    | $P(L > L_{max} FS)$ | $P(L > L_{max})_{section}$ |
| ref.           |      |       | 0.0424    | 0.434               | 0.0184                     | 0.0424     | 0.434               | 0.0184                     |
| 0.0            | 60.0 |       | 0.1652    | 0.508               | 0.084                      | 0.0424     | 0.387               | 0.0164                     |
| 5.0            | 55.0 |       | 0.1167    | 0.508               | 0.0593                     | 0.0424     | 0.428               | 0.0182                     |
| 10.0           | 50.0 |       | 0.0866    | 0.508               | 0.044                      | 0.0424     | 0.443               | 0.0188                     |
| 15.0           | 45.0 |       | 0.067     | 0.508               | 0.034                      | 0.0424     | 0.467               | 0.0198                     |
| 20.0           | 40.0 |       | 0.0536    | 0.508               | 0.0272                     | 0.0424     | 0.492               | 0.0209                     |
| 25.0           | 35.0 |       | 0.0442    | 0.508               | 0.0224                     | 0.0424     | 0.508               | 0.0216                     |
| 30.0           | 30.0 |       | 0.0424    | 0.509               | 0.0216                     | 0.0424     | 0.509               | 0.0216                     |
| 35.0           | 25.0 |       | 0.0424    | 0.508               | 0.0216                     | 0.0442     | 0.508               | 0.0224                     |
| 40.0           | 20.0 |       | 0.0424    | 0.492               | 0.0209                     | 0.0536     | 0.508               | 0.0272                     |
| 45.0           | 15.0 |       | 0.0424    | 0.467               | 0.0198                     | 0.067      | 0.508               | 0.034                      |
| 50.0           | 10.0 |       | 0.0424    | 0.443               | 0.0188                     | 0.0866     | 0.508               | 0.044                      |
| 55.0           | 5.0  |       | 0.0424    | 0.428               | 0.0182                     | 0.1167     | 0.508               | 0.0593                     |
| 60.0           | 0.0  |       | 0.0424    | 0.387               | 0.0164                     | 0.1652     | 0.508               | 0.084                      |

Table D.5: Probability flow slide for the narrow profile, scenario 3: variation in location for a scour hole with 25% of river width, depth=3.5m.

*(This page is intentionally left blank)*



## General method for risk assessment of scour holes

The general method for risk assessment of scour holes consists of 8 steps, as indicated in figure E.1. The starting point of the data-driven approach is a known scour hole location with a potential hazard for flow sliding. The steps for the risk assessment are shortly described in this Appendix. This Appendix can be seen as a summarization of the methods described in the main report and the other Appendixes. In Appendix G, the method is applied on a case study as an example.

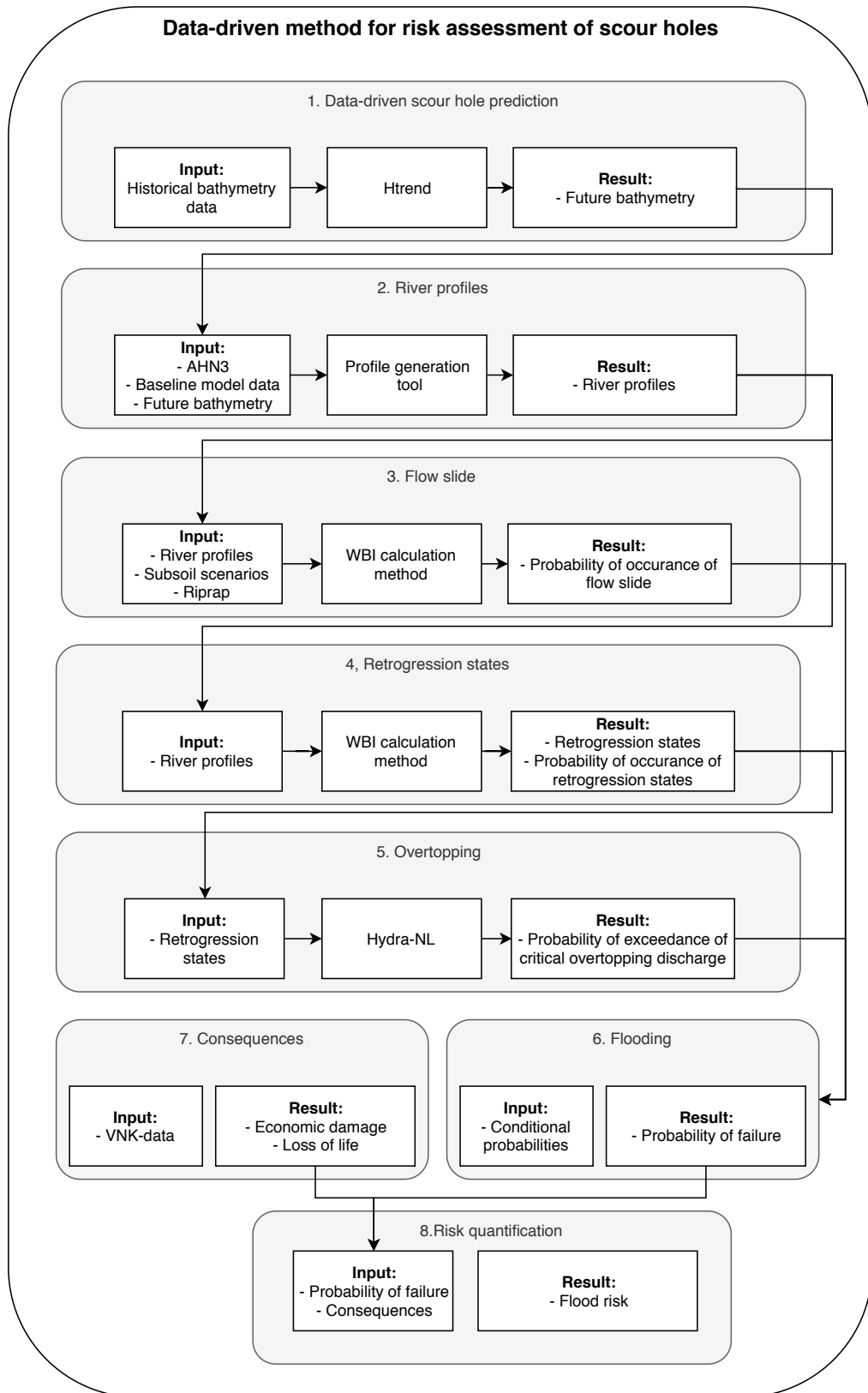


Figure E.1: Overview of the data-driven method for risk assessment of scour holes.

## 1. Data-driven approach for scour hole prediction

In this part of the method, the future scour hole dimensions are predicted. This entire step can be skipped if only insight is desired in the current state of the flood risk near scour holes.

### Input

The input for this step are bathymetry files. Only, the bed level data in the surrounding of a scour holes is required. This data can be selected from the bathymetry files of entire river branches. For the calibration and verification of the extrapolation tool, at least four historically measured bathymetry files are required. These files are also used for the determination of the bed level erosion rate relation. The usage of more bathymetry files, will improve the relation, especially for small scour holes.

### Method

The method for the scour hole prediction consists of the following steps, these steps are clarified in Appendix B:

1. Calibration and verification of Htrend for the specific scour hole.
2. Determination of bed level erosion rate relation for the specific scour hole.
3. Tool runs with Htrend, as described in figure 3.6 in the main report.
4. Determination for each bathymetry point, mean value and the 5% and 95% exceedance values.
5. Combining the 5%, mean and 95% values into scenarios for the future bathymetry.

### Result

The result of this step is the future bathymetry. For the future bathymetry, different scenarios can be defined based on the mean, the 5% and 95% exceedance values.

## 2. River profiles

In this step river profiles are generated, a river profile is a cross-section of the river containing both flood defences and everything in between them, like the foreshores and river channel. The intermediated distances between two river profiles should be determined based on the local variations and the desired density.

### Input

The input for the river profiles is one of the predicted future bathymetry scenarios or the historical measured scour hole bathymetry, together with the Actueel Hoogtebestand Nederland (AHN3) data and data from the baseline model of the Rhine-Meuse Delta.

### Method

The following steps are performed in order to determine the river profiles, these steps are done in this thesis with the river profile generation tool.

1. Selecting lines for the extraction of data based on the river geometry.
2. Extending and interpolation of the river lines.
3. Extraction data on the river lines.

### Result

River cross-section profiles with the elevation along the predefined river lines are the output of the river profile generation tool.

### 3. Flow slide

The probability of occurrence of a flow slide is determined in this step for each river profile.

#### Input

Next to the river profiles, the flow slide parameters are required in this step. The flow slide parameters are the subsoil scenarios with their probability of occurrence and the subsoil properties. Besides, the local parameters like the dynamic behaviour of the foreshore and the OLW-water level are required.

#### Method

The method applied to the river profiles in order to determine the probability of occurrence of a flow slide is described in the WBI (Rijkswaterstaat, 2016b). An example of the application is presented in Appendix C, in this Appendix the following steps are applied:

1. Determination of the characteristic profile points: Dike top and dike toe.
2. Per subsoil scenario, iterative determination of the geometry properties and the remaining characteristic profile points: insert river channel and bottom river channel.
3. Calculation of probability of occurrence of a flow slide per subsoil scenario
4. Combining the probabilities for all river profiles to one total probability for the entire scour hole per subsoil scenario.
5. Combining the probability per subsoil scenario to one general total probability.

#### Result

The result of this step is the total probability of occurrence of a flow slide next to the scour hole.

### 4. Retrogression states

The probability of occurrence of a certain retrogression state is determined in this step. A retrogression state is the state of the river profile after the occurrence of a flow slide. For example, affection of the entire foreshore or retrogression up to the dike crest.

#### Input

The input of this step is the river profiles determined in step 2. Based on the geometry of the river profiles a certain amount of retrogression states must be defined.

#### Method

The probability of occurrence of a retrogression states is determined with the method described in the WBI. This applied in the following way:

1. Determination of a certain amount of retrogression states.
2. Determination of retrogression length range representing each retrogression state.
3. Calculation of the post flow slide profile for the lower and upper bound of the retrogression length range, with the volume balance of the post flow slide profile.
4. Calculation of the probability of exceedance of the lower and upper bound of the retrogression length range.
5. Calculation of the probability of occurrence of each retrogression state.

#### Result

The results of this step are defined retrogression states together with their probability of occurrence. For each retrogression state a representative post flow slide profile is defined.

## 5. Overtopping

In this step, the probability of exceedance of the critical overtopping discharge is determined for each retrogression states.

### Input

The input for this step are the representative profiles for the retrogression states determined in step 4.

### Method

The probability of exceedance of the critical overtopping discharge is calculated with the software Hydra-NL. In which the representative profiles for the retrogression states are used as dike profiles and coupled with the hydraulic location of the WBI-Database.

### Result

With Hydra-NL, the probability of exceedance of the critical overtopping discharge is determined for each retrogression state.

## 6. Flooding

The total yearly probability of flooding is determined in this step.

### Input

The input for the total flooding probability are the conditional probabilities determined in the previous steps. These are the probability of occurrence of a flow slide (step 3), the probability of occurrence of a certain retrogression state (step 4) and the probabilities of exceedance of the retrogressions states (step 5). Moreover, the probability of successful repair after a flow slide is also required for the calculation of the flooding probability.

### Result

The result is the total yearly probability of flooding of the dike section next to the scour hole based on the scour hole bathymetry used as input for the generation of the river profiles in step 2.

## 7. Consequences

The consequences of a flood are determined in the nationwide flood risk assessment Veiligheid Nederland in Kaart (VNK2). The values determined in the reports of the VNK2 could be used in the risk assessment of the scour holes.

### Input

The input data for this step is the VNK2-report of the dike ring of the dike section next to the scour hole.

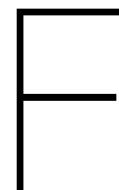
### Result

The result of this step are the expected loss of life of a flood together with the expected economic damages.

## 8. Risk quantification

The total flood risk can be calculated by multiplying the probability of flooding calculated in step 6 with the consequences determined in step 7.

*(This page is intentionally left blank)*



## Quickscan for the connecting branches

In this Appendix, a safety assessment is done for the indirect failure mechanism flows slide in three connecting branches: Spui, Oude Maas and Noord. The goal of the quickscan is to identified dike sections located near a scour hole with a moderated probability of damage due to flow slides.

### F.1. Spui

The river Spui connects the Oude Maas with the Haringvliet. The river branch has a length of 16 [km] from rkm 995 (begin: Oude Maas side) to rkm 1011 (end: Haringvliet). Compared with the other river branches in the Rhine-Meuse Delta, the Spui is a relatively narrow river branch. The average width of the river is namely 130 – 250 [m]. The nautical guaranteed depth is –3.5 [m NAP]. There is a lot of depth variation over the river branch. The average bottom level is –11.4 [m NAP], while due to the presence of 13 scour holes the bottom level is up to –18.5 [m NAP]. The bed level variation can be seen in figure F.1, in which the bottom level of the Spui is presented.

The flood defences on the left riverside are part of dike trajectories 20-3 and 20-4. The flood defences on the right side are part of dike trajectories 21-1 and 21-2.

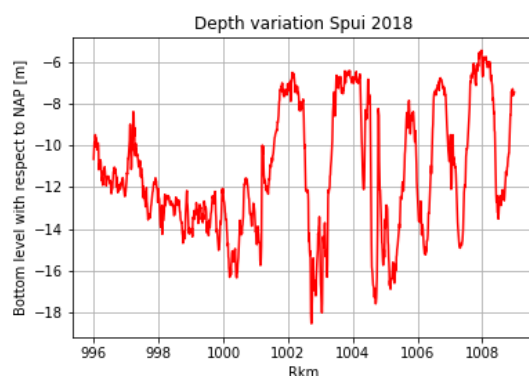


Figure F.1: Depth variation of the river Spui.

#### F.1.1. Foreshore filtering

The consequences of a flow slide depend on the length of the foreshore, as described in Rijkswaterstaat (2017). Based on the assessment profile presented in the rule of thumb part of the safety assessment regarding flow slide, it is assumed that the flood defence self of dike sections with a foreshore of at least 300 [m] will not be affected if a flow slide occurs. For this reason, the dike sections with a larger foreshore than 300 [m] will not be part of this quickscan. These locations are presented in figure F.2. The relevant dike sections for this quickscan are mentioned in table F.1.



Figure E2: Relevant sections for flow slide on the river Spui.

| Left side        | Right side       |
|------------------|------------------|
| rkm 996.0-997.1  | rkm 998.3-1008.5 |
| rkm 998.0-1007.5 |                  |

Table E1: Relevant dike sections for the quickscan on the river Spui.

### F.1.2. Parameter determination

For the safety assessment regarding flow slide, several parameters are required. The parameters are divided in three groups; geometry parameters, subsoil parameters and scaling parameters.

#### Geometry parameters

The geometry parameters are calculated from the characteristic profile points, which are determined from the river profiles as described in Appendix C. For the relevant sections of the Spui, each 10 [m] a river profile is generated from three datasets, the Actueel Hoogtebestand Nederland (AHN3), the baseline model and the multibeam bathymetry survey of June 2018. For the determination of the characteristic profile points, the water level is required next to the river profiles. The relevant water level is the agreed low water level (OLW) of Goidschalxoord.

$$OLW = -0.30 \text{ [m NAP]}$$

#### Subsoil parameters

According to Rijkswaterstaat (2017) subsoil scenarios must be used for the assessment regarding flow slide. For each subsoil scenario, the subsoil parameters must be determined. For this quickscan only one scenario will be used. Conservative parameters are chosen for the usages in this quickscan. The used subsoil scenario parameters are:

$$D_{50,mean.kar} = 150 \times 10^{-6}$$

$$\psi_{5m.kar} = -0.01$$

$$F_{cohesivelayers} = 3.0$$

#### Scaling parameters

The last group of parameters are the scaling parameters. The parameters in this group are the dynamic behaviour of the foreshore and the length of the section. The dynamic behaviour of the foreshore is determined from the conservative yearly-average erosion rate (0.02 [m/year]) multiplied with a conservative value of the slope of the foreshore (1 : 5). A default length of 1 [km] is used for the section length.

$$V_{local} = 0.1 \text{ [m/yr]}$$

### F.1.3. Probability of flow slide

#### Right riverside

In figure F.3, the  $P(L > L_{max})_{section}$  (Total probability of exceedance of the acceptable retrogression length for a dike section) is shown for the right riverside. As can be seen at nine location, the actually  $P(L > L_{max})_{section}$  is higher than the required  $P(L > L_{max})_{required}$  of 0.01 [1/year] according to Rijkswaterstaat (2017). The reason behind the high-value of these locations has been further analysed. The reasons can be seen in table F.2.

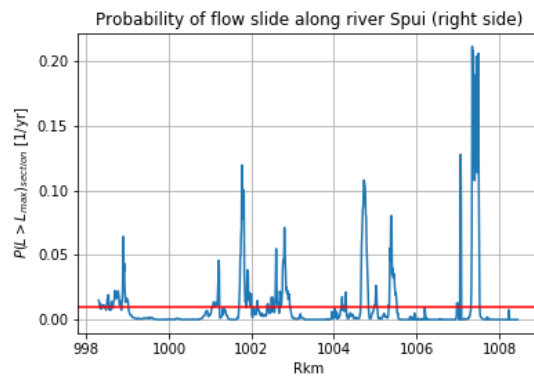


Figure F.3:  $P(L > L_{max})_{section}$  for the right side of the river Spui.

| Section              | Max $P(L > L_{max})_{section}$ |                        |
|----------------------|--------------------------------|------------------------|
| 1. rkm 998.3.0-999.0 | 0.064                          | Steep slope            |
| 2. rkm 1001.0-1001.2 | 0.045                          | Near scour hole        |
| 3. rkm 1001.7-1002.0 | 0.119                          | Steep slope            |
| 4. rkm 1002.4-1002.9 | 0.071                          | Near scour hole        |
| 5. rkm 1004.1-1004.2 | 0.021                          | Steep slope            |
| 6. rkm 1004.6-1005.0 | 0.108                          | Near scour hole        |
| 7. rkm 1005.2-1005.5 | 0.080                          | Near scour hole        |
| 8. rkm 1006.9-1007.0 | 0.128                          | Error in determination |
| 9. rkm 1007.2-1007.4 | 0.211                          | Near scour hole        |

Table F.2: Sections on the right riverside with  $P(L > L_{max})_{section} > 0.01$ .

#### Left riverside

For the left side, 10 location has a higher than allowable  $P(L > L_{max})_{section}$ , as can be seen in figure F.4. The length of these sections are smaller compared with the right riverside. The reasons of the high probabilities per section are shown in table F.3.

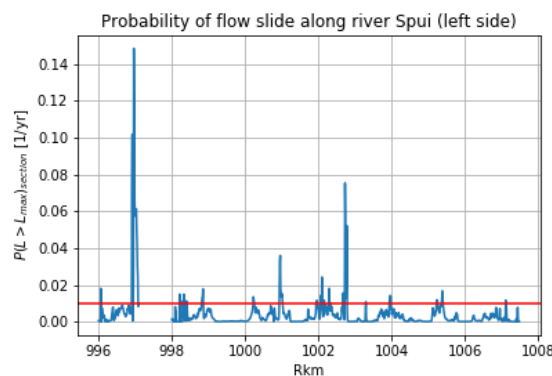


Figure F.4:  $P(L > L_{max})_{section}$  for the left side of the river Spui.

|     | Section            | Max $P(L > L_{max})_{section}$ |                        |
|-----|--------------------|--------------------------------|------------------------|
| 1.  | rkm 996.05         | 0.018                          | Error in determination |
| 2.  | rkm 996.9-1007.1   | 0.148                          | Steep slope            |
| 3.  | rkm 998.2-998.4    | 0.015                          | Error in determination |
| 4.  | rkm 998.8          | 0.017                          | Near scour hole        |
| 5.  | rkm 1000.2         | 0.013                          | Near scour hole        |
| 6.  | rkm 1000.9 -1001.0 | 0.036                          | Near scour hole        |
| 7.  | rkm 1002.0 -1002.3 | 0.024                          | Steep slope            |
| 8.  | rkm 1002.7 -1002.8 | 0.075                          | Near scour hole        |
| 9.  | rkm 1003.9 -1004.0 | 0.014                          | Steep slope            |
| 10. | rkm 1005.2 -1005.4 | 0.017                          | Near scour hole        |

Table E3: Sections on the left riverside with  $P(L > L_{max})_{section} > 0.01$ .

## Overview

An overview of the sections with  $P(L > L_{max})_{section} > 0.01$  is presented in figure E5. In this figure can be seen that these sections are spread over the entire river branch.



Figure E5: Sections with with  $P(L > L_{max})_{section} > 0.01$  on the river Spui.

### E1.4. Check for riprap

For the above mentioned sections with large probabilities of  $P(L > L_{max})_{section}$ , the presence of riprap must be checked. If riprap is present up to the bottom level, it can be assumed that the foreshore cannot erode and thus no trigger for flow slide can occur.

The presence of riprap is derived from historical bathymetry data. If no change of the slope between different years is observed it is assumed that the slope is stable due to the presence of riprap. The slopes retrieved from the bathymetry data of 2014, 2016, 2017 and 2018 are compared in table E4 and E5. Based on the difference in bathymetry, it can be concluded up to which level the riprap is presented per relevant river section.

Table F.4: Check for riprap on right riverside of Spui.

| Section              | Historical profile | Riprap   |
|----------------------|--------------------|--|
| 1. rkm 998.0-999.0   |                    | Riprap up to -11 m NAP                               |
| 2. rkm 1001.0-1001.2 |                    | Riprap up to -14 m NAP<br>Placed in period 2014-2016 |
| 3. rkm 1001.7-1002.0 |                    | Riprap up to -7 m NAP                                |

*Continued on next page*

Table F4 – Continued from previous page

| Section              | Historical profile                   | Riprap   |
|----------------------|--------------------------------------|--|
| 4. rkm 1002.3-1002.9 | <p>Historical profile rkm 1002.8</p> | <p>Riprap up to -17 m NAP<br/>Placed in period 2014-2016</p> |
| 5. rkm 1004.1-1004.2 | <p>Historical profile rkm 1004.3</p> | <p>Riprap up to -4 m NAP</p>                                 |
| 6. rkm 1004.6-1005.0 | <p>Historical profile rkm 1004.7</p> | <p>Riprap up to -5 m NAP</p>                                 |
| 7. rkm 1005.2-1005.4 | <p>Historical profile rkm 1005.3</p> | <p>Riprap up to -4 m NAP</p>                                 |

Continued on next page

Table F4 – Continued from previous page

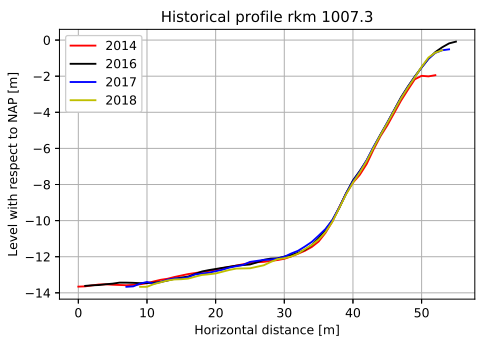
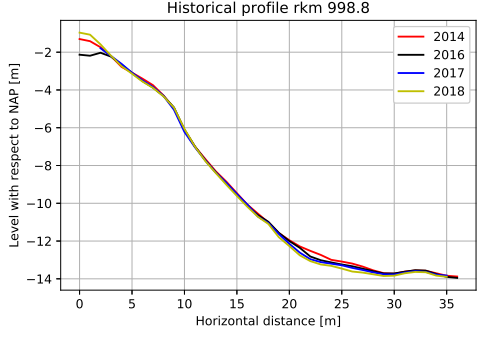
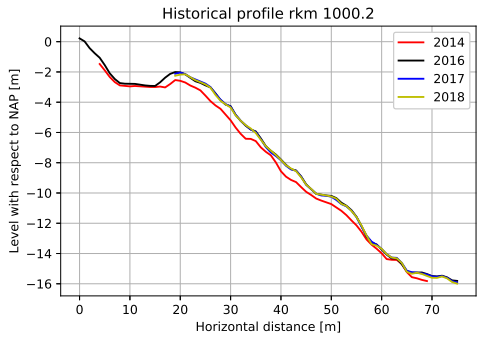
| Section              | Historical profile  | Riprap                 |
|----------------------|---|------------------------|
| 9. rkm 1007.2-1007.4 |  | Riprap up to -10 m NAP |

Table F5: Check for riprap on left riverside of Spui

| Section             | Historical profile  | Riprap   |
|---------------------|---|--|
| 2. rkm 996.9-1007.1 |   |  |
| 4. rkm 998.8        |  | Riprap up to -12 m NAP                               |
| 5. rkm 1000.2       |  | Riprap up to -14 m NAP<br>Placed in period 2014-2016 |

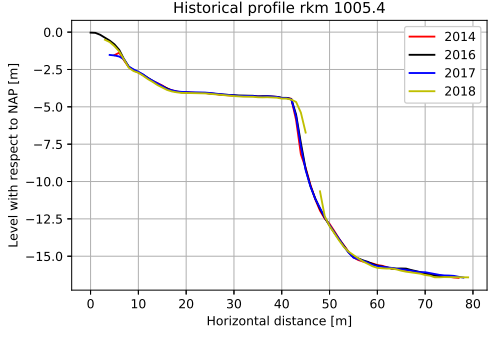
Continued on next page

Table E.5 – Continued from previous page

| Section               | Historical profile                   | Riprap                 |
|-----------------------|--------------------------------------|------------------------|
| 6. rkm 1000.9 -1001.0 | <p>Historical profile rkm 1001.1</p> | Riprap up to -12 m NAP |
| 7. rkm 1002.0 -1002.3 | <p>Historical profile rkm 1002.1</p> | Riprap up to -6 m NAP  |
| 8. rkm 1002.7 -1002.8 | <p>Historical profile rkm 1002.7</p> | Riprap up to -15 m NAP |
| 9. rkm 1003.9 -1004.0 | <p>Historical profile rkm 1004</p>   | Riprap up to -7 m NAP  |

Continued on next page

Table E5 – Continued from previous page

| Section                | Historical profile  | Riprap                |
|------------------------|---|-----------------------|
| 10. rkm 1005.2 -1005.4 |  | Riprap up to -5 m NAP |

**E1.5. Time development**

For the sections without riprap up to the river bottom and nearby a scour, the time development of  $P(L > L_{max})_{section}$  is interesting to analyse, in order to see if possibly scour growth enlarged the probability. The section taken into account for the time development analyse are for the right riverside 6,7 and 9, for the left riverside this is only section number 4 and 10. The other sections are not nearby a scour hole or have riprap up to the river bottom.

| Section              | Max $P_{2017}$ | Max $P_{2018}$ | $\Delta P_{max}$ | Mean $P_{2018}$ | Mean $P_{2018}$ | $\Delta P_{mean}$ |
|----------------------|----------------|----------------|------------------|-----------------|-----------------|-------------------|
| 6. rkm 1004.6-1005.0 | 0.104          | 0.108          | 0.003            | 0.0390          | 0.0409          | 0.0018            |
| 7. rkm 1005.2-1005.5 | 0.082          | 0.080          | -0.002           | 0.0367          | 0.0380          | 0.0013            |
| 9. rkm 1007.2-1007.4 | 0.268          | 0.211          | -0.057           | 0.1279          | 0.1340          | 0.0061            |

Table E6: Time development  $P(L > L_{max})_{section} > 0.01$  right side.

| Section               | Max $P_{2017}$ | Max $P_{2018}$ | $\Delta P_{max}$ | Mean $P_{2017}$ | Mean $P_{2018}$ | $\Delta P_{mean}$ |
|-----------------------|----------------|----------------|------------------|-----------------|-----------------|-------------------|
| 4. rkm 998.8          | 0.0165         | 0.0178         | 0.0013           | 0.0109          | 0.0116          | 0.0007            |
| 10. rkm 1005.2-1005.4 | 0.0170         | 0.0167         | -0.0003          | 0.0088          | 0.0091          | 0.0003            |

Table E7: Time development  $P(L > L_{max})_{section} > 0.01$  left side.

**E1.6. Conclusion quickscan Spui**

The most interesting dike sections are the dike sections between rkm 1004.6-1005.0 and 1007.2-1007.4 on the right side of the river branch, see figure E6. These two sections are located nearby scour holes and the probability of damage due to flow is above the allowable probability according to the safety standards. Moreover, the probability increased in the period between 2017 and 2018.

Besides these two sections, there are possible 14 dike sections on the river Spui, 6 on the left side and 8 on the right side, with a larger than allowable  $P(L > L_{max})_{section}$ . The actually probability depends on the actual presence of riprap, which is not verified yet, and the local subsoil parameters. These 14 sections will not be further analysed in the context of this research.

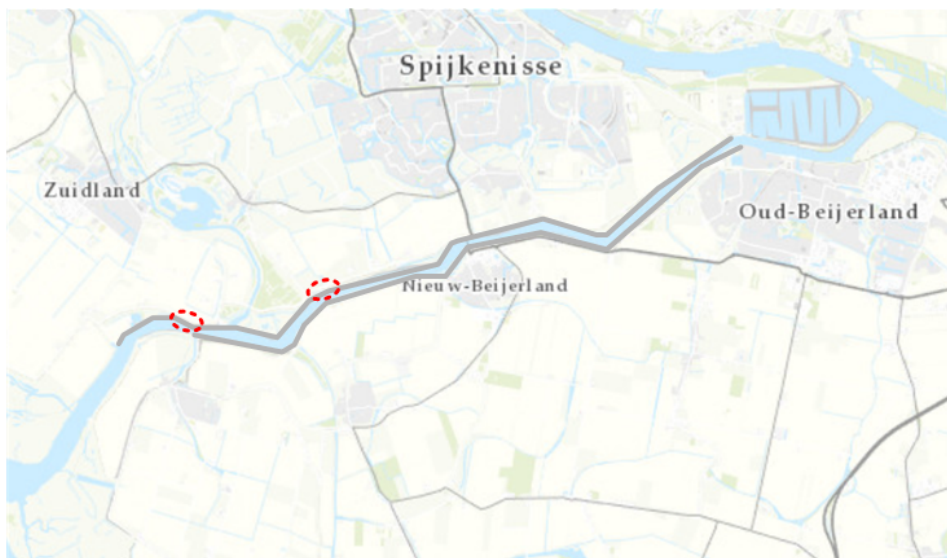


Figure E6: Most interesting dike sections for flow slide on the river Spui.

## E.2. Oude Maas

The part of the Oude Maas between the Dordtsche Kil and the Spui (rkm 980-995) is only considered for this quickscan. Downstream of this river part, Rijkswaterstaat is executing a pilot study on the scour holes, the available bathymetry do not represent the actual situation. There is an urban area with quay walls and other structures, upstream of the considered river part. The method for the calculation of the probability of flow slide is therefore not suitable.

The considered river branch is 15 [km] long. The nautical guaranteed depth is  $-5.0$  [m+NAP], making this river branch navigable for small sea-going vessels. There are nine scour holes located in the considered branch, six of those are located close to the river junction with the Dordtsche Kill.

### E.2.1. Foreshore filtering

For this quickscan, the relevant river sections depend on the length of the foreshore. Based on the WBI, it is assumed that the consequences of flow slide can be neglected for foreshores with a length of at least 300 [m]. The sections with a smaller foreshore than 300 [m] are indicated in green in figure E.7. Only these sections will be considered in the quickscan. In table E.8, the exact river sections are mentioned.

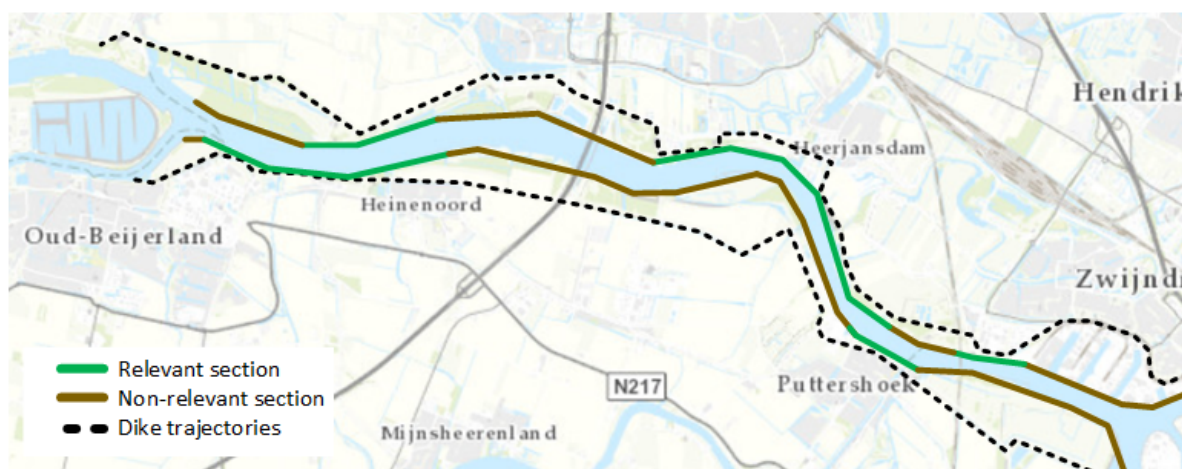


Figure E.7: Relevant sections for flow slide on the river Oude Maas.

| Left side       | Right side      |
|-----------------|-----------------|
| rkm 983.0-984.5 | rkm 982.0-982.8 |
| rkm 992.3-995.0 | rkm 984.1-988.6 |
|                 | rkm 990.3-993.7 |

Table F8: Relevant dike sections for the quickscan on the river Oude Maas, based on a smaller foreshore length than 300 m.

### Subsoil and scaling parameters

The same conservative subsoil and scaling parameters as used for the Spui are applied in the quickscan for the Oude Maas. These parameters are as follows:

$$D_{50.mean.kar} = 150 \times 10^{-6}$$

$$\psi_{5m.kar} = -0.01$$

$$F_{cohesivelayers} = 3.0$$

$$V_{local} = 0.1 \text{ [m/yr]}$$

## F.2.2. Probability of flow slide

### Right riverside

In figure F8, the  $P(L > L_{max})_{section}$  (Total probability of exceedance of the acceptable retrogression length for a dike section) is shown for the right riverside. As can be seen at three locations, the actual  $P(L > L_{max})_{section}$  is higher than the required  $P(L > L_{max})_{required}$  of 0.01 [1/year] according to Rijkswaterstaat (2017). The reason behind the high-value of these locations has been further analysed. The reasons can be seen in table F9.

Only at section 1 a scour hole is located, besides the foreshore is relatively small at this location. The other three high probabilities are due to an error in the determination, the dike profile was in all cases not good representative for the actual situation. In section 2 there is small basin located. In section 3, the dike profile is affected by a high elevation of the foreshore. In section 4, the entrance of the Heinoordtunnel is located. The presence of this entrance gives a wrong dike profile.

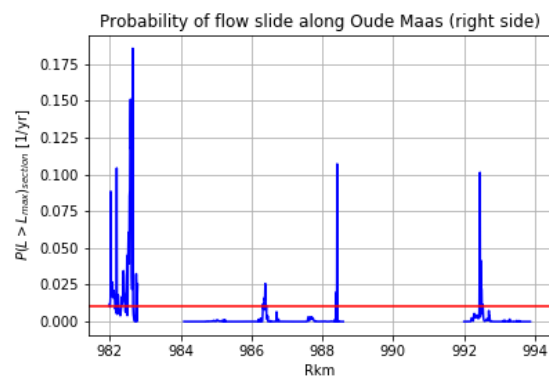


Figure F8:  $P(L > L_{max})_{section}$  for the right side of the river Oude Maas.

| Section             | Max $P(L > L_{max})_{section}$ |                              |
|---------------------|--------------------------------|------------------------------|
| 1. rkm 982.1-982.75 | 0.185                          | Scour hole & small foreshore |
| 2. rkm 986.4        | 0.026                          | Error in determination       |
| 3. rkm 988.4        | 0.107                          | Error in determination       |
| 4. rkm 992.5        | 0.102                          | Error in determination       |

Table F9: Sections on the Oude Maas right riverside with  $P(L > L_{max})_{section} > 0.01$ .

### Left riverside

For the left side, two location has a higher than allowable  $P(L > L_{max})_{section}$ , as can be seen in figure E.9. These sections are located close to each others. As mentioned in E.3, the high probability is for the first section due to a relative steep slope of the foreshore. For the second section, there is an error in the determination causing a high probability.

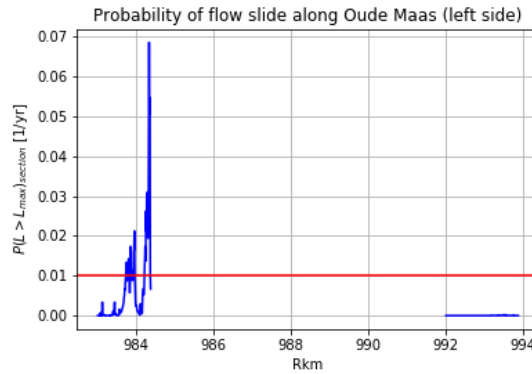


Figure E.9:  $P(L > L_{max})_{section}$  for the left side of the river Oude Maas.

| Section            | Max $P(L > L_{max})_{section}$ |                        |
|--------------------|--------------------------------|------------------------|
| 1. rkm 983.7-984.0 | 0.021                          | Steep slope            |
| 2. rkm 984.2-984.4 | 0.068                          | Error in determination |

Table E.10: Sections on the Oude Maas left riverside with  $P(L > L_{max})_{section} > 0.01$ .

### Overview

An overview of the sections with  $P(L > L_{max})_{section} > 0.01$  is presented for both riversides in figure E.10



Figure E.10: Sections with with  $P(L > L_{max})_{section} > 0.01$  on the river Oude Maas.

### F.2.3. Conclusion quickscan Oude Maas

There is only one location close to a scour hole with flow slide as a potential hazard in the Oude Maas. This location is indicated in figure E.11.

Besides, there is one location without a scour hole with a potential hazard of flow slide. At this location, the length of the foreshore is small and the slope of the foreshore is relatively steep.



Figure E11: Most interesting dike section for flow slide on the river Oude Maas.

### E3. Noord

The entire river Noord is analysed in this quickscan. The river branch has a length of 8.6 [km]. There are total six scour holes located in the Noord. Near Papendrecht, the Noord consists of two river part, the main fairway and a side-channel. Only the main fairway is considered in this quickscan, because of the side channel has a reduced depth of the side-channel.

#### E3.1. Foreshore filtering

Again, the sections with a foreshore length smaller than 300 [m] are analysed in the quickscan. The sections with a smaller foreshore than 300 [m] are indicated in green in figure E.12. Only these sections will be considered in the quickscan. In table E.11, the exact river sections are mentioned.

| Left side       | Right side      |
|-----------------|-----------------|
| rkm 979.8-980.5 | rkm 976.0-978.0 |
|                 | rkm 981.4-984.1 |

Table E11: Relevant dike sections for the quickscan on the river Noord, based on a smaller foreshore length than 300 m.

#### Subsoil and scaling parameters

The same conservative subsoil and scaling parameters as used for the Spui and the Oude Maas are applied in the quickscan for the Noord. However, the water level (OLW) differs, the OLW of Krimpen aan de Lek is used for the Noord. The used parameters are as follows:

$$D_{50.mean.kar} = 150 \times 10^{-6}$$

$$\psi_{5m.kar} = -0.01$$

$$F_{cohesivelayers} = 3.0$$

$$V_{local} = 0.1 \text{ [m/yr]}$$

$$OLW = -0.40 \text{ [m + NAP]}$$



Figure E12: Relevant sections for flow slide on the river Noord.

### F3.2. Probability of flow slide

#### Right side

There are three sections on the right side with a larger than probability of flow slide than  $P = 0.01$ . These sections are all located in the Northern part of the river branch.

| Section            | Max $P(L > L_{max})_{section}$ |                               |
|--------------------|--------------------------------|-------------------------------|
| 1. rkm 982.7       | 0.014                          | Steep slope & small foreshore |
| 2. rkm 983.5-983.7 | 1.0                            | Error in determination        |
| 3. rkm 983.8       | 0.023                          | Scour hole & small foreshore  |

Table F.12: Sections on the Noord right riverside with  $P(L > L_{max})_{section} > 0.01$ .

#### Left side

There are no relevant sections with a larger probability than 0.01 on the left side of the river branch Noord.

#### Overview

An overview of the sections with  $P(L > L_{max})_{section} > 0.01$  is presented in figure F.13

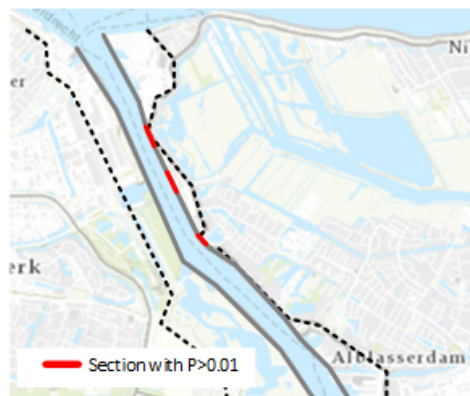


Figure F.13: Sections with with  $P(L > L_{max})_{section} > 0.01$  on the river Noord.

### F3.3. Conclusion quickscan Noord

There is only one location close to a scour hole with flow slide as a potential hazard in the Oude Maas. This location is indicated in figure F.14.

Besides, there is one location without a scour hole with a potential hazard of flow slide. At this location, the length of the foreshore is small and the slope of the foreshore is relatively steep.



Figure F.14: Most interesting dike sections for flow slide on the river Noord.

# G

## Risk assessment scour hole rkm 1004.8

In this Appendix the case study for the risk assessment of a scour hole is presented. As case study, the scour hole in the river spui near rkm 1004.8 is used. The results of the risk assessment are presented in the main report in section 5.3. In this Appendix, the calculations of the risk assessment are presented. Followed by the calibration of the scour hole extrapolation.

### G.1. Case Spui rkm 1004.8

At the Spui, around the river bend at rkm 1005, a cluster of three scour holes is located as shown in figure G.1. The eastern scour hole of these 3, is the most interesting scour hole in the context of this risk assessment since this scour hole is growing in depth and surface. Moreover, this scour hole is located close to the right riverbank and the foreshore near this scour hole is relatively small.

The risk assessment for this scour hole is only done for the right riverside. The flood defence on this side is part of dike trajectory 20-3. The safety standards for this dike trajectory is 1/10.000 [1/yr].

The edge level of this scour hole is determined at  $-12.8$  [m + NAP]. All bed level points, which are lower located than this level are considered as part of the scour hole (Huismans & van Duin, 2016).

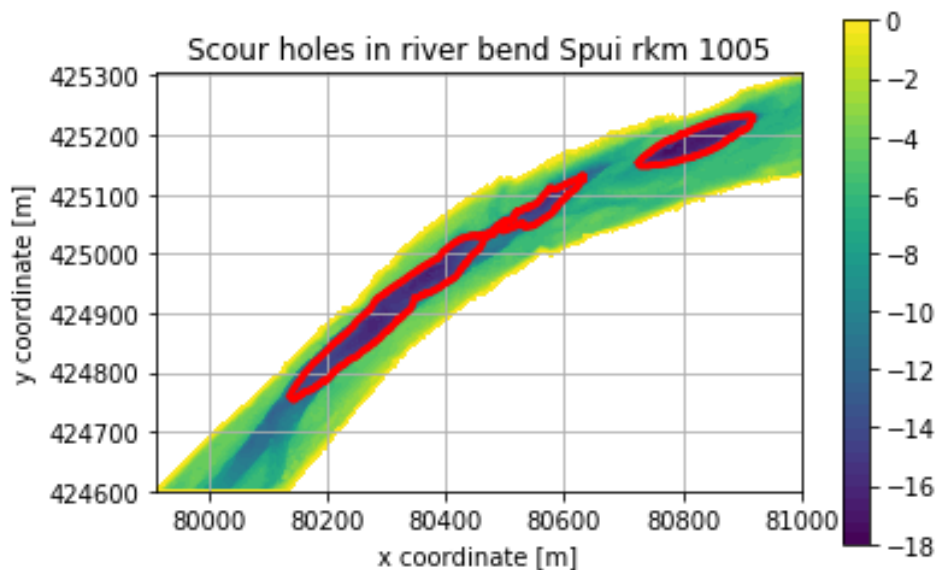


Figure G.1: Bathymetry around the river bend in the Spui near rkm 1005 with indication of three scour holes.

### G.1.1. Historical Scour hole development

This scour hole has currently a dynamic behaviour. The scour hole is growing in surface and in depth, as can be seen in table G.1. The deepest point of the scour hole increases with about 15-20 cm/year. The scour hole is growing in length at both ends. This can be seen in figure G.2. Besides, the scour hole is also growing in width. However, the growth in width is smaller than the growth in length. The scour hole is growing towards both riversides. The growth towards the left riverside (north-west) is larger than towards the right riverside (south/east).

| Year | Deepest point [m + NAP] | Surface [m <sup>2</sup> ] | Length [m] | $W_{max}$ [m] |
|------|-------------------------|---------------------------|------------|---------------|
| 2014 | -16.98                  | 6080                      | 182        | 44            |
| 2015 | -17.164                 | 6281                      | 182        | 44            |
| 2016 | -17.379                 | 6530                      | 190        | 46            |
| 2017 | -17.493                 | 6725                      | 200        | 46            |
| 2018 | -17.705                 | 6915                      | 200        | 47            |

Table G.1: Overview of development of the case scour hole.

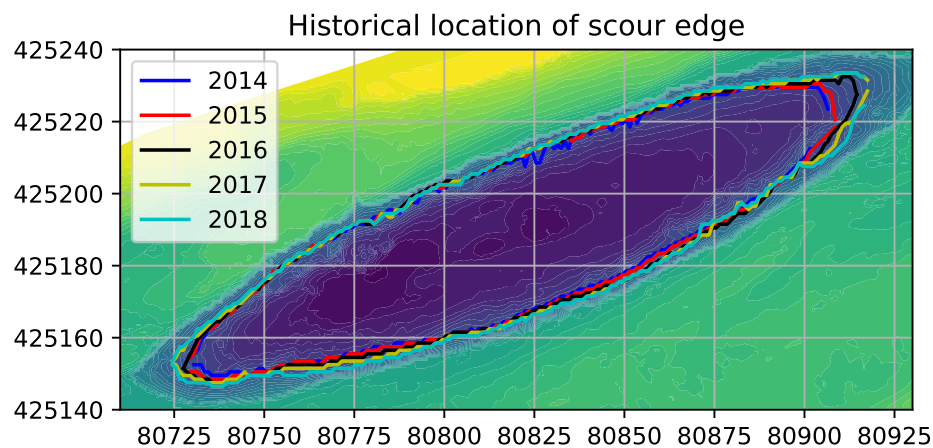


Figure G.2: Historical locations of the scour hole edges.

### G.1.2. Scour hole development prediction

The development of the scour hole is predicted with the probabilistic approach, explained in Appendix B. In this approach, the extrapolation tool Htrend is used. The set-up of this tool is together with the tool calibration and verification presented in this Appendix in section G.2.

With the probabilistic approach, 300 runs are made in order to predict the bathymetry in 2023. From the tool results, a range of the future scour hole bathymetry is determined. The properties of the mean, 5% and 95% scour holes are presented in table G.2. The prediction of the locations of the scour edges for these scour holes are indicated in figure G.3.

| Scenario       | Deepest point [m NAP] | Surface [m <sup>2</sup> ] | Length [m] | $W_{max}$ [m] |
|----------------|-----------------------|---------------------------|------------|---------------|
| 2018           | -17.705               | 6915                      | 200        | 47            |
| 5% percentile  | -17.895               | 6848                      | 206        | 46            |
| mean           | -18.252               | 7080                      | 210        | 48            |
| 95% percentile | -18.672               | 7282                      | 212        | 49            |

Table G.2: Overview of growth of case scour hole.

The scour hole surface in the 5% percentile scenario, is smaller than scour hole surface measured in 2018. An explanation for this predicted size is that in a part of the prediction runs, the bathymetry of 2016 and 2017 is

used as input. Extrapolating this bathymetry can result in a smaller scour hole than the actual scour hole of 2018.

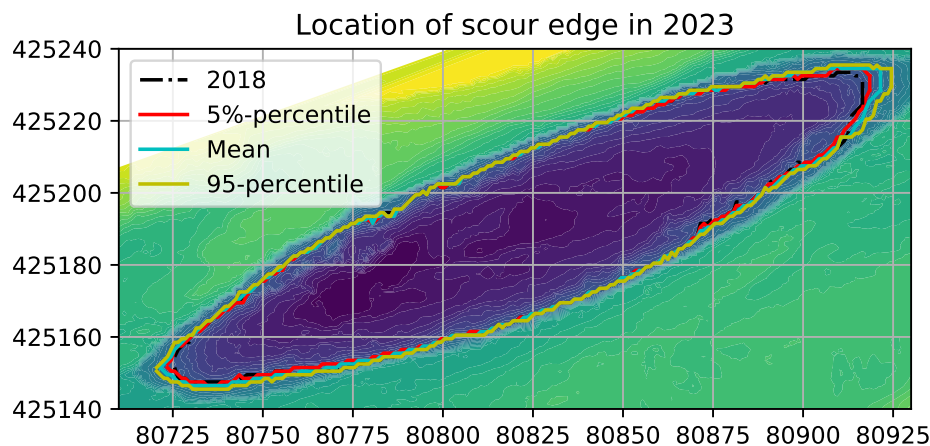


Figure G.3: Prediction of the location of the scour edge in 2023.

### G.1.3. Flow slide parameters

The flow slide parameters of this risk assessment differ from the parameters used in the quickscan of the river Spui. In the quickscan, conservative parameters are chosen such that they are applicable on the entire river branch. For this risk assessment, the parameters can be determined based on the conditions near the scour hole.

#### Riprap

In figure G.4, the riprap located next to the scour hole is indicated. As can be seen, the riprap is not placed on the scour hole edges or in the scour hole self. Based on the difference in bathymetry between 2014 and 2018, it is assumed that the riprap next to the scour hole is located until  $-8.0$  [m + NAP]. The presence of riprap can be neglected in the flow slide probability determination, because it is not located on the entire slope. In addition, the presence of riprap can also be neglected for the scour hole development prediction.

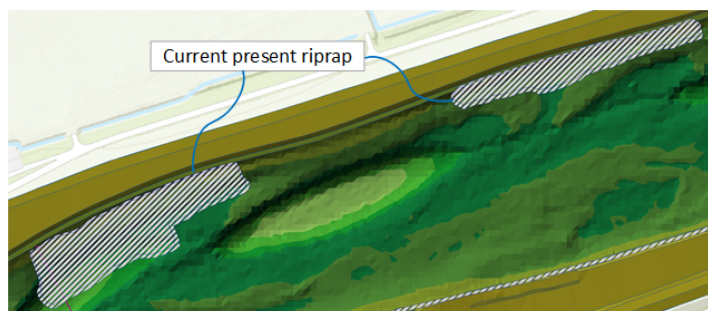


Figure G.4: Riprap next to the scour hole. Based on riprap information from WSHD (WSHD, 2019).

#### Subsoil parameters

The dike section next to the scour hole is located in dike-segment 20-01, for this dike-segment six subsoil scenarios are given in the WBI-Database. The subsoil scenarios are shown together with their probability of occurrence in figure G.5.

In table G.3, the subsoil parameters for these scenarios are presented. These parameters are estimated from the available information since no default values are (yet) available for this dike-segment. The thickest layers are the most important layers for the determination of  $D_{50,mean.kar}$ . This is the  $H\_Eg\_z&k$ -formation for scenario D1-D3 and the  $H\_Mg\_zm$ -formation for D4-D6. The  $H\_Eg\_z&k$  consists of very-fine till medium sand, while the  $H\_Mg\_zm$  consists of medium till coarse sand. Therefore it is assumed that the  $D_{50,mean.kar}$

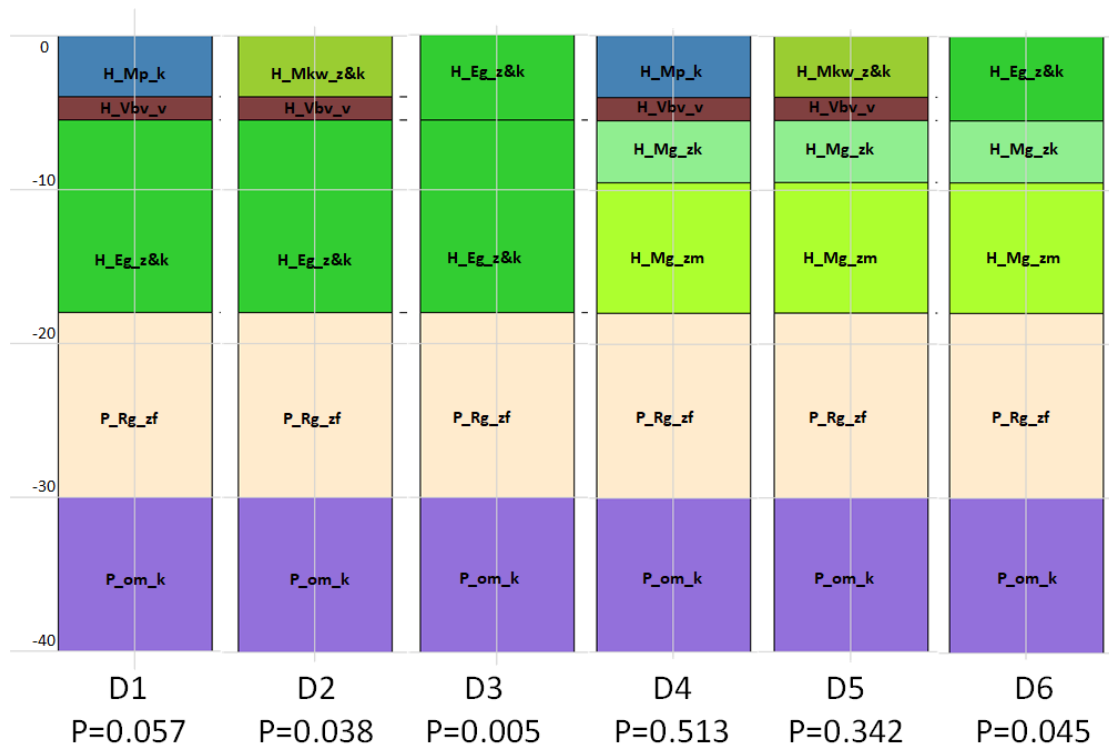


Figure G.5: Subsoil scenarios for dike-segment 20-01 from the SOS-database of the WBI.

is larger for the last three scenarios. According to Rijkswaterstaat (2016b) a good conservative assumption for the  $D_{50,mean.kar}$  is  $150 \times 10^{-6}$ .

A  $F_{cohesive}$ -value of 3.0 is given for the first three scenarios and 1.0 for the last three scenarios. These values are based on the soil layer between  $-10$  and  $-18$  [m + NAP]. Comparing the description of  $H\_Eg\_z&k$ -formation and the  $H\_Mg\_zm$ - formation, there are larger clay layers and more variation in the  $H\_Eg\_z&k$ -formation (Rijkswaterstaat, 2016a). Therefore, the scenarios with this soil formation is given a higher  $F_{cohesive}$ -value.

The  $\psi_{5m.kar}$ -values in table G.3 are based on the top layer. These are equal for D1 and D4, for D2 and D4 and for D3 and D6. In the scenarios D1 and D5, the top layer consists of clay and peat. While the top layer consists of sand, clay and peat for scenario D2 and D5. A sandy layer can be found as top layer in scenario D3 and D6. Good estimations for the  $\psi_{5m.kar}$ -values are in the range between  $-0.05$  and  $-0.15$ . Usually, sand layers have a larger value than clay or peat layers (Rijkswaterstaat, 2016b).

|                       | D1                   | D2                   | D3                   | D4                   | D5                   | D6                   |
|-----------------------|----------------------|----------------------|----------------------|----------------------|----------------------|----------------------|
| $D_{50,mean.kar}$ [m] | $100 \times 10^{-6}$ | $100 \times 10^{-6}$ | $100 \times 10^{-6}$ | $150 \times 10^{-6}$ | $150 \times 10^{-6}$ | $150 \times 10^{-6}$ |
| $\psi_{5m.kar}$       | -0.15                | -0.10                | -0.05                | -0.15                | -0.10                | -0.05                |
| $F_{cohesivelayers}$  | 3.0                  | 3.0                  | 3.0                  | 1.0                  | 1.0                  | 1.0                  |

Table G.3: Subsoil parameters for the subsoil scenarios for dike-segment 20-01.

### Scaling parameters

The scour hole had a length of 200 [m] in 2018. The scour hole is growing in length. In order to take future growth also into account, a larger section is considered. A length of 260 [m] is chosen, such that on both ends the scour hole can grow approximately 30 [m], see figure G.6.

$$L_{section} = 260 \text{ [m]}$$

The dynamic behaviour of the foreshore is determined from the yearly-average vertical erosion rate ( $0.05$  [m/year]) multiplied with a value of the slope of the foreshore (1 : 2).

$$V_{local} = 0.1 \text{ [m/yr]}$$

Lastly, the agreed low water level must be defined. For the flow slide probability determination, the OLW of Goidschalxoord is used.

$$OLW = -0.30 \text{ [m NAP]}$$

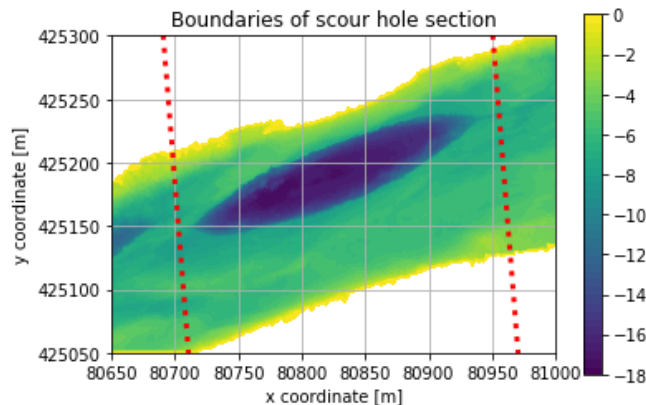


Figure G.6: Boundaries of the considered scour hole section.

#### G.1.4. Probability of a flow slide

For the selected section, 130 river profiles are generated with an intermediate distance of 2.0 [m]. This is done for the historical bathymetry (period 2014- 2018 ) and for the predict future bathymetry in 2023.

For each river profile, the probability of occurrence of a flow slide given the subsoil scenarios ( $P(FS|S_i)$ ) is calculated with Eq. A.10. In this calculation, a  $L_{section}$  of 0.002 [km] is used for each individual river profile. By summing the individual probabilities of occurrence of a flow slide, the total probability of occurrence can be determined, as shown with Eq. G.1.

$$P(FS|S_i) = \sum_{j=1}^{130} P(FS|S_i)_{prof.j} \quad (G.1)$$

In which:

$$P(FS|S_i)_{prof.j} = \text{Probability of occurrence of a flow slide given subsoil scenario } i \text{ for profile } j \quad [1/\text{yr}]$$

#### Historical probability of a flow slide

In table G.4, the historical probability of occurrence a flow slide is shown. As can be seen, the conditional probability for the first three subsoil scenarios is larger than for the last three. However, due to the smaller probability of occurrence of these scenarios, these higher probabilities per scenario have only a small contribution in the total probability of occurrence of a flow slide.

The total  $P(FS)$  was approximately the same in 2014, 2015 and 2016. However, the probability increased in 2017 and 2018. This is mainly due to the increase in the probability of occurrence for the profiles near the scour hole ends. As can be seen in figure G.7, the probability of occurrence of a flow slide for profile increased for the profiles near the scour hole ends, while it remained about equal or even decreased for the profiles in the centre of the scour hole.

| Year | $P(FS S_{D1})$ | $P(FS S_{D2})$ | $P(FS S_{D3})$ | $P(FS S_{D4})$ | $P(FS S_{D5})$ | $P(FS S_{D6})$ | $P(FS)$ |
|------|----------------|----------------|----------------|----------------|----------------|----------------|---------|
| 2014 | 0.0593         | 0.0556         | 0.0569         | 0.0068         | 0.0030         | 0.0044         | 0.0105  |
| 2015 | 0.0590         | 0.0553         | 0.0566         | 0.0067         | 0.0030         | 0.0043         | 0.0104  |
| 2016 | 0.0586         | 0.0549         | 0.0562         | 0.0067         | 0.0030         | 0.0043         | 0.0104  |
| 2017 | 0.0602         | 0.0564         | 0.0578         | 0.0070         | 0.0031         | 0.0045         | 0.0107  |
| 2018 | 0.0634         | 0.0596         | 0.0609         | 0.0072         | 0.0032         | 0.0046         | 0.0112  |

Table G.4: Probability of the occurrence of a flow slide given the subsoil scenarios, for the dike near the scour hole. Unit = [1/yr]

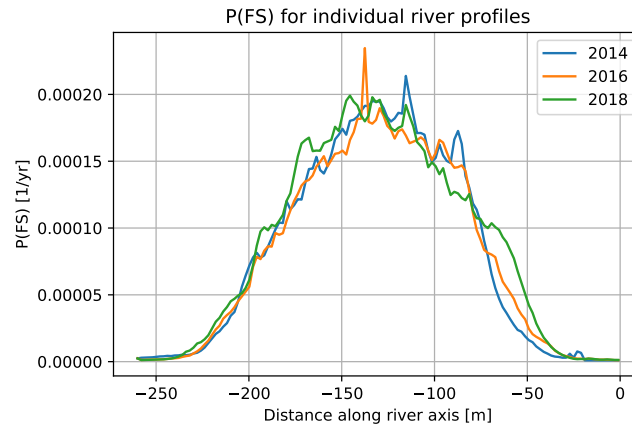


Figure G.7: Historical probability of occurrence of a flow slide for the individual river profiles of scour hole near rkm 1005 in the Spui.

### Future probability of a flow slide

The future  $P(FS)$  is calculated in the same way as the historical  $P(FS)$  for the mean expected and the 5% and 95% prediction scour hole in 2023. The results can be seen in table G.5. For all scenarios, the future probability increases. This was expected since the scour hole increases in depth and size.

| Scenario       | $P(FS S_{D1})$ | $P(FS S_{D2})$ | $P(FS S_{D3})$ | $P(FS S_{D4})$ | $P(FS S_{D5})$ | $P(FS S_{D6})$ | $P(FS)$ |
|----------------|----------------|----------------|----------------|----------------|----------------|----------------|---------|
| 5% percentile  | 0.071          | 0.0669         | 0.0684         | 0.0079         | 0.0036         | 0.0051         | 0.0124  |
| Mean           | 0.0877         | 0.0828         | 0.0845         | 0.0095         | 0.0044         | 0.0062         | 0.0152  |
| 95% percentile | 0.1129         | 0.1069         | 0.109          | 0.0118         | 0.0056         | 0.0078         | 0.0194  |

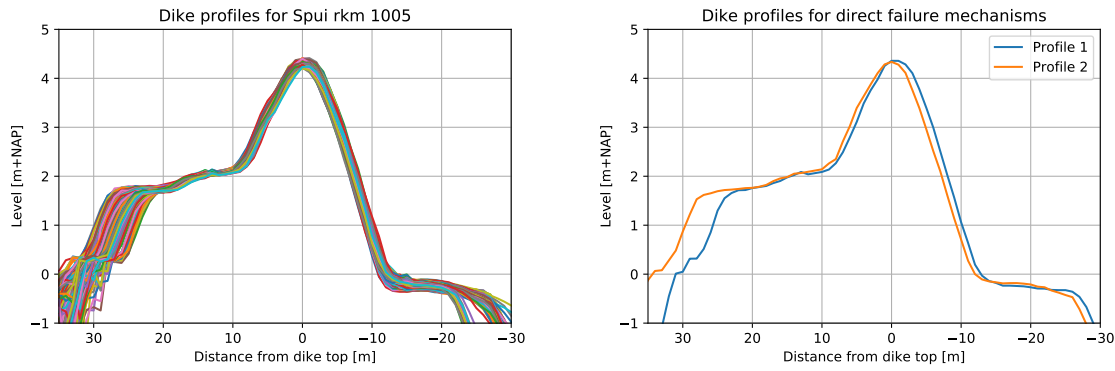
Table G.5: Probability of the occurrence of a flow slide in 2023 for different scour hole development scenarios. Unit = [1/yr]

## G.1.5. Direct failure mechanisms

### Dike profiles

In figure G.8a, the geometry of 130 dike profiles next to the scour hole is presented. The intermediate distance between the profiles is 2.0 [m]. As can be seen the geometry is quite uniform. There is only a small deviation in the foreshore lengths.

From these 130 profiles, two representative dike profiles are chosen for the determination of the effect on the direct failure mechanisms. These profiles have two different foreshore lengths, as can be seen in figure G.8b.



(a) Geometry of 130 dike profiles next to scour hole.

(b) Representative dike profiles for direct failure mechanisms.

Figure G.8: Dike geometry of the section next to the scour hole. The river Spui is located on the left sides of the profiles.

**Retrogression states**

The following states of retrogression are considered for the direct failure mechanisms:

1. Retrogression up to the dike toe ( $RS_1$ ).
2. Retrogression up to the dike top at landside ( $RS_2$ ).
3. Retrogression resulting of a dike height reduction of 2.0 m. ( $RS_3$ ).

For the two profiles, the lengths corresponding to these states are presented in table G.6. The corresponding retrogression state profiles are shown in figure G.9. The original profile presented in this figure is profile 1.

| Retrogression state | Profile 1 | Profile 2 |
|---------------------|-----------|-----------|
| State 1: $L_1$ [m]  | 17        | 21        |
| State 2: $L_2$ [m]  | 26        | 30        |
| State 3: $L_3$ [m]  | 31        | 35        |

Table G.6: Retrogression lengths for the representative profiles.

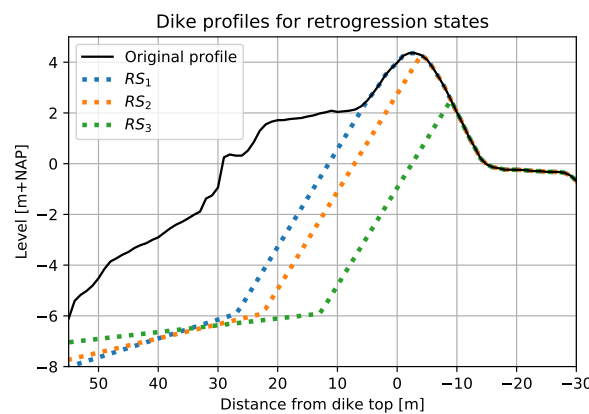


Figure G.9: Dike profiles after a flow slide for the three retrogression states.

The probabilities of exceedance of these retrogression lengths are shown in table G.7. These values are based on the 2018-geometry. Despite, the larger retrogression lengths for profile 2, the probabilities of exceedance are larger. This is due to the total profile geometry. Profile 2 is located near the deepest point of the scour

hole. Profile 1 is located close to end of the scour hole, where the scour hole is less deep. Which results in a lower probability of exceedance a certain retrogression length (mentioned as effect 2 in section 4.1.3).

|           | $P(L > L_1 FS)$ | $P(L > L_2 FS)$ | $P(L > L_3 FS)$ |
|-----------|-----------------|-----------------|-----------------|
| Profile 1 | 0.7207          | 0.4319          | 0.0177          |
| Profile 2 | 0.8475          | 0.6288          | 0.1523          |

Table G.7: Probability of the exceedance of the retrogression lengths for the 2018-geometry. Unit = [1/yr]

The probability of exceedance of a retrogression length is not equal to the probability of occurrence of a retrogression state. The probability of occurrence of the retrogression states are calculated with equation G.2. The probabilities corresponding to the two representative profiles are shown in table G.8.

The scour hole has a dynamic behaviour, therefore the probability of occurrence of the retrogression states will be different in the near-future. As can be seen in table G.9, G.10 and G.11 the probability of the states with the largest retrogression lengths increases and with the shortest retrogression lengths decreases for the 2023 profiles.

$$\begin{aligned}
 P(RS_1|FS) &= 1.0 - P\left(L > \frac{L_1 + L_2}{2} \middle| FS\right) \\
 P(RS_2|FS) &= P\left(L > \frac{L_1 + L_2}{2} \middle| FS\right) - P\left(L > \frac{L_2 + L_3}{2} \middle| FS\right) \\
 P(RS_3|FS) &= P\left(L > \frac{L_2 + L_3}{2} \middle| FS\right)
 \end{aligned} \tag{G.2}$$

|           | $P(RS_1 FS)$ | $P(RS_2 FS)$ | $P(RS_3 FS)$ |
|-----------|--------------|--------------|--------------|
| Profile 1 | 0.3449       | 0.5411       | 0.1140       |
| Profile 2 | 0.1966       | 0.5775       | 0.2259       |
| Average   | 0.2708       | 0.5593       | 0.1699       |

Table G.8: Probability of occurrence of the retrogression states based on the 2018 profiles. Unit = [1/yr]

|           | $P(RS_1 FS)$ | $P(RS_2 FS)$ | $P(RS_3 FS)$ |
|-----------|--------------|--------------|--------------|
| Profile 1 | 0.3249       | 0.5512       | 0.1239       |
| Profile 2 | 0.2004       | 0.5922       | 0.2074       |
| Average   | 0.2627       | 0.5717       | 0.1656       |

Table G.9: Probability of occurrence of the retrogression states based on the lowest 5% scour hole prediction in 2023. Unit = [1/yr]

|           | $P(RS_1 FS)$ | $P(RS_2 FS)$ | $P(RS_3 FS)$ |
|-----------|--------------|--------------|--------------|
| Profile 1 | 0.2802       | 0.5603       | 0.1595       |
| Profile 2 | 0.1717       | 0.5808       | 0.2475       |
| Average   | 0.226        | 0.57055      | 0.2035       |

Table G.10: Probability of occurrence of the retrogression states based on the mean expected profile in 2023. Unit = [1/yr]

|           | $P(RS_1 FS)$ | $P(RS_2 FS)$ | $P(RS_3 FS)$ |
|-----------|--------------|--------------|--------------|
| Profile 1 | 0.2385       | 0.5663       | 0.1952       |
| Profile 2 | 0.1434       | 0.5642       | 0.2924       |
| Average   | 0.1909       | 0.5652       | 0.2438       |

Table G.11: Probability of occurrence of the retrogression states based on the largest 95% scour hole prediction in 2023. Unit = [1/yr]

### Overtopping

The frequency of exceedance the critical overtopping discharge is calculated for the profiles of the three retrogression states. This is done with Hydra-NL. A critical overtopping discharge of 5.0 [l/s/m] is chosen. From the frequency, the probability of exceedance is calculated, as presented in Eq. A.11, and shown in table G.12. In this table, the probability of exceedance of the critical overtopping discharge for the original profile is presented as well.

|                             | $q_c = 5.0$ [l/s/m]    |                    |
|-----------------------------|------------------------|--------------------|
|                             |                        | Return period [yr] |
| $P(q_o > q_c   RS_1 \& FS)$ | $1.957 \times 10^{-8}$ | 51.100.000         |
| $P(q_o > q_c   RS_2 \& FS)$ | $1.570 \times 10^{-7}$ | 6.370.000          |
| $P(q_o > q_c   RS_3 \& FS)$ | $3.390 \times 10^{-2}$ | 29                 |
| $P(q_o > q_c   No FS)$      | $4.739 \times 10^{-9}$ | 211.000.000        |

Table G.12: Conditional probability of exceedance critical overtopping discharge. Unit = [1/yr]

The original probability of exceedance of the critical overtopping discharge is quite small. This is due to relatively high crest level on this location. Before, the closure of the Haringvliet, the Spui was an open channel to the North Sea and a high crest level was required. For the retrogression states, the probability of exceedance are larger, especially for  $RS_3$ , in which there is a considerable crest height reduction.

### G.1.6. Total probability

The total probability of exceedance of the critical overtopping discharge can be calculated with the following equation:

$$P(q_o > q_c) = P(q_o > q_c | No FS) \times (1 - P(FS)) + \sum_{i=1} (P(q_o > q_c | RS_i \& FS) \times P(RS_i | FS) \times P(FS)) \quad (G.3)$$

|                        | 2018                    |                     | 2023 <sub>mean</sub>    |                     |
|------------------------|-------------------------|---------------------|-------------------------|---------------------|
| $P(q_o > q_c   FS)$    | $5.760 \times 10^{-3}$  | $\times 0.0112$     | $6.899 \times 10^{-3}$  | $\times 0.0152$     |
| $P(q_o > q_c   No FS)$ | $4.739 \times 10^{-9}$  | $\times (1-0.0112)$ | $4.739 \times 10^{-9}$  | $\times (1-0.0152)$ |
| $P(q_o > q_c)$         | $=6.455 \times 10^{-5}$ |                     | $=1.049 \times 10^{-4}$ |                     |
| Return period [yr]     | 15500                   |                     | 9500                    |                     |

|                        | 2023 (5%)               |                     | 2023 (95%)              |                     |
|------------------------|-------------------------|---------------------|-------------------------|---------------------|
| $P(q_o > q_c   FS)$    | $5.614 \times 10^{-3}$  | $\times 0.0124$     | $8.264 \times 10^{-3}$  | $\times 0.0194$     |
| $P(q_o > q_c   No FS)$ | $4.739 \times 10^{-9}$  | $\times (1-0.0124)$ | $4.739 \times 10^{-9}$  | $\times (1-0.0194)$ |
| $P(q_o > q_c)$         | $=7.523 \times 10^{-5}$ |                     | $=1.603 \times 10^{-4}$ |                     |
| Return period [yr]     | 13300                   |                     | 6200                    |                     |

Table G.13: Probability of exceedance critical overtopping discharge ( $q=5$  l/s/m). Unit = [1/yr]

### Emergency repairs

If a flow slide happens, emergency or usual repairs can be made to restore the foreshore or the dike. Since the occurrence of flow slide is independent of the water level, there could be enough time for the repair without the occurrence of flooding. The average average required repair time for a successful repair is assumed to time 60 days. This assumption is based on Van der Krogt (2015), in which is stated that the  $p = 0.05$  for a successful repair within 14 days and  $p = 0.90$  for a successful repair within 100 days after the occurrence of a flow slide.

From this assumption follows that the probability of a successful repair after a flow slide is equal to  $P(\text{repair} | FS) = 1 - T_{\text{repair}}/365 \text{ days} = (1 - 60/365) = 0.835$ . With this assumption, the update total probability of exceedance of the critical overtopping discharge including repair measures are shown in table G.14

|             | Repair time =60 days |                    | without repairs      |                    |
|-------------|----------------------|--------------------|----------------------|--------------------|
|             | $P(q_o > q_c)$       | Return period [yr] | $P(q_o > q_c)$       | Return period [yr] |
| 2018        | $1.1 \times 10^{-5}$ | 94,300             | $6.5 \times 10^{-5}$ | 15,500             |
| 2023 (5%)   | $1.2 \times 10^{-5}$ | 80,800             | $7.5 \times 10^{-5}$ | 13,300             |
| 2023 (mean) | $1.7 \times 10^{-5}$ | 58,000             | $1.0 \times 10^{-4}$ | 9,500              |
| 2023 (95%)  | $2.6 \times 10^{-5}$ | 37,900             | $1.6 \times 10^{-4}$ | 6,200              |

Table G.14: Probability of exceedance and return period critical overtopping discharge ( $q=5$  l/s/m) for the case with and without dike repair after flow slide

### G.1.7. Other threats

#### Hydraulic structures

In the river Spui, no hydraulic structures like bridges or tunnels are located. There is, therefore, no danger for the stability problems with hydraulic structures. There are small groynes located in the Spui. However, the distance between the scour hole and the closest located groyne is over 200 [m], so the scour hole will not affect the stability of this groyne.

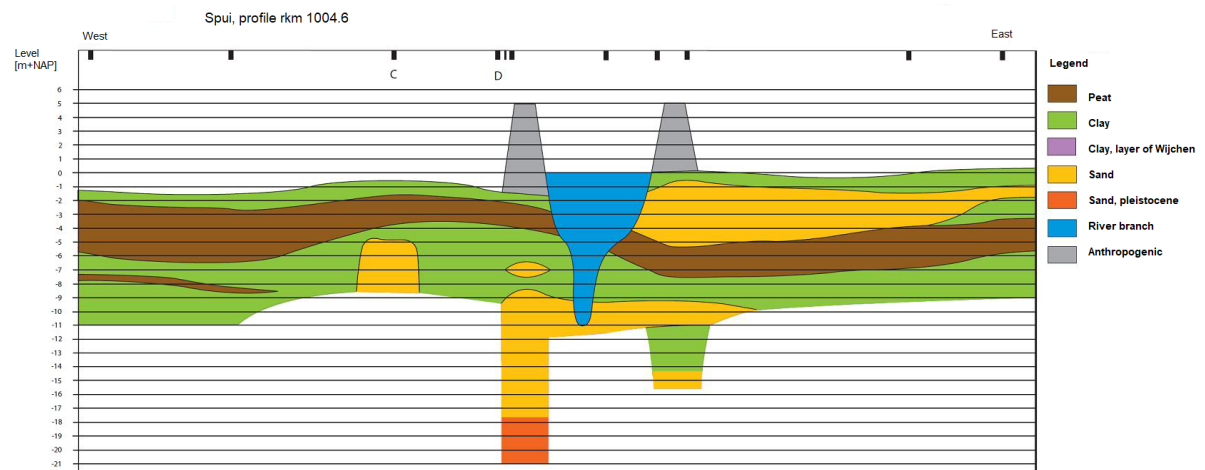
#### Cables and pipelines

There are no cables and pipelines in the direct surrounding of the scour hole. The scour hole is thus not a threat for damage to a cable or pipeline (Schoorman, 2018).

#### Sand layers

A lithological river cross-section is made by Stouthamer & de Haas (2011), close to the scour hole location, see figure G.10. The subsoil is determined with more details up to a level of  $-10$  [m + NAP]. For the lower located subsoil, fewer details are available. However, in the figure can be seen that at a level of approximately  $-18$  [m + NAP], the Pleistocene sand layer is located. The presence of this sand layer below the scour hole can result in a rapid scour depth increase if the above-located layers are totally eroded.

In 2018, the lowest located point of the scour hole was  $-17.70$  [m + NAP]. The Pleistocene sand layer is thus almost reached by the scour hole.



Source: Stouthamer & de Haas (2011)

Figure G.10: Lithological cross-section at rkm 1004.6 of the river Spui.

### G.1.8. Consequences

In Veiligheid Nederland in Kaart (VNK2), the consequences of a flood with a breach location near the scour hole are determined. The soil material influences the breaching pattern and thus subsequently the flood pattern. In VNK2, for breaches next to the Spui two cases are distinguished: a sand dike core and a clay core. The dike near the scour hole has a sand core, therefore the consequences of the sand core dike are used.

If there is a breach at the location and a flood occurs, the entire urban area of Spijkenisse and the rural areas up to the Bernisse will be flooded. The total consequences depends on the outer water level, and are shown in table G.15. (B. R. de Groot, 2014)

| Water level exceedance probability l | Economic damage [M€] | Loss of life |
|--------------------------------------|----------------------|--------------|
| 1/400 (tp-1d)                        | 2.495                | 80-330       |
| 1/4.000 (tp)                         | 2.910                | 100-415      |
| 1/40.000 (tp+1d)                     | 3.120                | 120-495      |

Source: B. R. de Groot (2014)

Table G.15: Consequences of a flood with a breach near the scour hole for different water levels associated with their exceedance probability.

### G.1.9. Risk estimation

Combining the probability of exceedance of the critical overtopping discharge with the consequences gives an estimation for the risk. According to B. R. de Groot (2014), the consequences corresponding to next, less favourable water level must be used for the risk estimation. For this scour hole, these are the consequences corresponding to a exceedance probability of 1/40.000 per year are used for the risk estimation.

The risk estimation is given in table G.16 for 2018 and in table G.17 for 2023. This is done fore the case with repair measures after a flow slide and the mean scenario with respect to the scour hole development. The two type of consequences can be combined with the value of statistic life. The common used value of €6.7 million per fatality is used with the mean of the range of expected loss of life.

|                   | Probability            | × | Consequences             | Risk                        |
|-------------------|------------------------|---|--------------------------|-----------------------------|
| Economical damage | $1.061 \times 10^{-5}$ | × | 3.120                    | = 33,099 [€/yr]             |
| Loss of life      | $1.061 \times 10^{-5}$ | × | (120 - 495)              | = 0.0013-0.0053 [People/yr] |
|                   | $1.061 \times 10^{-5}$ | × | $307.5 \times 6,700,000$ | = 21,1856 [€/yr]            |
| <b>Total</b>      |                        |   |                          | <b>= 54,955[€/yr]</b>       |

Table G.16: Risk estimation for scour hole in 2018.

|                   | Probability            | × | Consequences             | Risk                        |
|-------------------|------------------------|---|--------------------------|-----------------------------|
| Economical damage | $1.724 \times 10^{-5}$ | × | 3,430,000,000            | = 59,104 [€/yr]             |
| Loss of life      | $1.724 \times 10^{-5}$ | × | (120 - 495)              | = 0.0021-0.0085 [People/yr] |
|                   | $1.724 \times 10^{-5}$ | × | $307.5 \times 6,700,000$ | = 35,523[€/yr]              |
| <b>Total</b>      |                        |   |                          | <b>= 94.627[€/yr]</b>       |

Table G.17: Risk estimation for scour hole in 2023.

## G.2. Calibration and verification process

For the scour hole development prediction, the extrapolation tool Htrend is used. In this section the calibration and subsequently the verification of the tool set-up is presented. This is done for the scour hole at rkm1004.8 in the Spui.

In the calibration process, the input parameters of Htrend are varied, in order to set-up the tool such that the tool represent the actual situation. Subsequently, the calibrated parameters are checked with a verification. The calibrated parameters are kept fixed and are verified against an independent set of data. In figure G.11, the calibration and verification process is schematic shown.

There are four datasets required for the calibration and verification process of the tool. The first two datasets are used as input for htrend.exe. With these datasets, Htrend is calibrated such that the prediction of the scour hole bathymetry is close to the real bathymetry of the third dataset. Subsequently, the calibration must be verified, in order to see if the calibrated parameters also work on different datasets. For the verification,

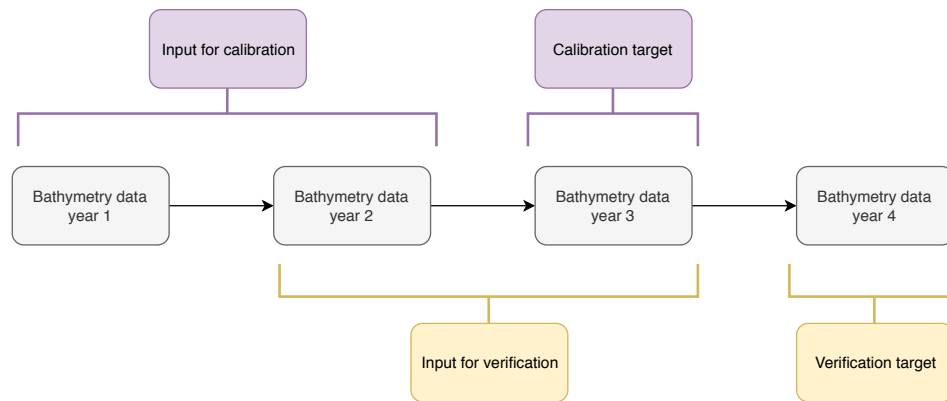


Figure G.11: Schematisation of usage of bathymetry datasets for the calibration and verification of the scour hole in Htrend.

different input datasets are required. For this verification, the bathymetry of year 2 and 3 are used as input data and the bathymetry is predicted for year 4.

### G.2.1. Calibration parameters

There are three input parameters in Htrend which have to be calibrated. The parameters are critical values for the detection of erosion and are used as a threshold for the horizontal displacements of the scour hole edges. The threshold is required to prevent the extrapolation of small local bed level changes.

These parameters are:

- Minimum erosion rate.
- Minimum length for erosion detection.
- Definition of a steep slope.

### G.2.2. Calibration targets

The tool will be used for the calculation of the probability of occurrence of a flow slide. In order to calculate this well, the tool must perform well on the prediction of the scour hole development in depth and size. The most important parts of the scour hole are the lowest parts of the scour hole.

The following targets are used for the calibration.

- Scour dimensions
  - Surface area of the scour hole
  - Length of the scour hole
  - Bed level of lowest located point
- Representation of lowest part
  - Profile development

The tool representation of the scour dimensions can be qualitatively assessed, while the representation of the profile development have to be done in a qualitative way. For the representation of the scour hole dimensions, next to the total surface area of the scour hole self, the area below a certain level are relevant. This is namely an indication for the representation of the depth increase of the scour hole

### G.2.3. Input data

As can be seen in figure G.11, the bathymetry of at least four different years is required for the calibration and verification. The four most recent available data is used, this is the bathymetry data of 2015, 2016, 2017 and 2018.

The historical mean vertical erosion rate is used in the calibration. This mean is based on the differences in bathymetry between 2014 and 2018. In figure G.12, the historical mean erosion rate is shown. The scour edge of the scour hole at rkm1004.8 in the Spui is defined at  $-12.8$  [m + NAP] (Huisman & van Duin, 2016).

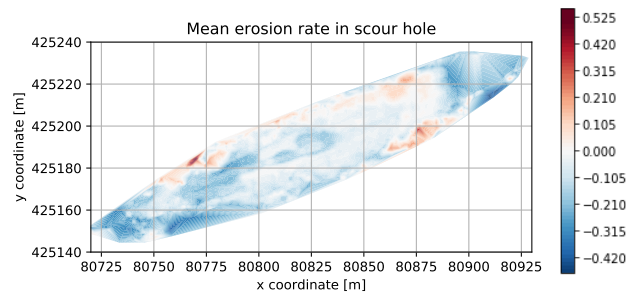


Figure G.12: Vertical erosion rate input data based on the historical average erosion in the period 2014-2018. Blue indicates local erosion while red indicates sedimentation.

### Surface area

In figure G.13, the historical surface areas below a certain level are indicated. The values corresponding to some levels are given in table G.18.

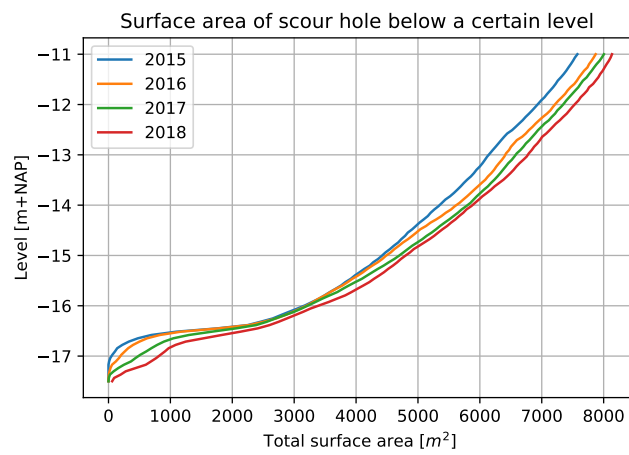


Figure G.13: Overview of historical surfaces of the scour hole below a certain level.

| Level [m + NAP] | 2015   | 2016   | 2017   | 2018   |
|-----------------|--------|--------|--------|--------|
| -11.5           | 7277.0 | 7580.0 | 7692.0 | 7892.0 |
| -12.0           | 6931.0 | 7213.0 | 7346.0 | 7530.0 |
| -12.8           | 6281.0 | 6530.0 | 6725.0 | 6915.0 |
| -14.0           | 5347.0 | 5618.0 | 5802.0 | 5884.0 |
| -15.0           | 4425.0 | 4490.0 | 4699.0 | 4805.0 |
| -16.0           | 3162.0 | 3189.0 | 3217.0 | 3385.0 |
| -17.0           | 50.0   | 196.0  | 480.0  | 810.0  |

Table G.18: Overview of historical surfaces of the scour hole below a certain level in [m<sup>2</sup>].

### Length and lowest located point

The historical length and the level of the lowest located point of the scour hole is presented in table G.19.

| Year | Deepest point [m NAP] | Length [m] |
|------|-----------------------|------------|
| 2015 | -17.164               | 182        |
| 2016 | -17.379               | 190        |
| 2017 | -17.493               | 200        |
| 2018 | -17.705               | 200        |

Table G.19: Overview of growth of Scour hole.

### G.2.4. Calibration

After varying of the input parameters, the following values give the best results for the calibration targets:

*Minimum erosion rate = 0.1 [m/yr]*

*Minimum length for erosion detection = 30 [m/yr]*

*Definition of a steep slope = 1:20*

The tool output with these input parameters is together with the target values and the differences between these two, presented in table G.20 and table G.21. In general, the surface are represented quite well with the used input parameters. Only the lowest located part is not good predicted with the tool. The tool gives a under prediction for the area lower located than -16.8 [m + NAP]

| Level [m + NAP] | Target | tool result | Difference      |
|-----------------|--------|-------------|-----------------|
| -11.5           | 7692.0 | 7699.0      | 7.0 (+0.1%)     |
| -12             | 7346.0 | 7333.0      | -13.0 (-0.2%)   |
| -12.8           | 6725.0 | 6703.0      | -22.0 (-0.3%)   |
| -14             | 5802.0 | 5800.0      | -2.0 (0.0%)     |
| -15             | 4699.0 | 4604.0      | -95.0 (-2.0%)   |
| -16             | 3217.0 | 3271.0      | 54.0 (+1.7%)    |
| -17             | 480.0  | 321.0       | -159.0 (-33.1%) |

Table G.20: Calibration targets and tool result for surface area in [m<sup>2</sup>].

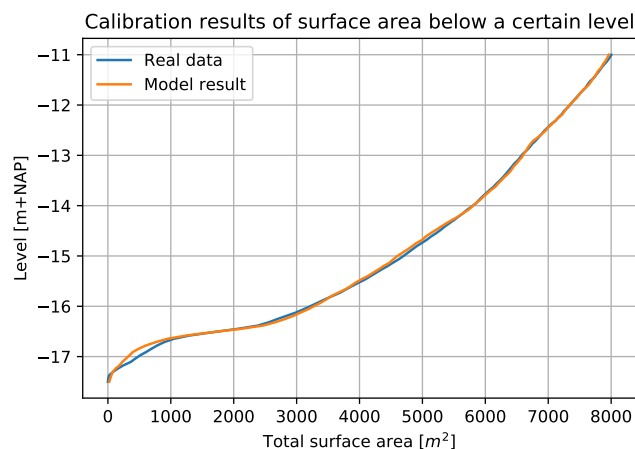


Figure G.14: Calibration results of surface area below a certain level.

|             | Deepest point [m NAP] | Length [m] |
|-------------|-----------------------|------------|
| Target      | -17.493               | 200        |
| tool result | -17.639               | 194        |
| Difference  | -0.146                | -6         |

Table G.21: Calibration targets and tool result for deepest point and length.

### G.2.5. Verification

The calibrated input parameters are used to predict the bathymetry of 2018, with as input data the bathymetry of 2016 and 2017. The tool output and the real values for the calibration targets are shown in table G.22 and table G.23.

As can be seen, the deepest point and the scour length is predicted very well. The difference between the surface areas are, with exception of the surface area below  $-17$  [m + NAP], less than 2.0%. There is small under prediction in the higher located parts of the scour hole and a small over prediction in the middle located parts.

The calibrated input values perform thus good on different input data and can be used for the prediction of the scour hole development.

| Level [m + NAP] | Target | tool result | Difference      |
|-----------------|--------|-------------|-----------------|
| -11.5           | 7892.0 | 7754.0      | -138.0 (-1.7%)  |
| -12             | 7530.0 | 7420.0      | -110.0 (-1.5%)  |
| -12.8           | 6915.0 | 6831.0      | -84.0 (-1.2%)   |
| -14             | 5884.0 | 5932.0      | 48.0 (+0.8%)    |
| -15             | 4805.0 | 4880.0      | 75.0 (+1.6%)    |
| -16             | 3385.0 | 3313.0      | -72.0 (-2.1%)   |
| -17             | 810.0  | 677.0       | -133.0 (-16.4%) |

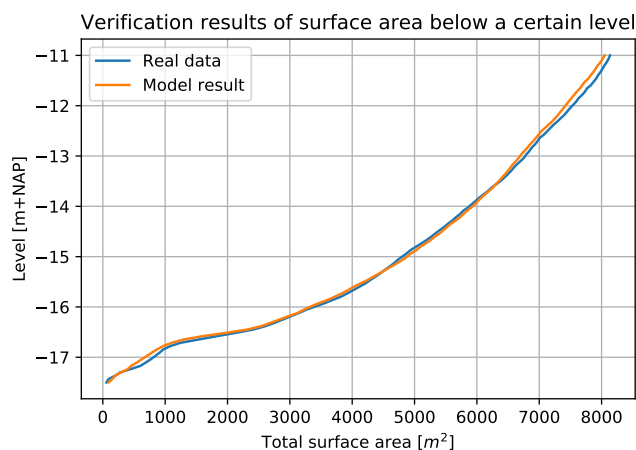
Table G.22: Verification targets and tool result for surface area in [m<sup>2</sup>].

Figure G.15: Verification results of surface area below a certain level.

|             | Deepest point [m NAP] | Length [m] |
|-------------|-----------------------|------------|
| Target      | -17.705               | 200        |
| tool result | -17.694               | 200        |
| Difference  | 0.011                 | 0          |

Table G.23: Verification targets and tool result for deepest point and length.